



JOURNAL OF A peer-reviewed open-access journal
Hymenoptera
The International Society of Hymenopterists **RESEARCH**

**ADVANCES IN THE
SYSTEMATICS OF
PLATYGASTROIDEA II**

EDITED BY
ELIJAH TALAMAS



Proterosceliopsis plurima Talamas, Shih & Ren

Advances in the Systematics of Platyastroidea II

Edited by
Elijah J. Talamas



Sofia–Moscow

2019

JOURNAL OF HYMENOPTERA RESEARCH 73 (SPECIAL ISSUE)

ADVANCES IN THE SYSTEMATICS OF PLATYGASTROIDEA II

Edited by Elijah J. Talamas

First published 2019

ISBN 978-954-642-985-8 (paperback)

Pensoft Publishers

12 Prof. Georgi Zlatarski Street, 1700 Sofia, Bulgaria

Fax: +359-2-870-42-82

info@pensoft.net

www.pensoft.net

Printed in Bulgaria, November 2019

Contents

- I Introduction**
Elijah J. Talamas
- 3 Proterosceliopsidae: A new family of Platygastroidea from Cretaceous amber**
Elijah J. Talamas, Norman F. Johnson, Chungkun Shih, Dong Ren
- 39 Revision of the Afrotropical genus *Pulchrisolia* Szabó (Hymenoptera, Platygasteridae, Sceliotrachelinae)**
Zachary Labey, Simon van Noort, Andrew Polaszek, Lubomír Masner, Norman F. Johnson
- 73 Revision of *Aleyroctonus* Masner & Huggert (Hymenoptera, Platygasteridae, Sceliotrachelinae)**
Zachary Labey, Lubomír Masner, Norman F. Johnson, Andrew Polaszek
- 95 First report of *Telenomus remus* parasitizing *Spodoptera frugiperda* and its field parasitism in southern China**
Yong-Lin Liao, Bin Yang, Miao-Feng Xu, Wei Lin, De-Sen Wang, Ke-Wei Chen, Hua-Yan Chen
- 103 *Paratelenomus anu* Rajmohana, Sachin & Talamas (Hymenoptera, Scelionidae): description and biology of a new species of phoretic egg parasitoid of *Megacopta cribraria* (Fab.) (Hemiptera, Plataspidae)**
Keloth Rajmohana, James P. Sachin, Elijah J. Talamas, Mukundan S. Shamyasree, S. K. Jalali, Ojha Rakshit
- 125 Field studies and molecular forensics identify a new association: *Idris elba* Talamas, sp. nov. parasitizes the eggs of *Bagrada hilaris* (Burmeister)**
J. Refugio Lomeli-Flores, Susana Eva Rodríguez-Rodríguez, Esteban Rodríguez-Levya, Héctor González-Hernández, Tara D. Garipey, Elijah J. Talamas
- 143 Scelionidae (Hymenoptera) parasitizing eggs of *Bagrada hilaris* (Hemiptera, Pentatomidae) in Mexico**
Moisés Felipe-Victoriano, Elijah J. Talamas, Sergio R. Sánchez-Peña

153 A morphological, biological and molecular approach reveals four cryptic species of *Trissolcus* Ashmead (Hymenoptera, Scelionidae), egg parasitoids of Pentatomidae (Hemiptera)

Francesco Tortorici, Elijah J. Talamas, Silvia T. Moraglio, Marco G. Pansa, Maryam Asadi-Farfar, Luciana Tavella, Virgilio Caleca

201 Molecular phylogeny of *Trissolcus* wasps (Hymenoptera, Scelionidae) associated with *Halyomorpha halys* (Hemiptera, Pentatomidae)

Elijah J. Talamas, Marie-Claude Bon, Kim A. Hoelmer, Matthew L. Buffington

Introduction

Elijah Talamas¹

¹ Florida Department of Agriculture and Consumer Service, Division of Plant Industry, Gainesville, Florida, USA

Corresponding author: *Elijah Talamas* (elijah.talamas@fdacs.gov)

Received 19 October 2019 | Accepted 6 November 2019 | Published 18 November 2019

<http://zoobank.org/72690716-CFF0-455F-8218-42CF531A7CAB>

Citation: Talamas E (2019) Introduction. In: Talamas E (Eds) *Advances in the Systematics of Platygastridae II*. Journal of Hymenoptera Research 73: 1–2. <https://doi.org/10.3897/jhr.73.47436>

The second installment of *Advances in the Systematics of Platygastridae* presents nine articles on an array of subjects that include paleontology, molecular phylogenetics and diagnostics, mating compatibility, field surveys, and a variety of taxonomic treatments. Designation of a new family name, Proterosciopsidae, portends further changes to family-level classification in Platygastridae and characterizes an extinct lineage. Two generic revisions bring much needed attention to Sceliotrachelinae, a group that has received relatively little attention. Importantly, the concepts of these genera are updated and synthesized through analysis of their constituent species and examination of related taxa.

From the remaining articles emerges the primary theme of this special issue: the systematics of scelionids that attack the eggs of invasive pests. During the past two decades, three pentatomoid pests of agricultural significance have invaded new continents, *Halyomorpha halys*, *Bagrada hilaris*, and *Megacopta cribraria*, generating impetus and funding for research on their parasitoids, particularly those in the scelionid genus *Trissolcus*. This issue contains treatments of scelionids that attack the eggs of each of these stink bugs, as well as a parasitoid of the widespread lepidopteran pest, *Spodoptera frugiperda*, highlighting the importance of these wasps in agricultural ecosystems. The molecular phylogeny of *Trissolcus* analyzes relationships between species found in the native and invaded ranges of *H. halys* and provides a context for delimiting species groups. This phylogeny independently confirms the results of a reanalysis of *Trissolcus*

species that were considered junior synonyms of *Trissolcus semistriatus* in the first issue of *Advances in the Systematics of Platygastroidea*. This complex contains some of the most common and widespread species in the genus, some of which have defied accurate diagnosis since their original description. Coupled with characterization of primary types described by Francis Walker in the 19th century, this marks a significant step in stabilizing the species-level taxonomy of *Trissolcus*.

This special issue is made possible by the work of contributors representing 24 institutions spread throughout ten countries and four continents. By presenting these publications as part of a cohesive unit, it is hoped that they will promote further collaboration and interest in the beneficial and beautiful taxon that is Platygastroidea.

Proterosceliopsidae: A new family of Platygastroidea from Cretaceous amber

Elijah J. Talamas^{1,2}, Norman F. Johnson³, Chungkun Shih^{1,4}, Dong Ren¹

1 College of Life Sciences, Capital Normal University, 105 Xisanhuanbeilu, Haidian District, Beijing 100048, China **2** Florida State Collection of Arthropods, Florida Department of Agriculture and Consumer Services, Gainesville, FL 32608, USA **3** Department of Evolution, Ecology and Organismal Biology, The Ohio State University, 1315 Kinnear Road, Columbus, Ohio 43212, USA **4** Department of Paleobiology, National Museum of Natural History, Smithsonian Institution, Washington, DC 20013-7012, USA

Corresponding author: *Elijah J. Talamas* (elijah.talamas@freshfromflorida.com); *Dong Ren* (rendong@mail.cnu.edu.cn)

Academic editor: *M. Yoder* | Received 7 December 2018 | Accepted 22 April 2019 | Published 18 November 2019

<http://zoobank.org/61D34EE7-13A3-48FB-8C55-30B76F60F1AA>

Citation: Talamas EJ, Johnson NF, Shih C, Ren D (2019) Proterosceliopsidae: A new family of Platygastroidea from Cretaceous amber. In: Talamas E (Eds) Advances in the Systematics of Platygastroidea II. Journal of Hymenoptera Research 73: 3–38. <https://doi.org/10.3897/jhr.73.32256>

Abstract

Proterosceliopsis was erected by Ortega-Blanco et al. (2014) in their treatment of scelionid genera in Cretaceous amber from Álava, Spain. The generic description appears to have been based on specimens in which only the dorsal aspects of the mesosoma and metasoma were visible, as characters of the mesopleuron, metapleuron, lateral pronotum, and ventral metasoma were not mentioned. We here provide a comprehensive description of the genus that includes characters from throughout the body and we reinterpret some of the characters presented by Ortega-Blanco et al. (2014). Our analysis of *Proterosceliopsis* in the context of extant and fossil platygastroids places this group as a lineage well outside of the current families. We here designate *Proterosceliopsis* as the type genus of a new family, Proterosceliopsidae Talamas, Johnson, Shih & Ren, **fam. nov.**, and describe five new species: *Proterosceliopsis ambulata* Talamas, Shih & Ren, **sp. nov.**, *P. nigon* Talamas, Shih & Ren, **sp. nov.**, *P. plurima* Talamas, Shih & Ren, **sp. nov.**, *P. torquata* Talamas, Shih & Ren, **sp. nov.**, and *P. wingerathi* Talamas, Shih & Ren, **sp. nov.** We provide a key to all presently known species in the genus. The oldest known specimen of Platygastriidae s.s., in Burmese amber, is presented and compared to Proterosceliopsidae **fam. nov.**

Keywords

fossil, morphology, Platygastriidae, Scelionidae

Introduction

Platygastroid wasps are numerous in Burmese amber, comprising 16% of Hymenoptera in a recent study by Zhang et al. (2018). Some Cretaceous taxa are recognizable among the extant fauna: Platygastridae, Sparasionini and *Archaeoteleia* Masner (Talamas et al. 2017a). Simultaneously, many cannot be confidently placed at the family level because of the morphological disparity of the Cretaceous fauna and because the classification of Platygastroidea is in a state of flux. Zhang et al. (2018) identified the Burmese amber specimens as Scelionidae, a family that has been used to accommodate taxa that are plesiomorphic, e.g. *Nixonia* Masner, *Archaeoteleia* Masner, *Sparasion* Latreille (Masner 1976), or feature characters that clearly exclude them from Platygastridae, e.g. *Janzenella* Masner & Johnson (Masner and Johnson 2007), *Plaumannion* Masner & Johnson (Masner et al. 2007), *Huddlestonium* Polaszek & Johnson (Masner et al. 2007) and *Neuroscelio* Dodd (Valerio et al. 2009).

The historical concept of Scelionidae was found to be polyphyletic in the molecular analysis of Murphy et al. (2007), which Sharkey (2007) used to treat Scelionidae as a junior synonym of Platygastridae. This resolved the issue of monophyly at the family level, but in doing so transferred the problem to the subfamilies, most of which are known to be polyphyletic. There is growing consensus among analyses that Platygastridae s.s. and the “main scelionid clade” of Murphy et al. (2007) are monophyletic lineages. The latter was retrieved in an analysis of the maxillo-labial complex by Popovici et al. (2017), and in unpublished molecular phylogenies of Platygastroidea that focus on relationships within Scelionidae (Chen et al.) and Platygastridae s.s. (Blaimer et al.). Both of these efforts include basal lineages and retrieve Platygastridae s.s. and the “main scelionid clade” as monophyletic taxa. A classification that employs the historical concept of Platygastridae and a modified concept of Scelionidae are thus well supported and provide cohesion with much of the taxonomic literature. Together, these taxa comprise the vast majority of platygastroid species, and a multi-family classification system provides better framework for higher taxonomy in the superfamily. We defer changes to family classification to the final results of the aforementioned analyses and note that while affinities are clearly present, we cannot place *Proterosceliopsis* in any of the existing or potential suprageneric taxa without drastically and unnecessarily altering their limits. Our analysis of *Proterosceliopsis* is made in the context of extant specimens from a broad geographic and taxonomic sampling, fossils from Lebanese, Burmese, Baltic, and Dominican amber, and with consideration of lineages for which additional families may be erected.

For the purposes of this paper, *Archaeoteleia*, *Neuroscelio*, *Huddlestonium* and *Plaumannion* are considered *incertae sedis* and are referenced by their generic names; Scelionidae refers to the “main scelionid clade” of Murphy et al. (2007); Platygastridae refers to the historical, pre-Sharkey (2007) concept of the family (=Platygastrinae + Sceliotrachelinae + *Orwellium* Johnson, Masner & Musetti); Nixonidae is treated as a monogeneric family (= *Nixonia*) sensu Mckellar and Engel (2012); and Sparasionini refers to the concept of Johnson et al. (2008a).

Criticism of previous taxonomy

Preservation artifacts complicate the taxonomic treatment of fossils. This problem is exacerbated when primary types do not display characters in sufficient detail to enable unambiguous determination at the species level. In the case of *Proterosceliopsis*, *P. masneri* Ortega-Blanco, McKellar & Engel can be reliably separated from the species here described from Burmese amber, but some of the most important generic characters are not visible in the specimens and are missing from the description presented by Ortega-Blanco et al. (2014). As a result, taxon-defining characters cannot presently be verified in the specimen that carries the name of a species, genus, and now, a family. We redefine *Proterosceliopsis* because we consider *P. masneri* and the specimens in Burmese amber to be congeneric based on the congruence of observable characters. In this case, attaching a concept to an existing name can be defended by the available data and reduces the number of superficially defined genera in Platygastroidea. We assert that dubiously delimited taxa can be avoided by a more rigorous approach to the treatment of fossils, one in which taxa are described only when based on well-preserved specimens and with the necessary background knowledge about the superfamily.

Material and methods

Informatics

The numbers prefixed with acronyms, e.g. “USNMENT” or “OSUC”, are unique identifiers for the individual specimens (note the blank space after some acronyms). Details on the data associated with these specimens may be accessed at the following link: purl.oclc.org/NET/hymenoptera/hol and entering the identifier in the form. Persistent URIs for each taxonomic concept were minted by xBio:D in accordance with best practices recommend by Hagedorn et al. (2013). Morphological terms were matched to concepts in the Hymenoptera Anatomy Ontology (Yoder et al. 2010) using the text analyzer function. A table of morphological terms and URI links is provided in Appendix 1. Taxonomic synopses and matrix-based descriptions were generated from the Hymenoptera Online Database (hol.osu.edu) and the online program vSysLab (vsyslab.osu.edu) in the format of character: state. Characters that were not visible because of preservation or orientation of the insects are coded as “not visible”.

Imaging and microscopy

The amber pieces were cut and polished to optimize the viewing and photography of specimens for taxonomic study. Direct examination of the specimens was made with a Zeiss V8 stereomicroscope and an Olympus BX51 compound microscope.

Photographs were captured with multiple imaging systems: a Z16 Leica lens with a JVC KY-F75U digital camera using Cartograph and Automontage software; an Olympus BX51 compound microscope with a Canon EOS 70D digital SLR camera; and a Leica DM2500 compound microscope with a Leica DFC425 camera. Illumination was achieved with a lighting dome or with LED gooseneck lamps and mylar light dispersers. Images were rendered from z-stacks with Automontage, Helicon Focus or Zerene Stacker. In some cases, multiple montage images were stitched together in Photoshop to produce larger images at high resolution and magnification. Full resolution images are archived at the image database at The Ohio State University (specimage.osu.edu).

Dissections for scanning electron microscopy were performed with a minuten probe and forceps and body parts were mounted to a 12 mm slotted aluminum mounting stub (EMS Cat. #75220) using a carbon adhesive tab (EMS Cat. #77825-12) and sputter coated with approximately 70 nm of gold/palladium using a Cressington 108 auto sputtercoater. Micrographs were captured using a Hitachi TM3000 Tabletop Microscope at 15 keV.

Author contributions

EJT: photography, scanning electron microscopy, taxon concepts, manuscript preparation; NFJ: manuscript preparation; CKS: manuscript preparation, provision of Burmese amber; DR: manuscript preparation, provision of Burmese amber.

Collections

The amber specimens of *Proterosceliopsis* studied here were collected from Kachin (Hukawng Valley) of northern Myanmar, which was dated at 98.79±0.62 Ma (Cruikshank and Ko 2003, Shi et al. 2012), equivalent to the earliest Cenomanian and approximately 1 Myr within the boundary between the Early and Late Cretaceous (Walker et al. 2012). This deposit yielded many well-preserved insect fossils (Chen et al. 2018a–b, Li et al. 2018, Wang et al. 2016, Zhang et al. 2018).

Specimens on which this work is based are deposited in the following repositories with abbreviations used in the text:

- CCHH** Hoffeins Collection, Hamburg, Germany
- CNCI** Canadian National Collection of Insects, Ottawa, Canada
- CNU** Key Lab of Insect Evolution and Environmental Changes, Capital Normal University, Beijing, China
- FSCA** Florida State Collection of Arthropods, Gainesville, FL, USA
- KUNH** Kansas University Natural History Museum, Lawrence, KS, USA
- OPPC** Ovidiu Popovici, personal collection, “A.I. Cuza” University, Faculty of Biology, Iasi, Romania

OSUC C.A. Triplehorn Insect Collection, The Ohio State University, Columbus, OH, USA

USNM National Museum of Natural History, Washington, DC, USA

Character annotations

1Rs (Fig. 15)	1 st radial sector vein
2Rs (Fig. 15)	2 nd radial sector vein
b (Fig. 15)	bullae
C, C+R (Fig. 15)	marginal vein
Cu (Fig. 15)	cubital vein
fas (Fig. 10)	facial striae
ff (Figs 43–44)	felt field
M (Fig. 15)	medial vein
mas (Fig. 10)	malar striae
mees (Figs 16, 20)	mesepimeral sulcus
ms (Figs 7–8, 10)	malar sulcus
net (Figs 16–17, 19)	netrion
p (Fig. 22)	cuticular pores
pp (Fig. 17)	mesopleural pit
prcs (Figs 16, 19, 21)	pronotal cervical sulcus
ps (Figs 1–6)	papillary (basiconic) sensilla
r (Fig. 15)	stigmatal vein
R1 (Fig. 15)	postmarginal vein
Rs+M (Fig. 15)	basal vein
sk (Figs 11–13)	skaphion
Sc+R (Fig. 15)	submarginal vein
S6 (Fig. 47)	metasomal sternites 6
T6–T8 (Figs 45–49, 55, 61)	metasomal tergites 6–8
tel (Figs 16, 19, 21)	transepisternal line

Results

Character discussion

Most of the diagnostic characters of *Proterosceliopsis* can be found in extant platygastroids but are present in a unique combination in this genus. Additionally, *Proterosceliopsis* exhibits significant differences from each of the taxa with which it shares characters. We present discussions of these characters and their distribution among platygastroid taxa as a prelude to the generic treatment.

Antenna

Bin (1981) defined the antennal clava in Telenominae (Scelionidae) based on the presence of papillary sensilla on the ventral side of the distal antennomeres (previously referred to as basiconic sensilla). The presence of these sensilla on female antennae is a synapomorphy for Platygastroidea (Austin et al. 2005), and Bin's definition of the clava has since been applied to all members of the superfamily. We continue to define the clava on the basis of papillary sensilla instead of relative antennomere size for multiple reasons: antennomeres can increase in size gradually (Figs 2–4); the size among antennomeres with papillary sensilla can be variable (Fig. 5); distinctly enlarged antennal segments may not have papillary sensilla, as in the clubbed antennae found in most males of *Helava* Masner & Huggert (Masner and Huggert 1989, Talamas and Masner 2016). The claval formula is often of taxonomic value, particularly at the species-level, and its use requires that specimens be preserved well enough to observe these structures. Small bubbles in the amber are sometimes visible at the tips of the sensilla (Fig. 6) and can be useful for identifying their presence.

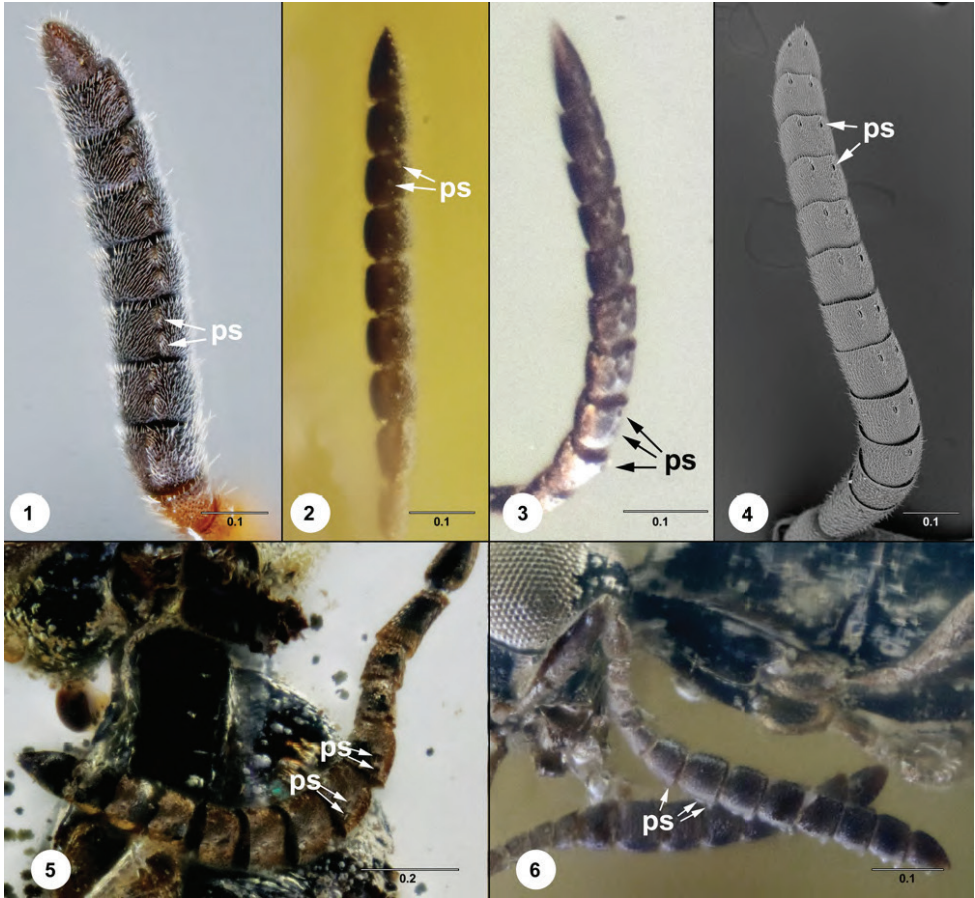
A transverse orientation of papillary sensilla is known only in *Nixonia* (Fig. 4) (Johnson and Masner 2006) whereas all other extant platygastroids have a longitudinal arrangement (Fig. 1). We found that in some species of *Proterosceliopsis* (Figs 3, 5) and Cretaceous *Electroteleia* Brues (Fig. 2) the sensilla are arranged at an oblique angle. This was found in multiple specimens in which the general shape of the antennomeres is intact, and thus we do not attribute this to taphonomic deformation. Instead, we consider that different arrangements of these sensilla were possible earlier in the history of Platygastroidea.

Malar sulcus

The malar sulcus found in *Proterosceliopsis* is unaccompanied by facial or malar striae (Fig. 7), a state which can be found in some Scelionidae (Fig. 8) and some Sparasionini (*Electroteleia*). In Platygastridae, the malar sulcus is present in only two genera: *Metacclisis* Förster and *Orseta* Masner & Huggert, each of which have both facial and malar striae (Fig. 10) (Masner and Huggert 1989), and *Orwellium*, which does not have facial or malar striae. The malar sulcus is entirely absent in *Nixonia* Masner (Fig. 9).

Palpal formula

Ortega-Blanco et al. (2014) recorded the palpal formula of *P. masner* to be 5:3. We observed 5-merous, cylindrical maxillary palps in *P. nigon*, *P. torquata*, and *P. wingerathi*; and at least 4 maxillary palpomeres in *P. plurima*. Two labial palpomeres are visible in *P. torquata*. Five-merous palpomeres were retrieved as the plesiomorphic condition for Platygastroidea in the phylogenetic analysis by Popovici et al. (2017) and are found in Sparasionini, *Nixonia*, and *Archaeoteleia*. This indicates that *Proterosceliopsis* is also

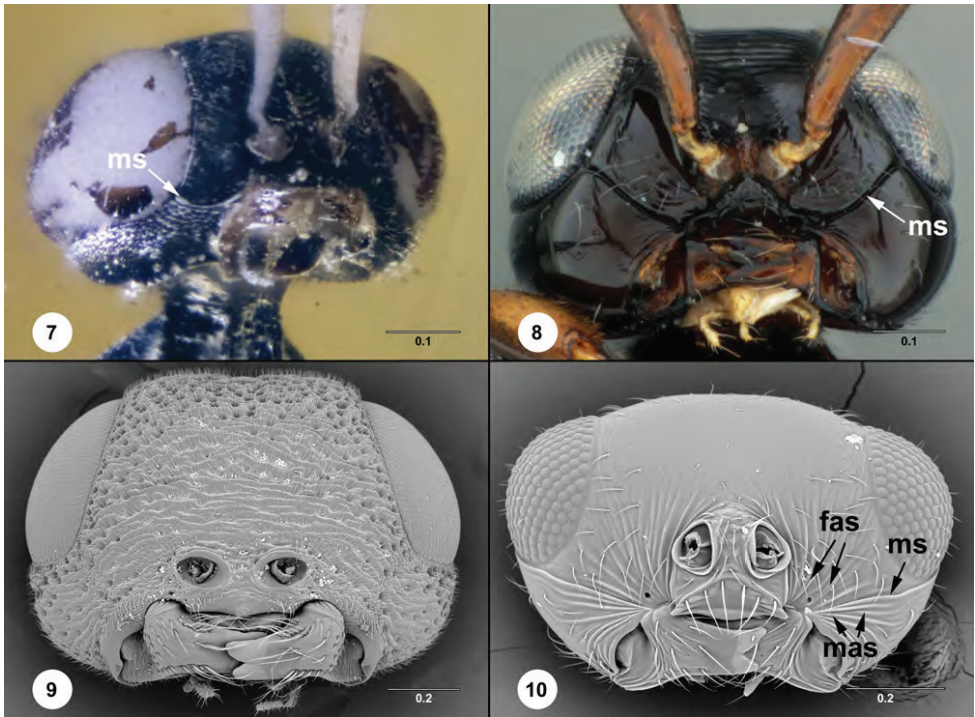


Figures 1–6. **1** *Sceliomorpha* Ashmead (DPI_FSCA 00008723), female antenna, ventral view **2** *Electroteleia* (DPI_FSCA 00010129), female antenna, ventral view **3** *Proterosceliopsis plurima* (CNU-HYM-MA-2016102), female antenna, ventral view **4** *Nixonia watshami* Johnson & Masner (OSUC 149432), female antenna, ventral view **5** *Proterosceliopsis nigon* (CNU-HYM-MA-2017566), female antenna, ventral view. **6** *Proterosceliopsis wingerathi* (CNU-HYM-MA-2016101), female antenna, lateral view. Scale bars in millimeters.

a basal lineage well outside of Scelionidae in which the palpal formula is 4:2 or less (Popovici et al. 2017), and Platygastridae in which the palpal formula is 2:1 or less (Popovici, personal communication).

Skaphion

The anterior mesoscutum in most species of *Proterosceliopsis* features a smooth, transverse structure to which we apply the term skaphion (Figs 11, 50, 58, 62). We do not assert that the skaphion of *Proterosceliopsis* is homologous with that found in scelionid genera (Figs 12–13) and note that it can be found in other Cretaceous taxa that do not belong to *Proterosceliopsis* or Scelionidae, e.g. *Electroteleia* (Fig. 14).



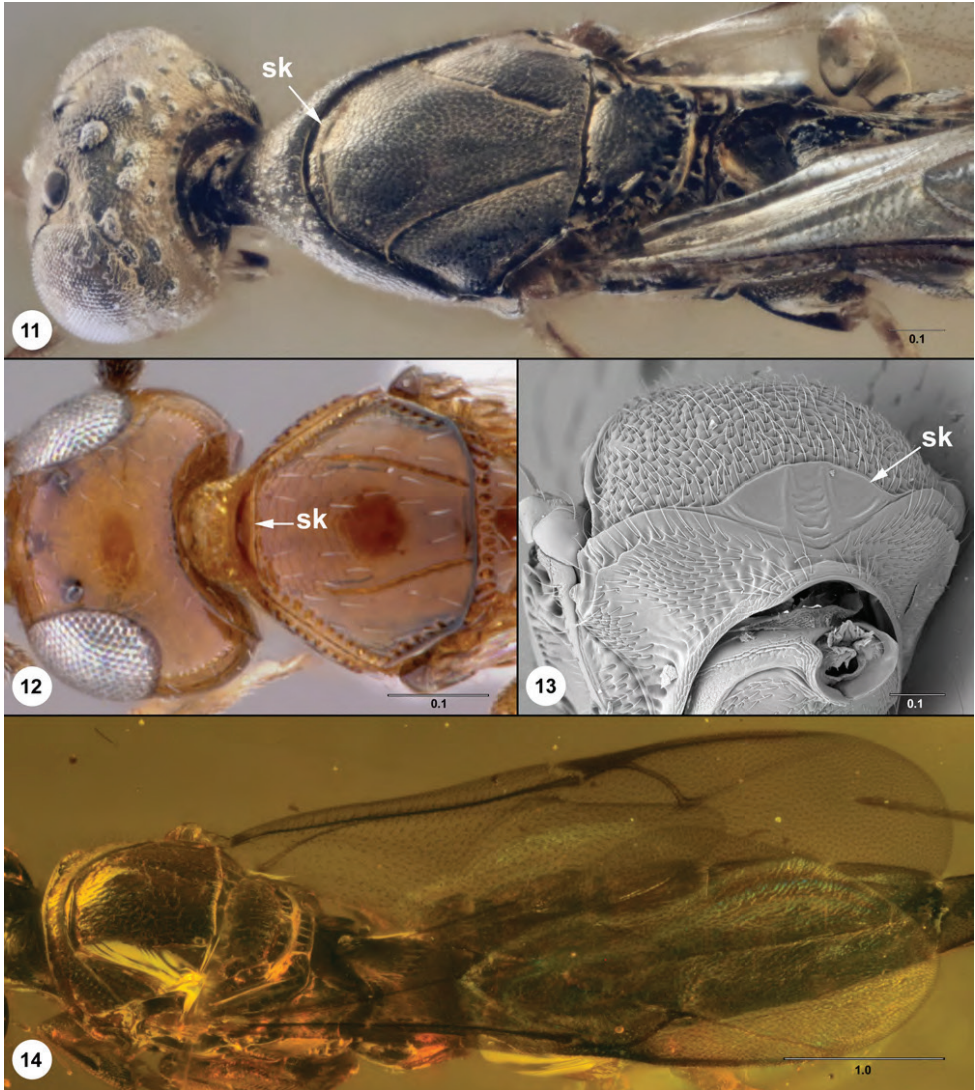
Figures 7–10. **7** *Proterosceliopsis plurima* (CNU-HYM-MA-2016102), head, anteroventral view **8** *Calliscelio* Ashmead (CNC494853), head, anteroventral view **9** *Nixonia watshami* (OSUC 149432), head, anteroventral view **10** *Metaclisis* (USNMENT01029162), head, anteroventral view. Scale bars in millimeters.

Costal vein

In *Proterosceliopsis*, the costal vein is present anterior to the fusion with R and extends proximally beyond the bulla (Fig. 15). This form is known from other Cretaceous platygastroids (Fig. 14), but not in extant taxa.

Setation of the pronotal cervical sulcus

The pronotal cervical sulcus can take many forms, including a distinct line of foveae (Fig. 18), a well-defined smooth groove (Fig. 19), or a weakly defined furrow along the lateral pronotal rim (Fig. 17). In *Nixonia*, Johnson and Masner (2006) reported an area of dense setation along the anterior margin of the lateral pronotum that is often associated with solidified exudate (Fig. 20). Setation along the pronotal cervical sulcus is found in *Proterosceliopsis* (Fig. 16, 52, 59) and many platygastroids (Figs 19, 26), and often contains what appears to be solidified exudate. The unpublished phylogenetic



Figures 11–14. **11** *Proterosceliopsis torquata* (CNU-HYM-MA-2016106), head and mesosoma, dorsal view **12** *Calotelea* Westwood (OSUC 56216), head and mesosoma, dorsal view **13** *Nyleta striaticeps* Dodd (OSUC 174452), mesosoma, anterior view **14** *Electroteleia* (CNU-HYM-MA-2016103), mesosoma and metasoma, dorsolateral view. Scale bars in millimeters.

analysis of Platygastriidae (Blaimer et al.) indicates that stem lineages of this family have a setose pronotal cervical sulcus. Figures 65–66 illustrate the oldest known platygastriid, in Burmese amber, that exhibits this character, consistent with our treatment of it as a plesiomorphy for Platygastriidae that varies significantly in some derived platygastriid lineages (Figs 21–26). Figures 21–22 illustrate the unusual form found in *Sacespalus*

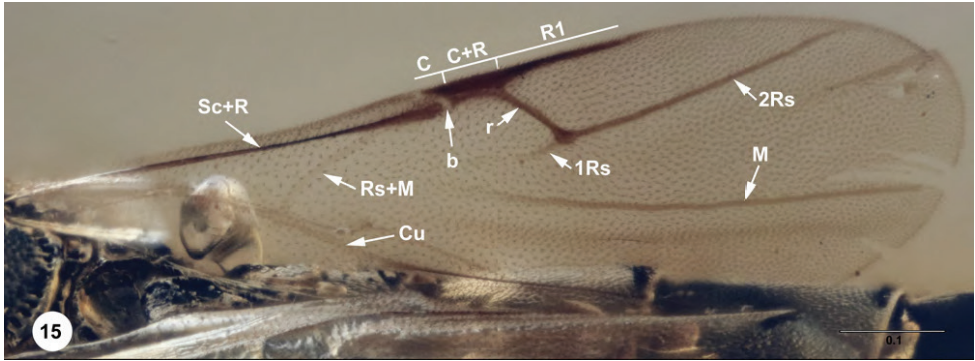


Figure 15. *Proterosceliopsis torquata* (CNU-HYM-MA-2016106), fore wing, dorsal view. Scale bar in millimeters.

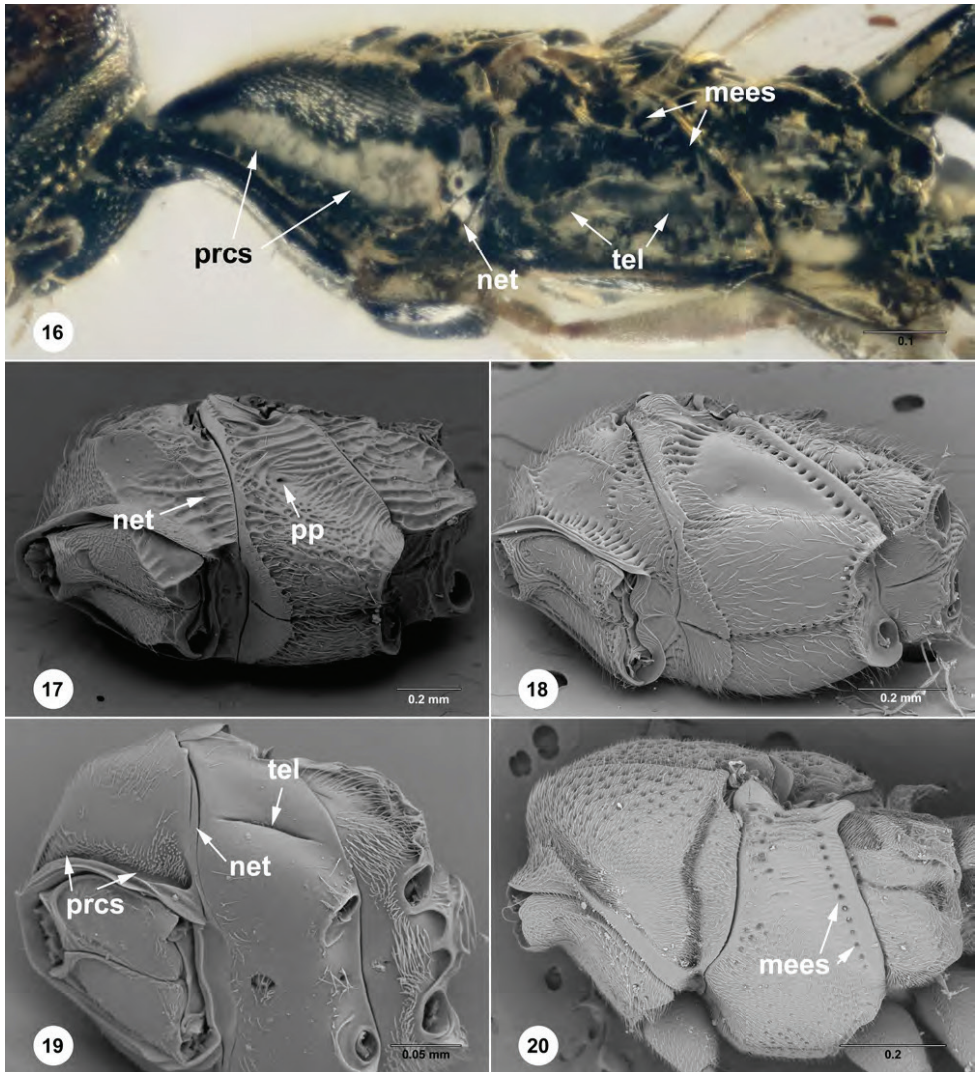
in which setation is absent and the pronotal cervical sulcus is broadly expanded. Pores can be seen in the ventral portion of the pronotal cervical sulcus of *Sacespalus* (Fig. 22), which is congruent with the hypothesis that this character is associated with glandular secretions. We do not know of any scelionids with a setal patch along the anterior portion of the lateral pronotum but note that the antespircular setal patch (sensu Yoder et al. 2012) in Scelionidae is associated with cuticular pores (Fig. 28). Based on the pronotal position of these setal patches, we suspect that they have similar function.

Netrion

A netrion is clearly present in 3 of the 5 species that we here describe. Mikó et al. (2007) reported that in *Nixonia* the trachea associated with the anterior thoracic spiracle extends ventrally between the netrion sulcus and the posterior pronotal inflection. Externally this results in the netrion sulcus dorsally terminating anterior to the anterior thoracic spiracle (Fig. 20). This character can be used to separate *Nixonia* from nearly all other platygastroids, in which the netrion sulcus, when present, terminates posterior or ventral to the anterior thoracic spiracle (Figs 16–18, 20).

Transepisternal line

Among extant platygastroids, the transepisternal line is found exclusively in Platygastriidae (Fig. 19). We treat it as a plesiomorphy for Platygastriidae based on its presence in the Cretaceous specimen illustrated in Figs 65–66, and because it is found in stem lineages of the family based on a preliminary analysis of molecular data (Blaimer et al.). The internal anatomy associated with this structure has yet to be examined in detail and will likely shed light on its function and evolution within Platygastriidae. The transepisternal line in *Proterosceliopsis* is clearly present in all specimens from Burmese amber (Figs 16, 53) suggesting a close relationship between Proterosceliopsidae and Platygastriidae.

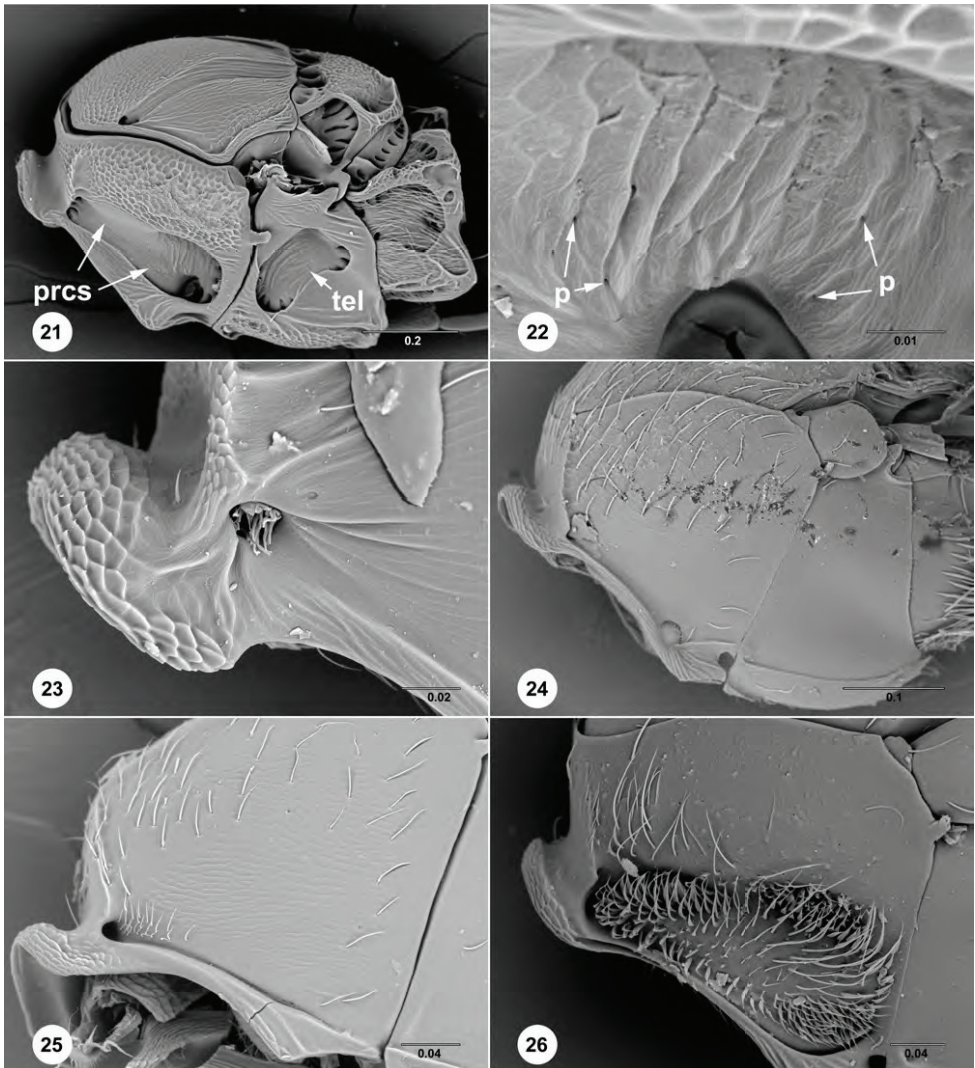


Figures 16–20. **16** *Proterosceliopsis plurima* (CNU-HYM-MA-2016102), mesosoma, lateral view **17** *Scelio* Latreille (USNMENT00989612_3), mesosoma, ventrolateral view **18** *Archaeoteleia gracilis* Masner (OSUC 163002), mesosoma, ventrolateral view **19** *Fidiobia* (USNMENT01197212_2), mesosoma, ventrolateral view **20** *Nixonia watshami* (OSUC 149432), head, lateral view. Scale bars in millimeters.

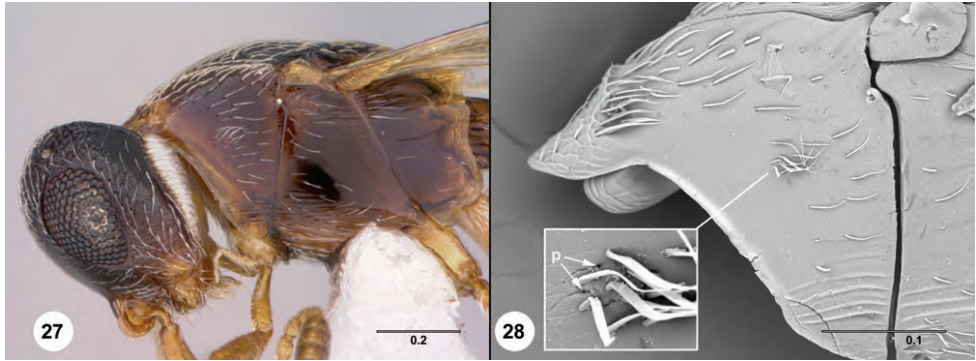
Mesepimeral sulcus

The presence of a fully developed mesepimeral ridge was retrieved by Vilhelmsen et al. (2010) as a potential autapomorphy for Proctotrupoidea s.s. This ridge corresponds externally to the mesepimeral sulcus, which is found in all platygastroid families except Platygastriidae (Figs 16–20). We consider the loss of the mesepimeral sulcus to be an apomorphy for Platygastriidae, but whether this internally corresponds to loss of the mesepimeral ridge has yet to be investigated. Some examples of an absent or weakly

indicated mesepimeral sulcus can be found in Scelionidae. In some cases, these are clearly secondary derivations that occurred at the species level (Fig. 17). In the unusual *Doddiella* Kieffer (Scelionidae) the mesepimeral sulcus is not indicated externally but the mesepimeral ridge can be seen through the semitransparent exoskeleton (Fig. 27). The presence of the mesepimeral sulcus in Proterosceliopsidae provides a reliable mesosomal character to separate it from Platygasteridae.



Figures 21–26. **21** *Sacspalus* Kieffer (USNMENT01197981_1), mesosoma, lateral view **22** *Sacspalus* (USNMENT01197981_1), ventral portion of pronotal cervical sulcus, lateral view **23** *Leptacis* Förster (USNMENT00872705), anterior portion of pronotal cervical sulcus, lateral view **24** *Synopeas* Förster (USNMENT00989616_3), mesosoma, lateral view **25** *Platygaster* Latreille (USNMENT01197214_1), pronotum, lateral view **26** *Trichacis* Förster (USNMENT00989620), pronotum, lateral view. Scale bars in millimeters.



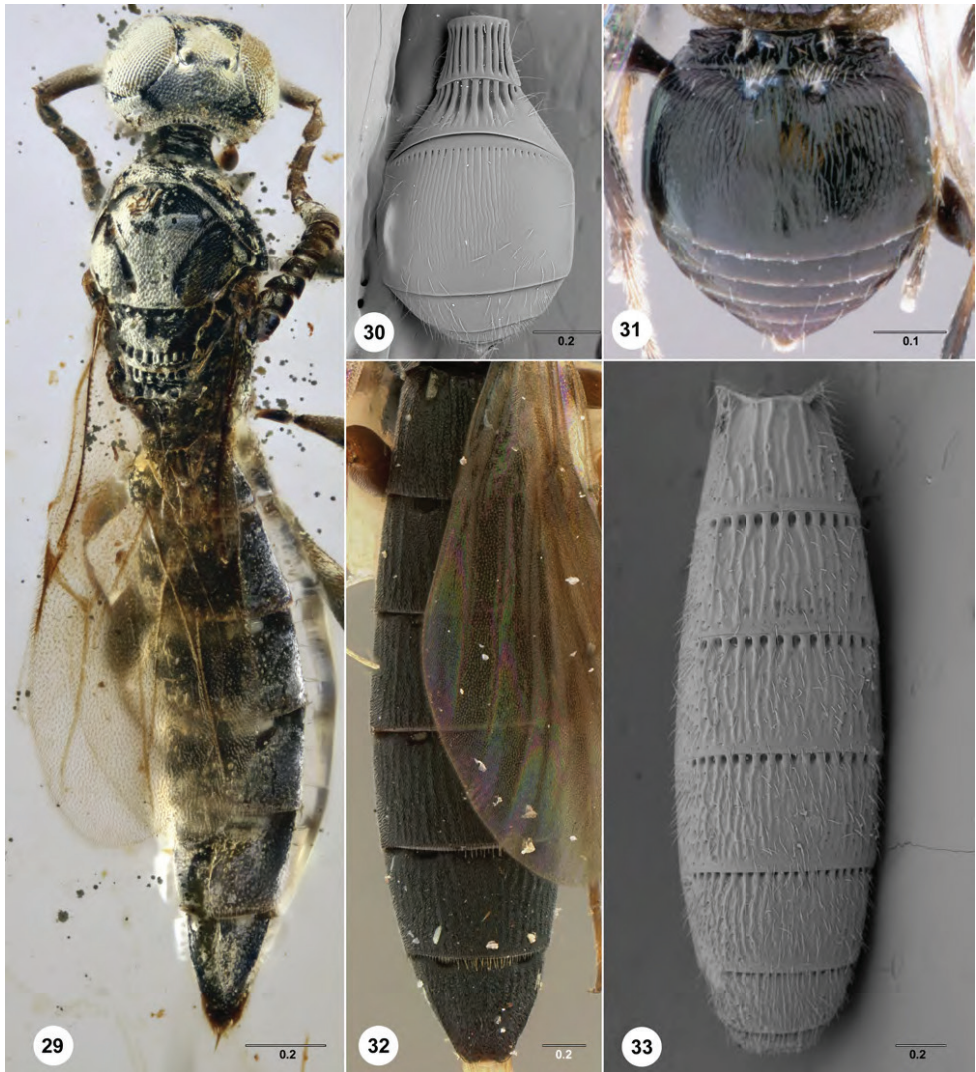
Figures 27, 28. **27** *Doddiella* (OSUC 56323), head and mesosoma, lateral view **28** *Doddiella* (USNM-ENT00872797), pronotum and mesopleuron, lateral view. Scale bars in millimeters.

Setation and sulci of the metasoma

Proterosceliopsis from Burmese amber and *Nixonia* share the presence of transverse, depressions along the anterior margins of T1–T5 (Figs 29, 32) and S1–S5 (Figs 34, 37). In *Nixonia*, these depressions have visible setation. In *Proterosceliopsis* they appear to have very fine setation, but the cloudy exudate prevents an unobscured view. In *P. torquata* these depressions are not clearly visible on T6, and in *P. plurima* they are not clearly present on S6. In the other Burmese species of *Proterosceliopsis*, and in all species of *Nixonia*, these depressions are present on T6 and S6. We suspect that they are present on T6 and S6 in all species of *Proterosceliopsis*, but the preservation of these specimens prevents us from reaching a confident conclusion.

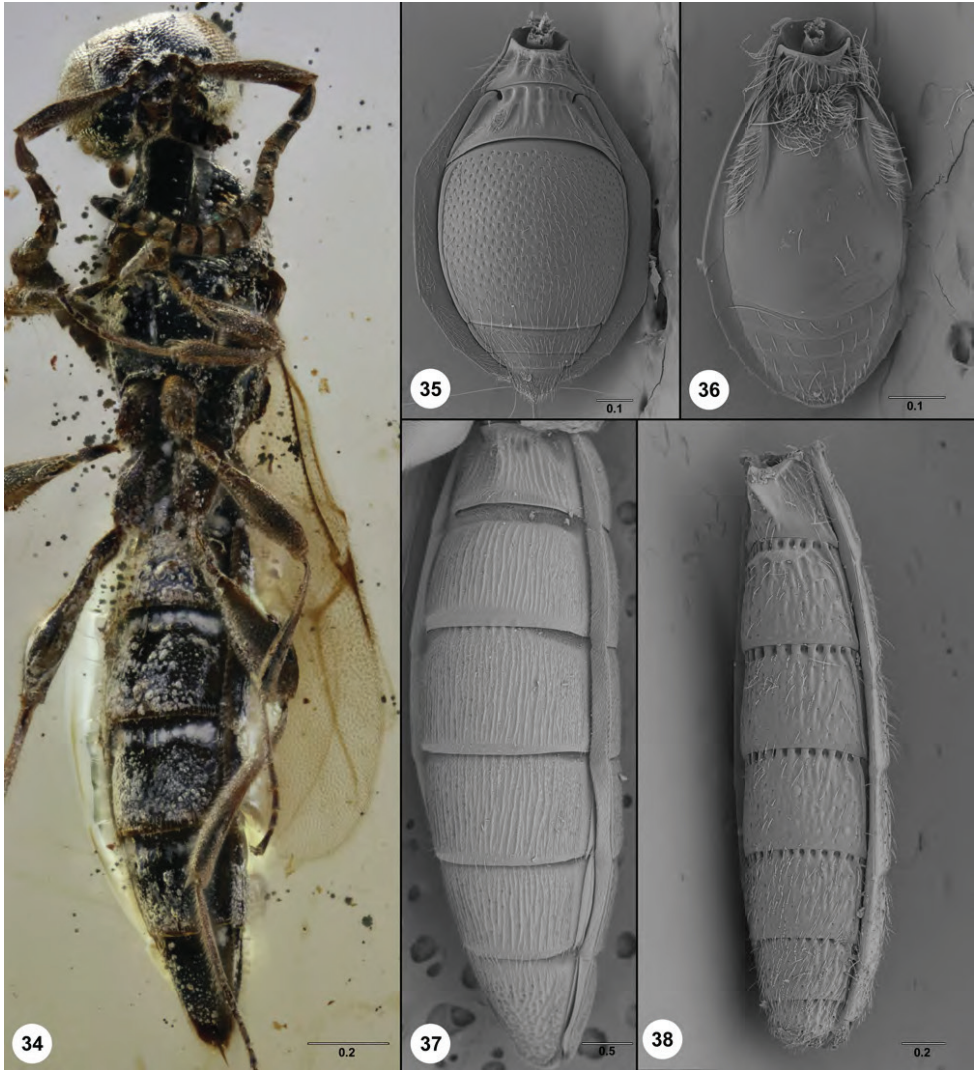
The two components of this character, setation/glandular secretion and sulci along the anterior tergites and sternites, vary independently among platygastroid families. Sparasionini and *Archaeoteleia* feature transverse sulci across the anterior margins of the external tergites and sternites (Figs 33, 38, 44), which may sometimes be reduced on T6 and S6 in females of *Electroteleia* (Sparasionini) and in *Archaeoteleia*. These sulci are found in all specimens that we examined in Lebanese amber, which constitute the oldest platygastroid fossils, and we consider it likely that this is the plesiomorphic condition for Platygastroidea. The metasoma in Sparasionini and *Archaeoteleia* lacks setation on the anterior tergites and sternites beyond T1 and S1, but there may be numerous felt fields (Fig. 44).

In Platygastriidae and Scelionidae, the anterior portions of T1–T2 and S1–S2 typically feature a transverse line of foveae or pits, which may or may not be clearly defined (Figs 30–31, 35–36). The transverse sulci in scelionids are not associated with setation, and patches of dense setae tend to be located on the lateral portion of the tergite, sometimes in well-defined pits (Figs 39–40). Some teleasines (Scelionidae) exhibit a transverse sulcus along anterior T3 and S3 (Fig. 30, 35) and setal patches with pores on T4–T5 (Fig. 42). Platygastriidae exhibits the greatest variation in the size, location, and shape of setal pits on metasomal segments 1 and



Figures 29–33. **29** *Proterosceliopsis nigron* (CNU-HYM-MA-2017566), head, mesosoma, metasoma, dorsal view **30** *Trimorus* Förster (USNMENT01197861), metasoma, dorsal view **31** *Amitus* Haldeman (OSUC 404941), metasoma, dorsal view **32** *Nixonia krombeini* Johnson & Masner (OSUC 146429), metasoma, dorsal view **33** *Sparasion philippinensis* Kieffer (USNMENT00872835), metasoma, dorsal view. Scale bars in millimeters.

2. They may be present laterally or medially, as a broad transverse patch that spans the width of the tergite or sternite (Fig. 43), in well-defined pits (Fig. 31), or they may be absent entirely (e.g. *Orwellium* Johnson, Masner & Musetti). Felt fields, which are absent in *Nixonia* and *Proterosceliopsis*, are found only on S2 in Platygastriidae and Scelionidae, with a few exceptions (e.g. *Heptascelio* Kieffer (Johnson

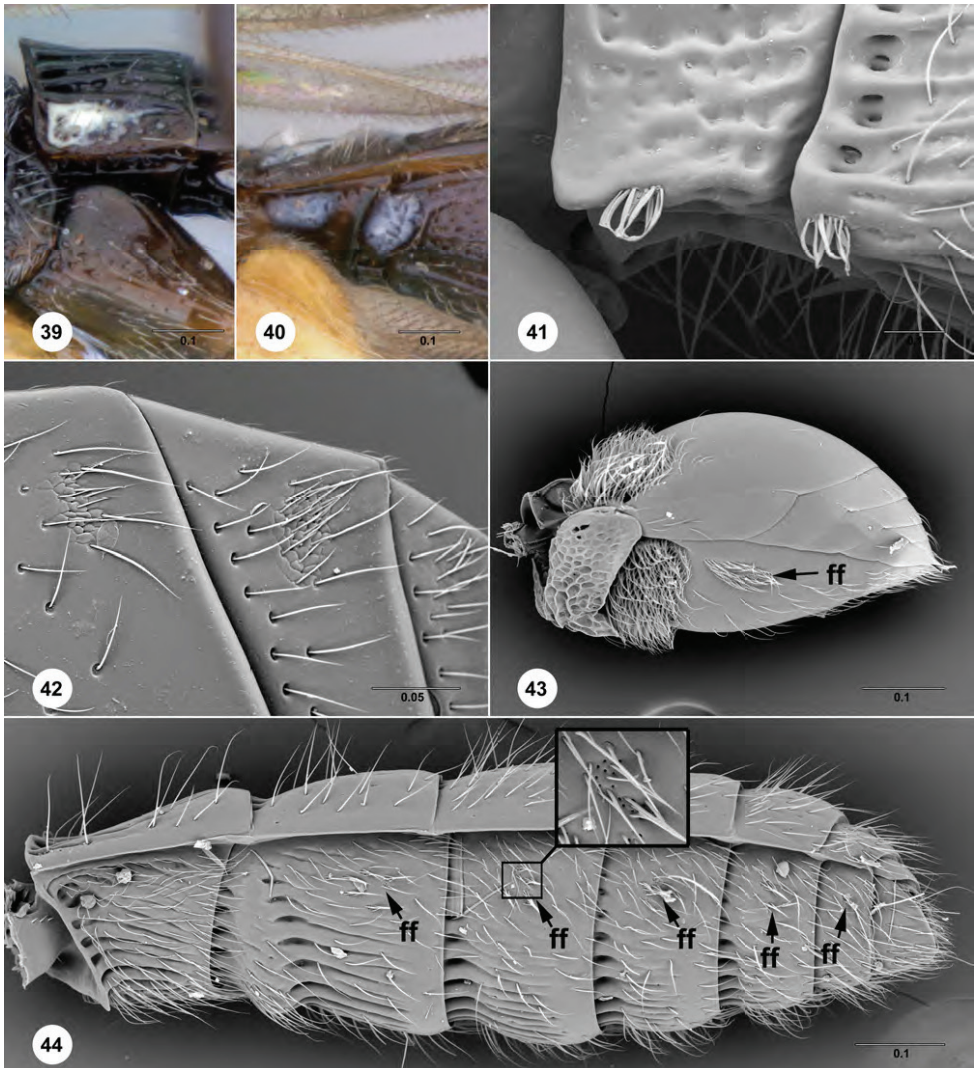


Figures 34–38. **34** *Proterosceliopsis nigon* (CNU-HYM-MA-2017566), head, mesosoma, metasoma, ventral view **35** *Dvivarnus mikuki* Talamas & Mikó (USNMENT01059135), metasoma, ventral view **36** *Trichacis* (USNMENT01059347), metasoma, ventral view **37** *Nixonia watshami* (OSUC 149432), metasoma, ventral view **38** *Sparasion philippinensis* (USNMENT00872835), metasoma, ventral view. Scale bars in millimeters.

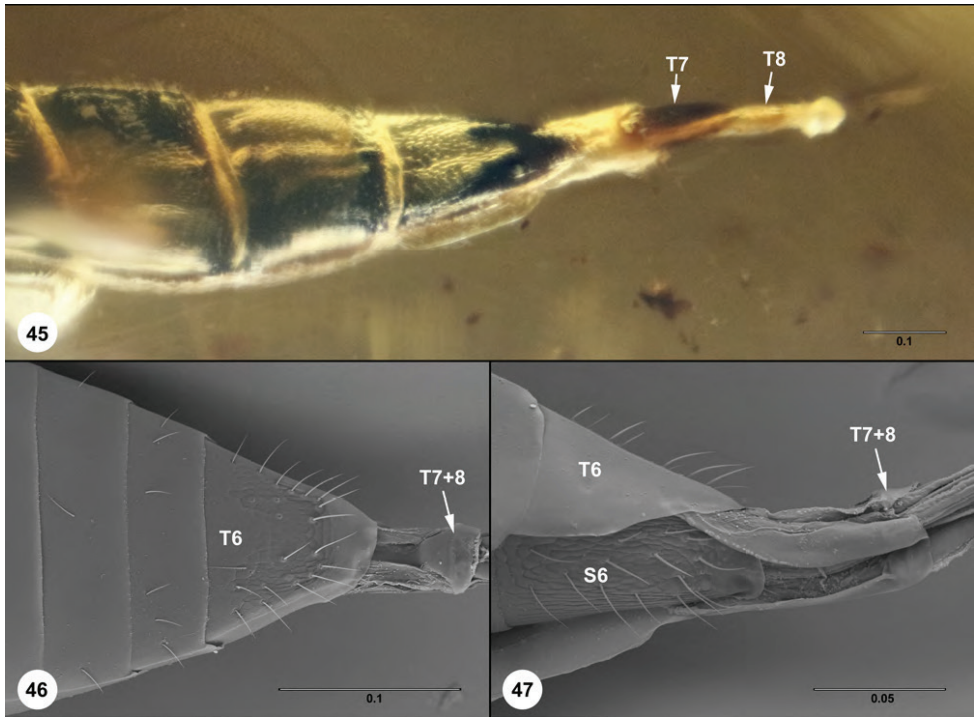
et al. 2008b)). *Neuroscelio doddi* Galloway, Austin & Masner exhibits an unusual and noteworthy form of sternal setation in which dense tufts are located medially on S1–S2 (Fig. 41).

Setal patches on the metasoma and pronotum, which are often associated with pores in the integument, clearly warrant further examination. A survey of platygas-

triod morphology with a scanning electron microscope has revealed an array of additional pore locations and forms on the head and mesosoma. Our present analysis of these characters, which provides only a broad overview as it relates to family level classification of *Proterosceliopsis*, will be developed further in future projects. The presence of cuticular pores and solidified exudate in the same locations point to the activity of internal glands.



Figures 39–44. **39** *Trichoteleia bidentata* Talamas (CASENT 2132802), T1, lateral view **40** Scelioninae (OSUC 254572), S1-S2, ventrolateral view **41** *Neuroscelio doddi* (OSUC 147252), S1-S2, ventrolateral view **42** *Dviivarnus mikuki* (USNMMENT01059135), T3-T5, dorsal view **43** *Helava alticola* Masner & Huggert (USNMMENT00989211), metasoma, lateral view **44** *Archaeoteleia gracilis* (OSUC 163002), metasoma, lateral view. Scale bars in millimeters.



Figures 45–47. **45** *Proterosceliopsis ambulata* (CNU-HYM-MA-2016105), distal metasoma, dorsal view **46** *Fidiobia* (USNMENT01197212_2), distal metasoma, dorsal view **47** *Fidiobia* (USNMENT01197212_2), distal metasoma, ventrolateral view.

Ovipositor system

Ortega-Blanco et al. (2014) interpreted T7+8 to be the ovipositor, which they described as short and broad. We here clarify that these sclerites are not the ovipositor, but they could be considered part of the *ovipositor system* sensu Austin and Field (1997). The known diversity of ovipositor systems in Platygastroidea has expanded in recent years, with at least two derivations of a telescoping ovipositor system found in Platygastriidae (Talamas et al. 2017b). Extension of the ovipositor system in *Proterosceliopsis* appears to operate via telescoping membrane between T6 and T7, with T7 and T8 clearly present as separate sclerites in some specimens (Fig. 45). The unpublished phylogenetic analyses suggest that conjunctival expansion between T6 and T7 occurred independently in Scelionidae and *Archaeoteleia*. The placement of *Proterosceliopsis* well outside of these families indicates that expansion of conjunctiva between T6 and T7 into a telescoping ovipositor system has occurred at least three times: in *Proterosceliopsis*, *Archaeoteleia*, and Scelionidae. We also have found evidence of conjunctival expansion between T6 and T7 in the platygastriid genus *Fidiobia* Ashmead. It does not appear to be telescoping but provides clear evidence of yet another independently derived elongation of conjunctiva between T6 and T7 (Figs 46–47), lending evidence to the plasticity of this morphological system.

Taxonomy

Proterosceliopsidae Talamas, Johnson, Shih & Ren, fam. nov.

<http://zoobank.org/A482A28F-562C-4318-A681-47F326D152E3>

Diagnosis. Antenna with 14 or 15 antennomeres; malar sulcus present (Fig. 7); facial striae absent (Fig. 7); malar striae absent (Fig. 7); pronotal cervical sulcus present as a furrow of fine setation associated with glandular excretion (Figs 16, 48–49, 51–53, 59); mesopleuron with transepisternal line and mesepimeral sulcus (Figs 16, 51–53, 59, 63); T3–T5 and S3–S5 anteriorly with depressions associated with glandular excretion (Figs 29, 34, 56, 58, 62).

***Proterosceliopsis* Ortega-Blanco, McKellar & Engel**

http://bioguid.osu.edu/xbiod_concepts/352921

Proterosceliopsis Ortega-Blanco, McKellar & Engel, 2014: 554 (original description.

Type: *Proterosceliopsis masneri* Ortega-Blanco, McKellar & Engel, by monotypy and original designation. Diagnosis); Talamas, Johnson, Buffington and Ren 2017: 251, 253 (description, keyed).

Diagnosis. See family diagnosis.

Description. Head: Facial striae: absent. Malar sulcus: present. Malar striae: absent. Orbital carina: absent. Setation of compound eye: absent. Torulus: opening anteriorly. Frontal ledge: absent. OOL: lateral ocellus separated from compound eye by less than one ocellar diameter. Macrosculpture of head: absent. Hyperoccipital carina: absent. Occipital carina: present, continuous dorsally and ventrally extending to posterior articulation of the mandible.

Mesosoma: Propleural epicoxal sulcus: absent. Posterolateral corner of propleuron: strongly pointed. Pronotal cervical sulcus: furrow of dense fine setae. Epomial carina: absent. Transverse pronotal carina: absent. Antero-admedian lines: absent. Macrosculpture of mesosoma: absent. Orientation of notauli: converging posteriorly. Mesoscutal humeral sulcus: indicated by smooth furrow. Posterior mesoscutellar sulcus: foveate. Sculpture of metanotal trough: foveate. Metascutellum: undifferentiated from metanotal trough. Ventral mesopleural furrow: present. Ventral mesopleural carina: present. Mesopleural carina: absent. Anterior mesepisternal area: absent. Episternal foveae: absent. Transepisternal line: present. Mesopleural pit: absent. Prespecular sulcus: absent. Mesepimeral sulcus: present. Metapleural carina: present. Ventral metapleural area: convex and without macrosculpture. Dorsal metapleural area: convex and without macrosculpture. Ventral surface of metapleuron: setose. Sculpture of dorsal propodeum: coarsely rugose. Setal patch on anterodorsal surface of hind coxa: present.

Fore Wing: submarginal (Sc+R), marginal (C+R), postmarginal (R1) and stigmal vein (r) present; C extending proximally past bulla; 1Rs short and nebulous; 2Rs sclerotized and extending to wing margin. Basal vein (Rs+M) and M+Cu nebulous to weakly sclerotized. Median vein (M) present as a nebulous line in distal portion of the wing; tibial spur formula: 1-2-2.

Metasoma: T1–T5 with depressions anteriorly (unclear in *P. masneri*); S1–S5 with depressions anteriorly; 6–7 visible tergites when ovipositor not extruded. T7+T8 extruded with ovipositor system (based on *P. ambulata*).

Distribution. The presence of *Proterosceliopsis* in Burmese and Álava (Spain) amber indicates that this was a widespread genus.

Comments. Our generic description of *Proterosceliopsis* is based largely on specimens from Burmese amber, which provide far greater detail than the original description, and the two descriptions are congruent as far as can be observed. However, it should be noted that depressions along the anterior margin of the metasomal tergites in *Proterosceliopsis masneri* are not mentioned or illustrated in Ortega-Blanco et al. (2014). In their photographs of the dorsal habitus (Fig. 6A–B) it is unclear if these depressions are present. In cases where exudate is absent, photography of these depressions can be difficult, particularly in darkly colored specimens and when the amber is turbid.

Key to species of *Proterosceliopsis* (females)

- | | | |
|---|--|--|
| 1 | Antenna with 15 antennomeres..... | <i>P. plurima</i> Talamas, Shih & Ren, sp. nov. |
| – | Antenna with 14 antennomeres | 2 |
| 2 | T1 with horn (Fig. 58)..... | 3 |
| – | T1 without horn (Figs 29, 48, 62) | 4 |
| 3 | T6 distinctly the longest tergite (Fig. 58) | |
| | | <i>P. torquata</i> Talamas, Shih & Ren, sp. nov. |
| – | T1–T6 approximately equal in length..... | |
| | | <i>P. masneri</i> Ortega-Blanco, McKellar & Engel |
| 4 | T1 evenly convex and without macrosculpture or raised area (Figs 48, 50); antenna with 7 clavomeres; A7 distinctly transverse (Fig. 49)..... | |
| | | <i>P. ambulata</i> Talamas, Shih & Ren, sp. nov. |
| – | T1 medially with raised area of longitudinal striation (Fig. 29); antenna with more than 7 clavomeres; A7 about as long as wide (Figs 5–6) | 5 |
| 5 | Antennae with 9 clavomeres (Fig. 5); T2 without striae posterior to transverse sulcus (Fig. 29) | <i>P. nigon</i> Talamas, Shih & Ren, sp. nov. |
| – | Antennae with 8 clavomeres (Fig. 6); anteromedial T2 with longitudinal striae posterior to transverse sulcus (Fig. 62) | |
| | | <i>P. wingerathi</i> Talamas, Shih & Ren, sp. nov. |

***Proterosceliopsis ambulata* Talamas, Shih & Ren, sp. nov.**<http://zoobank.org/96EBF28B-6654-48F5-8FD0-AE1B106985F3>http://bioguid.osu.edu/xbiod_concepts/451148

Figures 45, 48–50

Diagnosis. *Proteroscelio ambulata* shares with *P. wingerathi*, *P. nigon* and *P. masneri* the roughly equal lengths of metasomal segments 1–6. It can be separated from all of these by the evenly convex form of T1, which has a horn in *P. masneri* and an anteromedian area of prominent striae in *P. nigon* and *P. wingerathi*.

Description. Head: Number of antennomeres in female: 14. Number of clavomeres in female: 7. Claval formula in female: 1-2-2-2-2-2. Number of mandibular teeth: 3. Number of labial palpomeres: not visible. Number of maxillary palpomeres: not visible. Shape of clypeus: narrow, transverse. Central keel: absent. Antennal scrobe: undifferentiated sculpturally from remainder of frons. Anterior margin of occipital carina: simple.

Mesosoma: Pronotal prespiracular depression: present, without striation. Netrion: absent. Skaphion: present. Posterior notaulus: reaching posterior margin of mesoscutum. Width of notaulus: expanding posteriorly. Parapsidal lines: absent. Mesoscutal suprahumeral sulcus: indicated by smooth furrow. Scutoscutellar sulcus: simple. Postacetabular carina: absent. Postacetabular sulcus: absent. Mesopleural epicoxal sulcus: present. Episternal foveae: absent. Metapleural sulcus: present as a transverse furrow. Lateral propodeal carina: present laterally as two small posteriorly-pointing projections.

Metasoma: Horn on T1 in female: absent. Sculpture of T1: weakly longitudinally striate throughout. Macrosculpture of T2–T5: absent. Anterior tergal depressions: visible on T1–T6. Median keel on S2: absent. Macrosculpture of S3–S6: absent. Anterior sternal depressions: visible on S1–S6.

Etymology. This species is given the name “ambulata” because the holotype specimen appears to be walking.

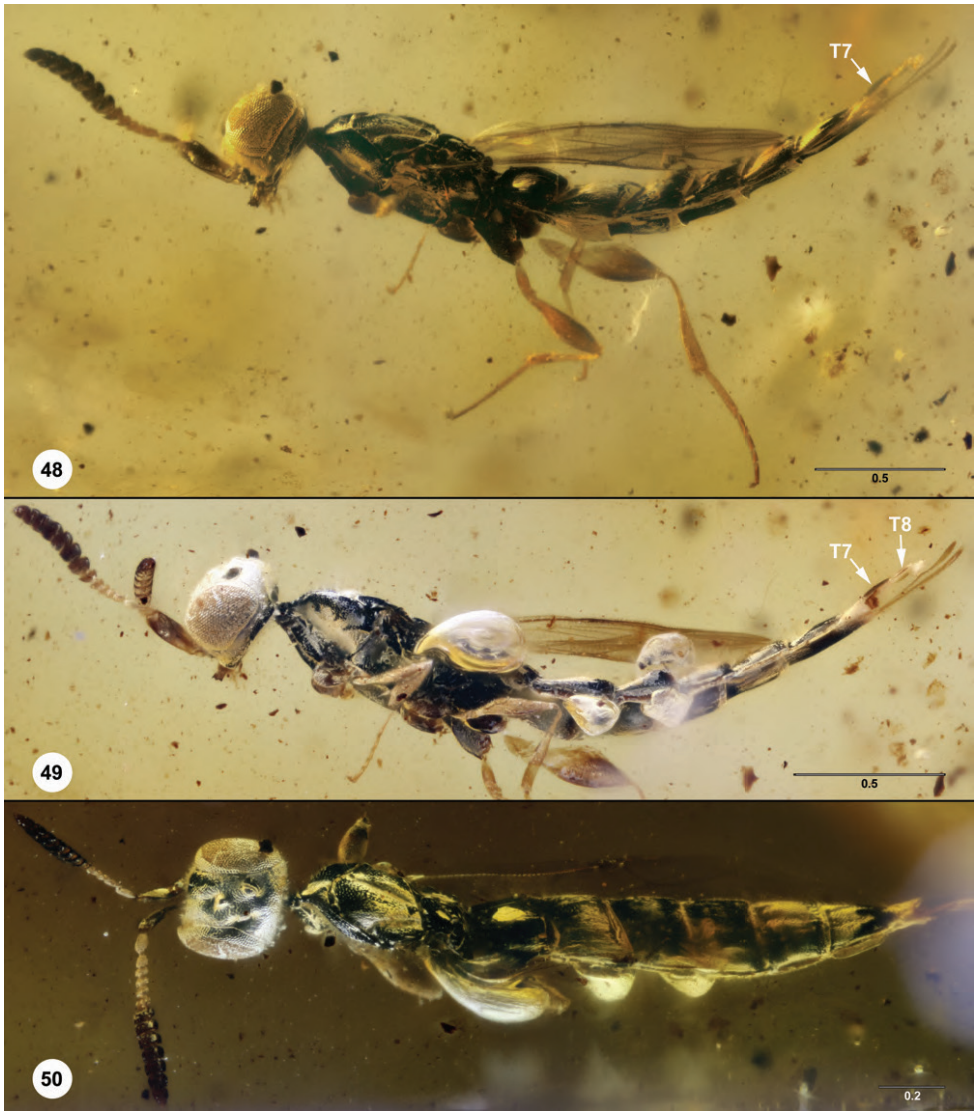
Link to distribution map. [<http://hol.osu.edu/map-large.html?id=451148>]

Material examined. Holotype female: **MYANMAR:** CNU-HYM-MA-2016105 (deposited in CNU).

***Proterosceliopsis masneri* Ortega-Blanco, McKellar & Engel**http://bioguid.osu.edu/xbiod_concepts/352922

Proterosceliopsis masneri Ortega-Blanco, McKellar & Engel, 2014: 555, 568 (original description, diagnosis, keyed).

Comments. *Proterosceliopsis masneri* may eventually be considered a *nomen dubium* as a species due to the paucity of detailed information on its morphology. The study of additional material from Álava amber is needed to clarify characters on this species, particularly the lateral mesosoma and structures on the anterior portions of the metasomal segments.



Figures 48–50. *Proterosceliopsis ambulata* (CNU-HYM-MA-2016105) **48** habitus, lateral view (left side) **49** habitus, lateral view (right side) **50** head, mesosoma, metasoma, dorsal view. Scale bars in millimeters.

***Proterosceliopsis nigon* Talamas, Shih & Ren, sp. nov.**

<http://zoobank.org/79232690-93E4-4F06-8157-76573017F84A>

http://bioguid.osu.edu/xbiod_concepts/463679

Figures 5, 29, 34

Diagnosis. *Proterosceliopsis nigon* is most similar to *P. wingerathi*, from which it can be separated by having 9 clavomeres and T2 without striation posterior to the transverse anterior depressions.

Description. Head: Number of antennomeres in female: 14. Number of clavomeres in female: 9. Claval formula in female: 1-2-2-2-2-2-2-2. Number of mandibular teeth: not visible. Number of labial palpomeres: not visible. Number of maxillary palpomeres: at least 5. Shape of clypeus: narrow, transverse. Central keel: absent. Antennal scrobe: indicated by faint transverse rugae. Anterior margin of occipital carina: crenulate.

Mesosoma: Pronotal prespiracular depression: present, without striation. Netrion: absent. Skaphion: present. Posterior notaulus: not reaching posterior margin of mesoscutum. Width of notaulus: expanding posteriorly. Parapsidal lines: present. Mesoscutal suprahumeral sulcus: simple, without furrow or cells. Scutoscutellar sulcus: crenulate. Postacetabular carina: present directly posterior to acetabulum. Postacetabular sulcus: present as simple furrow. Mesopleural epicoxal sulcus: present. Metapleural sulcus: present as a transverse furrow. Lateral propodeal carina: present and continuous dorsally, forming lamella surrounding metasomal depression, medial portion raised and projecting dorsally. Metasomal depression: excavate, interior surface with striae dorsomedially.

Metasoma: Horn on T1 in female: absent. Sculpture of T1: longitudinally striate medially. Macrosculpture of T2–T5: absent. Anterior tergal depressions: visible on T1–T6. Median keel on S2: absent. Macrosculpture of S3–S6: longitudinal median carina on S3–S4, otherwise absent. Anterior sternal depressions: visible on S1–S6.

Etymology. This word “nigon” is Anglo-Saxon for “nine”, referring to the number of clavomeres in this species, and is treated as a noun in apposition.

Link to distribution map. [<http://hol.osu.edu/map-large.html?id=463679>]

Material examined. Holotype female: **MYANMAR:** CNU-HYM-MA-2017566 (deposited in CNU). *Other material:* (1 female) **MYANMAR:** OPPC1718 (deposited in OPPC).

***Proterosceliopsis plurima* Talamas, Shih & Ren, sp. nov.**

<http://zoobank.org/8FBDF6FE-3BDC-499E-BDBF-BAF63B63943D>

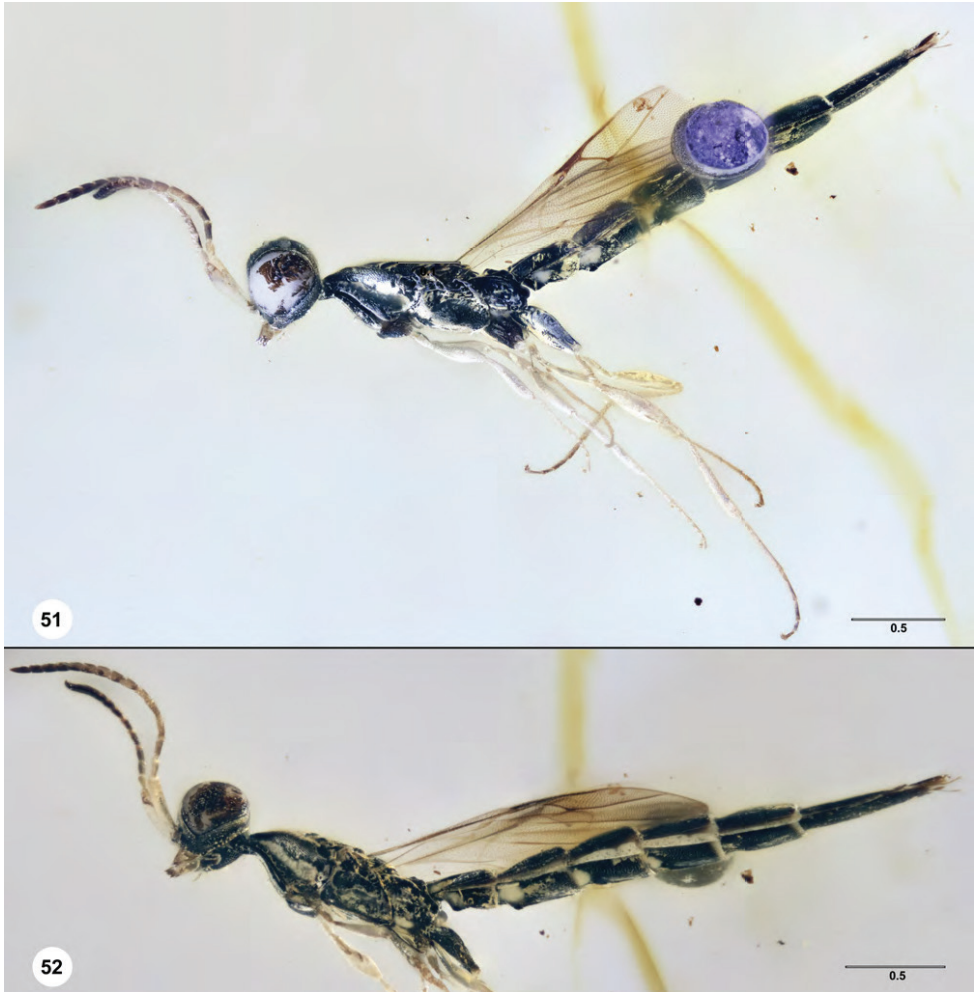
http://bioguid.osu.edu/xbiод_concepts/451147

Figures 3, 7, 16, 51–57

Diagnosis. The number of antennomeres in this species, 15, provides a simple means of separating it from other members of the genus. In *P. plurima* and *P. torquata* the 6th metasoma tergites and sternites are distinctly the longest. In the absence of antennal characters, these species can be separated on the form of the notaulus, which expands in width posteriorly in *P. plurima* and is of uniform width in *P. torquata*.

Description. Head: Number of antennomeres in female: 15. Number of clavomeres in female: 9. Claval formula in female: 1-2-2-2-2-2-2-1. Number of mandibular teeth: 3 on right mandible, 2 on left mandible. Number of labial palpomeres: not visible. Number of maxillary palpomeres: 4. Shape of clypeus: narrow, transverse. Central keel: present. Antennal scrobe: indicated by transverse rugae. Anterior margin of occipital carina: crenulate.

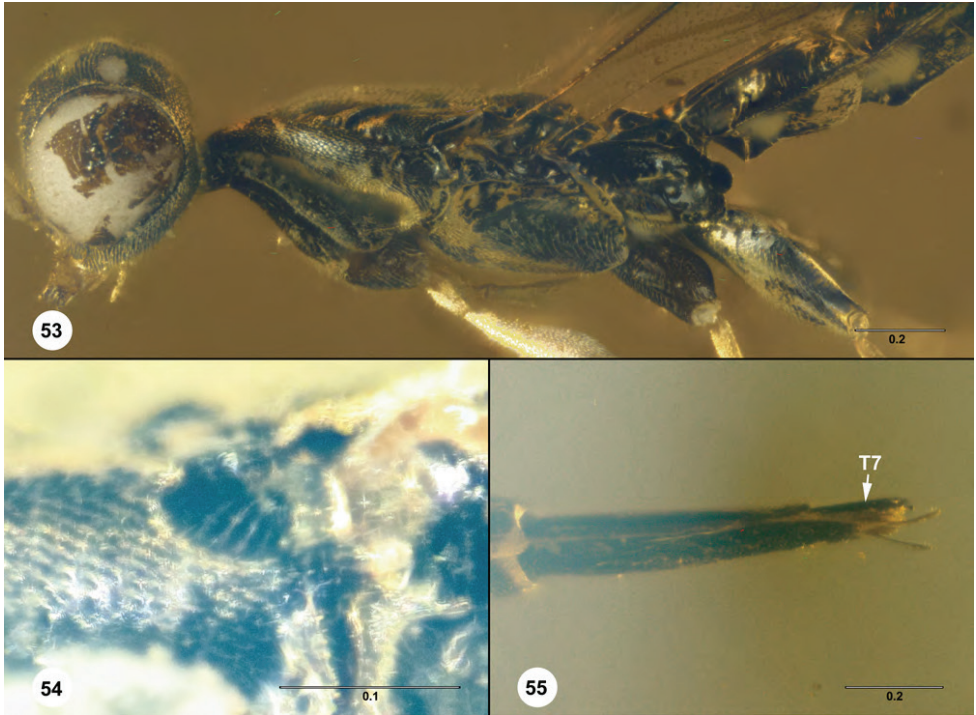
Mesosoma: Pronotal prespiracular depression: present, striate. Netrion: present. Skaphion: absent. Posterior notaulus: not reaching posterior margin of mesoscu-



Figures 51, 52. *Proterosceliopsis plurima* (CNU-HYM-MA-2016102) **51** habitus, lateral view (right side) **52** habitus, lateral view (left side). Scale bars in millimeters.

tum. Width of notaulus: expanding posteriorly. Parapsidal lines: absent. Mesoscutal suprahumeral sulcus: indicated by short line of cells. Scutoscutellar sulcus: simple. Postacetabular carina: present as short ridge laterally, carinae not meeting medially. Postacetabular sulcus: present as simple furrow. Mesopleural epicoxal sulcus: present. Episternal foveae: absent. Metapleural sulcus: present, anterodorsal portion comprised of cells. Lateral propodeal carina: present and continuous dorsally, forming lamella surrounding metasomal depression.

Metasoma: Horn on T1 in female: absent. Sculpture of T1: longitudinally striate medially. Macrosculpture of T2–T5: longitudinal median carina on T2 and T3, otherwise absent. Anterior tergal depressions: visible on T1–T6. Median keel on S2: present. Macrosculpture of S3–S6: longitudinal median carina on S3–S4, otherwise absent. Anterior sternal depressions: visible on S1–S5.



Figures 53–55. *Proterosceliopsis plurima* (CNU-HYM-MA-2016102) **53** head, mesosoma, anterior metasoma, lateral view (right side) **54** posterodorsal pronotum, lateral view **55** distal segments of metasoma, lateral view. Scale bars in millimeters.



Figures 56, 57. *Proterosceliopsis plurima* (CNU-HYM-MA-2016102) **56** habitus, dorsal view **57** head and mesosoma, ventral view. Scale bars in millimeters.

Etymology. The epithet “*plurima*”, meaning “abundant” or “numerous”, refers to the number of antennomeres in this species, which is the greatest known in Platygastroidea.

Link to distribution map. [<http://hol.osu.edu/map-large.html?id=451147>]

Material examined. Holotype female: **MYANMAR:** CNU-HYM-MA-2016102 (deposited in CNU).

Comments. The number of clavomeres is here coded as 9, a basiconic sensillum on A15 is visible, as are paired sensilla on A14–A8

***Proterosceliopsis torquata* Talamas, Shih & Ren, sp. nov.**

<http://zoobank.org/E0A610BA-26A4-4BBA-96F2-3EA25A202E59>

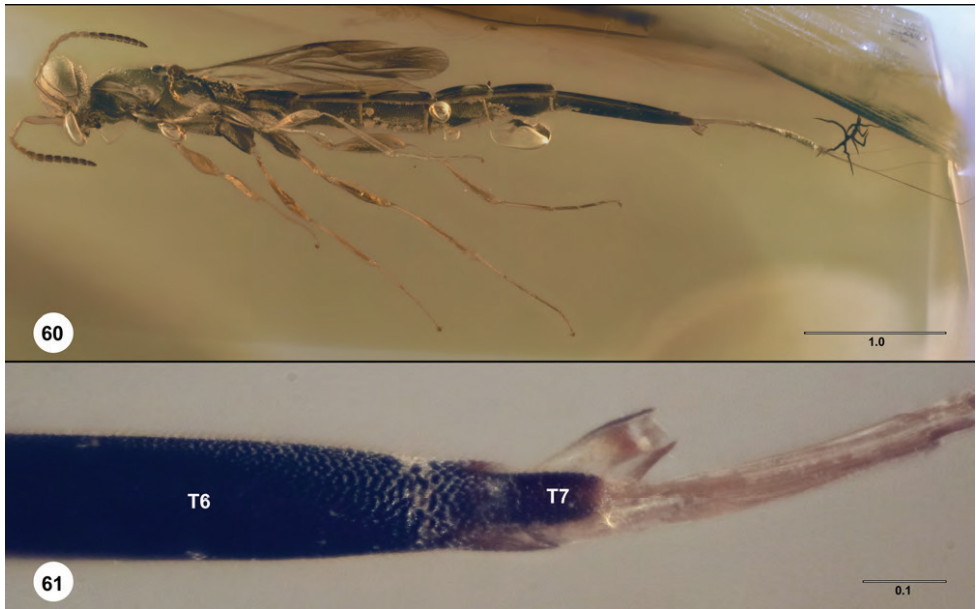
http://bioguid.osu.edu/xbiod_concepts/426419

Figures 11, 15, 58–61

Diagnosis. *Proterosceliopsis torquata* is most similar to *P. plurima*, with which it shares an elongate habitus, and having the 6th metasomal segment distinctly the longest. These



Figures 58, 59. *Proterosceliopsis torquata* (CNU-HYM-MA-2016106) **58** habitus, dorsolateral view **59** head and mesosoma, lateral view. Scale bars in millimeters.



Figures 60, 61. *Proterosceliopsis torquata* (CNU-HYM-MA-2016106) **60** habitus, ventrolateral view **61** distal segments of metasoma, dorsal view. Scale bars in millimeters.

can be separated by the presence of the horn on T1 in *P. torquata* (absent in *P. plurima*); the posteriorly expanded notauli in *P. plurima* (of uniform width in *P. torquata*), and by the number of antennomeres: 14 in *P. torquata* and 15 in *P. plurima*.

Description. Head: Number of antennomeres in female: 14. Number of clavomeres in female: 8. Claval formula in female: 1-2-2-2-2-2-1. Number of mandibular teeth: not visible. Number of labial palpomeres: at least 2. Number of maxillary palpomeres: at least 5. Shape of clypeus: not visible. Central keel: present. Antennal scrobe: indicated by transverse rugae. Anterior margin of occipital carina: crenulate.

Mesosoma: Pronotal prespiracular depression: present, without striation. Netrion: present. Skaphion: present. Posterior notaulus: not reaching posterior margin of mesoscutum. Width of notaulus: uniform. Parapsidal lines: present. Mesoscutal suprahumeral sulcus: indicated by smooth furrow. Scutoscutellar sulcus: simple. Postacetabular carina: present as short ridge laterally, carinae not meeting medially. Postacetabular sulcus: present as simple furrow. Mesopleural epicoxal sulcus: present. Episternal foveae: absent. Metapleural sulcus: present as a transverse furrow. Lateral propodeal carina: present and continuous dorsally, forming lamella surrounding metasomal depression. Metasomal depression: deeply excavate, interior surface smooth.

Metasoma: Horn on T1 in female: present. Sculpture of T1: longitudinally striate medially. Macrosculpture of T2–T5: longitudinal median carina on anterior T2 and T3, otherwise absent. Anterior tergal depressions: visible on T1–T5. Median keel on S2: present. Macrosculpture of S3–S6: absent. Anterior sternal depressions: visible on S1–S6.

Etymology. The Latin adjectival epithet “torquata”, meaning “adorned with a necklace or collar”, is given to this species for the collar-like shape of the pronotum in dorsal view.

Link to distribution map. [<http://hol.osu.edu/map-large.html?id=426419>]

Material examined. Holotype female: **MYANMAR:** CNU-HYM-MA-2016106 (deposited in CNU). *Other material:* (1 female) **MYANMAR:** OPPC1801 (deposited in OPPC).

***Proterosceliopsis wingerathi* Talamas, Shih & Ren, sp. nov.**

<http://zoobank.org/B2655449-13F3-42BE-A67B-2562D53CB003>

http://bioguid.osu.edu/xbiod_concepts/451152

Figures 6, 62–64

Diagnosis. *Proterosceliopsis wingerathi* is most similar to *P. nigon*, from which it can be separated by having eight clavomeres and the presence of longitudinal striation in the anteromedial portion of T2.

Description. Head: Number of antennomeres in female: 14. Number of clavomeres in female: 8. Claval formula in female: 1-2-2-2-2-2-1. Number of mandibular teeth: 3 on right mandible. Number of labial palpomeres: not visible. Number of maxillary palpomeres: at least 5. Shape of clypeus: narrow, transverse, medially concave. Central keel: absent. Antennal scrobe: undifferentiated sculpturally from remainder of frons. Anterior margin of occipital carina: crenulate.

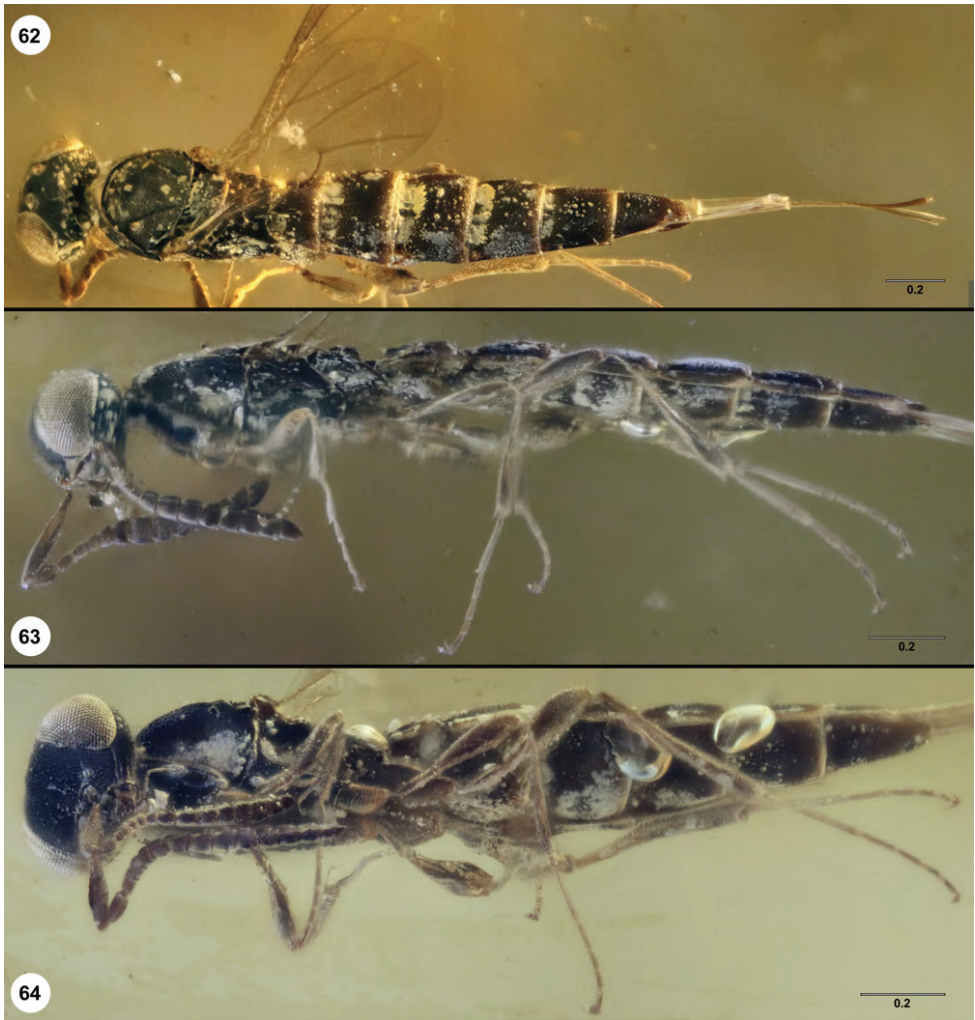
Mesosoma: Pronotal prespiracular depression: present, without striation. Netrion: present. Skaphion: present. Posterior notaulus: not reaching posterior margin of mesoscutum. Width of notaulus: uniform. Parapsidal lines: present. Mesoscutal suprahumeral sulcus: indicated by smooth furrow. Scutoscutellar sulcus: crenulate. Postacetabular carina: absent. Postacetabular sulcus: absent. Episternal foveae: absent. Metapleural sulcus: present as a transverse furrow. Lateral propodeal carina: present and continuous dorsally, forming lamella surrounding metasomal depression. Metasomal depression: excavate, interior surface with striae dorsomedially.

Metasoma: Horn on T1 in female: absent. Sculpture of T1: longitudinally striate medially. Macrosculpture of T2–T5: anteromedial T2 longitudinally striate, otherwise absent. Anterior tergal depressions: visible on T1–T6. Median keel on S2: absent. Macrosculpture of S3–S6: absent. Anterior sternal depressions: visible on S1–S6.

Etymology. This species is named for Jonathan Wingerath, Deputy Collections Manager for Paleobotany at the National Museum of Natural History, Washington, DC, to express our thanks for contributing his time and skills in preparing amber specimens for this and other projects.

Link to distribution map. [<http://hol.osu.edu/map-large.html?id=451152>]

Material examined. Holotype female: **MYANMAR:** CNU-HYM-MA-2016101 (deposited in CNU).



Figures 62–64. *Proterosceliopsis wingerathi* (CNU-HYM-MA-2016101) **62** habitus, dorsal view **63** habitus, lateral view **64** habitus, ventrolateral view. Scale bars in millimeters.

Comments on Cretaceous Platygastriidae

The specimen illustrated in Figures 65–66 is the oldest representative of Platygastriidae known to us. It complies with the current and historical concepts of the family: 10-merous antennae; T2 as the largest tergite; malar sulcus absent; pronotal cervical sulcus is a furrow with what appears to be solidified exudate; transepisternal line present (not clear in photographs); S1 and anterior S2 with setal patches. Perhaps most interesting, this specimen has marginal, stigmal and (short) postmarginal veins, as in *Orwellium enigmaticum* Johnson, Masner & Musetti, which Johnson et al. (2009) considered to be the sister to the rest of Platygastriidae. This specimen is not sufficiently



Figures 65, 66. Platygastriidae, female (KU-NHM-ENT Bu-007) **65** head, mesosoma, metasoma, dorso-lateral view **66** head, mesosoma, metasoma, ventrolateral view. Insets are portions of image that have had the color altered to emphasize wing venation. Scale bars in millimeters.

well preserved to be described at the species level, but we consider it relevant to this paper because it supports our contention that the transepisternal line and glandular nature of the pronotal cervical sulcus are plesiomorphies for Platygastriidae.

Acknowledgements

We are grateful to Jonathan Wingerath (USNM), Minyue Ren, Huijia Cao, and Bingyu Zheng (CNU) for cutting and polishing amber. Lubomír Masner (CNCI) provided insightful discussion. Michael Engel generously provided a loan of Burmese

amber to EJT, including platygastriid specimen KU-NHM-ENT Bu-007, and facilitated examination of Lebanese amber. Former Smithsonian interns Dylan Johnston-Jordan, Melanie Anderson, Luke Kresslein, Anthony Cuminale, Colin Schwantes and Cate Paxton contributed many of the scanning electron micrographs. Ovidiu Popovici (“A.I. Cuza” University, Faculty of Biology, Iasi, Romania) provided images that enabled species determination of two female specimens in his collection. We thank the Florida Department of Agriculture and Consumer Services – Division of Plant Industry for their support on this contribution. This research was supported by the National Natural Science Foundation of China (No. 31730087 and 31672323), the Program for Changjiang Scholars and Innovative Research Team in University (grant number IRT-17R75), and Project of High-level Teachers in Beijing Municipal Universities (grant number IDHT20180518).

References

- Austin AD, Field SA (1997) The ovipositor system of scelionid and platygastriid wasps (Hymenoptera: Platygastroidea): comparative morphology and phylogenetic implications. *Invertebrate Taxonomy* 11: 1–87. <https://doi.org/10.1071/IT95048>
- Austin AD, Johnson NF, Downton M (2005) Systematics, evolution, and biology of scelionid and platygastriid wasps. *Annual Review of Entomology*, 50: 553–582. <https://doi.org/10.1146/annurev.ento.50.071803.130500>
- Bin F (1981) Definition of female antennal clava based on its plate sensilla in Hymenoptera Scelionidae Telenominae. *Redia* 64: 245–261.
- Chen S, Yin XC, Lin XD, Shih CK, Zhang RZ, Gao TP, Ren D (2018) Stick insect in Burmese amber reveals an early evolution of lateral lamellae in the Mesozoic. *Proceedings of the Royal Society B*, 285(1877): 20180425. <https://doi.org/10.1098/rspb.2018.0425>
- Chen S, Deng SW, Shih CK, Zhang WW, Zhang P, Ren D, Zhu YN, Gao TP (2018) The earliest Timematids in Burmese amber reveal diverse tarsal pads of stick insects in the mid-Cretaceous. *Insect Science* 2018: 1–13. <https://doi.org/10.1111/1744-7917.12601>
- Cruikshank RD, Ko K (2003) Geology of an amber locality in the Hukawng Valley, Northern Myanmar. *Journal of Asian Earth Sciences* 21: 441–455. [https://doi.org/10.1016/S1367-9120\(02\)00044-5](https://doi.org/10.1016/S1367-9120(02)00044-5)
- Hagedorn G, Catapano T, Güntsch A, Mietchen D, Endresen D, Sierra S, Groom Q, Biserkov J, Glöckler F, Morris R (2013) Best practices for stable URIs.
- Johnson NF, Masner L (2006) Revision of world species of the genus *Nixonia* Masner (Hymenoptera: Platygastroidea, Scelionidae). *American Museum Novitates* 3518: 1–32. [https://doi.org/10.1206/0003-0082\(2006\)3518\[1:ROWSOT\]2.0.CO;2](https://doi.org/10.1206/0003-0082(2006)3518[1:ROWSOT]2.0.CO;2)
- Johnson NF, Masner L, Musetti L (2008a) Review of Genera of the Tribe Sparasionini (Hymenoptera: Platygastroidea, Scelionidae), and Description of Two New Genera from the New World. *American Museum Novitates* 3629: 1–24. <https://doi.org/10.1206/578.1>

- Johnson NF, Masner L, Musetti L, van Noort S, Rajmohana K, Darling DC, Guidotti A, Polaszek A (2008b) Revision of world species of the genus *Heptascelio* Kieffer (Hymenoptera: Platygastroidea, Platygastriidae). *Zootaxa* 1776:1–51. <https://doi.org/10.3897/zookeys.6.67>
- Johnson NF, Masner L, Musetti L (2009) *Orwellium*, a new genus of Valdivian Platygastriidae (Hymenoptera). *ZooKeys*, 20: 21–30. <https://doi.org/10.3897/zookeys.20.204>
- Li L, Rasnitsyn AP, Shih CK, Labandeira CC, Buffington ML, Li D, Ren D (2018) Phylogeny of Evanioidea (Hymenoptera, Apocrita), with descriptions of new Mesozoic species from China and Myanmar. *Systematic Entomology* 43: 810–842. <https://doi.org/10.1111/syen.12315>
- Masner L (1976) Revisionary notes and keys to world genera of Scelionidae (Hymenoptera: Proctotrupeoidea). *Memoirs of the Entomological Society of Canada* 97: 1–87. <https://doi.org/10.4039/entm10897fv>
- Masner L, Huggert L (1989) World review and keys to genera of the subfamily Inostemmatinae with reassignment of the taxa to the Platygastriinae and Sceliotrachelinae (Hymenoptera: Platygastriidae). *Memoirs of the Entomological Society of Canada* 147: 1–214. <https://doi.org/10.4039/entm121147fv>
- Masner L, Johnson NF, Polaszek A (2007) Redescription of *Archaeoscelio* Brues and description of three new genera of Scelionidae (Hymenoptera): a challenge to the definition of the family. *American Museum Novitates*. 3550: 1–24. [https://doi.org/10.1206/0003-0082\(2007\)3550\[1:ROABAD\]2.0.CO;2](https://doi.org/10.1206/0003-0082(2007)3550[1:ROABAD]2.0.CO;2)
- Masner L, Johnson NF (2007) *Janzenella*, an enigmatic new genus of scelionid wasp from Costa Rica (Hymenoptera: Platygastroidea, Scelionidae). *American Museum Novitates*, 3574: 1–7. [https://doi.org/10.1206/0003-0082\(2007\)3574\[1:JAENGO\]2.0.CO;2](https://doi.org/10.1206/0003-0082(2007)3574[1:JAENGO]2.0.CO;2)
- McKellar RC, Engel MS (2012) Hymenoptera in Canadian Cretaceous amber (Insecta). *Cretaceous Research*, 35: 258–279. <https://doi.org/10.1016/j.cretres.2011.12.009>
- Mikó I, Vilhelmsen L, Johnson NF, Masner L, Péntzes Z (2007) Skeletomusculature of Scelionidae (Hymenoptera: Platygastroidea): head and mesosoma. *Zootaxa*, 1571:1–78. <https://doi.org/10.11646/zootaxa.1571.1.1>
- Murphy NP, Carey D, Castro LR, Downton M, Austin AD (2007) Phylogeny of the platygastroid wasps (Hymenoptera) based on sequences from the 18S rRNA, 28S rRNA and cytochrome oxidase I genes: implications for the evolution of the ovipositor system and host relationships. *Biological Journal of the Linnean Society* 91: 653–669. <https://doi.org/10.1111/j.1095-8312.2007.00825.x>
- Ortega-Blanco J, McKellar RC, Engel MS (2014) Diverse scelionid wasps in Early Cretaceous amber from Spain (Hymenoptera: Platygastroidea). *Bulletin of Geosciences* 89: 553–571. <https://doi.org/10.3140/bull.geosci.1463>
- Popovici OA, Vilhelmsen L, Masner L, Mikó I, Johnson N (2017) Maxillolabial complex in scelionids (Hymenoptera: Platygastroidea): morphology and phylogenetic implications. *Insect Systematics & Evolution* 48: 315–439. <https://doi.org/10.1163/1876312X-48022156>
- Sharkey MJ (2007) Phylogeny and classification of Hymenoptera. *Zootaxa* 1668: 521–548.

- Shi G, Grimaldi DA, Harlow GE, Wang J, Wang J, Yang MC, Lei WY, Li XH (2012) Age constraint on Myanmar amber based on U–Pb dating of zircons. *Cretaceous Research* 37: 155–163. <https://doi.org/10.1016/j.cretres.2012.03.014>
- Talamas E, Masner L (2016) Revision of New World *Helava* Masner & Huggert (Platygastridae, Sceliotrachelinae). *Journal of Hymenoptera Research* 53: 1–24. <https://doi.org/10.3897/jhr.53.10217>
- Talamas EJ, Johnson NF, Buffington ML, Dong R (2017a) *Archaeoteleia* Masner in the Cretaceous and a new species of *Proteroscelio* Brues (Hymenoptera, Platygastroidea). In: Talamas EJ, Buffington ML (Eds) *Advances in the Systematics of Platygastroidea*. *Journal of Hymenoptera Research* 56: 241–261. <https://doi.org/10.3897/jhr.56.10388>
- Talamas EJ, Mikó I, Johnston-Jordan D (2017b) Convergence in the ovipositor system of platygastroid wasps (Hymenoptera). In: Talamas EJ, Buffington ML (Eds) *Advances in the Systematics of Platygastroidea*. *Journal of Hymenoptera Research* 56: 263–276. <https://doi.org/10.3897/jhr.56.12300>
- Valerio AA, Masner L, Austin AD, Johnson NF (2009) The genus *Neuroscelio* Dodd (Hymenoptera: Platygastridae s.l.) reviewed: new species, distributional update, and discussion of relationships. *Zootaxa*. 2306: 29–43.
- Vilhelmsen L, Mikó I, Krogmann L (2010) Beyond the wasp-waist: structural diversity and phylogenetic significance of the mesosoma in apocritan wasps (Insecta: Hymenoptera). *Zoological Journal of the Linnean Society* 159: 22–194. <https://doi.org/10.1111/j.1096-3642.2009.00576.x>
- Walker JD, Geissman JW, Bowring SA, Babcock LE (2012) The Geological Society of America time scale. *Bulletin of the Geological Society of America* 125: 259–272. <https://doi.org/10.1130/B30712.1>
- Wang M, Rasnitsyn AP, Li H, Shih CK, Sharkey MJ, Ren D (2016) Phylogenetic analyses elucidate the inter-relationships of Pamphilioidea (Hymenoptera, Symphyta). *Cladistics* 32: 239–260. <https://doi.org/10.1111/cla.12129>
- Yoder MJ, Mikó I, Seltmann K, Bertone MA, Deans AR (2010) A gross anatomy ontology for Hymenoptera. *PLoS ONE* 5(12): e15991. <https://doi.org/10.1371/journal.pone.0015991>
- Yoder MJ, Valerio AA, Polaszek A, van Noort S, Masner L, Johnson NF (2014) Monograph of the Afrotropical species of *Scelio* Latreille (Hymenoptera, Platygastridae), egg parasitoids of acridid grasshoppers (Orthoptera, Acrididae). *ZooKeys* 380: 1–188. <https://doi.org/10.3897/zookeys.380.5755>
- Zhang Q, Rasnitsyn AP, Wang B, Zhang H (2018) Hymenoptera (wasps, bees, and ants) in mid-Cretaceous Burmese amber: A review of the fauna. *Proceedings of the Geologists' Association* 129: 736–747. <https://doi.org/10.1016/j.pgeola.2018.06.004>
- Zhang WT, Li H, Shih CK, Zhang AB, Ren D (2018) Phylogenetic analyses with four new Cretaceous bristletails reveal inter-relationships of Archaeognatha and Gondwana origin of Meinertellidae. *Cladistics* 34: 384–406. <https://doi.org/10.1111/cla.12212>

Appendix I

asdasd

Term	Concept	URI	Preferred Term
T8	The tergum that is located on abdominal segment 8.	http://purl.obolibrary.org/obo/HAO_0000061	abdominal tergum 8
acetabulum	The scrobe that is located anteroventrally on the mesopsectus and accommodates the procoxa.	http://purl.obolibrary.org/obo/HAO_0000294	epinemium
antenna	The appendage that is composed of ringlike sclerites and the anatomical structures encircled by these sclerites and that is articulated with the cranium.	http://purl.obolibrary.org/obo/HAO_0000101	antenna
antennal scrobe	The scrobe that is located dorsally of the antennal foramen and is for the reception of the antenna.	http://purl.obolibrary.org/obo/HAO_0001432	antennal scrobe
antennomere	The anatomical structure that is delimited by the proximal and distal margins of the antennal sclerite.	http://purl.obolibrary.org/obo/HAO_0000107	antennomere
anterior mesepisternal area	The area delimited anteriorly by the pronotal-mesoplectal suture, posterodorsally by the ventral limit of the subacropleurial sulcus, and posteroventrally by the episternal foveal line.	http://purl.obolibrary.org/obo/HAO_0002459	anterior mesepisternal area
anterior thoracic spiracle	The spiracle that is located on the border of the pronotum and mesopleuron.	http://purl.obolibrary.org/obo/HAO_0000582	anterior thoracic spiracle
antepitracular scutal patch	The setiferous patch that is located just anteriorly of the anterior thoracic spiracle.	http://purl.obolibrary.org/obo/HAO_0001985	antepitracular scutal patch
basal vein	The wing vein that is basally located on the fore wing and connects or nearly connects the submarginal vein and the medial plus cubital veins.	http://purl.obolibrary.org/obo/HAO_0000170	basal vein
bullula	The anatomical region of the wing vein that is less melanized and more flexible than surrounding anatomical wing vein regions and corresponds to the intersection of the wing vein with a flexion line.	http://purl.obolibrary.org/obo/HAO_0000184	bullula
carina	The process that is elongate and external.	http://purl.obolibrary.org/obo/HAO_0000188	carina
central keel	The frontal line that is a carina.	http://purl.obolibrary.org/obo/HAO_0001929	central keel
clava	The anatomical cluster that is composed of apical flagellomeres bearing multiporous plates in female organism.	http://purl.obolibrary.org/obo/HAO_0000203	clava
clypeus	The area that corresponds to the site of origin of the clypeo-epipharyngeal muscle.	http://purl.obolibrary.org/obo/HAO_0000212	clypeus
conjunctiva	The area of the cuticle that is weakly sclerotized, with thin exocuticle.	http://purl.obolibrary.org/obo/HAO_0000221	conjunctiva
costa	The wing vein that is anterior to the subcosta and is connected to the humeral plate.	http://purl.obolibrary.org/obo/HAO_0000225	costa
coxa	The leg segment that is connected to the body and to the trochanter via conjunctivae and muscles.	http://purl.obolibrary.org/obo/HAO_0000228	coxa
cubital vein	The longitudinal vein that is posterior to the marginal vein.	http://purl.obolibrary.org/obo/HAO_0000237	cubital vein
dorsal metapleurial area	The area that is delimited posterodorsally by the metapleurial carina and anteroventrally by the metapleurial sulcus.	http://purl.obolibrary.org/obo/HAO_0000261	dorsal metapleurial area
egg	.	http://purl.obolibrary.org/obo/HAO_0000286	egg
episternal foveae	The row of impressions that is located on the anteroventral edge of the mesopleuron and is correspond to the site of origin of the mesopleuro-mesobasalar muscle.	http://purl.obolibrary.org/obo/HAO_0001509	episternal foveae
eye	The compound organ that is composed of ommatidia.	http://purl.obolibrary.org/obo/HAO_0000217	eye

Term	Concept	URI	Preferred Term
facial striae	The anatomical cluster anterior to the malar sulcus that is composed of carinae radiating from the pleurotomial condyle.	http://purl.obolibrary.org/obo/HAO_0002376	facial striae
felt field	The setiferous patch that is located sublaterally on an abdominal sternum.	http://purl.obolibrary.org/obo/HAO_0000322	felt field
fore wing	The wing that is located on the mesothorax.	http://purl.obolibrary.org/obo/HAO_0000351	fore wing
frons	The area that is located dorsally of the ventral margin of the antennal rim and ventrally of the anterior ocellus medial to the inner margins of the eye and malar line.	http://purl.obolibrary.org/obo/HAO_0001044	upper face
frontal ledge	The edge that traverses the upper face between the antennal foramen and the median ocellus separating a more horizontal dorsal and a more vertical ventral area.	http://purl.obolibrary.org/obo/HAO_0001886	frontal ledge
head	The tagma that is located anterior to the thorax.	http://purl.obolibrary.org/obo/HAO_0000397	head
hyperocipital carina	The carina that extends on the vertex between the outer orbits.	http://purl.obolibrary.org/obo/HAO_0000406	hyperocipital carina
integument	The anatomical system that forms the covering layer of the animal, ectodermal in origin and composed of epidermal cells producing the cuticle.	http://purl.obolibrary.org/obo/HAO_0000421	integument
lateral ocellus	The ocellus that is paired.	http://purl.obolibrary.org/obo/HAO_0000481	lateral ocellus
lateral propodeal carina	The carina that arises submedially from the anterior margin of the metapleural-propodeal complex, is longitudinal and extends towards the propodeal foramen.	http://purl.obolibrary.org/obo/HAO_0001919	lateral propodeal carina
malar striae	The anatomical cluster posterior to the malar sulcus that is composed of carinae radiating from the pleurotomial condyle.	http://purl.obolibrary.org/obo/HAO_0002373	malar striae
malar sulcus	The sulcus that extends between the ventral margin of the compound eye and the base of the mandible.	http://purl.obolibrary.org/obo/HAO_0000504	malar sulcus
mandible	The appendage that is encircled by one sclerite that is connected to the cranium proximolaterally and to the maxillo-labial complex proximomedially via conjunctivae and articulates with the cranium via the anterior and posterior cranio-mandibular articulations.	http://purl.obolibrary.org/obo/HAO_0000506	mandible
margin	The line that delimits the periphery of an area.	http://purl.obolibrary.org/obo/HAO_0000510	margin
mesepimeral ridge	The ridge that extends along the posterior margin of the mesoplectus.	http://purl.obolibrary.org/obo/HAO_0000537	mesepimeral ridge
mesepimeral sulcus	The sulcus that extends along the posterior margin of the mesoplectus, delimits the mesepimeral area and corresponds to the mesepimeral ridge.	http://purl.obolibrary.org/obo/HAO_0000538	mesepimeral sulcus
mesopleural carina	The carina that crosses the mesopleuron and limits ventrally the femoral depression.	http://purl.obolibrary.org/obo/HAO_0000559	mesopleural carina
mesopleural epicoxal sulcus	The epicoxal sulcus that is located on the mesopleuron.	http://purl.obolibrary.org/obo/HAO_0000560	mesopleural epicoxal sulcus
mesopleural pit	The pleural pit that is located on the mesopleuron.	http://purl.obolibrary.org/obo/HAO_0000561	mesopleural pit
mesopleuron	The pleuron that is located in the mesothorax.	http://purl.obolibrary.org/obo/HAO_0001354	mesopleuron
mesoscutal humeral sulcus	The sulcus that extends medially along the parasutural carina and corresponds to a shallow ridge.	http://purl.obolibrary.org/obo/HAO_0000569	mesoscutal humeral sulcus
mesoscutal supra-humeral sulcus	The sulcus that extends along the anterior margin of the mesoscutum between the anterior-most point of the preaxilla and the anteromedian line and corresponds to the vertical lobe of the mesoscutum.	http://purl.obolibrary.org/obo/HAO_0000570	mesoscutal supra-humeral sulcus
mesoscutum	The scutum that is located on the mesonotum.	http://purl.obolibrary.org/obo/HAO_0000575	mesoscutum

Term	Concept	URI	Preferred Term
mesosoma	The anatomical cluster that is composed of the prothorax, mesothorax and the metapetal-propodeal complex.	http://purl.obolibrary.org/obo/HAO_0000576	mesosoma
metanotal trough	The area that is concave, and is delimited medially by the mesoscutellum, laterally by the supraalar area and posteriorly by the mesoscutellar arm.	http://purl.obolibrary.org/obo/HAO_0000600	metanotal trough
metapleural carina	The carina that delimits the metapleuron dorsally from the propodeum, extends from just ventral of the metapleural arm to the metacoxal articulation and passes anteroventral to the propodeal spiracle.	http://purl.obolibrary.org/obo/HAO_0000609	metapleural carina
metapleural sulcus	The line that corresponds with the metapleural ridge.	http://purl.obolibrary.org/obo/HAO_0000614	metapleural sulcus
metapleuron	The area of the metapetal-propodeal complex that is located laterally of the metadiscrimen.	http://purl.obolibrary.org/obo/HAO_0000621	metapleuron
mesoscutellum	The area that is located posteromedially on the mesonotum, is delimited laterally by the metanotal trough and corresponds to the reservoir of the dorsal vessel.	http://purl.obolibrary.org/obo/HAO_0000625	mesoscutellum
metasoma	The tagna that is connected anteriorly to the metapetal-propodeal complex at the propodeal foramen and consists of abdominal segments.	http://purl.obolibrary.org/obo/HAO_0000626	metasoma
metasomal depression	The acetabulum that is concave, surrounds the nucha and accommodates the base of the metasoma.	http://purl.obolibrary.org/obo/HAO_0000627	metasomal depression
metasomal segment	The abdominal segment that is located in the metasoma.	http://purl.obolibrary.org/obo/HAO_0001969	metasomal segment
netrion	The area that is located posteroventrally on the pronotum and corresponds to the site of origin of first flexor of the fore wing muscle.	http://purl.obolibrary.org/obo/HAO_0000644	netrion
netrion sulcus	The sulcus that anteriorly delimits the netrion.	http://purl.obolibrary.org/obo/HAO_0000646	netrion sulcus
notaullus	The line that extends submedially along the mesoscutum and corresponds to the median border of the site of origin of the first mesopleuro-mesonotal muscle.	http://purl.obolibrary.org/obo/HAO_0000647	notaullus
occipital carina	The carina that surrounds dorsolaterally the occiput.	http://purl.obolibrary.org/obo/HAO_0000653	occipital carina
ocellar diameter	The diameter of the ocellus.	http://purl.obolibrary.org/obo/HAO_0002107	ocellar diameter
ocellus	The multi-tissue structure that is located on the top of the head, composed of the corneal lens, pigment cell, rhabdoms and synaptic plexus.	http://purl.obolibrary.org/obo/HAO_0000661	ocellus
orbital carina	The carina that is located on the face, parallels the inner orbit and is paired.	http://purl.obolibrary.org/obo/HAO_0000810	preorbital carina
ovipositor	The anatomical cluster that is composed of the first valvulae, second valvulae, third valvulae, first valvifers, second valvifers and female T9.	http://purl.obolibrary.org/obo/HAO_0000679	ovipositor
postacetabular sulcus	The sulcus that extends posteriorly along the epicnemial carina.	http://purl.obolibrary.org/obo/HAO_0000741	postacetabular sulcus
posterior mesoscutellar sulcus	The line that extends along the posterior margin of the mesoscutellum and corresponds to the posterior mesoscutellar ridge.	http://purl.obolibrary.org/obo/HAO_0000757	posterior mesoscutellar sulcus
posterior pronotal inflection	The inflection that extends along the posterior margin of the pronotum and articulates with the anterior mesopleural inflection.	http://purl.obolibrary.org/obo/HAO_0000761	posterior pronotal inflection
postmarginal vein	The abscissa that is marginal and located distal to the marginal vein.	http://purl.obolibrary.org/obo/HAO_0000783	postmarginal vein
prespecular sulcus	The sulcus that delimits anteriorly the speculum and corresponds to the anterior margin of the speculum.	http://purl.obolibrary.org/obo/HAO_0000816	prespecular sulcus
pronotal cervical sulcus	The sulcus that extends along the anterior margin of the pronotum and delimits the anterior rim of pronotum.	http://purl.obolibrary.org/obo/HAO_0000831	pronotal cervical sulcus

Term	Concept	URI	Preferred Term
pronotum	The notum that is located in the prothorax.	http://purl.obolibrary.org/obo/HAO_0000853	pronotum
propleural epicoxal sulcus	The epicoxal sulcus that sets of the epicoxal lobe from the ventral part of the ventral propleural area.	http://purl.obolibrary.org/obo/HAO_0000858	propleural epicoxal sulcus
propleuron	The pleuron that is articulated with the fore leg, connected dorsolaterally (anterolaterally) with the pronotum and ventrally (posteriorly) with the prosternum.	http://purl.obolibrary.org/obo/HAO_0000862	propleuron
propodeal carina	The carina that is located on the propodeum.	http://purl.obolibrary.org/obo/HAO_0000864	propodeal carina
propodeum	The area of the metapleural-propodeal complex that is located posterior to the metapleural carina.	http://purl.obolibrary.org/obo/HAO_0001249	propodeum
sculpture	The area that is located on the sclerite and that is composed of repetitive anatomical structures.	http://purl.obolibrary.org/obo/HAO_0000913	sculpture
scutoseutellar sulcus	The sulcus that extends along the scutoseutellar suture.	http://purl.obolibrary.org/obo/HAO_0000919	scutoseutellar sulcus
segment	An anatomical structure that is metameric and is connected to other metameric subdivisions by muscles and is delimited by its sclerites.	http://purl.obolibrary.org/obo/HAO_0000929	segment
sensillum	A sense organ embedded in the integument and consisting of one or a cluster of sensory neurons and associated sensory structures, support cells and glial cells forming a single organized unit with a largely bonafide boundary.	http://purl.obolibrary.org/obo/HAO_0000933	sensillum
skaphion	The area that is anteriorly on the mesonotum and delimited posteriorly by the skaphion carina.	http://purl.obolibrary.org/obo/HAO_0000940	skaphion
spiracle	The anatomical cluster that is composed of the distal end of the trachea and the margin of the sclerite or conjunctiva surrounding the spiracular opening.	http://purl.obolibrary.org/obo/HAO_0000950	spiracle
sternite	The sclerite that is located on the sternum.	http://purl.obolibrary.org/obo/HAO_0000955	sternite
stigmatal vein	The vein that is adjacent proximally to the preostigma.	http://purl.obolibrary.org/obo/HAO_0002428	stigmatal vein
submarginal vein	Basal-most portion of the forewing vein complex that occurs behind the costal cell; measured from the constriction that delimits the humeral plate to the point at which the vein touches the leading edge of the wing apically.	http://purl.obolibrary.org/obo/HAO_0000972	submarginal vein
sulcus	The groove that corresponds to a ridge.	http://purl.obolibrary.org/obo/HAO_0000978	sulcus
tergite	The sclerite that is located on the tergum.	http://purl.obolibrary.org/obo/HAO_0001005	tergite
trachea	The cuticular invagination that is tubular, branched into tracheoles and bears the taenidia.	http://purl.obolibrary.org/obo/HAO_0002415	trachea
transpleural line	The line that is longitudinal, extends ventrolaterally on the mesopleuron and corresponds with the site of origin of the second and third mesopleuro-third axillary sclerite of fore wing muscle and the second mesopleuro-mesonotal muscle.	http://purl.obolibrary.org/obo/HAO_0001205	transpleural line
transverse pronotal carina	The carina that delimits posteriorly the pronotal neck.	http://purl.obolibrary.org/obo/HAO_0001031	transverse pronotal carina
venation	The anatomical cluster that is composed of abscissae.	http://purl.obolibrary.org/obo/HAO_0001096	venation
ventral metapleural area	The area that is located on the metapleuron anteroventrally of the metapleural sulcus.	http://purl.obolibrary.org/obo/HAO_0001062	ventral metapleural area
wing	The appendage that is between the notum and the pectus and is connected to the body by the axillary sclerite muscles.	http://purl.obolibrary.org/obo/HAO_0001089	wing

Revision of the Afrotropical genus *Pulchrisolia* Szabó (Hymenoptera, Platygasteridae, Sceliotrachelinae)

Zachary Lahey¹, Simon van Noort^{2,3}, Andrew Polaszek⁴,
Lubomír Masner⁵, Norman F. Johnson¹

1 Department of Evolution, Ecology, and Organismal Biology, The Ohio State University, 1315 Kinnear Road, Columbus, Ohio 43212, USA **2** Department of Research & Exhibitions, Iziko South African Museum, PO Box 61, Cape Town 8000, South Africa **3** Department of Biological Sciences, University of Cape Town, Private Bag, Rondebosch, 7701, South Africa **4** Department of Life Sciences, Natural History Museum, Cromwell Road, London SW7 5BD, United Kingdom **5** Agriculture and Agri-Food Canada, K.W. Neatby Building, Ottawa, Ontario K1A 0C6, Canada

Corresponding author: Zachary Lahey (lahey.18@osu.edu)

Academic editor: *Elijah Talamas* | Received 14 February 2019 | Accepted 13 May 2019 | Published 18 November 2019

<http://zoobank.org/388A2BB4-D653-42C1-BF5F-4AB5CB614EB2>

Citation: Lahey Z, van Noort S, Polaszek A, Masner L, Johnson NF (2019) Revision of the Afrotropical genus *Pulchrisolia* Szabó (Hymenoptera, Platygasteridae, Sceliotrachelinae). In: Talamas E (Eds) *Advances in the Systematics of Platygastroidea II*. Journal of Hymenoptera Research 73: 39–71. <https://doi.org/10.3897/jhr.73.33876>

Abstract

The genus *Pulchrisolia* Szabó is revised. *Pulchrisolia maculata* Szabó is redescribed and nine species are described as new: *P. ankremos* Lahey, **sp. nov.** (Ghana, Ivory Coast), *P. asantesana* van Noort & Lahey, **sp. nov.** (South Africa), *P. diehoekensis* van Noort & Lahey, **sp. nov.** (South Africa), *P. ellieae* Lahey, **sp. nov.** (Madagascar), *P. nephelae* Lahey, **sp. nov.** (Benin, Burkina Faso, Gambia, Ivory Coast, Mali, Nigeria), *P. robynae* van Noort & Lahey, **sp. nov.** (South Africa), *P. sanbornei* Lahey & Masner, **sp. nov.** (South Africa), *P. teras* Lahey, **sp. nov.** (Madagascar), and *P. valerieae* Polaszek & Lahey, **sp. nov.** (Zambia). The genus is diagnosed from *Afrisolia* Masner & Huggert, *Isolia* Förster, and *Sceliotrachelus* Brues, and a key is provided to the platygastriid genera of the *Isolia*-cluster.

Keywords

Afrisolia, *Isolia*, Parasitoid, Platygastroidea, *Sceliotrachelus*, taxonomy

Introduction

The genus *Pulchrisolia* Szabó was erected for the species *Pulchrisolia maculata* Szabó based on a single female collected in Shirati (Tanzania) by Kálmán Kittenberger in 1909 (Szabó 1959). Masner (1964) examined the type and treated *Pulchrisolia* as a junior synonym of *Sceliotrachelus* Brues. Upon accumulation of new material and re-examination of the type, Masner and Huggert (1989) reinstated *Pulchrisolia* as a valid genus based on a series of characters not found in *Sceliotrachelus*: fore wing with a short, tubular submarginal vein; a transverse frontal ledge just above the toruli; and a ventrally-produced, apically-bifurcated interantennal process. As revealed by this revision, the latter two characters are present in most, but not all, species. *Pulchrisolia* also resembles *Isolia* Förster and *Afrisolia* Masner & Huggert but can be separated from those genera using some of the characters mentioned above as well as characters unique to each genus.

The purpose of this study is to revise the species-level taxonomy of *Pulchrisolia* and update its generic concept. The contributions of the authors are as follows: Z. Lahey: character definition, generic concept development, species concept development, imaging, key development, manuscript preparation; S. van Noort: character definition, key development, provision of specimens; imaging; A. Polaszek: initial proposal for redefinition of the *Isolia*-cluster, character definition, provision of specimens; L. Masner: character definition, generic concept development, species concept development, provision of specimens; N.F. Johnson: character definition, generic concept development, species concept development.

Materials and methods

The numbers prefixed with “CASENT”, “HNHM”, “NHMUK”, “OSUC”, “SAM”, and “USNMENT” are unique identifiers for the individual. Details of the data associated with these specimens may be accessed at the following link: <https://hol.osu.edu> and entering the identifier in the form.

Abbreviations and morphological terms used in the text: sensillar formula of clavomeres: distribution of papillary sensilla on the ventral clavomeres of the female (Yang et al. 2016), with the segment interval specified followed by the number of papillary sensilla (PS) per segment (e.g., A10–A8/1-2-2) (Bin 1981; Bin et al. 1989); T1, T2, ... T6: metasomal tergite 1, 2, ... 6; S1, S2, ... S6: metasomal sternite 1, 2, ... 6. Morphological terminology generally follows Masner and Huggert (1989), Mikó et al. (2007), Talamas and Masner (2016), and Lahey et al. (2019). Morphological terms were matched to concepts in the Hymenoptera Anatomy Ontology (Yoder et al. 2010) using the text analyzer function.

Images were captured at OSUC with a Leica MC170 HD digital camera attached to a Leica Z16 APOA microscope using Leica Application Suite (LAS; version 4.12.0).

Image stacks were combined into a single montage image using Zerene Stacker (version 1.04). Montage images at OSUC were postprocessed with Adobe Photoshop CC and are archived at <http://specimage.osu.edu>, the image database at The Ohio State University, which includes supplementary images not included in this paper. Images were acquired at SAMC with a Leica LAS 4.9 imaging system, comprising a Leica Z16 APOA microscope (using either a 2× or 5× objective) with a Leica DFC450 Camera and 0.63× video objective attached. The imaging process, using an automated Z-stepper, and subsequent image stacking was managed using the LAS (version 4.9) software installed on a desktop computer. Diffused lighting was achieved using a Leica LED5000 HDI dome. All images presented in this paper, as well as supplementary images, are available at <http://www.waspweb.org>.

Scanning electron micrographs were produced with a Hitachi TM300 Tabletop Microscope. The specimen was disarticulated with a minuten probe and forceps, mounted on a 12 mm slotted aluminum mounting stub (EMS Cat. #75220) using carbon adhesive tabs (EMS Cat. #77825-12), and sputter coated with approximately 70 nm of gold/palladium.

Collections

This work is based on specimens deposited in the following repositories:

CAS	California Academy of Sciences, San Francisco, California, USA
CNCI	Canadian National Collection of Insects, Ottawa, Ontario, Canada
NHMUK	Natural History Museum, London, United Kingdom
HNHM	Hungarian Natural History Museum, Budapest, Hungary
OSUC	C.A. Triplehorn Collection, The Ohio State University, Columbus, Ohio, USA
SAMC	Iziko South African Museum, Cape Town, South Africa
USNM	Smithsonian National Museum of Natural History, Washington, DC, USA

Abbreviations and characters annotated in the figures

aad	antero-admedian depression (Figure 5)
atp	anterior tentorial pit (Figures 54, 55)
auc	axillular carina (Figure 5)
axu	axillula (Figure 57)
cly	clypeus (Figures 54, 55)
diap	dorsal surface of interantennal process (Figures 54, 55)
dmpa	dorsal metapleural area (Figure 56)
epc	epomium (Figure 56)
fld	frontal ledge (Figure 54)

fs	foamy structures (Figure 58)
fsS1	foamy structures on S1 (Figures 61, 62)
iap	interantennal process (Figure 55)
loc	lateral ocellus (Figure 5)
lpar	lateral propodeal area (Figure 57)
lpc	lateral propodeal carina (Figures 5, 57)
lt1	lateral tergite 1 (Figure 61)
lt2	lateral tergite 2 (Figure 61)
mc	mesopleural carina (Figure 56)
mdb	mandible (Figure 54)
metp	metapleural pit (Figure 58)
mml	median mesoscutal line (Figure 5)
mnt	metanotal trough (Figures 57, 59)
msct	metascutellum (Figure 57)
mtsr	metascutellar carina (Figure 5)
not	notaulus (Figure 5)
pad	paraocellar depression (Figure 5)
plc	plica (Figure 57)
pns	pronotal shoulder (Figure 5)
prcs	pronotal cervical sulcus (Figure 56)
prd	preocellar depression (Figure 52)
prsl	parapsidal line (Figure 5)
pts	protibial spur (Figure 63)
R (sbmv)	radial vein (submarginal vein) (Figure 5)
scu	mesoscutellum (Figures 5, 57)
sss	scutoscutellar sulcus (Figure 5)
vmpa	ventral metapleural area (Figure 56)

Taxonomy

Pulchrisolia Szabó

Pulchrisolia Szabó, 1959: 395 (original description. Type: *Pulchrisolia maculata* Szabó, by monotypy and original designation); Masner 1964: 11 (treated as a synonym of *Sceliotrachelus* Brues); Masner and Huggert 1989: 29, 108 (keyed, description, diagnosis, species list); Vlug 1995: 73 (cataloged, catalog of world species); Veena-kumari et al. 2019: 453 (key to genera of the *Isolia*-cluster, keyed).

Description. Coloration: yellow; orange; light to dark red; brown to brownish-black. Antennal formula: 10-10. Male antennae: filiform. Clava: subcompact. Number of clavomeres: 3. Arrangement of setae on ventral surface of clavomeres: chevron-shaped

leading to posterior-most papillary sensillum. Sensillar formula of clavomeres: A10–A8/1-2-2. Position of lateral ocellus: remote from inner margin of compound eye by > 3 ocellar diameters. Hyperoccipital carina: present. Frontal ledge: present; absent. Interantennal process: present. Shape of clypeus: ovoid, abruptly widening below ventral surface of interantennal process. Labrum: concealed by clypeus. Facial striae: absent. Malar striae: absent. Malar sulcus: absent. Epomium: incomplete dorsally. Notaulus: present; absent. Anterior admedian depression: present; absent. Axilla: absent. Axillary carina: present, potentially fused with transaxillar carina, sometimes with the posterior margin projecting over metanotal trough. Sculpture of anterior margin of mesoscutellum: smooth; weakly crenulate. Scutoscutellar sulcus: undifferentiated from transcutal articulation. Posterior mesoscutellar sulcus: undifferentiated from mesoscutellar disc. Metascutellum: differentiated from metanotal trough by metascutellar carinae. Sculpture of metascutellum: smooth. Sculpture of metanotal trough: smooth. Netrion: absent. Sculpture of dorsal mesopleuron: transversely ridged. Transepisternal line: absent. Mesopleural carina: present. Foamy structures on metapleuron: present posteriorly. Metapleuron carina: concealed by foamy structures. R (submarginal vein) of fore wing: present, < 1/10 length of fore wing. Marginal cilia of fore wing: present; absent. Shape of fore and hind wing microtrichia: scale-like pegs, some nearly as wide as long. Shape of T1 in dorsal view: transverse. Foamy structures on T1: present anterolaterally. Foamy structures on S1: present, transverse, sometimes projecting between hind coxae. Transverse felt field on S2: absent. Tibial spur formula: 1-2-2. Protibial spur: combed. Setation of dorsal metatibia: present as linear tract of dense setae.

Diagnosis. Species of *Pulchrisolia* may be diagnosed from other platygastroids by the following combination of characters: fore wing with incredibly short, tubular R vein terminating in a knob and at least some microtrichia of the fore and hind wings in the form of short, scale-like pegs. The coloration of the adult (most species are yellow, orange, red, or a combination thereof); frontal ledge on the lower frons; bilobed, protuberant interantennal process; and tract of dense setae on the metatibia are additional characters that may aid in the recognition of the genus.

Definition of the *Isolia*-cluster

As part of their treatment of the subfamily Sceliotrachelinae, Masner and Huggert (1989) grouped genera into clusters based on combinations of characters shared between their constituent species. Genera within the *Isolia*-cluster are recognizable by the combed fore tibial spur (Figure 63) and the microtrichia on the fore and hind wings that are distinctly spike- or scale-like in most, but not all, species (e.g., certain *Isolia*). Masner and Huggert (1989) also placed emphasis on the compact arrangement of the ocelli; however, this character is highly variable between species and between sexes within a species (Veenakumari et al. 2019). There are no host records for any of the genera within this cluster.

Key to genera of the *Isolia*-cluster

- 1 Microtrichia of fore wing distinctly bicolored, giving the appearance of patches or stripes (Figures 1, 2, 48, 64).....2
- Microtrichia of fore wing not bicolored (Figures 3, 4).....3
- 2 Fore wing with short, tubular submarginal vein terminating in knob (Figs 1, 5, 23, 31, 38); microtrichia on fore wing in the form of scale-like pegs (Figs 1, 12, 31, 38); mesoscutum longer than visible portion of pronotum in dorsal view (Figures 5, 23, 50); S2 glabrous; inner margin of metatibia with comb of setae (Figures 15, 22) ***Pulchrisolia* Szabó**
- Fore wing veinless (Figure 2); microtrichia on fore wing dense, overlapping, and needle-like (see Masner and Huggert 1989, p. 197); S2 with long setae; mesoscutum transverse, shorter than visible portion of pronotum (Figure 2); inner margin of metatibia without comb of setae ***Sceliotrachelus* Brues**
- 3 Fore wing with tubular submarginal vein (Figure 3); transepisternal line present; anterior notaular pits present (Figure 3).. ***Afrisolia* Masner & Huggert**
- Fore wing veinless (Figure 4); transepisternal line absent; anterior notaular pits absent (Figure 4) ***Isolia* Förster**

Key to species of *Pulchrisolia* (males and females)

- 1 Fore wing with one black band or a black band and a circular black area (Figs 8, 38); marginal cilia of female fore wing absent; costal margin of hind wing without dark, thick sclerotization posterior to hamuli; frontal ledge present or absent (Figures 5, 10, 21)2
- Fore wing with two black bands (Figures 15, 20, 28); marginal cilia of female fore wing present or absent; costal margin of hind wing with dark, thick sclerotization posterior to hamuli; frontal ledge present (Figures 5, 14, 16, 19, 21)5
- 2 Frontal ledge absent (Figure 10)..... ***P. ankremos* Lahey, sp. nov.**
- Frontal ledge present (Figures 14, 16, 30, 36, 51, 54)3
- 3 Fore wing with a circular arrangement of black microtrichia (Figure 38); mesoscutellum longitudinally striate (Figure 33)..... ***P. nephelae* Lahey, sp. nov.**
- Fore wing without circular pattern of black microtrichia (Figure 22); mesoscutellum smooth (Figures 12, 31)4
- 4 Notaulus present (Figures 5, 50) ***P. teras* Lahey, sp. nov.**
- Notaulus absent (Figure 23)..... ***P. ellieae* Lahey, sp. nov.**
- 5 Antero-admedian depression present (Figures 5, 23, 50)6
- Antero-admedian depression absent (Figures 31, 45)8
- 6 Antero-admedian lines present (Figure 66); mesoscutum and mesoscutellum darker than head and pronotum (Figures 65, 66).....
- ***P. valerieae* Polaszek & Lahey, sp. nov.**
- Antero-admedian lines absent; pronotum, mesoscutum and mesoscutellum concolorous and lighter than head and metasoma (Figures 12, 31)7

- 7 Mesoscutellum approximately twice as wide as long (Figure 39); frontal ledge of male distinctly concave medially (Figure 43); forewing microtrichia of female not overlapping; forewing distinctly longer than body length (Figure 42).....*P. robynae* van Noort & Lahey, sp. nov.
- Mesoscutellum approximately 3 times as wide as long (Figure 12); frontal ledge of male straight, not concave medially (Figure 16); forewing microtrichia of female and male overlapping; forewing approximately as long as body length (Figure 15).....*P. asantesana* van Noort & Lahey, sp. nov.
- 8 Metapleuron completely covered by foamy structures, without setae along anterior margin (Figure 47); posterolateral corners of pronotal shoulders acute (Figures 45, 49).....*P. sanbornei* Lahey & Masner, sp. nov.
- Metapleuron with anterior margin distinctly setose (Figure 18); posterolateral corners of pronotal shoulders round (Figures 17, 31).....9
- 9 Posterolateral corners of pronotal shoulders remote from anterior margin of tegula (Figures 28, 31); head concolorous with mesosoma (Figures 28, 31); clavomeres distinctly darker than funicle (Figure 28)..... *P. maculata* Szabó
- Posterolateral corners of pronotal shoulders closer to anterior margin of tegula (Figures 17, 20); head of female distinctly darker than mesosoma (Figures 17, 18); clavomeres concolorous with funicle.....
..... *P. diehoekensis* van Noort & Lahey, sp. nov.

Character discussion

Antero-admedian depression

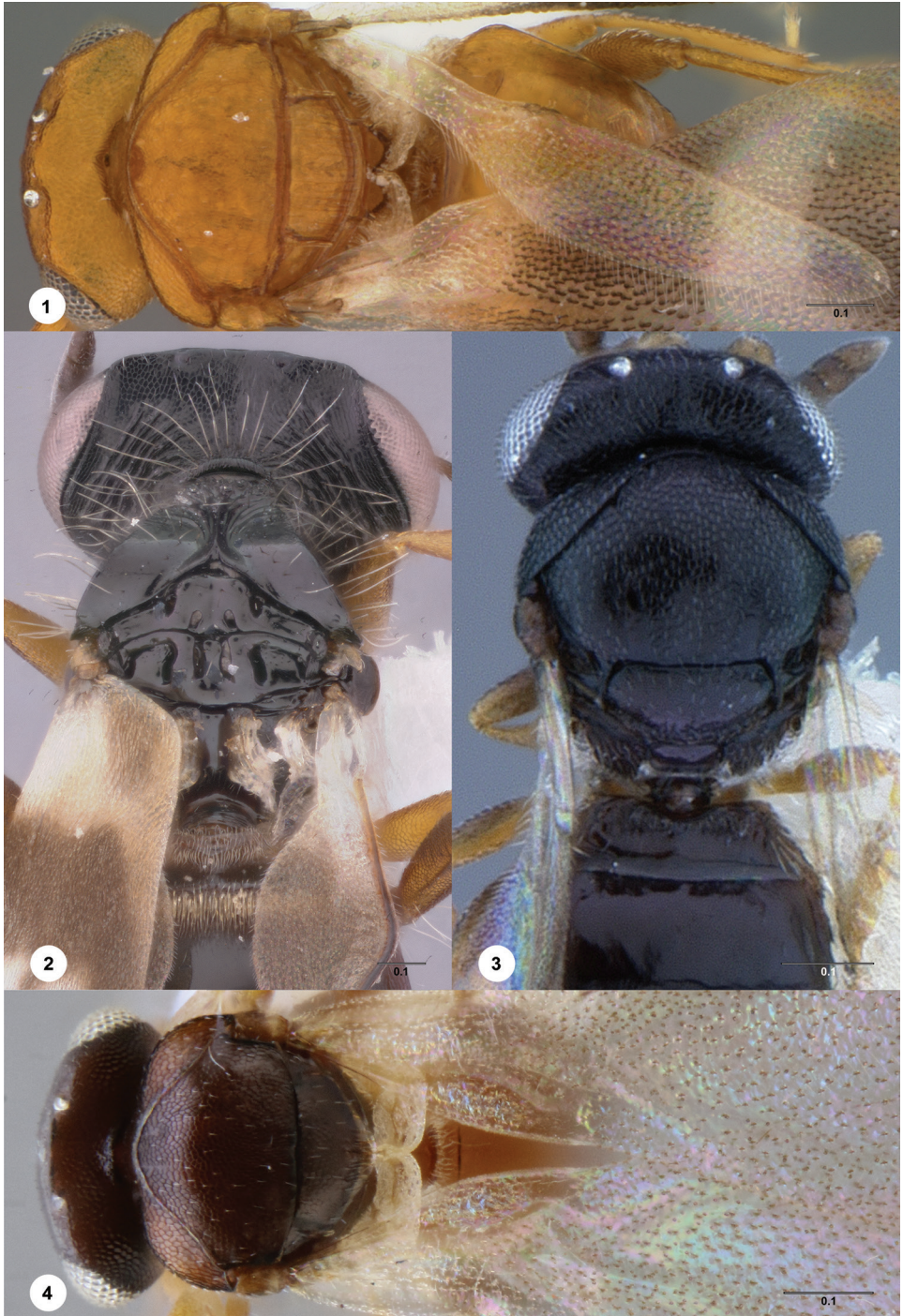
We coin this term for the depression that is located anteromedially on the mesoscutum and is usually separated by a horizontal septum (Figures 1, 5, 23, 50). This character shows little intraspecific or sexual variation, with the notable exception that it may be absent or present in *P. ankremos*.

Interantennal process

All species of *Pulchrisolia* have a distinct, protuberant interantennal process. The dorsal portion ranges in shape from a thin strip that is shorter than the radicle (Figure 10), to an apically bilobate projection longer than the radicle (Figures 16, 21).

Foamy structures and metapleural setation

All species of *Pulchrisolia* have the posterior (Figures 9, 35), and most of the anterior (Figs 40, 47), portion of the metapleuron covered in foamy structures. Foamy structures are extensions of cuticle that usually emanate from carinae on the propodeum and metapleuron but may also occur on T1 and S1. Their structure and coloration (i.e., translucent to yellowish-white) resemble that of a bubbly liquid, with an irregular arrangement of open and closed



Figures 1–4. Genera of the *Isolia*-cluster. *Pulchrisolia nephelae*, male (USNMENT00916688) **1** head, mesosoma, metasoma, dorsal view. *Sceliotrachelus braunsi* Brues, female (OSUC 231999) **2** head, mesosoma, metasoma, dorsal view. *Afrisolia* sp., female (USNMENT00916676) **3** head, mesosoma, metasoma, dorsal view. *Isolia* sp., female (USNMENT00197883) **4** head, mesosoma, metasoma, dorsal view. Scale bars in millimeters.

cells. We hypothesize that they function as an evaporating surface for undetermined glandular products secreted from pores on the associated sclerites. The degree to which the foamy structures are developed and the setation of the anterior margin of the metapleuron are important characters in species identification. We distinguish the anterodorsal from the anteroventral portion of the metapleuron by the location of the metapleural pit (Figures 56, 58), which, although nearly obscured by foamy structures, is generally indicated by an invagination or 'break' along the anterior margin of the foamy structures.

Papillary sensillum

Platygastroids are characterized by the presence of papillary sensilla located on the ventral surface of the distal antennomeres of the adult female (Bin 1981; Bin et al. 1989; Isidoro et al. 2001). These sensilla have been referred to by various names, including plate sensilla (Bin 1981), basiconic sensilla (Bin 1981), multiporous gustatory sensilla (Isidoro et al. 2001), and papillary sensilla (Bin et al. 1989; Yang et al. 2016). We here adopt the term papillary sensilla to describe these structures and suggest other workers on Platygastroidea do the same for the following reasons: (1) the specific function of these sensilla is yet to be elucidated, which obviates the use of terms placing them into a functional category, and (2) the term basiconic has been misapplied to these structures, as histological examinations have confirmed that hundreds, not a few, sensory neurons innervate each sensillum (Isidoro et al. 2001).

Preocellar and paraocellar depressions

We coin these terms to describe the depressions that flank the anterior (preocellar) and/or lateral (paraocellar) margins of the anterior and lateral ocelli, respectively. We prefer not to use the term 'pit' when describing these structures because they may not be homologous with the preocellar pit possessed by some Telenominae, which corresponds internally with an apodeme (Isidoro and Bin 1994). These structures are most noticeable in *P. teras*, where they are semilunar in shape and deep (Figures 5, 50, 52).

Sexual dimorphism

The hyperoccipital carina of some male *Pulchrisolia* is less pronounced than that of conspecific females (Figures 19, 21, 40, 42). In contrast, the interantennal process of males is generally more pronounced and, in species where the interantennal process is apically bilobed, the invagination separating each lobe is longer (Figures 19, 21, 41, 43). Minimal variation was observed in other character systems used to differentiate between males and females of the same species.

Wing microtrichia

The fore and hind wings of *Pulchrisolia* are covered in specialized microtrichia that appear scale-, disc- or paddle-like depending on the angle at which they are observed

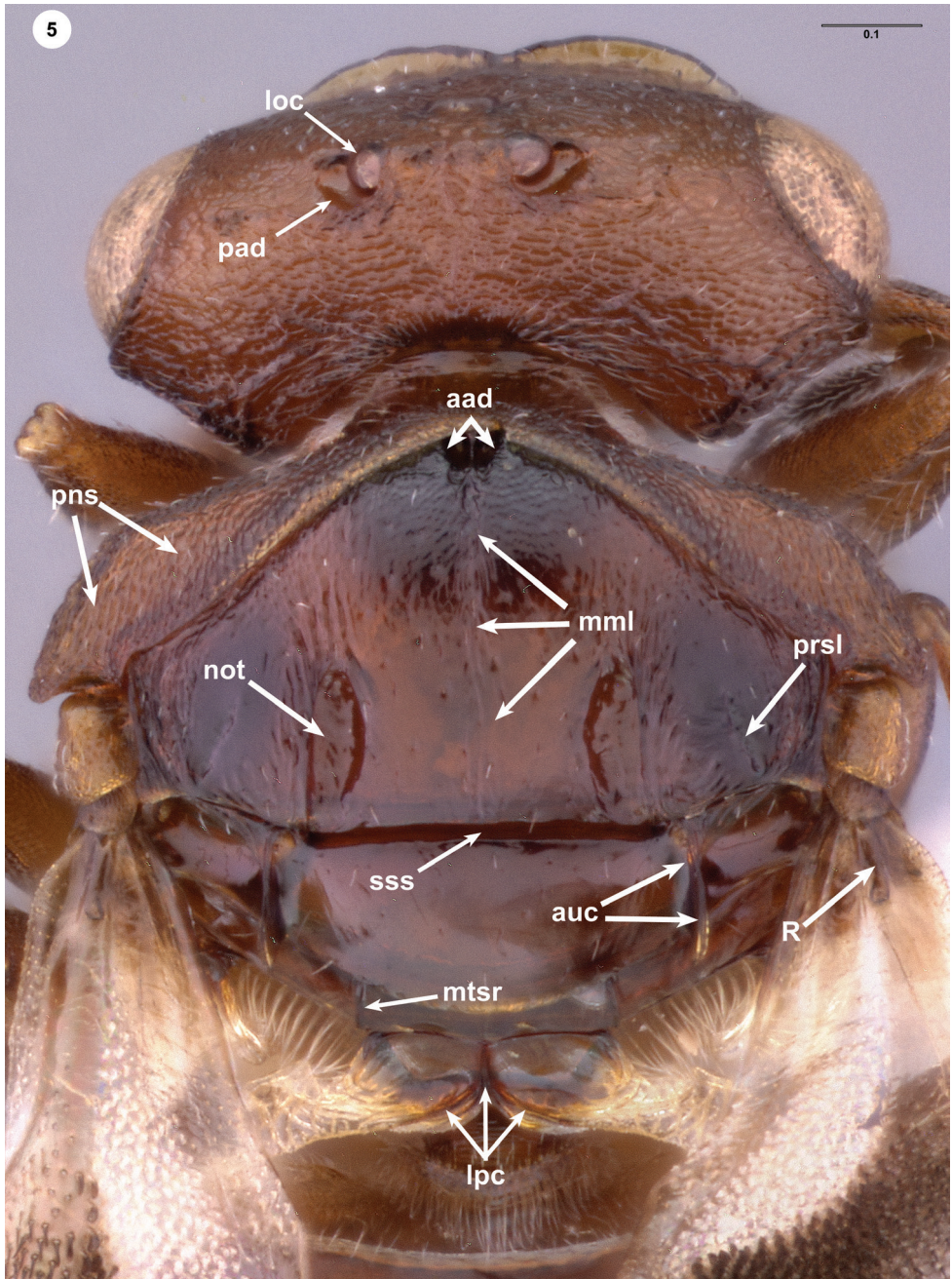


Figure 5. *Pulchrisolia teras*, male (CASENT 2043867), head, mesosoma, T1, dorsal view. Scale bar in millimeters.

(Figures 1, 5, 12, 38, 48, 50). All species possess these structures on at least some portion of their fore and hind wings, but their density and position are species-specific and may require viewing the animal at different angles.

***Pulchrisolia ankremos* Lahey, sp. nov.**

<http://zoobank.org/30BE42DD-D219-4643-90CC-25DFA45D263A>

Figures 6–11

Description. Female body length: 0.74–1.02 mm (n = 10). Coloration of head, female: concolorous with mesosoma. Shape of dorsal interantennal process: simple, not strongly projecting. Length of interantennal process: shorter than radicle. Frontal ledge: absent. Preocellar depressions: absent. Setation of pronotal cervical sulcus: absent. Setation of cervical pronotal area: absent. Sculpture of pronotal shoulders: reticulate. Sculpture of anterior margin of pronotal shoulders: carinate. Posterolateral margin of pronotal shoulders: sharply angled. Posterior margin of pronotal shoulders: rounded. Antero-admedian line: absent. Anterior admedian depression or pit: absent; present. Parapsidial line: present. Median mesoscutal line: absent. Notaulus: absent. Color of mesoscutum: concolorous with pronotum. Shape of mesoscutum in lateral view: flat to slightly convex. Sculpture of mesoscutum: reticulate. Sculpture of mesoscutellum: longitudinally striate. Setation of anterodorsal metapleuron: present. Length of setation of anterodorsal metapleuron: long. Setation of anteroventral metapleuron: present. Length of setation of anteroventral metapleuron: short. Foamy structures on anterior metapleuron: absent. Shape of fore wing: elliptical. Infusate banding of fore wing: absent. Costal margin of hind wing: fuscous posterior to hamuli. Marginal cilia of female fore wing: absent.

Diagnosis. The lack of a frontal ledge on the lower frons and simple interantennal process that does not extend past the radicle separates *P. ankremos* from all other species of *Pulchrisolia*.

Etymology. Taken from the Greek word for cliff (γκρεμὸς), in reference to the lack of a frontal ledge on the lower frons. The epithet is treated as a noun in apposition.

Link to distribution map. [<http://hol.osu.edu/map-large.html?id=457749>]

Material examined. Holotype, female: GHANA: Ashanti Reg., 06°42'N, 01°20'W, Bobiri Forest Reserve, II-2002, flight intercept trap, C. Carlton & O. Frimpong, OSUC 666426 (deposited in CNCI). Paratypes: (8 females) GHANA: 7 females, OSUC 666420–666422, 666424–666425, 666427–666428 (CNCI). IVORY COAST: 1 female, OSUC 666404 (CNCI).

Comments. *Pulchrisolia ankremos* is most similar to *P. nephelae* both morphologically and in geographic distribution. Nearly all the specimens examined have an antero-admedian depression, but this character is absent from the holotype, despite being present in other specimens collected during the same collecting event.

***Pulchrisolia asantesana* van Noort & Lahey, sp. nov.**

<http://zoobank.org/A1125BB0-BF57-4317-AB4B-CF9F13B9E040>

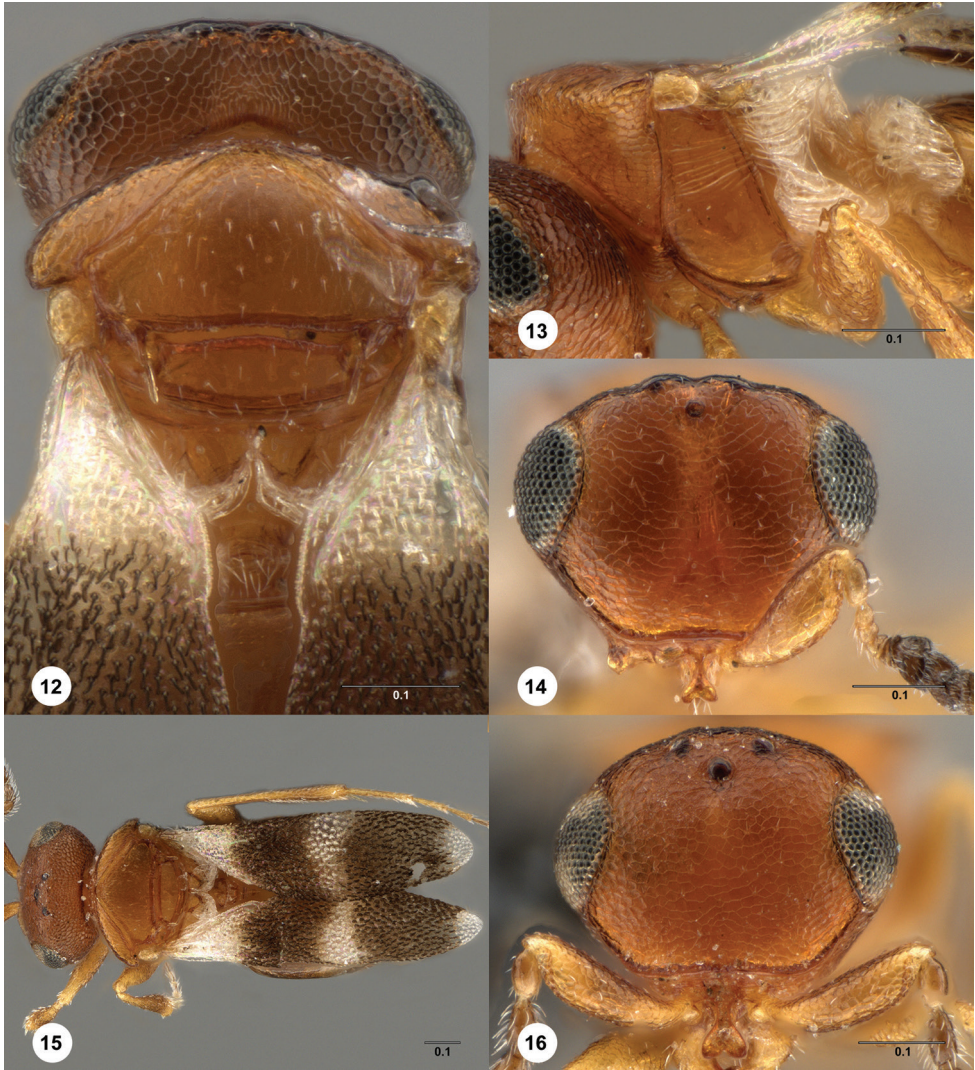
Figures 12–16

Description. Female body length: 0.88–0.96 mm (n = 10). Male body length: 0.74–0.88 mm (n = 10). Coloration of head, female: concolorous with mesosoma. Shape of dorsal interantennal process: apically bilobed. Length of interantennal process: longer



Figures 6–11. *Pulchrisolia ankremos*, female holotype (OSUC 666426) **6** head, mesosoma, metasoma, dorsal view **7** mesosoma, dorsal view **8** head, mesosoma, metasoma, lateral view **9** mesosoma, lateral view **10** head, anterior view **11** metasoma, dorsal view. Scale bars in millimeters.

than radicle. Coloration of clavomeres: darker than funicle. Hyperoccipital carina: sunken between lateral ocelli. Frontal ledge: present. Preocellar depressions: absent. Setation of pronotal cervical sulcus: absent. Setation of cervical pronotal area: present. Sculpture of pronotal shoulders: reticulate. Sculpture of anterior margin of pronotal shoulders: carinate. Posterolateral margin of pronotal shoulders: sharply angled. Posterior margin of pronotal shoulders: rounded. Antero-admedian line: absent. Anterior admedian depression or pit: present. Parapsidial line: absent. Median mesoscutal line: absent. Notaulus: absent. Color of mesoscutum: concolorous with pronotum. Shape of mesoscutum in lateral view: flat to slightly convex. Sculpture of mesoscutum: reticu-



Figures 12–16. *Pulchrisolia asantesana*, female holotype (SAM-HYM-P046628) **12** head, mesosoma, T1, T2, dorsal view **13** head, mesosoma, S1, lateral view **14** head, anterior view **15** male paratype (SAM-HYM-P046628), head, mesosoma, metasoma, dorsal view **16** head, anterior view. Scale bars in millimeters.

late. Sculpture of mesoscutellum: absent. Setation of anterodorsal metapleuron: present. Length of setation of anterodorsal metapleuron: long. Setation of anteroventral metapleuron: absent. Foamy structures on anterior metapleuron: absent. Shape of fore wing: oblong. Infusate banding of fore wing: present. Costal margin of hind wing: darkly sclerotized posterior to hamuli. Marginal cilia of female fore wing: absent.

Diagnosis. The straight frontal ledge and short fore wings with dense microtrichia readily separate this species from other *Pulchrisolia*.

Etymology. Named after the game reserve where the holotype was collected. Asante Sana is Swahili for “thank you very much”. The epithet is treated as a noun in apposition.

Link to distribution map. [<http://hol.osu.edu/map-large.html?id=467907>]

Material examined. Holotype, female: SOUTH AFRICA: Eastern Cape Prov., Zuurkloof, Camdeboo Escarpment Thicket / tall grass stands / scattered outhos / shrubs, T2S3d, 1621m, 32°16.011'S, 25°00.244'E, Asante Sana Game Reserve, 23.X.2010, pitfall trap, J. Midgley, SAM-HYM-P046628a (deposited in SAMC). Paratypes: SOUTH AFRICA: 16 females, 23 males, SAM-HYM-P037363, P038988, P046626, P046627, P046628b-d; P046629, P046630, P046631, P046632, P046633, P046634, P046635, P046636, P046637, P046638, P046639, P046640, P046641, P046642 (SAMC).

***Pulchrisolia dieboekensis* van Noort & Lahey, sp. nov.**

<http://zoobank.org/B7E4613D-560A-4BAA-BDC5-6B3447E3F82E>

Figures 17–21

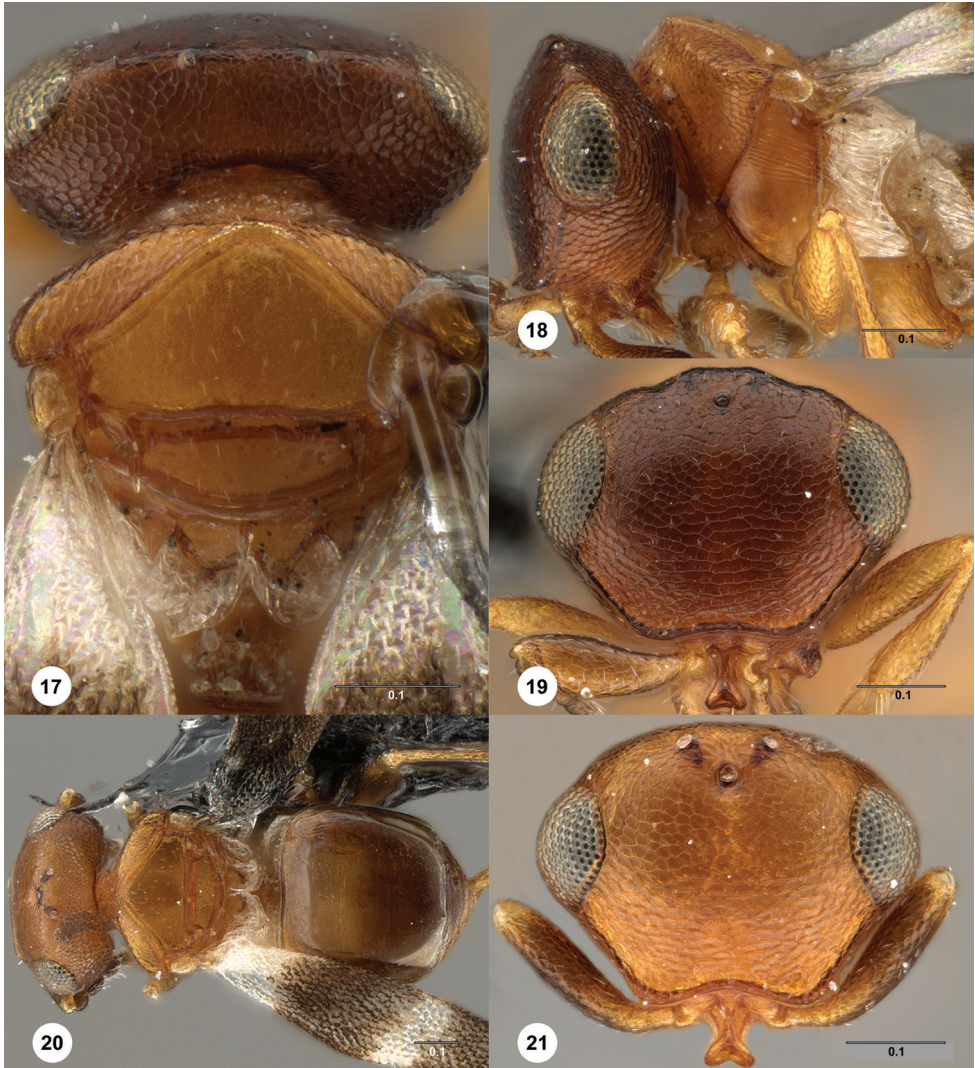
Description. Female body length: 1.04 mm (n = 1). Male body length: 0.80–1.18 mm (n = 4). Coloration of head, female: darker than mesosoma. Shape of dorsal interantennal process: apically bilobed. Length of interantennal process: longer than radicle. Coloration of clavomeres: concolorous with funicle. Hyperoccipital carina: raised between lateral ocelli. Frontal ledge: present. Preocellar depressions: absent. Setation of pronotal cervical sulcus: absent. Setation of cervical pronotal area: present. Sculpture of pronotal shoulders: reticulate. Sculpture of anterior margin of pronotal shoulders: carinate. Posterolateral margin of pronotal shoulders: sharply angled. Posterior margin of pronotal shoulders: rounded. Antero-admedian line: absent. Anterior admedian depression or pit: absent. Parapsidial line: absent. Median mesoscutal line: absent. Notaulus: absent. Color of mesoscutum: concolorous with pronotum. Shape of mesoscutum in lateral view: flat to slightly convex. Sculpture of mesoscutum: mostly smooth. Sculpture of mesoscutellum: absent. Setation of anterodorsal metapleuron: present. Length of setation of anterodorsal metapleuron: long. Setation of anteroventral metapleuron: absent. Foamy structures on anterior metapleuron: absent. Shape of fore wing: oblong. Infusate banding of fore wing: present. Costal margin of hind wing: darkly sclerotized posterior to hamuli. Marginal cilia of female fore wing: absent.

Diagnosis. Separated from other species by the absence of an antero-admedian depression, posterolateral corners of the pronotal shoulders that are nearly articulate with the tegula, deep scutoscutellar sulcus, and coloration of the female.

Etymology. Named after the farm where the type series was collected. Die Hoek is Afrikaans for “the corner”. The epithet is treated as a noun in apposition.

Link to distribution map. [<http://hol.osu.edu/map-large.html?id=467906>]

Material examined. Holotype, female: SOUTH AFRICA: Eastern Cape Prov., Winterberg, Amathole Mistbelt Grassland, WTB09-GRA1-Y04, 1879m, 32°21.260'S, 26°23.001'E, The Hoek Farm, 9.IV–26.VII.2010, yellow pan trap, S. van Noort, SAM-HYM-P038987 (deposited in SAMC). Paratypes: SOUTH AFRICA: 4 males, SAM-HYM-P038989, P038990 (SAMC).



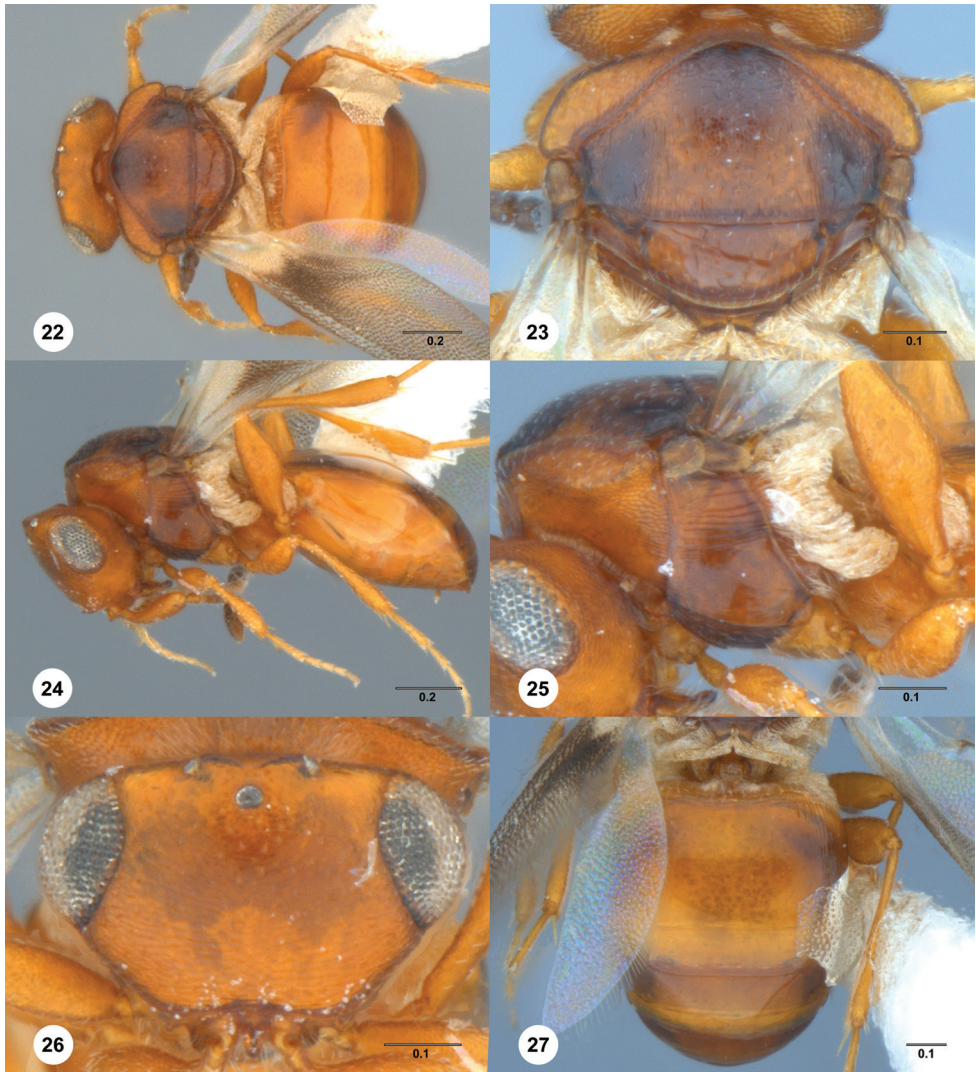
Figures 17–21. *Pulchrisolia diehoekensis*, female holotype (SAM-HYM-P038987) **17** head, mesosoma, T1, T2, dorsal view **18** head, mesosoma, S1, lateral view **19** head, anterior view **20** male paratype (SAM-HYM-P038989), head, mesosoma, metasoma, dorsal view **21** head, anterior view. Scale bars in millimeters.

***Pulchrisolia ellieae* Lahey, sp. nov.**

<http://zoobank.org/CB7B8FBF-DB38-4367-9879-686BEA83D13A>

Figures 22–27

Description. Female body length: 0.97–1.41 mm (n = 2). Coloration of head, female: concolorous with pronotum. Shape of dorsal interantennal process: apically rounded. Length of interantennal process: longer than radicle. Hyperoccipital carina: raised be-



Figures 22–27. *Pulchrisolia ellieae*, female holotype (OSUC 666430) **22** head, mesosoma, metasoma, dorsal view **23** mesosoma, dorsal view **24** head, mesosoma, metasoma, lateral view **25** mesosoma, lateral view **26** head, anterior view **27** metasoma, dorsal view. Scale bars in millimeters.

tween lateral ocelli. Frontal ledge: present. Preocellar depressions: present. Setation of pronotal cervical sulcus: present. Setation of cervical pronotal area: present. Sculpture of pronotal shoulders: reticulate. Sculpture of anterior margin of pronotal shoulders: carinate. Posterolateral margin of pronotal shoulders: sharply angled. Posterior margin of pronotal shoulders: rounded. Antero-admedian line: absent. Anterior admedian depression or pit: present. Parapsidial line: present. Median mesoscutal line: present; indicated posteriorly. Notaulus: absent. Coloration of mesoscutum: darker anteromedially and posterolaterally. Shape of mesoscutum in lateral view: flat to slightly convex.

Sculpture of mesoscutum: reticulate. Sculpture of mesoscutellum: absent. Setation of anterodorsal metapleuron: present. Length of setation of anterodorsal metapleuron: long. Setation of anteroventral metapleuron: present. Length of setation of anteroventral metapleuron: long. Foamy structures on anterior metapleuron: absent. Shape of fore wing: elliptical. Infusate banding of fore wing: absent. Costal margin of hind wing: fuscous posterior to hamuli. Marginal cilia of female fore wing: absent. Marginal cilia of male fore wing: absent.

Diagnosis. *Pulchrisolia ellieae* is identifiable by the apically rounded interantennal process and absence of notauli.

Etymology. This species is named to honor Ellie, the first author's beloved Coton de Tuléar, the royal dog of Madagascar. The epithet is treated as a noun in the genitive case.

Link to distribution map. [<http://hol.osu.edu/map-large.html?id=457304>]

Material examined. Holotype, female: MADAGASCAR: Toliara Auto. Prov., 60km NE Morondava, Beroboka Avaratra, 18.V–23.V.1983, J. S. Noyes & M. C. Day, OSUC 666430 (deposited in NHMUK). Paratype: MADAGASCAR: 1 female, OSUC 666429 (CNCI).

Pulchrisolia maculata Szabó

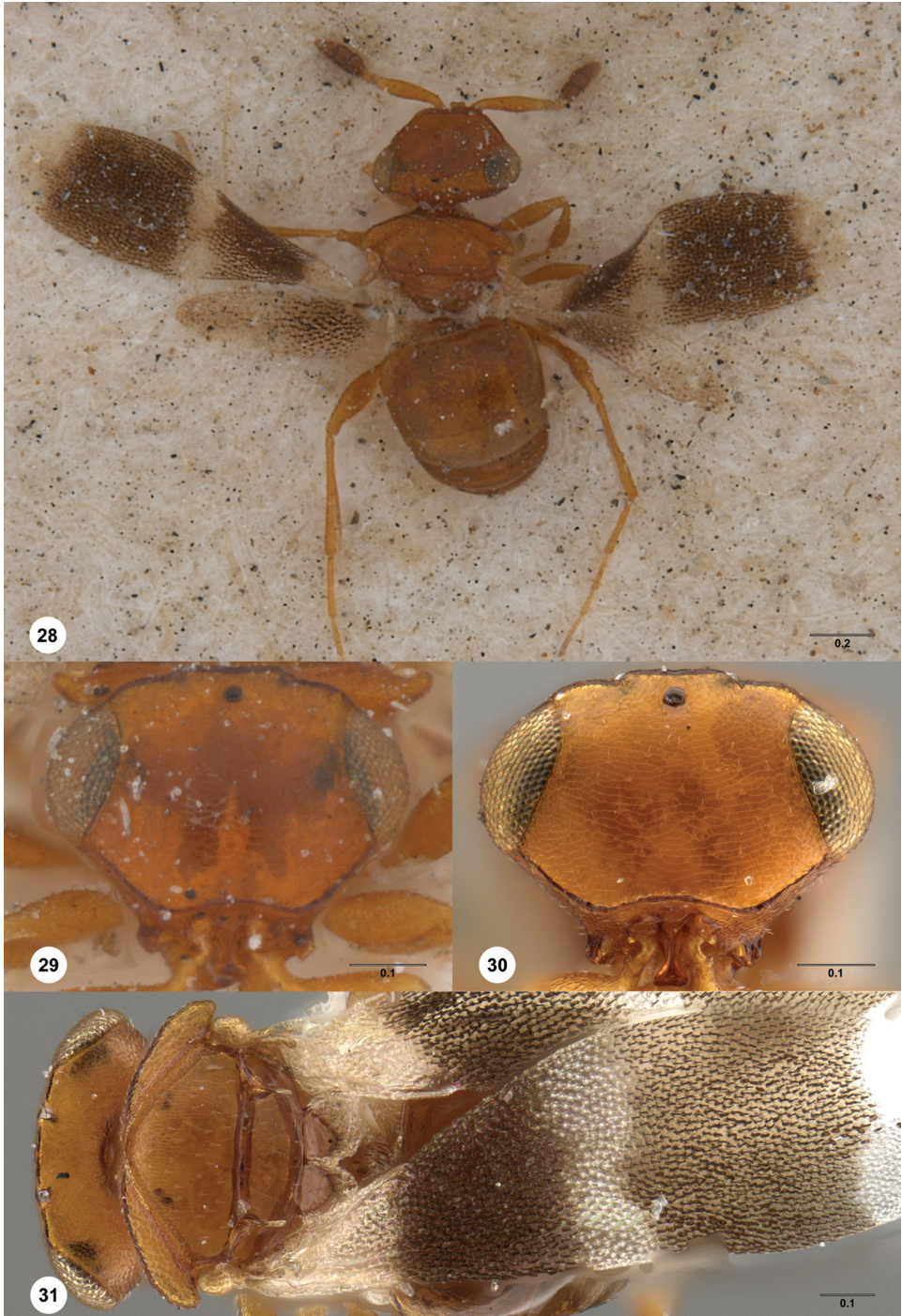
<http://zoobank.org/FEFD0E42-14D3-4687-90F5-4D4D91601F08>

Figures 28–31

Pulchrisolia maculata Szabó, 1959: 396 (original description); Vlug 1995: 73 (cataloged, type information).

Sceliotrachelus maculatus (Szabó): Masner 1964: 11 (generic transfer); Kozlov 1972: 134 (keyed).

Description. Female body length: 1.15–1.16 mm (n = 2). Coloration of head, female: concolorous with mesosoma. Shape of dorsal interantennal process: apically bilobed. Length of interantennal process: longer than radicle. Hyperoccipital carina: indicated as lateral tubercles; raised between lateral ocelli; sunken between lateral ocelli. Frontal ledge: present. Preocellar depressions: absent. Setation of pronotal cervical sulcus: absent. Setation of cervical pronotal area: present. Sculpture of pronotal shoulders: reticulate. Sculpture of anterior margin of pronotal shoulders: carinate. Posterolateral margin of pronotal shoulders: sharply angled. Posterior margin of pronotal shoulders: rounded. Antero-admedian line: absent. Anterior admedian depression or pit: absent. Parapsidal line: absent. Median mesoscutal line: absent. Notaulus: absent. Coloration of mesoscutum: concolorous with pronotum. Shape of mesoscutum in lateral view: flat to slightly convex. Sculpture of mesoscutum: reticulate. Sculpture of mesoscutellum: absent. Setation of anterodorsal metapleuron: present. Length of setation of anterodorsal metapleuron: long. Setation of anteroventral metapleuron: present. Length of setation of anteroventral metapleuron: short. Foamy structures on anterior metapleuron: absent. Shape of fore wing: elliptical. Infusate banding of fore wing: present. Costal



Figures 28–31. *Pulchrisolia maculata* **28** female holotype (HNHM 152909), head, mesosoma, metasoma, dorsal view **29** female holotype (HNHM 152909), head, anterior view **30** female (SAM-HYM-P020261), head, anterior view **31** female (SAM-HYM-P020261), head, mesosoma, metasoma, dorsal view. Scale bars in millimeters.

margin of hind wing; darkly sclerotized posterior to hamuli. Marginal cilia of female fore wing: present.

Diagnosis. *Pulchrisolia maculata* is identifiable by the absence of an antero-admedian depression, posterolateral corners of the pronotal shoulders that are remote from the tegula, and the anteroventral margin of the metapleuron that is glabrous or sparsely setose.

Link to distribution map. [<http://hol.osu.edu/map-large.html?id=12362>]

Material examined. Holotype, female: TANZANIA: Mara Reg., Shirati, V-1909, Katona, Hym. Typ. No. 9583 Mus. Budapest (deposited in HNHM). Other material: (6 females) KENYA: 3 females, OSUC 697903, 697951 (OSUC); USNM-MENT01448452 (USNM). TANZANIA: 3 females, HYM-P019793, P020252, P020261 (SAMC).

Comments. The holotype female is in relatively good condition despite being covered in debris, a result of the method used by Szabó to mount and examine specimens. Additional material collected in Kenya and Tanzania were found to be conspecific with *P. maculata*.

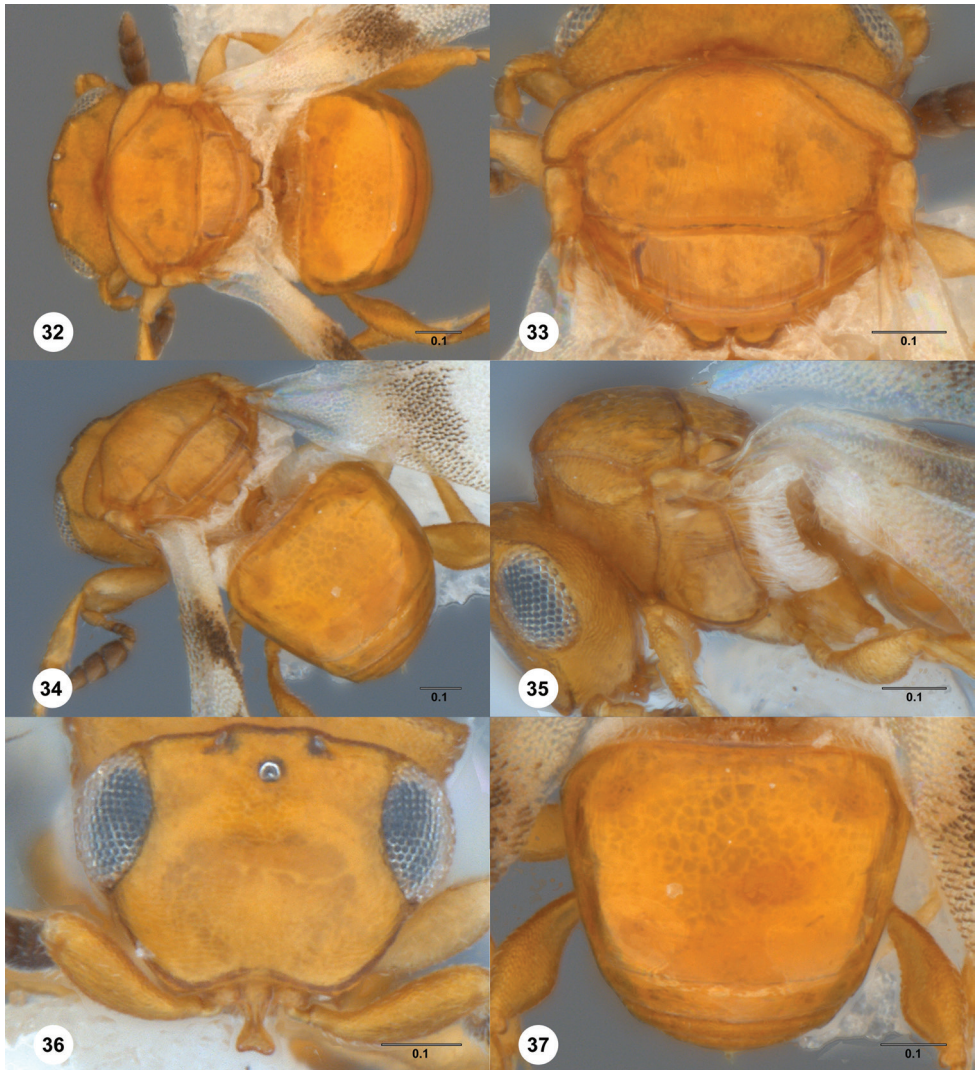
***Pulchrisolia nephelae* Lahey, sp. nov.**

<http://zoobank.org/AF822308-21BA-45B1-8EF9-5E1B070A64FE>

Figures 32–38

Description. Female body length: 0.73–1.14 mm (n = 10). Male body length: 0.73–1.07 mm (n = 10). Coloration of head, female: concolorous with mesosoma. Shape of dorsal interantennal process: simple; apically bilobed. Length of interantennal process: longer than radicle. Hyperoccipital carina: indicated as lateral tubercles; sunken between lateral ocelli. Frontal ledge: present; not traceable to ventral margin of compound eye. Preocellar depressions: present. Setation of pronotal cervical sulcus: absent. Setation of cervical pronotal area: absent. Sculpture of pronotal shoulders: reticulate. Sculpture of anterior margin of pronotal shoulders: carinate. Posterolateral margin of pronotal shoulders: evenly rounded. Posterior margin of pronotal shoulders: rounded. Antero-admedian line: absent. Anterior admedian depression or pit: present. Parapsidal line: absent. Median mesoscutal line: present; indicated posteriorly. Notaulus: absent. Coloration of mesoscutum: concolorous with pronotum. Shape of mesoscutum in lateral view: strongly convex. Sculpture of mesoscutum: longitudinally striate. Sculpture of mesoscutellum: longitudinally striate. Setation of anterodorsal metapleuron: present. Length of setation of anterodorsal metapleuron: long. Setation of anteroventral metapleuron: present. Length of setation of anteroventral metapleuron: long. Foamy structures on anterior metapleuron: absent. Shape of fore wing: elliptical. Infusate banding of fore wing: absent. Costal margin of hind wing: fuscous posterior to hamuli. Marginal cilia of female fore wing: absent. Marginal cilia of male fore wing: present.

Diagnosis. *Pulchrisolia nephelae* closely resembles *P. ankremos* but can be separated from all other *Pulchrisolia* species due to the circular arrangement of black microtrichia in the disc of the fore wing.



Figures 32–37. *Pulchrisolia nephelae*, female holotype (OSUC 666433) **32** head, mesosoma, metasoma, dorsal view **33** mesosoma, dorsal view **34** head, mesosoma, metasoma, posterodorsal view **35** mesosoma, lateral view **36** head, anterior view **37** metasoma, dorsal view. Scale bars in millimeters.

Etymology. Named for the cloud nymphs of Greek mythology. The epithet is treated as a noun in the genitive case.

Link to distribution map. [<http://hol.osu.edu/map-large.html?id=457303>]

Material examined. Holotype, female: MALI: Koulikoro Reg., Mourdiah, 25.VIII–5.IX.1986, Malaise trap, M. Matthews, OSUC 666433 (deposited in CNCI). Paratypes: (29 females, 12 males) BENIN: 3 females, OSUC 666440–666441 (CNCI); OSUC 418469 (OSUC). BURKINA FASO: 4 females, 8 males, OSUC 666409–666416–666419, 666442–666443 (CNCI). GAMBIA: 2 females, OSUC



Figure 38. *Pulchrisolia nephelae*, female (OSUC 697956) **38** fore wing, slide mount. Scale bar in micrometers.

666438–666439 (CNCI). IVORY COAST: 18 females, 1 male, OSUC 666444–666462 (CNCI). MALI: 1 female, 3 males, OSUC 666432, 666434–666436 (CNCI). NIGERIA: 1 female, OSUC 666437 (CNCI).

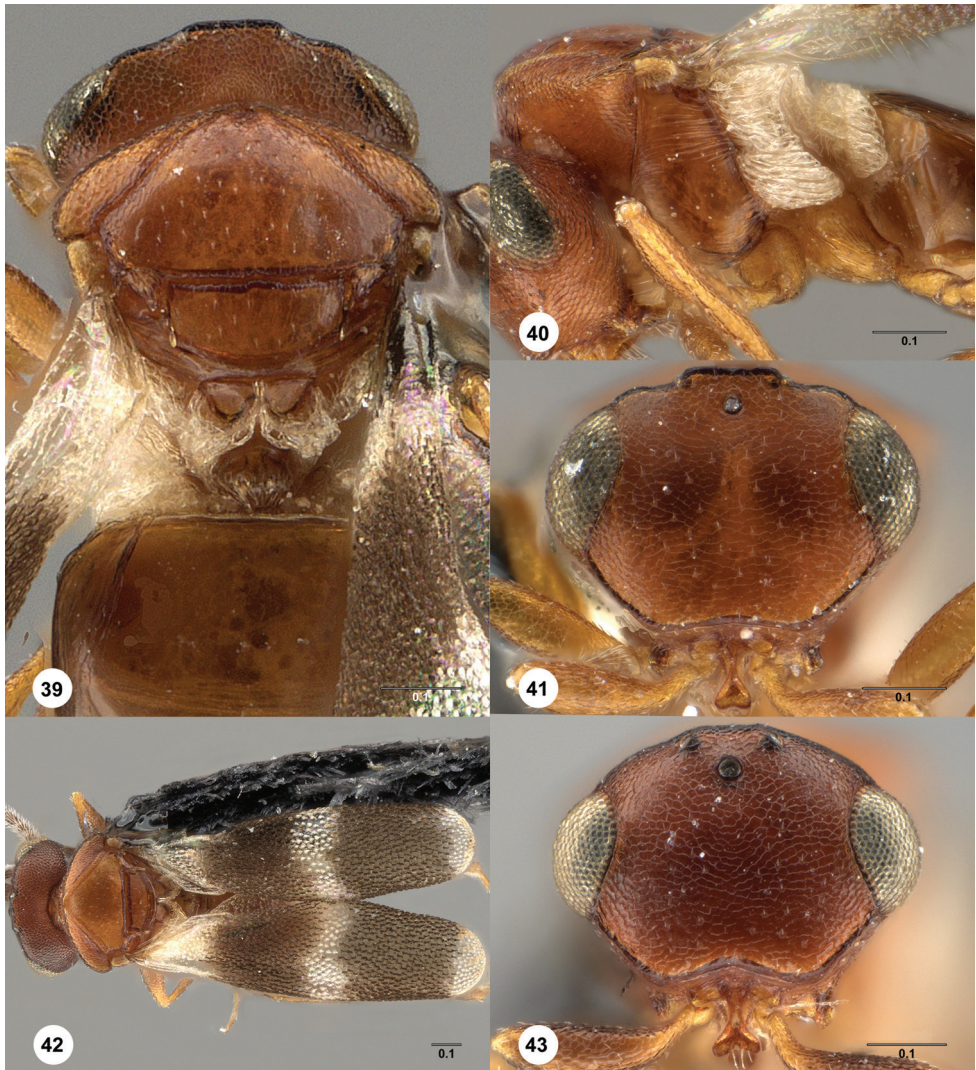
Comments. The most abundant and widely distributed *Pulchrisolia* species currently known. *Pulchrisolia nephelae* is the species figured in the line drawings of Masner and Huggert (1989).

***Pulchrisolia robynae* van Noort & Lahey, sp. nov.**

<http://zoobank.org/A8DD409E-A457-4C08-9AF3-DD3A29532972>

Figures 39–43

Description. Female body length: 0.93–1.10 mm ($n = 6$). Male body length: 0.84–1.40 mm ($n = 8$). Coloration of head, female: concolorous with mesosoma. Shape of dorsal interantennal process: apically bilobed. Length of interantennal process: longer than radicle. Coloration of clavomeres: darker than funicle. Hyperoccipital carina: indicated as lateral tubercles; raised between lateral ocelli. Frontal ledge: present. Pre-cellular depressions: present. Setation of pronotal cervical sulcus: present. Setation of cervical pronotal area: present. Sculpture of pronotal shoulders: reticulate. Sculpture of anterior margin of pronotal shoulders: carinate. Posterolateral margin of pronotal shoulders: evenly rounded. Posterior margin of pronotal shoulders: rounded. Antero-admedian line: absent. Anterior admedian depression or pit: present. Parapsidial line: absent. Median mesoscutal line: present. Notaulus: absent. Coloration of mesoscutum: concolorous with pronotum. Shape of mesoscutum in lateral view: flat to slightly convex. Sculpture of mesoscutum: mostly smooth. Sculpture of mesoscutellum: absent. Setation of anterodorsal metapleuron: present. Length of setation of anterodorsal metapleuron: long. Setation of anteroventral metapleuron: absent. Foamy structures on anterior metapleuron: absent. Shape of fore wing: elliptical; oblong. Infusate banding



Figures 39–43. *Pulchrisolia robynae*, female holotype (SAM-HYM-P031619) **39** head, mesosoma, T1, dorsal view **40** head, mesosoma, S1, lateral view **41** head, anterior view **42** male paratype (SAM-HYM-033748), head, mesosoma, metasoma, dorsal view **43** head, anterior view. Scale bars in millimeters.

of fore wing: present. Costal margin of hind wing: darkly sclerotized posterior to hamuli. Marginal cilia of female fore wing: present.

Diagnosis. *Pulchrisolia robynae* is morphologically similar to *P. maculata* but differs from that species by the presence of an antero-admedian depression, the posterolateral margin of the pronotal shoulders that are nearly articulate with the tegula, and the scutoscutellar sulcus that is weakly crenulate.

Etymology. Named in honor of Robyn Tourle, who was employed as a research assistant on the GEF-funded Conservation Farming project that produced these speci-

mens, in recognition of all her hard work in the field as well as her sorting and curation of specimens. The epithet is treated as a noun in the genitive case.

Link to distribution map. [<http://hol.osu.edu/map-large.html?id=467905>]

Material examined. Holotype, female: SOUTH AFRICA: Eastern Cape Prov., 25.6km (254°) W Kirkwood, valley bushveld (goat trashed), VB01-R4T-P06, 33°32.635'S, 25°13.678'E, Marais Hoop Farm, 10.II–17.II.2001, pitfall trap, H. G. Robertson & R. Tourle, SAM-HYM-P031619 (deposited in SAMC). Paratypes: SOUTH AFRICA: Eastern Cape Province: 5 females, 5 males, SAM-HYM-P031616, P031617, P031618, P033082, P033745, P033746, P033747, P033748 (SAMC); Western Cape Province, Gamkaberg Nature Reserve: 3 males, SAM-HYM-P035656, P038480, P038642 (SAMC).

***Pulchrisolia sanbornei* Lahey & Masner, sp. nov.**

<http://zoobank.org/0B2AA4D0-2345-4D8D-977A-D8A9A719495B>

Figures 44–49

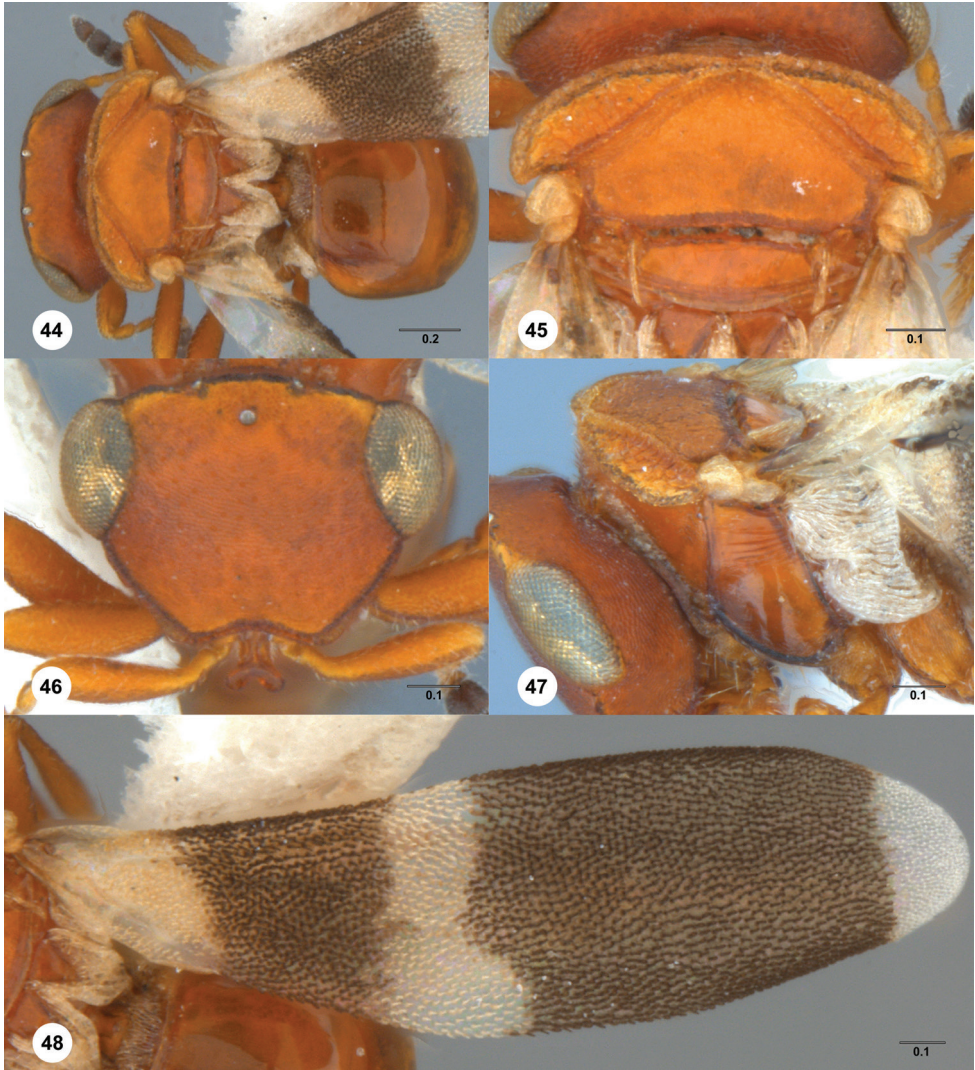
Description. Female body length: 1.61–1.98 mm (n = 10). Male body length: 1.56–1.74 mm (n = 8). Coloration of head, female: concolorous with mesosoma. Shape of dorsal interantennal process: apically bilobed. Length of interantennal process: longer than radicle. Hyperoccipital carina: indicated as lateral tubercles; raised between lateral ocelli. Frontal ledge: present. Preocellar depressions: absent. Setation of pronotal cervical sulcus: absent. Setation of cervical pronotal area: absent. Sculpture of pronotal shoulders: rugose. Sculpture of anterior margin of pronotal shoulders: serrate. Posterolateral margin of pronotal shoulders: sharply angled. Posterior margin of pronotal shoulders: carinate. Antero-admedian line: absent. Anterior admedian depression or pit: absent. Parapsidal line: absent. Median mesoscutal line: absent. Notaulus: absent. Coloration of mesoscutum: concolorous with pronotum. Shape of mesoscutum in lateral view: flat to slightly convex. Sculpture of mesoscutum: longitudinally striate. Sculpture of mesoscutellum: absent. Setation of anterodorsal metapleuron: absent. Setation of anteroventral metapleuron: absent. Foamy structures on anterior metapleuron: present. Shape of fore wing: oblong. Infusate banding of fore wing: present. Costal margin of hind wing: darkly sclerotized posterior to hamuli. Marginal cilia of female fore wing: present. Marginal cilia of male fore wing: present.

Diagnosis. The metapleuron completely covered in foamy structures and the rugose sculpture of the pronotal shoulders separates *P. sanbornei* from other species of *Pulchrisolia*.

Etymology. Named in honor of the late Michael Sanborne (Carleton University, Ottawa, Canada) for his efforts during a field expedition to South Africa which yielded a long series of this beautiful species. The epithet is treated as a noun in the genitive case.

Link to distribution map. [<http://hol.osu.edu/map-large.html?id=457751>]

Material examined. Holotype, female: SOUTH AFRICA: Limpopo Prov., 15km E Klaserie, Guernsey Farm, 19.XII–31.XII.1985, pan trap, M. Sanborne, OSUC 666387 (deposited in SAMC). Paratypes: SOUTH AFRICA: 8 females, 9 males, OSUC 666386, 666388–666403 (CNCI).



Figures 44–48. *Pulchrisolia sanbornei*, female holotype (OSUC 666387) **44** head, mesosoma, metasoma, dorsal view **45** mesosoma, dorsal view **46** head, anterior view **47** mesosoma, lateral view **48** fore wing, dorsal view. Scale bars in millimeters.

***Pulchrisolia teras* Lahey, sp. nov.**

<http://zoobank.org/22736A8D-13BE-4518-BB7C-B251CA2EE713>

Figures 5, 50–63

Description. Female body length: 2.37 mm (n = 1). Male body length: 1.17–1.95 mm (n = 7). Coloration of head, female: concolorous with pronotum. Shape of dorsal interantennal process: apically rounded. Length of interantennal process: longer than radicle. Hyperoccipital carina: indicated as lateral tubercles; raised between lateral ocel-



Figure 49. *Pulchrisolia sanbornei*, male paratype (OSUC 666396) **49** head, mesosoma, metasoma, dorsal view. Scale bars in millimeters.

li. Frontal ledge: present. Preocellar depressions: present. Setation of pronotal cervical sulcus: present. Setation of cervical pronotal area: present. Sculpture of pronotal shoulders: rugose. Sculpture of anterior margin of pronotal shoulders: carinate. Posterolateral margin of pronotal shoulders: sharply angled. Posterior margin of pronotal shoulders: carinate. Antero-admedian line: absent. Anterior admedian depression or pit: present. Parapsidial line: present. Median mesoscutal line: absent; present. Notaulus: present in posterior portion of mesoscutum. Shape of notaulus: broad, deep, abbreviated anteri-



Figure 50. *Pulchrisolia teras*, female holotype (CASENT 2043862) 50 head, mesosoma, T1, T2, dorsal view. Scale bar in millimeters.

only. Coloration of mesoscutum: darker anteromedially and posterolaterally. Shape of mesoscutum in lateral view: flat to slightly convex. Sculpture of mesoscutum: mostly smooth. Sculpture of mesoscutellum: absent. Setation of anterodorsal metapleuron: present. Length of setation of anterodorsal metapleuron: long. Setation of anteroventral metapleuron: present. Length of setation of anteroventral metapleuron: long. Foamy



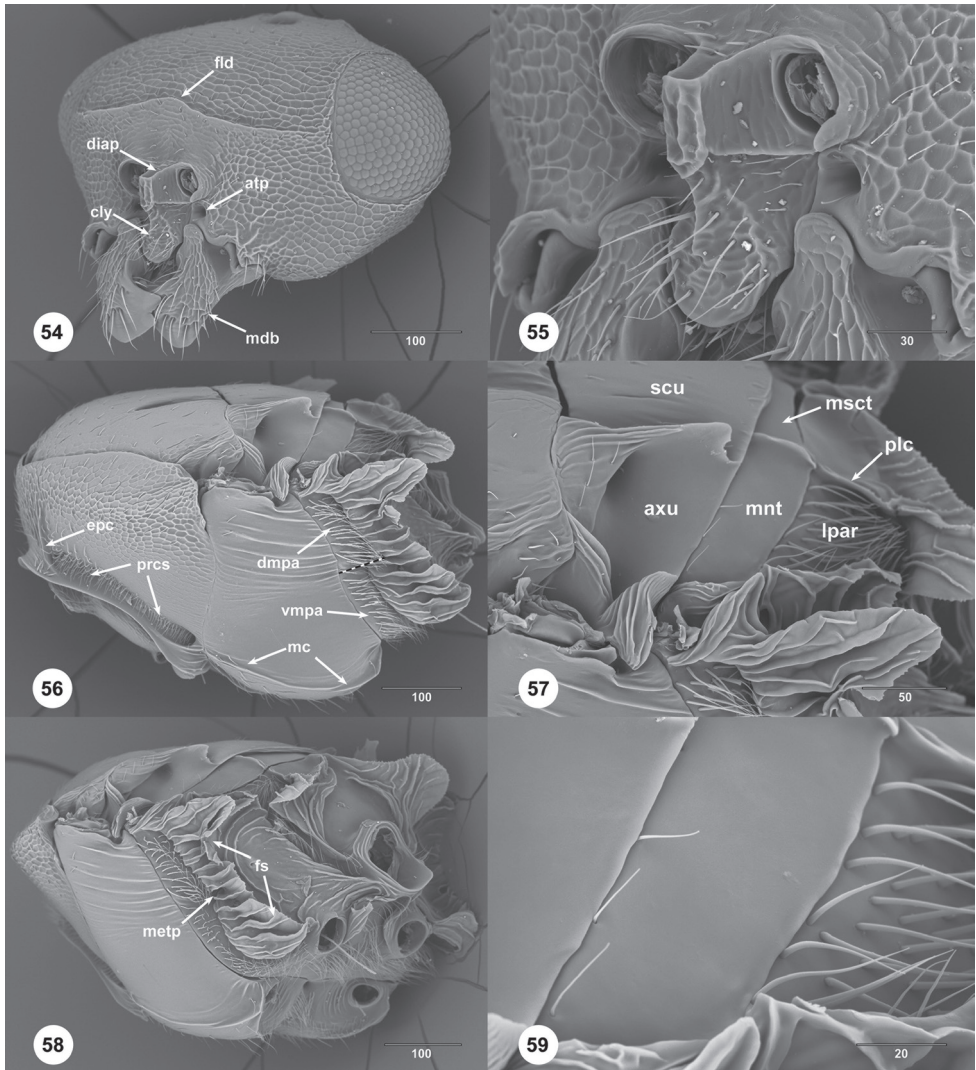
Figures 51–53. *Pulchrisolia teras*, female holotype (CASENT 2043862) **51** head, mesosoma, lateral view **52** head, anterior view **53** head, anteroventral view. Scale bars in millimeters.

structures on anterior metapleuron: absent. Shape of fore wing: elliptical. Infusate banding of fore wing: absent. Costal margin of hind wing: fuscous posterior to hamuli. Marginal cilia of female fore wing: absent. Marginal cilia of male fore wing: absent.

Diagnosis. *Pulchrisolia teras* is separated from all other species by the presence of deep notauli and well-defined preocellar depressions.

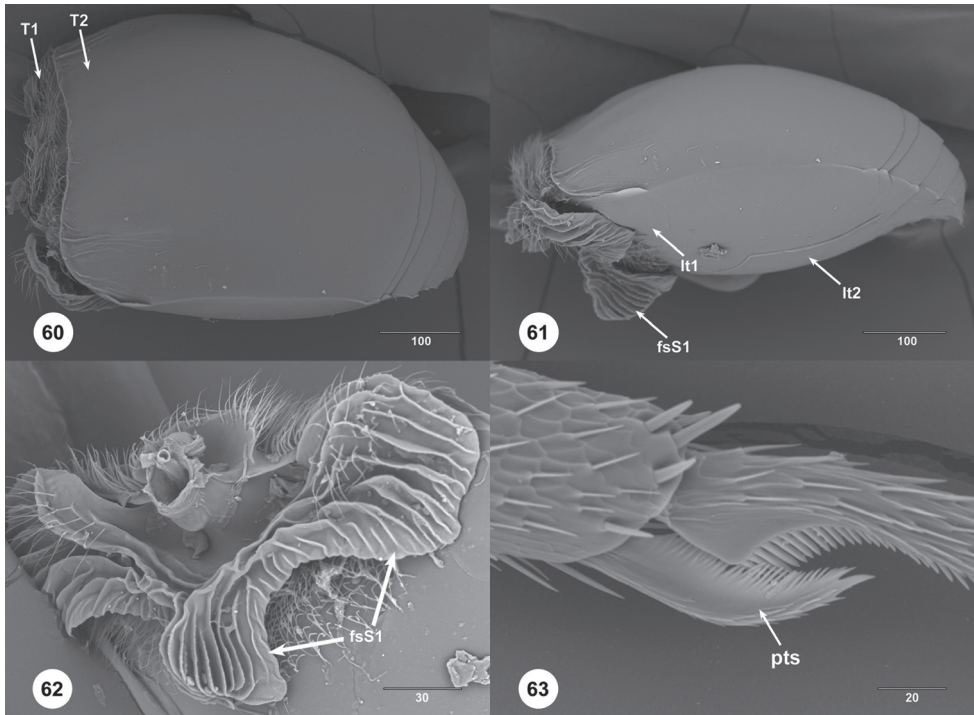
Etymology. Taken from the Greek word for monster (τέρας), in reference to the size and appearance of this formidable creature. The epithet is treated as a noun in apposition.

Link to distribution map. [<http://hol.osu.edu/map-large.html?id=457302>]



Figures 54–59. *Pulchrisolia teras*, female (OSUC 698062) **54** head, anterolateral view **55** interantennal process, clypeus, anterolateral view **56** mesosoma, lateral view **57** axillar complex, metanotum, propodeum, dorsolateral view **58** mesosoma, posterolateral view **59** metanotal trough, dorsal view. Scale bars in micrometers.

Material examined. Holotype, female: MADAGASCAR: Toliara Auto. Prov., 36.1km (308°) NW Tolagnaro, 1.7km (61°) ENE Tsimelahy, Ambohibory Forest, tropical dry forest, BLF4915, 300m, 24°55'48"S, 46°38'44"E, Andohahela National Park, 16.I-20.I.2002, pitfall trap, Fisher, Griswold et al., [CASENT 2043862](#) (deposited in CAS). Paratypes: MADAGASCAR: 7 males, [CASENT 2043863–2043869](#) (CAS).



Figures 60–63. *Pulchrisolia teras*, female (OSUC 698062) **60** metasoma, dorsolateral view **61** metasoma, lateral view **62** S1, S2, anteroventral view **63** protibial spur, lateral view. Scale bars in micrometers.

Comments. The holotype of *P. teras* is considerably larger and more robust than most of the type series, which may indicate polyphagy or intraspecific variability in the size of its host(s).

***Pulchrisolia valerieae* Polaszek & Lahey, sp. nov.**

<http://zoobank.org/6A48C19F-3196-47B6-B9C2-93D607C13A08>

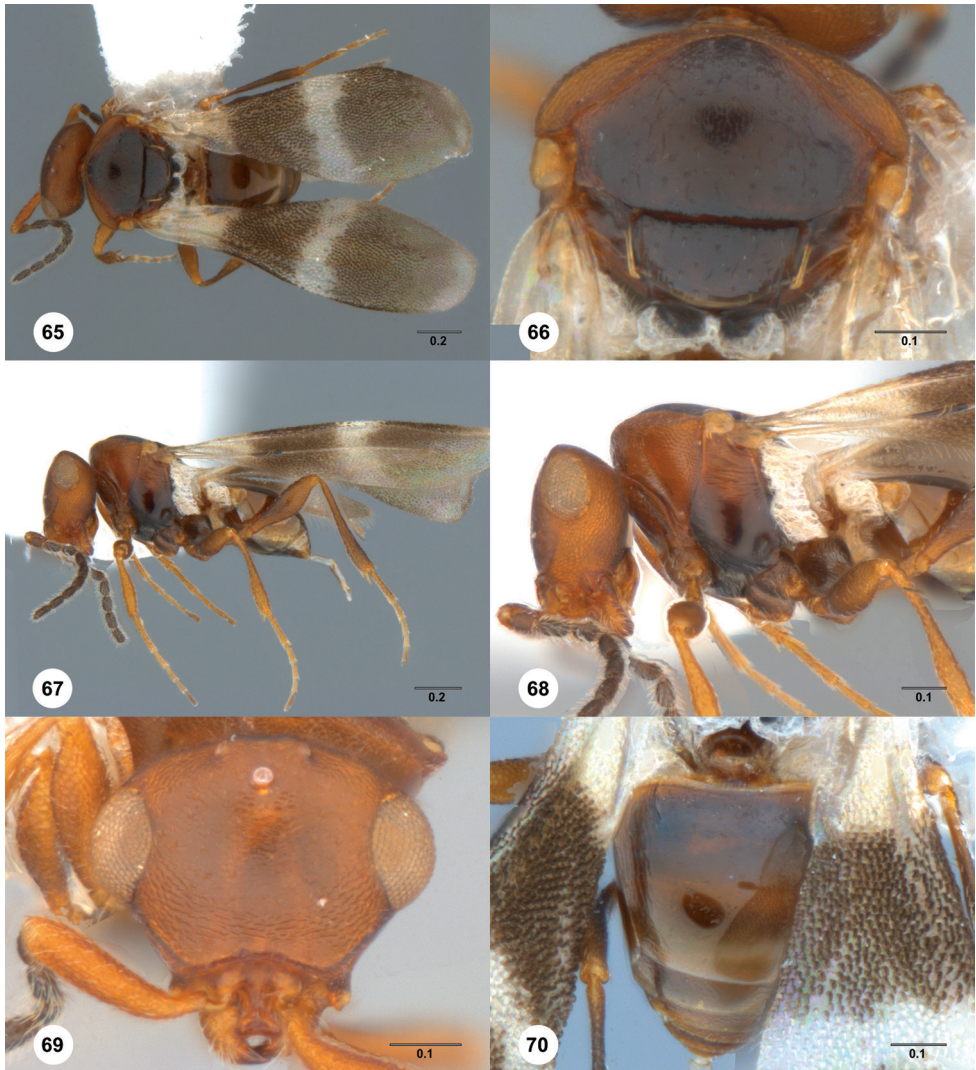
Figures 64–70

Description. Male body length: 1.18 mm (n = 1). Shape of dorsal interantennal process: apically bilobed. Length of interantennal process: longer than radicle. Hyperocipital carina: raised between lateral ocelli. Frontal ledge: present. Preocellar depressions: present. Setation of pronotal cervical sulcus: absent. Setation of cervical pronotal area: absent. Sculpture of pronotal shoulders: reticulate. Sculpture of anterior margin of pronotal shoulders: carinate. Posterolateral margin of pronotal shoulders: sharply angled. Posterior margin of pronotal shoulders: rounded. Antero-admedian line: present. Anterior admedian depression or pit: present. Parapsidial line: absent. Median mesoscutal line: absent. Notaulus: absent. Coloration of mesoscutum: darker than



Figures 64. *Pulchrisolia valerieae*, male holotype (BMNH 010823075) **64** head, mesosoma, metasoma, lateral view (top), dorsal view (bottom).

pronotum. Shape of mesoscutum in lateral view: flat to slightly convex. Sculpture of mesoscutum: reticulate. Sculpture of mesoscutellum: absent. Setation of anterodorsal metapleuron: present. Length of setation of anterodorsal metapleuron: long. Setation of anteroventral metapleuron: absent. Foamy structures on anterior metapleuron: absent. Shape of fore wing: elliptical. Infusate banding of fore wing: present. Costal



Figures 65–70. *Pulchrisolia valerieae*, male holotype (BMNH 010823075) **65** head, mesosoma, metasoma, dorsal view **66** mesosoma, dorsal view **67** head, mesosoma, metasoma, lateral view **68** mesosoma, lateral view **69** head, anterior view **70** metasoma, dorsal view. Scale bars in millimeters.

margin of hind wing: darkly sclerotized posterior to hamuli. Marginal cilia of male fore wing: present.

Diagnosis. *P. valerieae* is unique among the species described due to the presence of antero-admedian lines and for its dark mesoscutum, mesoscutellum, legs, and metasoma.

Etymology. Named in honor of the late Valerie Coughlan, a friend of Andrew Polaszek. The epithet is treated as a noun in the genitive case.

Link to distribution map. [<http://hol.osu.edu/map-large.html?id=457948>]

Material examined. Holotype, male: ZAMBIA: Lukwakwa, open Dambo, 12°39'40"S; 24°26'13"E, 1147m, 4–8.ix.13, Yellow Pan, leg. Smith, Takano and Oram, NHMUK010823075, type number 9.1020 (deposited in NHMUK).

Comments. We describe *P. valerieae* from a single male based on our observations of interspecific, intraspecific, and intersexual variation within the genus. The coloration of all *Pulchrisolia* species known from males and females is virtually identical, with slight differences having been observed on the head (Figures 19, 21) and mesoscutum (Figures 5, 50) of certain species. Most species in the genus are light yellow, orange, or dark red in color; however, the male of *P. valerieae* has most of its mesosoma, and portions of its metasoma and legs, brownish-black (Figures 65–68, 70). The only other species that approximates the coloration of *P. valerieae* is *P. teras*, but this species has notauli and the antero-admedian depression is prominent and hemispherical in shape, even in smaller specimens. Based on what we have observed in other species of the genus, we expect both male and female *P. valerieae* to share similar coloration patterns and possess antero-admedian lines that flank a shallow antero-admedian depression of similar size, making it unlikely that the holotype male is conspecific with *P. maculata* or any of the newly described species of *Pulchrisolia* known only from females.

Acknowledgements

We recognize and thank Sara Hemly and Luciana Musetti (OSUC) for their help with specimen databasing and curation, Elijah Talamas (FSCA) for scanning electron micrographs and comments on an earlier version of the manuscript; Zoltán Vas and Tamás Németh (HNHM) for the loan and images of the *Pulchrisolia maculata* holotype; and Hitoshi Takano (NHMUK) for the donation of the *P. valerieae* holotype. Cape Nature and Eastern Cape Department of Economic Development and Environmental Affairs are thanked for providing collecting permits. This material is based upon work supported in part by the National Science Foundation of the USA under grant No. DEB-0614764 to N.F. Johnson and A.D. Austin, and in part by the South African National Research Foundation under grants GUN 81139 and GUN 98115 to S. van Noort.

References

- Bin F (1981) Definition of female antennal clava based on its plate sensilla in Hymenoptera Scelionidae Telenominae. *Redia* 64: 245–261.
- Bin F, Colazza S, Isidoro N, Solinas M, Vinson SB (1989) Antennal chemosensillar and glands, and their possible meaning in the reproductive behavior of *Trissolcus basal* (Woll.) (Hym.: Scelionidae). *Entomologica* 24: 33–97. <https://doi.org/10.15162/0425-1016/623>
- Isidoro N, Bin F (1994) Fine structure of the preocellar pit in *Trissolcus basal* (Woll.) (Hymenoptera : Scelioindae). *International Journal of Insect Morphology and Embryology* 23: 189–196. [https://doi.org/10.1016/0020-7322\(94\)90017-5](https://doi.org/10.1016/0020-7322(94)90017-5)

- Isidoro N, Romani R, Bin F (2001) Antennal multiporous sensilla: their gustatory features for host recognition in female parasitic wasps (Insecta, Hymenoptera: Platygastroidea). *Microscopy Research and Technique* 55: 350–358. <https://doi.org/10.1002/jemt.1183>
- Kozlov MA (1972) [A Palearctic representative of the genus *Sceliotrachelus* Brues, 1908 (Hymenoptera, Platygasteridae) from the Mongolian People's Republic.] *Entomologicheskoye Obozreniye* 61: 133–135. <https://doi.org/10.5281/zenodo.24377>
- Lahey Z, Masner L, Johnson NF (2019) *Calixomeria*, a new genus of Sceliotrachelinae (Hymenoptera, Platygasteridae) from Australia. *ZooKeys* 830: 63–73. <https://doi.org/10.3897/zookeys.830.32463>
- Masner L (1964) Remarks on *Sceliotrachelus* Brues and allied genera (Hymenoptera, Platygasteridae). *Psyche* 71: 8–11. <https://doi.org/10.1155/1964/40282>
- Masner L, Huggert L (1989) World review and keys to genera of the subfamily Inostemmatinae with reassignment of the taxa to the Platygastriinae and Sceliotrachelinae (Hymenoptera: Platygasteridae). *Memoirs of the Entomological Society of Canada* 147: 1–214. <https://doi.org/10.4039/entm121147fv>
- Mikó I, Vilhelmsen L, Johnson NF, Masner L, Péntzes Z (2007) Skeletomusculature of Scelionidae (Hymenoptera: Platygastroidea): head and mesosoma. *Zootaxa* 1571: 1–78. <https://doi.org/10.11646/zootaxa.1571.1>
- Szabó JB (1959) Notes on the new tribus Amitini with the descriptions of a new genus and some new species of the Aretogaea (Hymenoptera, Proctotrupoidea, Platygasteridae). *Annales Historico-Naturales Musei Nationalis Hungarici* 51: 389–396.
- Talamas EJ, Masner L (2016) Revision of New World *Helava* Masner & Huggert (Platygasteridae, Sceliotrachelinae). *Journal of Hymenoptera Research* 53: 1–24. <https://doi.org/10.3897/jhr.53.10217>
- Veenakumari K, Buhl PN, Mohanraj P (2019) Review of the genus *Isolia* Förster (Platygastroidea: Platygasteridae: Sceliotrachelinae) with description of two new species from India. *Zootaxa* 4565: 451–474. <https://doi.org/10.11646/zootaxa.4565.4.1>
- Vlug HJ (1995) Catalogue of the Platygasteridae (Platygastroidea) of the world (Insecta: Hymenoptera). *Hymenopterorum Catalogus* 19: 1–168. <https://doi.org/10.5281/zenodo.24358>
- Yang SY, Zhong YZ, Zhang JP, Wang XP, Zhang F (2016) A comparative scanning electron microscopy study on antennal sensilla of *Trissolcus japonicus* and *Trissolcus plautiae*, egg parasitoids of stink bugs (Pentatomidae). *Annals of the Entomological Society of America* 109: 112–120. <https://doi.org/10.1093/aesa/sav104>
- Yoder MJ, Mikó I, Seltmann K, Bertone MA, Deans AR (2010) A gross anatomy ontology for Hymenoptera. *PLoS ONE* 5(12): e15991. <https://doi.org/10.1371/journal.pone.0015991>

Revision of *Aleyroctonus* Masner & Huggert (Hymenoptera, Platygasteridae, Sceliotrachelinae)

Zachary Lahey¹, Lubomír Masner², Norman F. Johnson¹, Andrew Polaszek³

1 Department of Evolution, Ecology, and Organismal Biology, The Ohio State University, 1315 Kinnear Road, Columbus, Ohio 43212, USA **2** Agriculture and Agri-Food Canada, K.W. Neatby Building, Ottawa, Ontario K1A 0C6, Canada **3** Department of Life Sciences, Natural History Museum, Cromwell Road, London SW7 5BD, United Kingdom

Corresponding author: Zachary Lahey (lahey.18@osu.edu)

Academic editor: *Elijah Talamas* | Received 19 July 2019 | Accepted 29 August 2019 | Published 18 November 2019

<http://zoobank.org/25BD1DF6-268B-4B48-AAA4-9F24A5D38193>

Citation: Lahey Z, Masner L, Johnson NF, Polaszek A (2019) Revision of *Aleyroctonus* Masner & Huggert (Hymenoptera, Platygasteridae, Sceliotrachelinae). In: Talamas E (Eds) Advances in the Systematics of Platygastroidea II. Journal of Hymenoptera Research 73: 73–93. <https://doi.org/10.3897/jhr.73.38383>

Abstract

The genus *Aleyroctonus* Masner & Huggert is revised. *Aleyroctonus pilatus* Masner & Huggert is redescribed, and two species are described as new: *A. miasmus* Lahey & Polaszek, **sp. nov.** (Australia) and *A. stanslyi* Lahey & Polaszek, **sp. nov.** (Australia). We consider *Aleyroctonus* to be most closely related to a complex of three morphologically similar genera: *Aphanomerus* Perkins, *Austromerus* Masner & Huggert, and *Helava* Masner & Huggert. *Aleyroctonus* is diagnosed from other genera of Sceliotrachelinae and a key is provided to the platygastriid genera of the *Aphanomerus*-cluster.

Keywords

Aleuroctarthrus, *Aleurodicus*, Aleurodicinae, Platygastroidea, taxonomy, whitefly

Introduction

Masner and Huggert (1989) erected the genus *Aleyroctonus* Masner & Huggert for the type species *A. pilatus* Masner & Huggert, a parasitoid of *Aleuroctarthrus destructor* (Mackie) (Hemiptera, Aleyrodidae, Aleurodicinae) in Indonesia. Masner and Huggert (1989) included *Aleyroctonus* in the ‘*Amitus*-cluster’, composed of *Amitus* Haldeman, *Alfredella* Masner & Huggert, and *Nanomerus* Masner & Huggert based on its compact antennal clava, opisthognathous mouthparts, and ‘stocky’ habitus. Morphologi-

cally, however, *Aleyroctonus* more closely resembles *Aphanomerus* Perkins than it does *Amitus*. The densely setose axillar area (Figures 28, 32), tubular submarginal vein that is distant from the fore wing margin (Figure 46), lack of foamy structures on the propodeum and metasoma (Figures 28, 31, 38), and structure of the meso- and metasomally the two genera (Figures 3, 35, 41). For this reason, we transfer *Aleyroctonus* to the *Aphanomerus*-cluster of genera *sensu* Masner and Huggert (1989).

This research is part of an ongoing effort to revise the genera of Sceliotrachelinae, with priority given to the monotypic genera described by Masner and Huggert (1989). The purpose is to update the generic concept of *Aleyroctonus*, describe new species of this economically important genus, and provide an identification key to the genera of the *Aphanomerus*-cluster.

Materials and methods

The numbers prefixed with “NHMUK”, “OSUC”, and “USNMENT” are unique identifiers for the individual specimens (note the blank space after some acronyms). Details of the data associated with these specimens may be accessed at the following link: <http://hol.osu.edu> and entering the identifier in the form.

Abbreviations and morphological terms used in the text: sensillar formula of clavomeres: distribution of large papillary sensilla on the ventral clavomeres of the female (Yang et al. 2016), with the segment interval specified followed by the number of papillary sensilla (PS) per segment (e.g., A10–A8/1-2-2) (Bin 1981); LOL: lateral ocellar line, shortest distance between outer margins of the lateral and median ocellus (Masner 1980); OD: ocellar diameter, greatest width of ocellus; OOL: ocular ocellar line, shortest distance between inner orbit and outer margin of posterior ocellus (Masner 1980); POL: posterior ocellar line, shortest distance between inner margins of lateral ocelli (Masner 1980); T1, T2, ... T6: metasomal tergite 1, 2, ... 6; S1, S2, ... S6: metasomal sternite 1, 2, ... 6. Morphological terminology follows Masner and Huggert (1989), Mikó et al. (2007), and Lahey et al. (2019), except for that of the male genitalia which follows Johnson (1984). Morphological terms were matched to concepts in the Hymenoptera Anatomy Ontology (Yoder et al. 2010) using the text analyzer function. A table of morphological terms and URI links is provided in Suppl. material 1: Table S1.

Photographs of card- or point-mounted insects were captured with a Z16 Leica lens, JVC KY-F75U digital camera, and Cartograph software, or using a Macroscopic Solutions Macropod Micro Kit with optical slices rendered in Helicon Focus. Image stacks of card- or point-mounted insects were processed with CombineZP to produce single montage images. Photographs of slide-mounted insects were captured with a Nikon DS-Fi1 camera attached to a Nikon Eclipse 90i compound microscope with DIC illumination. Image stacks of slide-mounted insects were processed with NIS Elements BR (version 3.22.01, Build 715) to produce single montage images. The single scanning electron micrograph was produced using the methods of Talamas et al. (2016). Montage images from the various imaging systems were postprocessed for exposure and contrast with Adobe Photoshop CC.

Collections

This work is based on specimens deposited in the following repositories:

ANIC	Australian National Insect Collection, Canberra, ACT, Australia
CNCI	Canadian National Collection of Insects, Ottawa, Ontario, Canada
FSCA	Florida State Collection of Arthropods, Gainesville, Florida, USA
NHMMUK	Natural History Museum, London, United Kingdom
OSUC	C.A. Triplehorn Collection, The Ohio State University, Columbus, Ohio, USA
USNM	Smithsonian National Museum of Natural History, Washington, DC, USA

Abbreviations and characters annotated in the figures

2Rs	second abscissa of the radial sector vein (Figure 46)
apT2	anterior setal patch of T2 (Figure 3)
bcT2	basal costae of T2 (Figure 19)
bsT2	basal striae of T2 (Figure 27)
clv	clava (Figures 16, 17, 25)
fs	foamy structures (Figures 13, 14)
gc	genal carina (Figure 36)
M	median vein (Figure 46)
mfp	metafemoral spines (Figure 7)
mlc	median carina on mesoscutellum (Figure 18)
msc	mesoscutum (Figure 8)
mssp	median mesoscutellar projection (Figure 10)
ps	papillary sensilla (Figure 4, 12, 25)
psu	posterior mesoscutellar sulcus (Figures 11, 26)
R	radial vein (submarginal vein) (Figure 46)
RS+M	basal vein (Figures 1, 46)
sce	setation of compound eye (Figure 20)
scu	mesoscutellum (Figure 8)
tel	transepisternal line (Figures 2, 6, 14)
tf	transverse furrow (Figure 24)

Character discussion

Facial and malar striae

Aleyroctonus is one of the few sceliotracheline genera with facial and malar striae. Normally, the malar sulcus serves as the boundary separating the facial striae (dorsal to the malar sulcus) from the malar striae (ventral to the malar sulcus). In *Aleyroc-*

tonus, the precise position of this boundary is not clear because the malar sulcus is inseparable from the facial and malar striae in terms of surface sculpture. Despite this uncertainty, we use these terms to refer to the striae on either side of where we would expect the malar sulcus to be located based on our experience with other platygastroid genera.

Metascutellar setae

Setation of the metascutellum is uncommon within Platygastroidea, occurring in several genera of Scelionidae (e.g., *Bracalba* Dodd, *Chromoteleia* Ashmead, *Microthoron* Masner, *Oxyscelio* Kieffer, *Paridris* Kieffer, *Romilius* Walker, *Sceliacanthella* Dodd, *Tanaodytes* Masner, *Thoron* Haliday, *Thoronidea* Masner & Huggert, *Tiphodytes* Bradley, *Trichoteleia* Kieffer, and *Trimorus* Förster) and at least one species of *Metaclisis* Förster (Platygastriidae; USNMENT01197956). *Aleyroctonus* is the only sceliotracheline known to us with a setose metascutellum, a character best observed when viewed posteriorly.

***Aphanomerus*-cluster**

The *Aphanomerus*-cluster was loosely defined by Masner and Huggert (1989) and includes genera with or without foamy structures on the propodeum or metasoma; with basal costae, striae, or anterolateral pits on T2; different numbers of clavomeres; and an articulated, subcompact, or compact antennal clava. We retain use of this cluster until relationships among these genera are better understood, knowing full well that the genera included in this cluster may not form a monophyletic group.

Key to genera of the *Aphanomerus*-cluster

- 1 T1 fused with T2 and S1 fused with S2, without sutures (Figures 22, 23); frons with transverse furrow above torulus (Figure 24); eyes strongly diverging ventrally (Figure 24)..... ***Parabaeus* Kieffer**
- T1 and T2 and S1 and S2 separated by distinct sutures, sometimes obscured by dense setation (Figure 3); frons without transverse furrow above torulus (Figure 7); eyes not strongly diverging ventrally **2**
- 2 Anterior margin of T2 costate or striate medially, without lateral pits (Figures 1, 19, 26, 27)..... **3**
- Anterior margin of T2 smooth medially, usually with 2 pits laterally (Figures 3, 8, 28)..... **7**
- 3 Female antenna 7- or 8-merous; clava without sutures (Figure 12)..... **4**
- Female antenna 9- or 10-merous; clava with sutures (Figures 16, 17)..... **5**

- 4 Female antenna 7-merous (Figure 25); clava with 3 papillary sensilla (Figure 25); posterior mesoscutellar sulcus complete (Figure 26); posteromedial surface of mesoscutellum flat ***Pseudaphanomerus Szelenyi***
- Female antenna 8-merous; clava with 4 papillary sensilla (Figure 12); posterior mesoscutellar sulcus incomplete medially (Figure 11); posteromedial surface of mesoscutellum with projection (Figure 10) ***Calomerella Masner & Huggert***
- 5 Claval formula 1-2-2-1; eyes distinctly setose (Figure 20); mesoscutellum with longitudinal median carina (Figure 18); transepisternal line not extending to anterior and posterior margins of mesopleuron ***Indomerella Buhl***
- Claval formula 1-2-2-2; eyes glabrous or without distinct setation; mesoscutellum without longitudinal median carina; transepisternal line complete (Figure 2) **6**
- 6 RS+M of fore and hind wings nebulous (Figure 1) ***Aphanomerella Dodd***
- RS+M of fore and hind wings absent or spectral ***Tetrabaesus Kieffer***
- 7 Foamy structures on posterior surface of metapleuron present (Figures 6, 14) **8**
- Foamy structures on posterior surface of metapleuron absent (Figures 9, 36, 42) **9**
- 8 Clava composed of articulated segments (Figure 7); ventral surface of metafemur with one or two rows of erect, stout setae (Figure 7); transepisternal line wide and straight, not reaching anterior margin of mesopleuron (Figure 6) ***Austromerus Masner & Huggert***
- Clava compact, segments not articulated (Figures 16, 17); ventral surface of metafemur without rows of erect, stout setae; transepisternal line absent or thin, length variable (Figure 14) ***Helava Masner & Huggert***
- 9 Malar and facial striae present (Figures 29, 37, 43, 44); distal margin of clypeus pointed (Figures 29, 37, 43) ***Aleyroctonus Masner & Huggert***
- Malar and facial striae absent (Figure 7); distal margin of clypeus truncate, not pointed (Figures 4, 5) **10**
- 10 Mesoscutellum approximately as long as mesoscutum (Figure 8); transepisternal line absent (Figure 9) ***Calixomeria Lahey & Masner***
- Mesoscutellum clearly shorter than mesoscutum (Figure 13); transepisternal line present ***Aphanomerus Perkins***

Key to species of *Aleyroctonus*

- 1 Genal carina present (Figure 36); antennal clava approximately as long or longer than A3–A7 (Figure 33); notauli of uniform width throughout, not strongly converging posteriorly (Figures 32, 35) ***A. pilatus Masner & Huggert***
- Genal carina absent; antennal clava distinctly shorter than A3–A7 (Figure 45); notauli dilated or strongly converging posteriorly (Figures 28, 41) **2**
- 2 Notauli strongly converging posteriorly, of uniform width throughout (Figures 28, 31); posterior mesoscutellar sulcus complete (Figure 28); length of POL

- greater than 2 OD (Figure 28); metasoma xanthic (Figures 28, 29).....
 *A. miasmus* Lahey & Polaszek, sp. nov.
- Notauli not strongly converging posteriorly, dilated posteriorly (Figure 41); posterior mesoscutellar sulcus incomplete medially (Figure 41); length of POL less than or equal to 2 OD (Figure 41); metasoma black (Figures 41, 42).....
 *A. stanslyi* Lahey & Polaszek, sp. nov.

Taxonomy

Aleyroctonus Masner & Huggert

<http://zoobank.org/012252F4-956E-4A7E-ADBE-955697F0F236>

Aleyroctonus Masner & Huggert, 1989: 36 (original description. Type: *Aleyroctonus pilatus*. Masner & Huggert, by monotypy and original designation); Vlug 1995: 10 (cataloged, catalog of world species).

Description. Head. Color of head: black. Shape of head in dorsal view: transverse. Occipital carina: present. Setation of compound eye: present. Hyperoccipital carina: absent. Occipital pit: absent. Preocellar depressions: present. Position of lateral ocellus: less than 1 OD from inner margin of compound eye. Antennal scrobe: present. Sculpture of antennal scrobe: transversely striate. Sculpture of upper frons: densely reticulate. Sculpture of vertex: densely reticulate. Malar striae: present. Malar sulcus: not apparent, undifferentiated from facial and malar striae. Facial striae: present. Epistomal sulcus: absent. Central keel: present. Shape of clypeus: almost V-shaped, projecting over mandibles. Anteclypeus: undifferentiated from postclypeus. Orientation of mandibular teeth: transverse. Mandibular dentition: bidentate. Number of maxillary palpomeres: 1. Number of labial palpomeres: 1. Number of antennomeres, female: 10. Number of antennomeres, male: 9. Number of clavomeres: 3. Sensillar formula of clavomeres: 1-2-2. Condition of A7: not fused with A8, separated by a deep suture.

Mesosoma. Epomial carina: present. Pronotal shoulders: lateral portion visible in dorsal view, not angled. Sculpture of mesoscutum: reticulate. Anterior admedian line: present as pits. Median mesoscutal line: absent. Notaulus: percurrent. Parapsidial line: present. Mesoscutal humeral sulcus: present as a thin groove. Netrion: present. Scutoscutellar sulcus: present as a deep, noncrenulate groove. Sculpture of mesoscutellum: reticulate. Shape of mesoscutellum: nearly hexagonal, widest anteriorly. Setation of axillula: dense. Metascutellum: obscured medially by posterior margin of mesoscutellum. Setation of metascutellum: present. Transepisternal line: present, terminating in anterior and posterior pits. Mesopleural carina: absent. Metapleural carina: present. Metapleural sulcus: present posteriorly. Paracoxal sulcus: absent. Number of mesofurcal pits: 3. Setation of plical area: dense. Color of legs: yellow. Protibial spur: bifid. Tibial spur formula: 1-2-2. Tarsal formula: 5-5-5. Length of tarsal claws: equal.



Figures 1,2. *Aphanomerella* sp., female (USNMENT00916678) **1** head, mesosoma, metasoma, dorsal view **2** head, mesosoma, metasoma, lateral view. Scale bars: in millimeters.



Figures 3–5. *Aphanomerus* spp. **3** female (USNMENT01109890), head, mesosoma, metasoma, dorsal view **4** female (USNMENT00916681), head, anterior view **5** female (USNMENT00916681), head, lateral view. Scale bars: in millimeters.



Figures 6,7. *Austromerus grandis* Masner & Huggert, female (USNMENT00916679) **6** head, mesosoma, metasoma, lateral view **7** head, mesosoma, metasoma, ventrolateral view. Scale bars: in millimeters.

Metasoma. Foamy structures: absent. Number of visible terga in female: 6. Number of visible terga in male: 8. Setation of laterotergites: present. Number of visible sterna: at least 6. Sculpture of terga: absent. Laterotergites: present. Laterosternites: absent. Nucha: present, visible in dorsal view. Sculpture of nucha: costate. Shape of T1: transverse. Anterolateral pits on T2: present. Longest tergite: T2. Transverse felt field on anterior S2: present, sparsely setose. Ovipositor: *Ceratobaeus*-type (Austin and Field 1997).

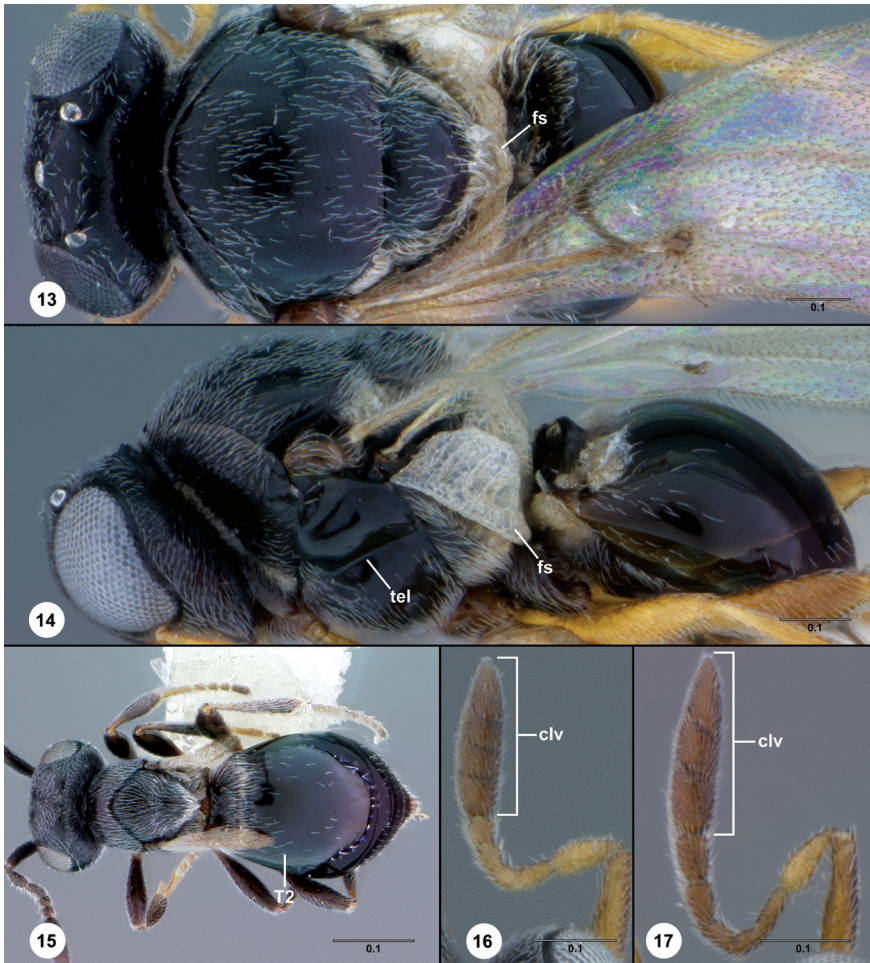
Wings. Color of wings: hyaline. Wing development: macropterous. Length of fore wing: exceeding apex of metasoma. Marginal cilia of fore wing: present. Length of fore wing R: 1/3 length of fore wing. R of fore wing: tubular, remote from costal margin. Shape of knob of R: truncate. Cu of fore wing: spectral. M+Cu of fore wing: spectral. Marginal cilia of hind wing: present, longest along ventral margin. R of hind wing: present, 1/8 length of hind wing.



Figures 8,9. *Calixomeria lasallei* Lahey & Masner, female (USNMENT01197947) **8** head, mesosoma, metasoma, dorsal view **9** head, mesosoma, metasoma, lateral view. Scale bars: in millimeters.



Figures 10–12. *Calomerella scutellata* Masner & Huggert, female (USNMENT00916680) **10** head, mesosoma, metasoma, lateral view **11** mesosoma, dorsal view **12** antenna, ventral view. Scale bars: in millimeters.



Figures 13–17. *Helava* spp. **13** *Helava samantha* Masner & Talamas, male paratype (USNMENT00989200), head, mesosoma, metasoma, dorsal view **14** *Helava samantha* Masner & Talamas, female holotype (USNMENT00989199), head, mesosoma, metasoma, lateral view **15** *Helava microptera* Masner & Talamas, female holotype (USNMENT00989197), head, mesosoma, metasoma, dorsal view **16** *Helava samantha* Masner & Talamas, female holotype (USNMENT00989199), antenna, lateral view **17** *Helava allomera* Masner & Talamas, female holotype (USNMENT00989217), antenna, lateral view. Scale bars: in millimeters.

Male genitalia. Length of basal ring: $2/3$ length of aedeago-volsellar shaft.

Diagnosis. The presence of facial and malar striae, a distally pointed clypeus, 3-merous antennal clava, compound eyes with long setae, setation of the metascutellum, and the absence of foamy structures on the propodeum and metasoma separates *Aleyroctonus* from other members of Sceliotrachelinae. Excluding the clava, these characters are also present in males of the genus, facilitating the identification of specimens of either sex.

Link to distribution map. [<https://hol.osu.edu/map-large.html?id=7857>]



Figures 18–21. *Indomerella vanachterbergi* Buhl, female holotype (RMNH.INS1104989) **18** head, mesosoma, metasoma, dorsal view **19** head, mesosoma, metasoma, lateral view **20** head, anterodorsal view **21** specimen labels.

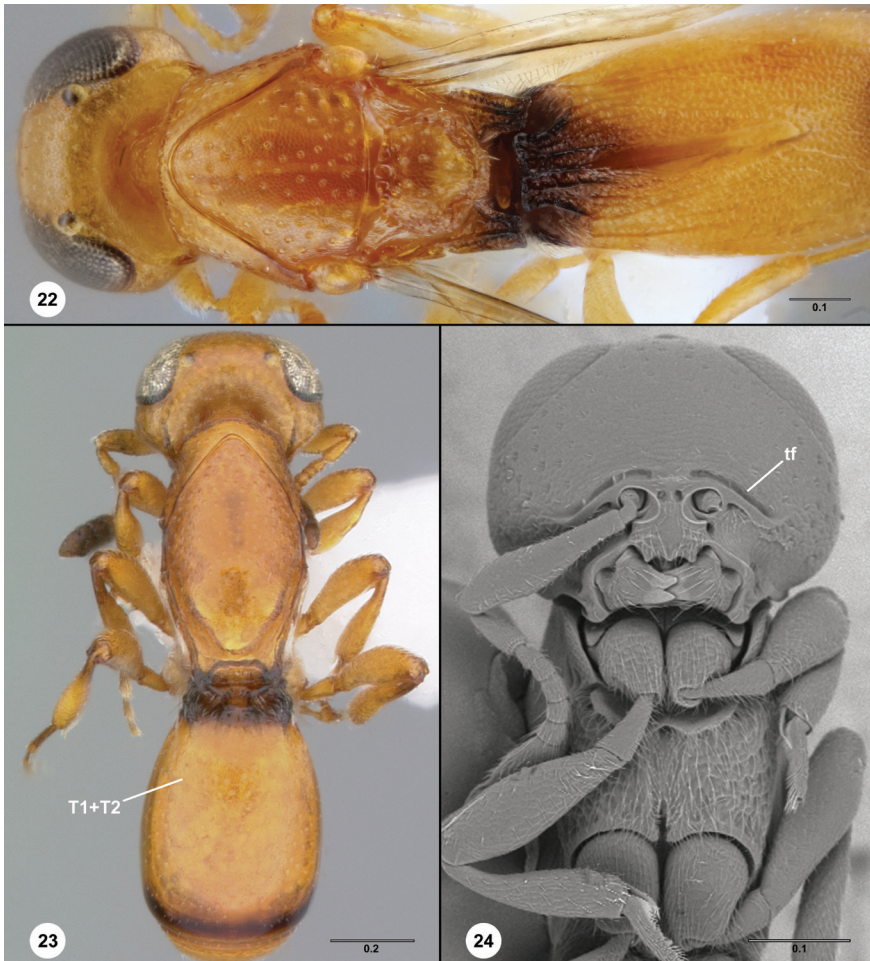
***Aleyroctonus miasmus* Lahey & Polaszek, sp. nov.**

<http://zoobank.org/90A8E729-876E-4297-8A70-BC325E9D401E>

Figures 28–31

Description. Body length of female: 0.96–1.06 mm (n=3). Color of radicle: yellow. Color of mesosoma: brown. Color of metasoma: yellow. Length of LOL: equal to or greater than 2 OD. Length of POL: greater than 2 OD. Genal carina: absent. Length of clava: not longer than A3–A7. Length of A4: approximately as long as A3. Shape of mesoscutum in lateral view: convex. Path of notauli: strongly converging posteriorly. Shape of notaulus: same width throughout. Posterior mesoscutellar sulcus: continuous. Setation of posterior mesoscutellar sulcus: sparse. Sculpture of posterior mesoscutellar sulcus: foveolate. Rim of posterior mesoscutellar sulcus: present. Sculpture of metanotal trough: costate. Prespecular sulcus: present. Sculpture of prespecular sulcus: costate. Setation of metapleuron: dense. Length of metabasitarsus: shorter than tarsomeres 2–5. Setation of anterolateral pits on T2: thin. Rs of fore wing: spectral. M of fore wing: spectral. Rs+M of fore wing: spectral.

Diagnosis. The strongly converging notauli, complete posterior mesoscutellar sulcus, and light coloration of the metasoma make *A. miasmus* a charismatic species that in unlikely to be confused with *A. pilatus* or *A. stanslyi*.



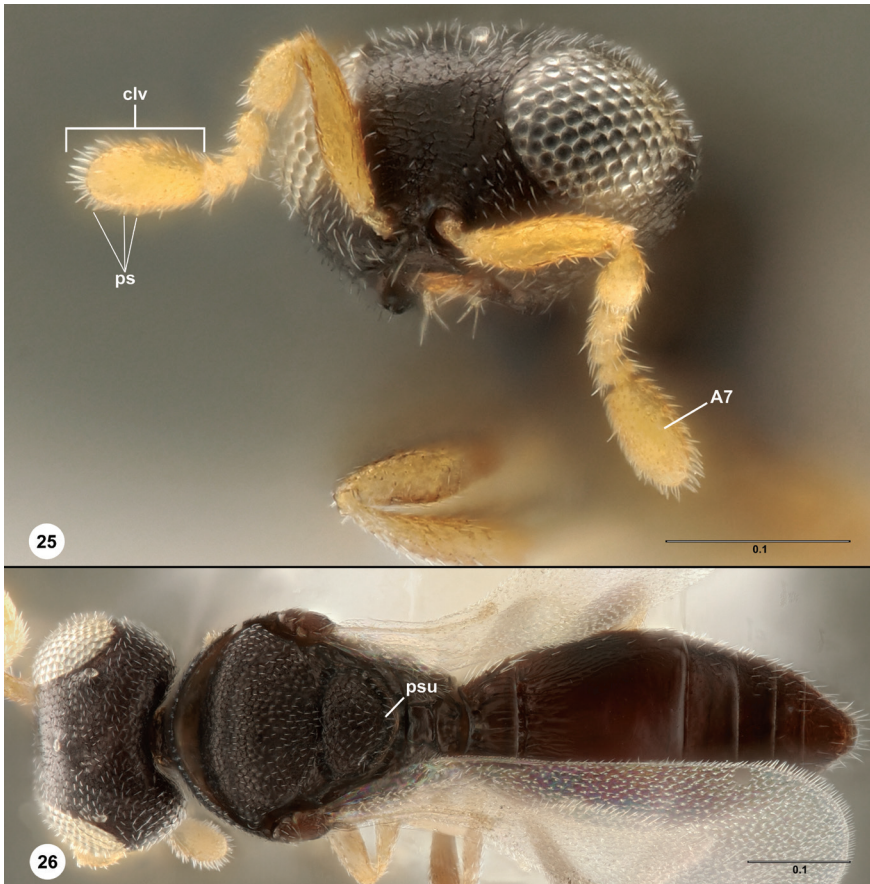
Figures 22–24. *Parabaeus* spp. **22** *Parabaeus* sp., female (USNMENT01197847), head, mesosoma, T1+T2, dorsal view **23** *Parabaeus* sp., female (OSUC 526295), head, mesosoma, metasoma, dorsal view **24** *Parabaeus* sp., female (USNMENT01059128), head, mesosoma, ventral view. Scale bars: in millimeters.

Etymology. The epithet was inspired by the miasma theory of disease, particularly the beaked masks worn by plague doctors during the Black Death of the 12th Century. The epithet is treated as a noun.

Link to distribution map. [<https://hol.osu.edu/map-large.html?id=466911>]

Material examined. Holotype, female: **AUSTRALIA:** QLD, rainforest, Q-23, 17°28'14"S 146°03'48"E, Ella Bay National Park, 21.IX–23.IX.2004, yellow pan trap, L. Masner, OSUC 697908 (deposited in ANIC). Paratypes: **AUSTRALIA:** 2 females, OSUC 697906–697907 (CNCI).

Comments. No significant variation in size was observed in the material examined. The host of *A. miamus* is unknown.



Figures 25, 26. *Pseudaphanomerus hyalinatus* Szelényi, female (FSCA 00090462) **25** head, anterior view **26** head, mesosoma, metasoma, dorsal view. Scale bars: in millimeters.

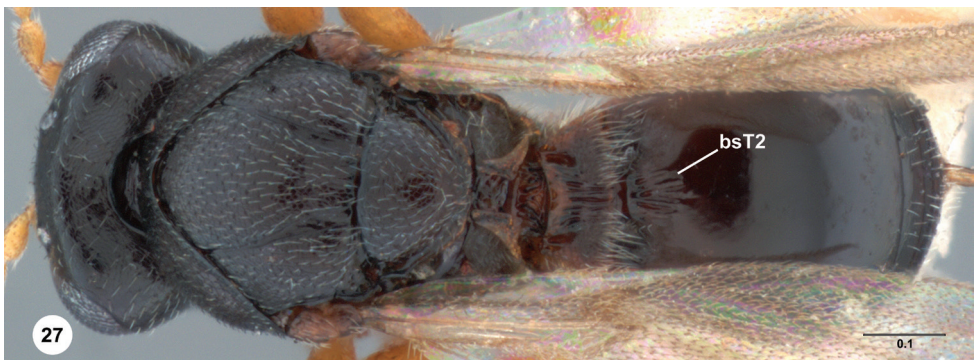
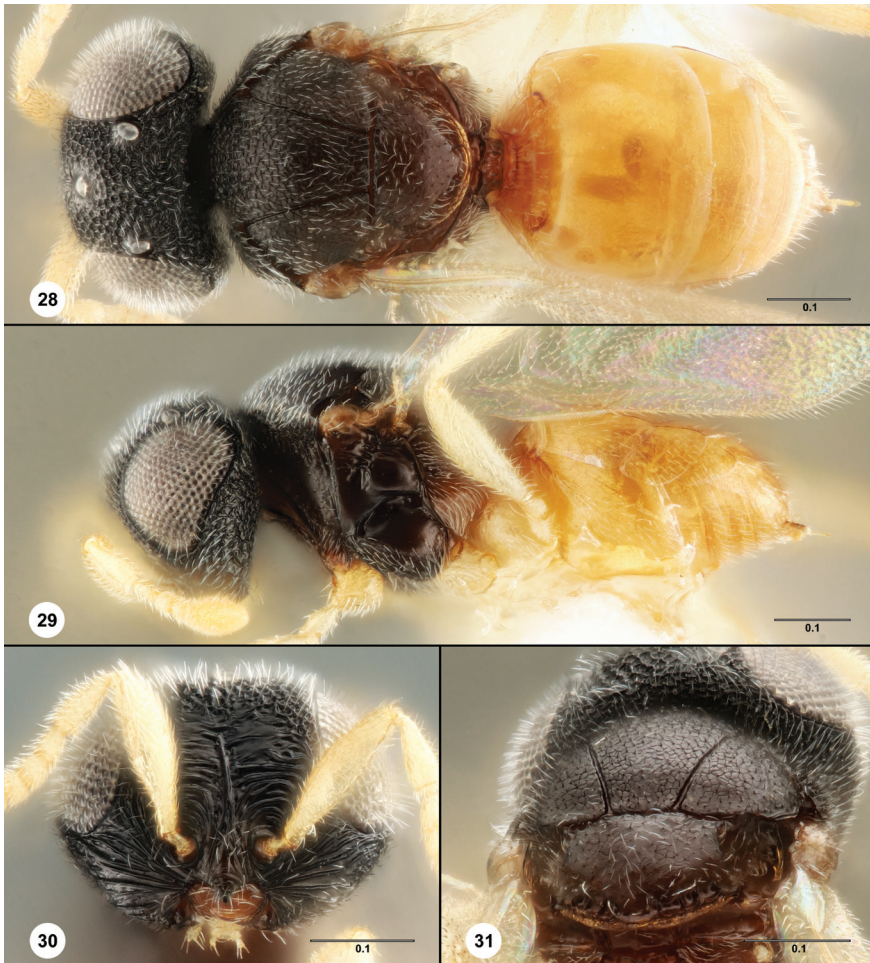


Figure 27. *Tetrabaesus americanus* (Brues), female (USNMENT01109486) **27** head, mesosoma, metasoma, dorsal view. Scale bars: in millimeters.



Figures 28–31. *Aleyroctonus miasmus*, female holotype (OSUC 697908) **28** head, mesosoma, metasoma, dorsal view **29** head, mesosoma, metasoma, lateral view **30** head, anterior view **31** mesosoma, posterodorsal view. Scale bars: in millimeters.

***Aleyroctonus pilatus* Masner & Huggert**

<http://zoobank.org/3245B5E8-3C0A-435E-A389-EED848B464FF>

Figures 32–40

Aleyroctonus pilatus Masner & Huggert, 1989: 38 (original description); Vlug 1995: 10 (cataloged, type information).

Description. Body length of female: 1.18–1.23 mm (n=2). Body length of male: 0.99–1.06 mm (n=2). Color of radicle: yellow; black. Color of mesosoma: black. Color of metasoma: black. Length of LOL: equal to or greater than 2 OD. Length of POL:



Figures 32–34. *Aleyroctonus pilatus*, female holotype (USNMENT01059255) **32** head, mesosoma, metasoma, dorsal view **33** head, mesosoma, metasoma, lateral view **34** head, anterior view. Scale bars: in millimeters.

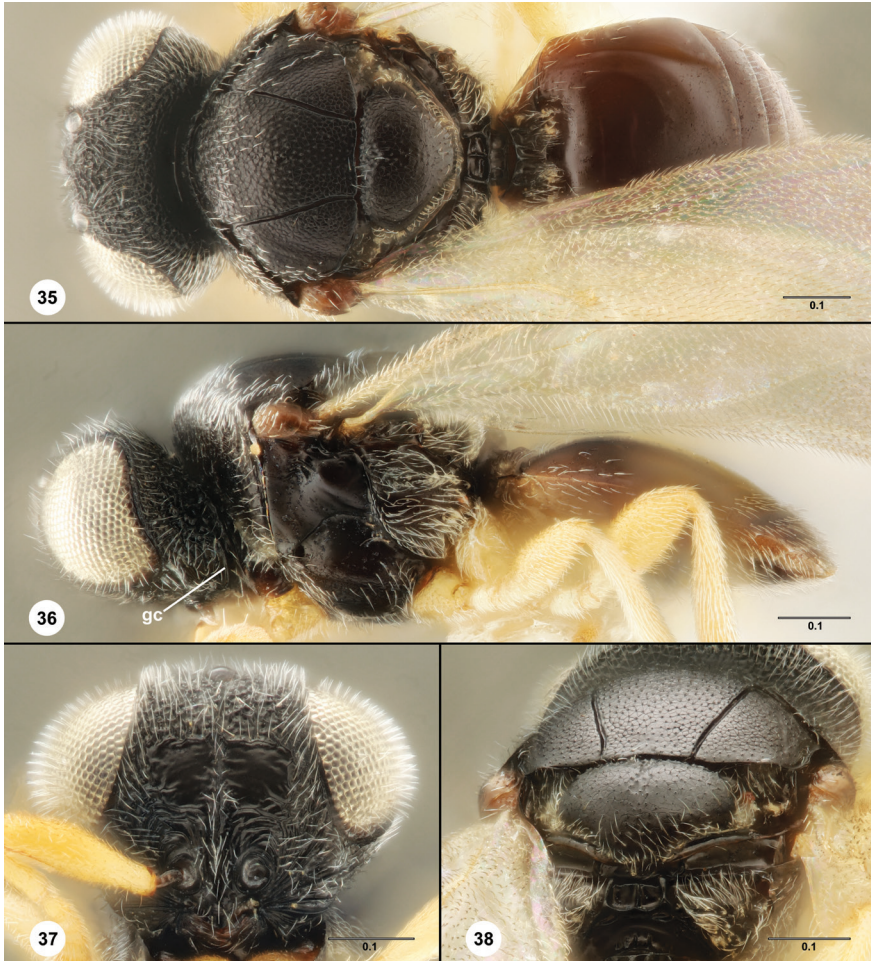
greater than 2 OD. Genal carina: present. Length of clava: longer than A3–A7. Length of A4: approximately as long as A3. Shape of mesoscutum in lateral view: flat to slightly convex. Path of notauli: subparallel. Shape of notaulus: same width throughout. Posterior mesoscutellar sulcus: incomplete medially. Setation of posterior mesoscutellar sulcus: dense. Sculpture of posterior mesoscutellar sulcus: smooth. Rim of posterior mesoscutellar sulcus: absent. Sculpture of metanotal trough: smooth. Prespecular sulcus: absent; present. Sculpture of prespecular sulcus: smooth; weakly costate. Setation of metapleuron: dense. Length of metabasitarsus: shorter than tarsomeres 2–5. Setation of anterolateral pits on T2: dense. Rs of fore wing: spectral. M of fore wing: nebulous. Rs+M of fore wing: nebulous. Shape of ventral aedeagal lobe: rounded.

Diagnosis. The genal carina and ovoid clava that is longer than A3–A7 readily separates *A. pilatus* from other species in the genus.

Link to distribution map. [<https://hol.osu.edu/map-large.html?id=12274>]

Material examined. Paratypes: **MALAYSIA:** 6 females, 2 unsexed, OSUC 697943–697945 (BMNH); OSUC 697946–697950 (CNCI). Other material: **AUSTRALIA:** 3 females, 5 males, OSUC 697909, 697911–697912 (ANIC); OSUC 697918, 697921–697922 (CNCI); NHMUK010370460, OSUC697954 (NHMUK).

Comments. The distribution of this species is expanded to include northeast and southeast Queensland, Australia. In addition, Carver and Reid (1996) mentioned the presence of *A. pilatus* in Papua New Guinea; however, we did not examine specimens from that location.



Figures 35–38. *Aleyroctonus pilatus*, female (OSUC 697921) **35** head, mesosoma, metasoma, dorsal view **36** head, mesosoma, metasoma, lateral view **37** head, anterior view **38** mesosoma, posterodorsal view. Scale bars: in millimeters.



Figure 39. *Aleyroctonus pilatus*, male (OSUC 697912) **39** head, mesosoma, metasoma, lateral view. Scale bar: in millimeters.



Figure 40. *Aleyroctonus pilatus*, male (OSUC 697954) **40** antenna, lateral view. Scale bar: in micrometers.

***Aleyroctonus stanslyi* Lahey & Polaszek, sp. nov.**

<http://zoobank.org/0AAAD651-E536-4DEE-8B00-46DF1FB25DE5>

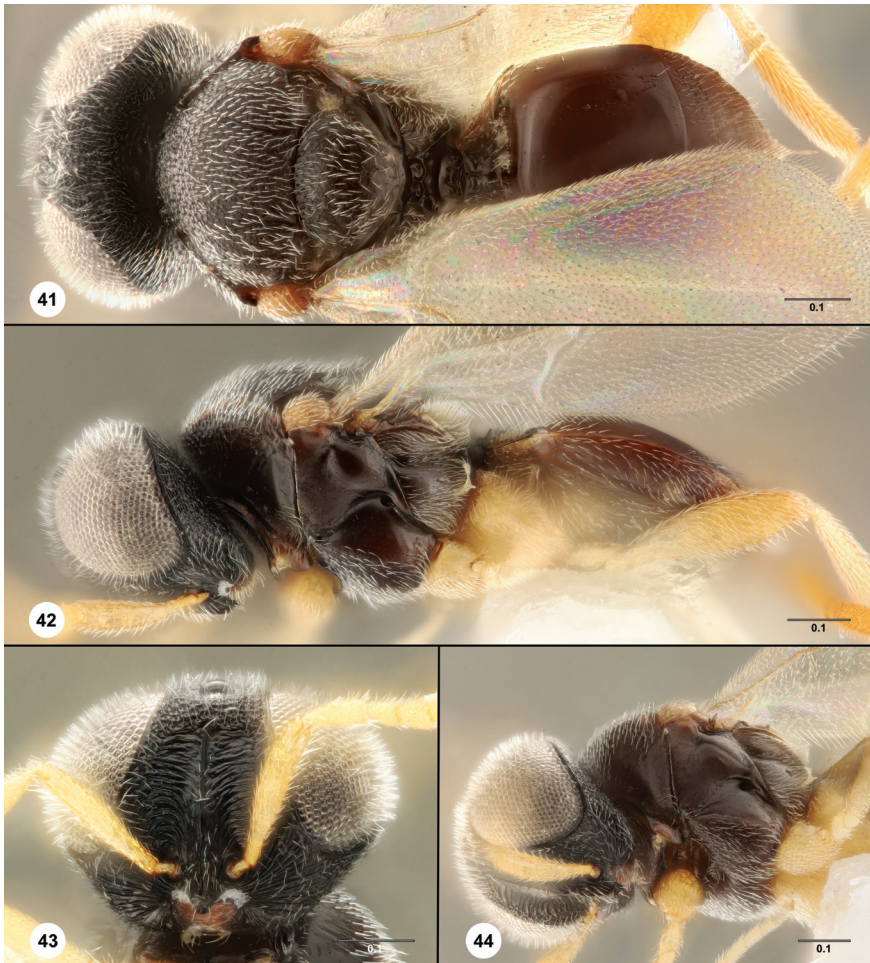
Figures 41–47

Description. Body length of female: 1.21 mm (n=1). Color of radicle: black. Color of mesosoma: black. Color of metasoma: black. Length of LOL: less than 2 OD. Length of POL: approximately 2 OD. Genal carina: absent. Length of clava: not longer than A3–A7. Length of A4: clearly longer than A3. Shape of mesoscutum in lateral view: flat to slightly convex. Path of notauli: subparallel. Shape of notaulus: posteriorly dilated. Posterior mesoscutellar sulcus: incomplete medially. Setation of posterior mesoscutellar sulcus: sparse. Sculpture of posterior mesoscutellar sulcus: smooth. Rim of posterior mesoscutellar sulcus: absent. Sculpture of metanotal trough: smooth. Prespecular sulcus: present. Sculpture of prespecular sulcus: smooth. Setation of metapleuron: medially sparse. Length of metabasitarsus: as long or longer than tarsomeres 2–5. Setation of anterolateral pits on T2: dense. Rs of fore wing: nebulous. M of fore wing: nebulous. Rs+M of fore wing: spectral. Shape of ventral adeagal lobe: truncate.

Diagnosis. *Aleyroctonus stanslyi* is immediately recognizable by its short POL and posteriorly dilated notauli.

Etymology. Named in memory of Philip Anzolut Stansly (Professor of Entomology, University of Florida), former graduate advisor of the first author, authority on integrated pest management, and a world-renowned expert on the biological control of whiteflies. The epithet is treated as a noun in the genitive case.

Link to distribution map. [<https://hol.osu.edu/map-large.html?id=475493>]



Figures 41–44. *Aleyroctonus stanslyi*, female holotype (OSUC 697919) **41** head, mesosoma, metasoma, dorsal view **42** head, mesosoma, metasoma, lateral view **43** head, anterior view **44** head, mesosoma, ventrolateral view. Scale bars: in millimeters.

Material examined. Holotype, female: **AUSTRALIA:** QLD, Beechmont, 4.V.1991, W. I. Farno, OSUC 697919 (deposited in ANIC). Paratypes: **AUSTRALIA:** 15 females, 4 males, OSUC 697910 (ANIC); OSUC 697913–697917, 697920, 697924 (CNCI); 697936–697942, 97952–697953, 697955 (NHMUK); OSUC 697923 (OSUC).

Comments. Host records indicate that *A. stanslyi* is a solitary parasitoid of immature *Aleuroctarthrus destructor* (Mackie) (Hemiptera, Aleyrodidae, Aleyrodicinae) on *Cordyline stricta* (Sims) Endl. (Asparagales, Asparagaceae), the narrow-leaved pond lily. *Aleyroctonus stanslyi* is the ‘*Aleyroctonus* sp. nov.’ discussed by Carver and Reid (1996).

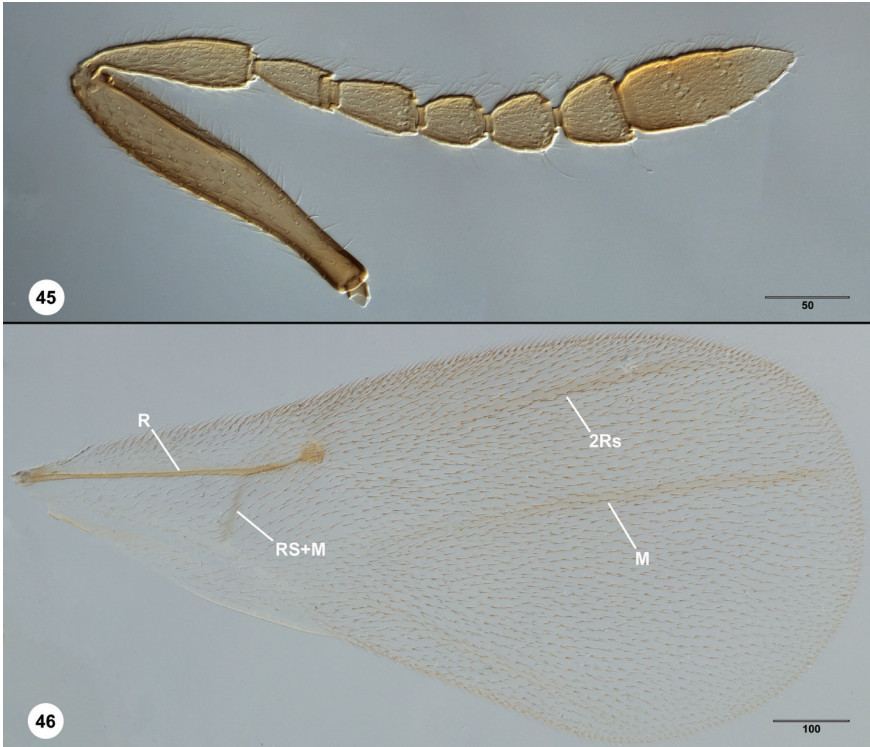


Figure 45, 46. *Aleyroctonus stanslyi*, female paratype (OSUC 697952) **45** antenna, lateral view **46** fore wing, dorsal view. Scale bars: in micrometers.

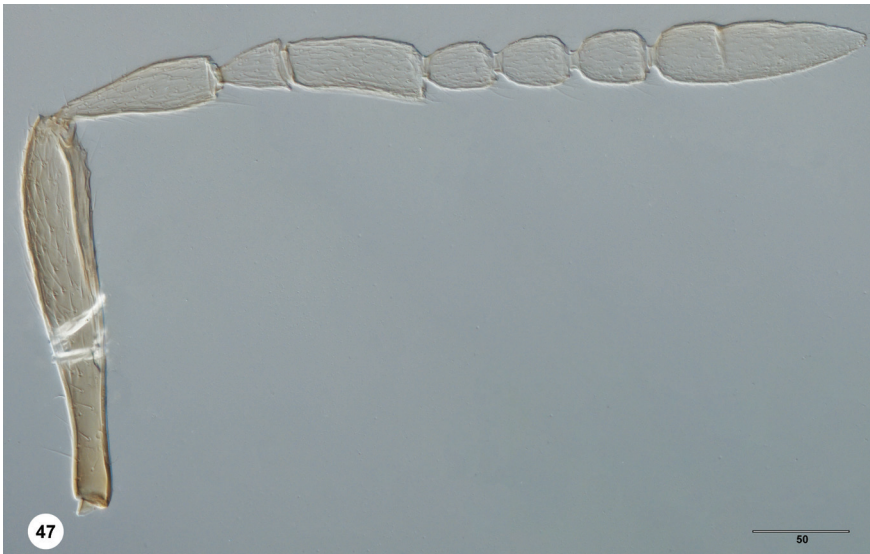


Figure 47. *Aleyroctonus stanslyi*, male paratype (OSUC 697953)

Acknowledgements

We thank L. Musetti and S. Hemly (OSUC) for critical assistance with specimen handling and databasing. Frédérique Bakker (Naturalis Biodiversity Center) for providing images of the *Indomerella vanachterbergi* holotype, and Elijah Talamas (Florida State Collection of Arthropods) and interns at the USNM for providing most of the images used in the manuscript.

References

- Austin AD, Field SA (1997) The ovipositor system of scelionid and platygastriid wasps (Hymenoptera: Platygastroidea): comparative morphology and phylogenetic implications. *Invertebrate Taxonomy* 11: 1–87. <https://doi.org/10.1071/IT95048>
- Bin F (1981) Definition of female antennal clava based on its plate sensilla in Hymenoptera Scelionidae Telenominae. *Redia* 64: 245–261.
- Carver M, Reid IA (1996) Aleyrodidae (Hemiptera: Sternorrhyncha) of Australia – Systematic catalogue, host plant spectra, distribution, natural enemies and biological control. CSIRO Division of Entomology Technical Paper 37: 1–55.
- Johnson NF (1984) Systematics of Nearctic *Telenomus*: classification and revisions of the *podisi* and *phymatae* species groups (Hymenoptera: Scelionidae). *Bulletin of the Ohio Biological Survey* 6: 1–113.
- Lahey Z, Masner L, Johnson NF (2019) *Calixomeria*, a new genus of Sceliotrachelinae (Hymenoptera, Platygastriidae) from Australia. *ZooKeys* 830: 63–73. <https://doi.org/10.3897/zookeys.830.32463>
- Masner L (1980) Key to genera of Scelionidae of the Holarctic region, with descriptions of new genera and species (Hymenoptera: Proctotrupeoidea). *Memoirs of the Entomological Society of Canada* 113: 1–54. <https://doi.org/10.4039/entm112113fv>
- Masner L, Huggert L (1989) World review and keys to genera of the subfamily Inostemmatinae with reassignment of the taxa to the Platygastriinae and Sceliotrachelinae (Hymenoptera: Platygastriidae). *Memoirs of the Entomological Society of Canada* 147: 1–214. <https://doi.org/10.4039/entm121147fv>
- Mikó I, Vilhelmsen L, Johnson NF, Masner L, Péntzes Z (2007) Skeletomusculature of Scelionidae (Hymenoptera: Platygastroidea): head and mesosoma. *Zootaxa* 1571: 1–78. <https://doi.org/10.11646/zootaxa.1571.1>
- Talamas EJ, Johnson NF, Buffington ML, Dong R (2016) *Archaeoteleia* Masner in the Cretaceous and a new species of *Proteroscelio* Brues (Hymenoptera, Platygastroidea). In: Talamas EJ, Buffington ML (Eds) *Advances in the Systematics of Platygastroidea*. *Journal of Hymenoptera Research* 56: 241–261. <https://doi.org/10.3897/jhr.56.10388>
- Vlug HJ (1995) Catalogue of the Platygastriidae (Platygastroidea) of the world (Insecta: Hymenoptera). *Hymenopterorum Catalogus* 19: 1–168. <https://doi.org/10.5281/zenodo.24358>
- Yang SY, Zhong YZ, Zhang JP, Wang XP, Zhang F (2016) A comparative scanning electron microscopy study on antennal sensilla of *Trissolcus japonicus* and *Trissolcus plautiae*, egg

parasitoids of stink bugs (Pentatomidae). *Annals of the Entomological Society of America* 109: 112–120. <https://doi.org/10.1093/aesa/sav104>

Yoder MJ, Mikó I, Seltmann K, Bertone MA, Deans AR (2010) A gross anatomy ontology for Hymenoptera. *PLoS ONE* 5(12): e15991. <https://doi.org/10.1371/journal.pone.0015991>

Supplementary material I

Table S1

Authors: Zachary Lahey, Lubomír Masner, Norman F. Johnson, Andrew Polaszek

Data type: species data

Copyright notice: This dataset is made available under the Open Database License (<http://opendatacommons.org/licenses/odbl/1.0/>). The Open Database License (ODbL) is a license agreement intended to allow users to freely share, modify, and use this Dataset while maintaining this same freedom for others, provided that the original source and author(s) are credited.

Link: <https://doi.org/10.3897/jhr.37.38383.suppl1>

First report of *Telenomus remus* parasitizing *Spodoptera frugiperda* and its field parasitism in southern China

Yong-Lin Liao^{1*}, Bin Yang^{2*}, Miao-Feng Xu³, Wei Lin³, De-Sen Wang⁴,
Ke-Wei Chen⁴, Hua-Yan Chen⁵

1 Institute of Plant Protection, Guangdong Academy of Agricultural Science, Guangdong Provincial Key Laboratory High Technology for Plant Protection, Guangzhou, 510640, China **2** State Key Laboratory for Biology of Plant Diseases and Insect Pests, Institute of Plant Protection, Chinese Academy of Agricultural Sciences, Beijing 100193, China **3** Technical Center of Gongbei Customs District, Zhuhai, 519001, China **4** College of Agriculture, South China Agricultural University, Guangzhou, 510642, China **5** State Key Laboratory of Biocontrol, School of Life Sciences, Sun Yat-sen University, Guangzhou, 510275, China

Corresponding author: Hua-Yan Chen (chenhuayan@mail.sysu.edu.cn)

Academic editor: *Elijah Talamas* | Received 16 August 2019 | Accepted 13 September 2019 | Published 18 November 2019

<http://zoobank.org/E0438BE1-393A-483C-8F12-290AEFD5CF63>

Citation: Liao Y-L, Yang B, Xu M-F, Lin W, Wang D-S, Chen K-W, Chen H-Y (2019) First report of *Telenomus remus* parasitizing *Spodoptera frugiperda* and its field parasitism in southern China. In: Talamas E (Eds) Advances in the Systematics of Platygastridae II. Journal of Hymenoptera Research 73: 95–102. <https://doi.org/10.3897/jhr.73.39136>

Abstract

The fall armyworm, *Spodoptera frugiperda*, is a lepidopteran pest that feeds on many economically important cereal crops such as corn, rice, sorghum, and sugarcane. Native to the Americas, it has become a serious invasive pest in Africa and Asia. Recently, this pest was found in China and has spread quickly across the country. As *S. frugiperda* will most likely become a major pest in China, Integrated Pest Management strategies, including biological control methods, should be developed to manage its populations. Here, we report the detection of *Telenomus remus* parasitizing *S. frugiperda* eggs in cornfields in southern China based on morphological and molecular evidence. Our preliminary surveys indicated that the parasitism rates of *T. remus* on *S. frugiperda* could reach 30% and 50% for egg masses and per egg mass, respectively. Further application of *T. remus* against *S. frugiperda* in biological control programs are discussed.

Keywords

Scelionidae, egg parasitoid, parasitism rates, biological control

* These two authors contributed equally to this work.

Introduction

The fall armyworm, *Spodoptera frugiperda* (Smith) (Lepidoptera: Noctuidae), which originates from tropical and subtropical areas of North, Central, and South America, has become an invasive pest of cereals in Africa, India, Myanmar, Thailand, etc, where it has caused serious damage (Kenis et al. 2019). In China, this species was first detected in the southeast province of Yunnan in January, 2019, and it has quickly spread northward to 17 other provinces (Cui et al. 2019, Jiang et al. 2019). Geographic distribution models have indicated that large parts of China are potentially suitable for the survival of this devastating pest (Lin et al. 2019).

In its native and introduced ranges, *S. frugiperda* feeds on a wide range of crops. Over 350 different host plants in numerous families have been recorded, and almost 40% of them are economically important (Montezano et al. 2018). It is estimated that, just for corn, rice, sorghum and sugarcane, this pest could cause up to 13 billion USD per annum in crop losses in Africa (Day et al. 2017). Given that corn, sugarcane, and rice are widely grown in southern China, *S. frugiperda* will most likely establish as a major pest in this region (Wang et al. 2019). Currently, chemical control is still the main strategy against this pest in China, although some biological control experiments using predators (*Picromerus lewisi* Scott (Hemiptera: Pentatomidae)) have been conducted in the laboratory (Tang et al. 2019). However, in the long run, more biological control strategies should be adopted to against *S. frugiperda* under the perspectives of Integrated Pest Management (IPM).

Among the ~150 parasitoid species that attack *S. frugiperda*, the egg parasitoid species *Telenomus remus* Nixon (Hymenoptera: Scelionidae) appears to be a promising biological control candidate (Kenis et al. 2019) and is reported to attack eggs of various *Spodoptera* species that are known from China (Chou 1987, Tang et al. 2010). In this study, we report the detection of *T. remus* parasitizing *S. frugiperda* eggs and its parasitism rates in cornfields in southern China.

Materials and methods

Field sampling

Eggs of *S. frugiperda* were collected from cornfields of three sites in Guangzhou and Foshan, China, in May and June, 2019 (Table 1). Egg masses were brought to the laboratory and individual egg masses were placed in a 10 cm glass tube and kept in a growth chamber set at $26\text{ }^{\circ}\text{C}\pm 1\text{ }^{\circ}\text{C}$, 40–60% humidity and a 12L:12D light cycle and checked daily for emergence of *S. frugiperda* or parasitoids. Larvae of *S. frugiperda* from the non-parasitized eggs in the same egg mass usually emerged first and were transferred to artificial diet (originally designed for rearing the tobacco cutworm, *Spodoptera litura* (Fabricius)) and reared to adulthood to confirm the identification of the hosts. Any parasitoids that emerged were placed in 100% ethanol for morphological and molecular analyses. The number of eggs in each egg mass, emerged larvae, parasitism and sex ratio of the parasitoids were recorded.

Table 1. Details of the sampling, numbers, and accession numbers of parasitoids sequenced.

Locality (City)	Coordinates	Collection date	Host plant	No. egg mass	No. barcoded	Code & GenBank accession number
Huadu District, Guangzhou	23°29'6.11"N, 113°16'11.99"E	8.vi.2019	corn	28	2	Huadu_F (MN123241) Huadu_M (MN123242)
Panyu District, Guangzhou	23°3'21"N, 113°24'41"E	7.vi.2019	corn	5	2	Panyu_F (MN123243) Panyu_M (MN123244)
Gaoming, Foshan	22°48'22.28"N, 112°34'19.83"E	18.vi.2019	corn	3	2	Gaoming_F (MN123239) Gaoming_M (MN123240)

Species identification

Species of *Telenomus* were determined using the characters of Johnson (1984). Considering the similarity of females between *Telenomus* species, genitalia of males collected from each locality were examined. To confirm morphological identifications, genomic DNA was extracted from a female and male collected from each locality using a nondestructive DNA extraction protocol as described in Taekul et al. (2014). Voucher specimens for all molecular data are deposited in the Museum of Biology at Sun Yat-sen University, Guangzhou, China. Following extraction, the “barcode” region of the mitochondrial cytochrome oxidase subunit 1 (*COI*) was amplified using the LCO1490/HCO2198 primer pair (Folmer et al. 1994). Polymerase chain reactions (PCRs) were performed using Tks Gflex DNA Polymerase (Takara) and conducted in a T100 Thermal Cycler (Bio-Rad). Thermocycling conditions were: an initial denaturing step at 94 °C for 1 min, followed by 5 cycles of 98 °C for 10s, 45 °C for 15s, 68 °C for 30s; 35 cycles of 98 °C for 10s, 52 °C for 15s, 68 °C for 30s and an additional extension at 68 °C for 5 min. Amplicons were directly sequenced in both directions with forward and reverse primers on an Applied Biosystems (ABI) 3730XL by Sangon Biotech (Shanghai, China). Chromatograms were assembled with Sequencing Analysis 6 (ThermoFisher Scientific, Gloucester, UK). All the amplified sequences were deposited into GenBank (accession numbers in Table 1).

Sequences obtained in this study were compared with those analyzed by Kenis et al. (2019). Sequences were aligned by codons using MUSCLE implemented in MEGA6 (Tamura et al. 2013). The alignment was then analyzed using RAXML as implemented in Geneious 11.0.3 with *Gryon cultratum* Masner and *Gryon largi* (Ashmead) (Hymenoptera: Scelionidae) used as outgroups to root the tree.

Photography

Images of live specimens were captured using a Keyence VHX-6000 digital microscope. Images of mounted specimens were produced with Combine ZP and Auto-Montage extended-focus software, using a JVC KY-F75U digital camera, Leica Z16 APOA microscope, and 1X objective lens.

Results

Only one parasitoid species, *Telenomus remus* (Figure 1D), emerged from the 36 egg masses collected from the three sites. The specimens (Figure 1B, 1C) collected from the three sites show no morphological variation and match well with the holotype (Figure 1A) of *T. remus* (deposited in British Museum of Natural History, **BMNH**) as well as the description of this species developed by Nixon (1937) and Chou (1987). The *COI* sequences were identical among females and males sampled from the three collecting sites, and over 99% of the pairs of bases were identical to a series of sequences labeled as *T. remus* available from the Barcoding of Life Data system and the GenBank database. Phylogenetic analysis based on *COI* sequences generated from this study and those used by Kenis et al. (2019) showed that the six specimens collected from the three sites of southern China were grouped well within the clade of *T. remus* specimens collected from Asia, Africa, and the Americas (Figure 2).

Twenty-eight, five, and three egg masses of *S. frugiperda* were collected from Huadu, Panyu, and Gaoming, respectively (Table 1). Of the 36 egg masses collected, 11 egg masses (30.6%) were parasitized by *T. remus*. For the 28 egg masses collected from Huadu, we counted the number of layers of each egg mass, parasitism per egg

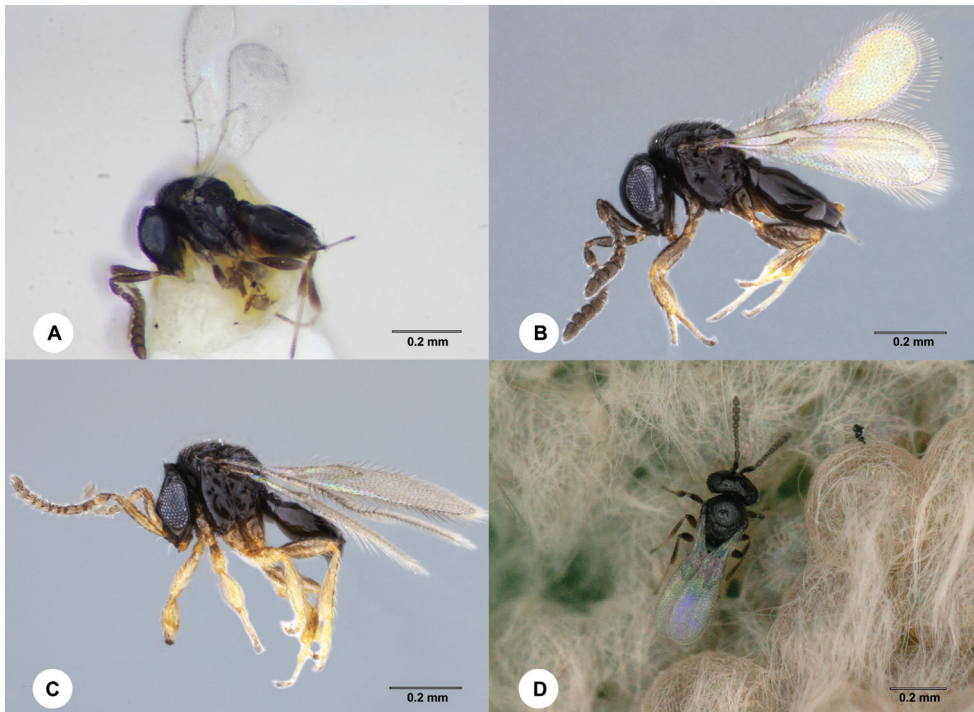


Figure 1. *Telenomus remus* Nixon. **A** Holotype (NHMUK010576395), female, lateral habitus **B** female (SCAU 3040967), lateral habitus **C** male (SCAU 3040968), lateral habitus **D** a female on egg mass of *Spodoptera frugiperda*.

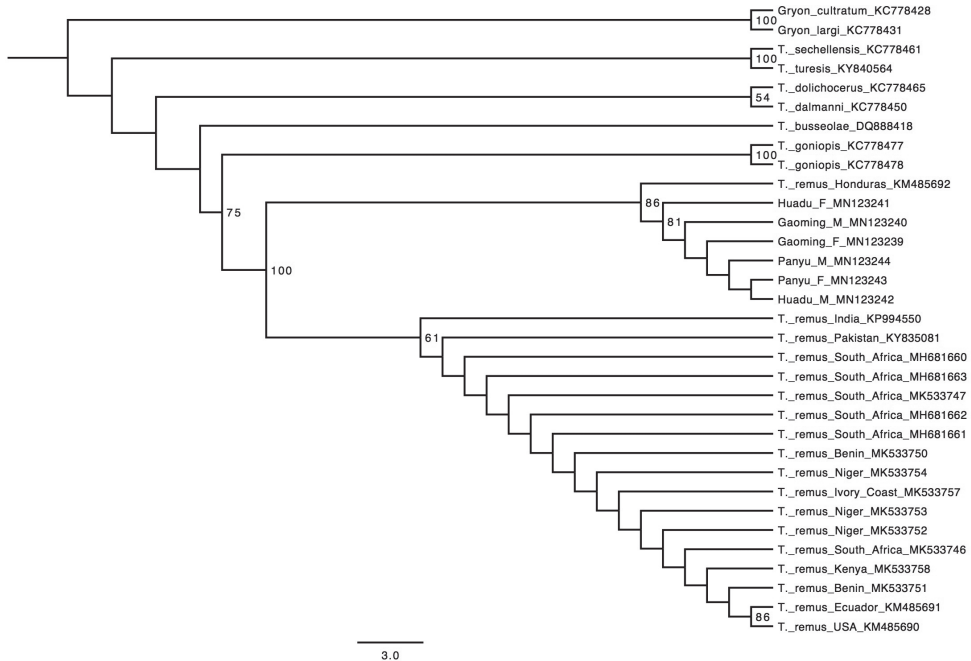


Figure 2. Phylogenetic analysis of *Telenomus remus* and related species by maximum likelihood method based on *COI* sequences. The six sequences generated from this study are indicated with codes and GenBank accession numbers (see Table 1). Bootstrap values above 50 indicated on branches.

mass and parasitoid sex ratio in detail (Figure 3 and Table 2). Of the 28 egg masses, one-layer and two-layer egg masses seem to be dominant (13 of each), followed by three-layer egg masses (3). Of the seven parasitized egg masses, six were two-layer and one was one-layer. The number of eggs of each parasitized egg masses ranges from 64 to 163. The number of emerged *T. remus* adults from these parasitized egg masses ranges from 29 to 87, with $79.2\% \pm 2.14$ females, resulting in an approximate $50.86\% \pm 2.24$ parasitism rate per egg mass.

Discussion

Both morphological and molecular analyses in this study showed that the *Telenomus* species we found attacking *S. frugiperda* eggs in southern China is the promising biological control agent, *T. remus*. In China, this parasitoid species was reported to attack eggs of other *Spodoptera* species, including *S. litura* and *S. exigua* (Hübner) (Chou 1987, Tang et al. 2010), but its identity was not well established. Both our morphological and molecular data confirmed the presence of *T. remus* and its parasitism on *S. frugiperda* eggs in China. *Telenomus* species are generally small and morphologically simplified, rendering them difficult to distinguish and identify. However, in the case

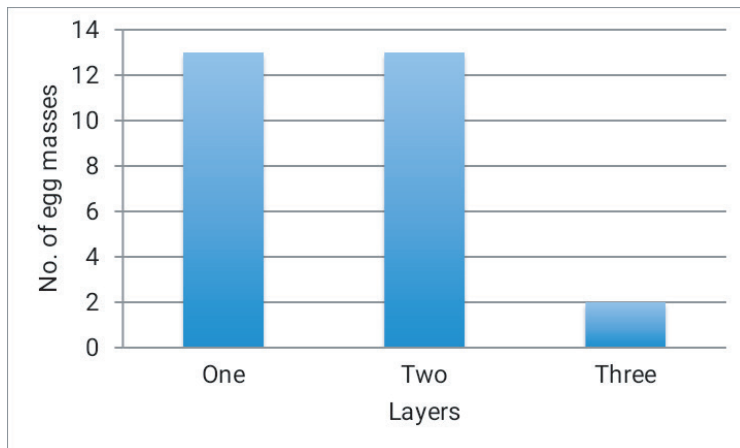


Figure 3. Number of layers in *Spodoptera frugiperda* egg masses.

Table 2. Status of parasitized *Spodoptera frugiperda* egg masses, field parasitism and sex ratio of *Telenomus remus* collected from Huadu, Guangzhou.

Layers per egg mass	No. eggs	No. parasitoids	% parasitism	No. female parasitoids	% female parasitoids
1	76	33	43.42105263	24	72.72727273
2	64	29	45.3125	22	75.86206897
2	103	62	60.19417476	48	77.41935484
2	99	48	48.48484848	38	79.16666667
2	163	87	53.37423313	66	75.86206897
2	79	44	55.69620253	37	84.09090909
2	113	56	49.55752212	50	89.28571429
Total	99.57±12.40	51.29±7.41	50.86±2.24	40.71±5.83	79.2±2.14

of using *T. remus* against *Spodoptera* pests, biological control practitioners should note that the color of the legs is sexually dimorphic (confirmed by *COI* sequences from both sexes) and not indicative of different species. We recommend that a strategy of integrated taxonomy should be applied to identify *Telenomus* species, especially in the case of introducing a parasitoid species into a new region for biological control of pests.

Eggs of *S. frugiperda* are usually laid in masses of approximately 100–200 eggs which are laid in one to three layers on the surface of a leaf (Guo et al. 2019) and the egg mass is usually covered with a layer of scales (setae) from the female abdomen. Our observations showed that *S. frugiperda* females usually lay one-layer and two-layer egg masses and rarely three-layers in cornfields (Figure 3). Although our current data do not allow us to analyze the preference of different egg masses attacked by *T. remus* due to small sample size (Table 2), this parasitoid species seems to be able to parasitize multiple-layer egg masses. We observed that even the bottom layer of a three-layer egg mass can be parasitized by *T. remus*. Determination of how architecture of *S. frugiperda* egg masses affects parasitism rates of *T. remus* requires further investigation and is crucial for mass rearing of *T. remus*.

Studies have shown that *T. remus* has great potential use in augmentative biological control against *S. frugiperda* in the field (Cave 2000). Our observations showed that natural parasitism rates of *T. remus* in corn fields in southern China can reach 30% and 50% for egg masses and per egg mass, respectively. In a study conducted in cornfields in Venezuela, parasitism rates of *T. remus* on *S. frugiperda* reached 90% through inundative release in corn cultivation areas (Ferrer 2001). Further research programs, such as long-term monitoring of natural parasitism and mass release in the field, should be developed for *T. remus* to evaluate its impact on *S. frugiperda* populations in China.

Acknowledgments

We are grateful to David Notton (BMNH) for imaging the holotype of *Telenomus remus*. This study was supported by grants from the Optimization and Popularization of Plant Central Hospital's Information Platform for Remote Diagnosis and Prevention of Diseases and Pests (2016B080802004) and China Postdoctoral Science Foundation (2019M653187).

References

- Cave RD (2000) Biology, ecology and use in pest management of *Telenomus remus*. *Biocontrol News and Information* 21: 21–26.
- Chou LY (1987) [Note on *Telenomus remus* (Hymenoptera: Scelionidae).] *Bulletin of Society of Entomology, National Chung-Hsing University* 20: 15–20.
- Cui L, Rui CH, Li YP, Wang QQ, Yang DB, Yan XJ, Guo YW, Yuan HZ (2019) Research and application of chemical control technology against *Spodoptera frugiperda* (Lepidoptera: Noctuidae) in foreign countries. *Plant Protection*. <https://doi.org/10.16688/j.zwbh.2019300>
- Day R, Abrahams P, Bateman M, Beale T, Clotey V, Cock M, Colmenarez Y, Maizeiani N, Early R, Godwin J, Gomez J, Moreno PG, Murphy ST, Oppong-Mensah B, Phiri N, Pratt C, Silvestri S, Witt A (2017) Fall armyworm: Impacts and implications for Africa. *Outlooks on Pest Management* 28(5): 196–201. https://doi.org/10.1564/v28_oct_02
- Ferrer F (2001) Biological control of agricultural insect pests in Venezuela; advances, achievements, and future perspectives. *Biocontrol News and Information* 22(3): 67–74.
- Folmer O, Black M, Hoeh W, Lutz R, Vrijenhoek R (1994) DNA primers for amplification of mitochondrial cytochrome c oxidase subunit I from diverse metazoan invertebrates. *Molecular Marine Biology and Biotechnology* 3: 294–299.
- Guo JF, Jing DP, Tai HK, Zhang AH, He KL, Wang ZY (2019) Morphological characteristics of *Spodoptera frugiperda* in comparison with three other lepidopteran species with similar injury characteristics and morphology in cornfields. *Plant Protection* 45(2): 7–12.
- Jiang YY, Liu J, Zhu XM (2019) Occurrence and trend of *Spodoptera frugiperda* invasion in China. *China Plant Protection* 39(2): 33–35.

- Johnson NF (1984) Systematics of Nearctic *Telenomus*: classification and revisions of the *podisi* and *phymatae* species groups (Hymenoptera: Scelionidae). Bulletin of the Ohio Biological Survey 6(3): 1–113.
- Kenis M, du Plessis H, Van den Berg J, Ba MN, Goergen G, Kwadjo KE, Baoua I, Tefera T, Buddie A, Cafà G, Offord L, Rwomushana I, Polaszek A (2019) *Telenomus remus*, a candidate parasitoid for the biological control of *Spodoptera frugiperda* in Africa, is already present on the continent. Insects 10(4): 1–92. <https://doi.org/10.3390/insects10040092>
- Lin W, Xu MF, Quan YB, Liao L, Gao L (2019) Potential geographic distribution of *Spodoptera frugiperda* in China based on MaxEnt model [J/OL]. Plant Quarantine. <https://kns.cnki.net/kcms/detail/11.1990.s.20190422.1026.002.html>
- Montezano DG, Sosa-Gómez DR, Roque-Specht VF, Sousa-Silva JC, Paula-Moraes SV, Peterson JA, Hunt TE (2018) Host plants of *Spodoptera frugiperda* (Lepidoptera: Noctuidae) in the Americas. African Entomology 26(2): 286–300. <https://doi.org/10.4001/003.026.0286>
- Nixon GEJ (1937) Some Asiatic Telenominae (Hym., Proctotrupoidea). Annals and Magazine of Natural History 10(20): 444–475. <https://doi.org/10.1080/00222933708655367>
- Taekul C, Valerio AA, Austin AD, Klompen H, Johnson NF (2014) Molecular phylogeny of telenomine egg parasitoids (Hymenoptera: Platygastridae s.l.: Telenominae): evolution of host shifts and implications for classification. Systematic Entomology 39: 24–35. <https://doi.org/10.1111/syen.12032>
- Tamura K, Stecher G, Peterson D, Filipiński A, Kumar S (2013) MEGA6: Molecular Evolutionary Genetics Analysis version 6.0. Molecular Biology and Evolution 30: 2725–2729. <https://doi.org/10.1093/molbev/mst197>
- Tang YL, Chen KW, Xu ZF (2010) Study on ontogenesis of *Telenomus remus* Nixon (Hymenoptera: Scelionidae). Journal of Changjiang Vegetables 18: 1–3.
- Tang YT, Wang MQ, Chen HY, Wang Y, Zhang HM, Chen FS, Zhao XQ, Zhang LS (2019) Predation and behavior of *Picromerus lewisi* Scott to *Spodoptera frugiperda* (J. E. Smith). Chinese Journal of Biological Control. <https://doi.org/10.16409/j.cnki.2095-039x.2019.04.005>
- Wang L, Chen KW, Zhong GH, Xian JD, He XF, Lu YY (2019) Progress for occurrence and management and the strategy of the fall armyworm *Spodoptera frugiperda* (Smith). Journal of Environmental Entomology. <https://kns.cnki.net/kcms/detail/44.1640.Q.20190523.1748.004.html>

Paratelenomus anu Rajmohana, Sachin & Talamas (Hymenoptera, Scelionidae): description and biology of a new species of phoretic egg parasitoid of *Megacopta cribraria* (Fab.) (Hemiptera, Plataspidae)

Keloth Rajmohana¹, James P. Sachin², Elijah J. Talamas³,
Mukundan S. Shamyasree², S. K. Jalali⁴, Ojha Rakshit⁴

1 Zoological Survey of India, P.O New Alipore, Kolkata-700053, West Bengal, India **2** PG & Research Department of Zoology, Malabar Christian College, Calicut-673001, Kerala, India **3** Florida Department of Agriculture and Consumer Services, Division of Plant Industry, Gainesville, FL, USA **4** National Bureau of Agriculturally Important Insects, Bangalore 560024, India

Corresponding author: *Elijah J. Talamas* (talamas.1@osu.edu)

Academic editor: *Matthew Yoder* | Received 3 March 2019 | Accepted 4 June 2019 | Published 18 November 2019

<http://zoobank.org/B367648F-1696-4487-883D-4CD455D316B0>

Citation: Rajmohana K, Sachin JP, Talamas EJ, Shamyasree MS, Jalali SK, Rakshit O (2019) *Paratelenomus anu* Rajmohana, Sachin & Talamas (Hymenoptera, Scelionidae): description and biology of a new species of phoretic egg parasitoid of *Megacopta cribraria* (Fab.) (Hemiptera, Plataspidae). In: Talamas E (Eds) Advances in the Systematics of Platygastridae II. Journal of Hymenoptera Research 73: 103–123. <https://doi.org/10.3897/jhr.73.34262>

Abstract

Paratelenomus anu Rajmohana, Sachin & Talamas, **sp. nov.** (Hymenoptera: Scelionidae) is an egg parasitoid of the kudzu bug, *Megacopta cribraria* (Fab.) (Hemiptera: Plataspidae). It is morphologically and genetically distinct from *P. saccharalis* (Dodd), a well-known egg parasitoid of the same host. *Paratelenomus anu* is here described from India and diagnosed from other species of *Paratelenomus* Dodd. This parasitoid can be reared easily, has high rates of parasitism, and thus may be significant for the biological control of *M. cribraria*. Phoresy is documented in *P. anu* and provides the first known example of this behavior in *Paratelenomus*. *Paratelenomus longus* (Kozlov & Lê) **syn. nov.** and *P. mangrovus* Rajmohana & Narendran, **syn. nov.** are treated as junior synonyms of *P. tetartus* (Crawford), and *P. obtusus* (Lê) **syn. nov.** is treated as a junior synonym of *P. saccharalis*.

Keywords

kudzu bug, phoresy, India, invasive species, biological control

Introduction

Megacopta cribraria (Fab.) (Hemiptera: Plataspidae), commonly called the kudzu bug, the lablab bug, the bean plataspid, or the globular stink bug, is native to Asia, including the Indian subcontinent, and Australia (Srinivasaperumal et al. 1992, Hua 2000, Eger et al. 2010). This bug is a voracious feeder on kudzu and numerous agricultural crops including soy bean (Zhang 1985), lablab bean (Schaeffer and Panizzi 2000), pigeon pea (Hoffmann 1932), *Phaseolus* group (Hoffmann 1931, Easton and Pun 1997), broad beans (Ishihara 1950), peach (*Amygdalus persica* L.), and jujube (*Ziziphus jujube* Mill.) (Wang et al. 1996, Li et al. 2001, Wang et al. 2004). The invaded range now includes the United States where it feeds on the kudzu plant, *Pueraria montana* Lour. (Merr.) (Zhang et al. 2012), an economically important invasive weed (Suiter et al. 2010, Gardner et al. 2013b).

Eger et al. (2010) reported several hymenopteran parasitoids from the eggs of *M. cribraria*, including *Encarsia boswelli* (Girault) (Aphelinidae), *Ablerus* Howard (Aphelinidae), *Ooencyrtus nezarae* Ishi (Encyrtidae), *Trissolcus latusulcus* (Crawford) (Scelionidae), and *Paratelenomus saccharalis* (Dodds) (Scelionidae). *Paratelenomus saccharalis*, which was once restricted to the eastern Hemisphere, has been found in the United States parasitizing the eggs of *M. cribraria* (Gardner et al. 2013a, Medal et al. 2013). In this paper we describe another egg parasitoid from India, *Paratelenomus anu* Rajmohana, Sachin and Talamas sp. nov., from the same host, and provide notes on its behavior, distribution and parasitism rate, and provide updates to the taxonomy of other species of *Paratelenomus*.

Materials and methods

Collection of parasitoid and host

Surveys were conducted at five different localities in Calicut district, in the South Indian state of Kerala, from June 2015 until 2017, where *Lablab purpureus* (L.) plants were grown and incidence of *M. cribraria* was noticed (Table 1). Adult bugs, on which the parasitoids were phoretic, were also collected from the field (Fig.1). Several egg masses of *M. cribraria* were collected from these localities and brought into the laboratory. The egg masses were kept for rearing in small transparent plastic containers (8×11 cm) and kept at ambient temperature. The number of host bugs and the parasitoids that emerged from the eggs were recorded. The parasitoids recovered were preserved in ethyl alcohol (100%) for taxonomic study or kept alive in the laboratory by providing 20% honey solution as food. The rates of parasitism and bug emergence were calculated from field-collected and laboratory-reared eggs by comparing the number of parasitoids and nymphs that emerged from each egg mass to the number of eggs collected, respectively. The identity of *M. cribraria* was confirmed by the expertise available at the University of Agricultural Sciences, Bangalore, Karnataka, and the identity of the legumes were confirmed by the Department of Botany, University of Calicut, Kerala.

Microscopy

The preserved wasps were glued to the tip of point cards and examined with Leica M 205A and Zeiss V8 stereo microscopes. Extended-focus images were produced with two systems: a Leica DFC 500 camera attached to a Leica M 205 A stereomicroscope with images combined using the Leica Application Suite, and a Macroscopic Solutions Macropod Micro Kit with images combined in Helicon Focus. Scanning electron microscopy was performed with a Hitachi SU6600 Variable Pressure Field Emission Scanning Electron Microscope (FESEM) and a Hitachi TM3000 Tabletop Microscope.

Cybertaxonomy

The data associated with these specimens is deposited in the Hymenoptera Online Database (hol.osu.edu). The online systematics and taxonomy tool, vSysLab (vsyslab.osu.edu), was used to generate the material examined sections and taxonomic synopses. Morphological terms were matched to concepts in the Hymenoptera Anatomy Ontology using the text analyzer function and a table of these terms and URI links is provided in Suppl. material 1.

Collections

This study is based on specimens deposited in the following institutions.

CNCI	Canadian National Collection of Insects, Ottawa, Canada
IEBR	Institute for Ecology and Biological Resources, Hanoi, Vietnam
USNM	National Museum of Natural History, Washington, DC, USA
ZSIC	National Zoological Collection, Zoological Survey of India, Kolkata, India
ZSIK	National Zoological Collection, Zoological Survey of India, Calicut, India

DNA barcoding

DNA was extracted from the whole insect using Qiagen DNeasy kit, following the manufacturer's protocols. The extracts were subjected to PCR amplification of a 658 bp region near the 5' terminus of the CO1 gene following standard protocol (Hebert et al. 2004). Primers used were: forward primer (LCO 1490: 5'-GGTCAACAAATCAT-AAAGATATTGG-3'), and reverse primer (HCO 2198: 5'-TAAACTTCAGGGT-GACCAAAAATCA-3'). PCR reactions were carried out in 96-well plates, 50 µL reaction volume containing: 5 µL GeNei™ Taq buffer, 1 µL GeNei™ 10mM dNTP mix, 2.5 µL (20 pmol/µL) forward primer, 2.5 µL (20 pmol/µL) reverse primer, 1 µL GeNei™ Taq DNA polymerase (1 U/µL), 2 µL DNA (50 ng/µL), and 36 µL sterile

Table 1. Egg emergence data for nymphs of *Megacopta cribraria* and adults of *Paratelenomus anu* by egg mass.

Locality	Date eggs were laid	# of eggs in mass	# of days until first emergence	# of male <i>P. anu</i> emerged	# of female <i>P. anu</i> emerged	# of nymphs emerged	# of unhatched eggs
Calicut – Malaparamba near providence college, Lat. 11.292975 Long -75.803572	9/6/15	22	13	2	16	3	1
	12/6/15	24	12	3	12	2	7
	16/6/15	18	12	1	13	4	0
	27/6/15	16	12	3	8	2	3
	8/7/15	26	13	4	16	1	5
	16/7/15	24	12	3	17	3	1
	24/7/15	18	13	2	12	0	4
	27/7/15	24	14	1	17	0	6
	28/7/15	26	13	2	18	5	1
	1/8/15	24	13	3	18	0	3
	6/8/15	16	13	2	10	0	3
	6/8/15	22	12	4	14	2	2
	20/8/15	24	13	4	16	3	1
	20/8/15	20	13	1	14	2	3
26/8/15	22	13	3	16	2	1	
Calicut University, Lat. 11.131442 Long -75.894595	6/10/15	28	14	2	16	4	6
	6/10/15	26	14	3	17	2	4
	6/10/15	38	13	4	22	7	5
	6/10/15	36	14	2	30	2	2
	6/10/15	24	12	1	17	3	3
	6/10/15	28	13	2	20	0	6
	12/10/15	24	12	2	16	0	6
	12/10/15	26	13	2	18	5	1
	12/10/15	24	14	3	18	0	3
	8/12/15	22	12	1	15	2	4
Koylandi- Nelluli tazham, Lat. 11.472937 Long -75.676152	8/12/15	16	14	2	11	0	3
	8/12/15	24	13	3	14	4	3
	8/12/16	22	13	3	12	3	4
	8/12/16	16	14	1	11	1	3
	8/12/16	16	14	2	9	0	5
	8/12/16	10	12	1	7	0	2
	8/12/16	30	13	4	13	9	4
	8/12/16	27	13	3	18	3	3
Kunnamangalam Markaz, Lat. 11.306922 Long -75.894595	8/12/16	32	14	2	21	4	5
	8/12/16	29	12	3	17	5	4
	3/9/16	22	14	2	11	3	6
	3/9/16	24	14	3	15	4	2
	3/9/16	18	13	2	12	1	3
	3/9/16	25	12	3	13	5	4
	6/9/16	12	14	1	8	0	3
	6/9/16	14	12	2	8	0	4
6/9/16	20	13	1	16	0	3	
6/9/16	25	14	4	14	2	2	

Locality	Date eggs were laid	# of eggs in mass	# of days until first emergence	# of male <i>P. anu</i> emerged	# of female <i>P. anu</i> emerged	# of nymphs emerged	# of unhatched eggs
Palayattunada Maniyoora Rd Pathiyarakkara Kerala India, Latitude: 11.573128 Longitude: 75.617743	2/2/17	10	12	1	6	0	3
	2/2/17	24	13	2	16	2	4
	2/2/17	25	14	4	15	3	3
	2/2/17	26	13	3	14	5	4
	2/2/17/2/17	26	13	2	17	0	7
	2/2/17	28	14	3	17	5	3
	2/2/17	29	13	4	18	3	4
	2/2/17	30	14	3	15	7	5
	2/2/17	22	12	2	14	3	3
	9/2/17	36	14	3	23	4	6
	9/2/17	40	14	4	27	2	7
	9/2/17	17	13	1	9	3	4
	9/2/17	23	13	2	15	2	4
	18/2/17	18	12	2	13	0	3
	18/2/17	14	14	2	9	0	3
18/2/17	12	14	1	8	0	3	
18/2/17	12	13	1	6	2	3	
Nallalam-padam bus stop, Lat 11.258753N Long 75.780411E	19/7/18	66	14	9	37	10	10

water. Thermo cycling consisted of an initial denaturation of 94 °C for 5 minutes, followed by 30 cycles of denaturation at 94 °C for 1 minute, annealing at 55 °C for 1 minute and extension at 72 °C for 1 minute using a C1000™ Thermal Cycler. The amplified products were analyzed on a 1.5% agarose gel electrophoresis as described by Sambrook and Russell (2001), sequenced, and uploaded to Genbank (accession number KT896660.1, see Suppl. material 2).

Results

Taxonomy

Paratelenomus anu Rajmohana, Sachin & Talamas, sp. nov.

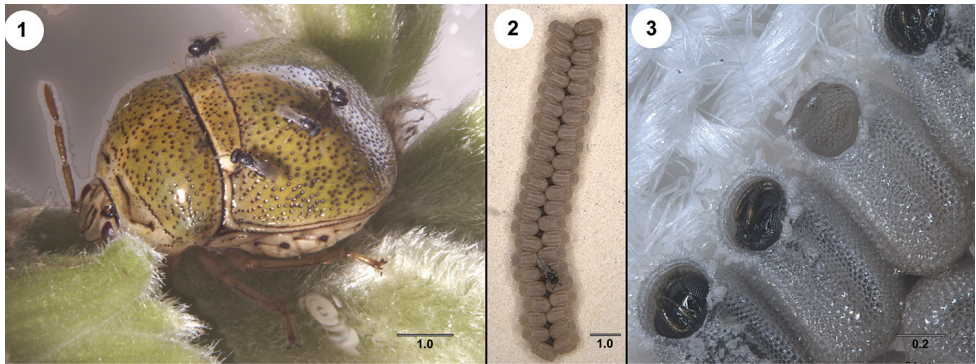
<http://zoobank.org/B367648F-1696-4487-883D-4CD455D316B0>

http://bioguid.osu.edu/xbiod_concepts/486304

Figures 1–8

Description. Body length. Female: 0.65–0.71mm. Male: 0.66–0.68mm.

Color. Body black to honey brown; first metasomal tergite slightly xanthic, weakly contrasting with posterior metasomal segments; antenna and legs yellow to brown; wings hyaline; wing venation brown.



Figures 1–3. 1 *Megacocta cribraria* with phoretic *Paratelenomus anu* 2 female of *P. anu* on eggs of *M. cribraria* 3 individuals of *P. anu* prior to emergence from eggs of *M. cribraria*.

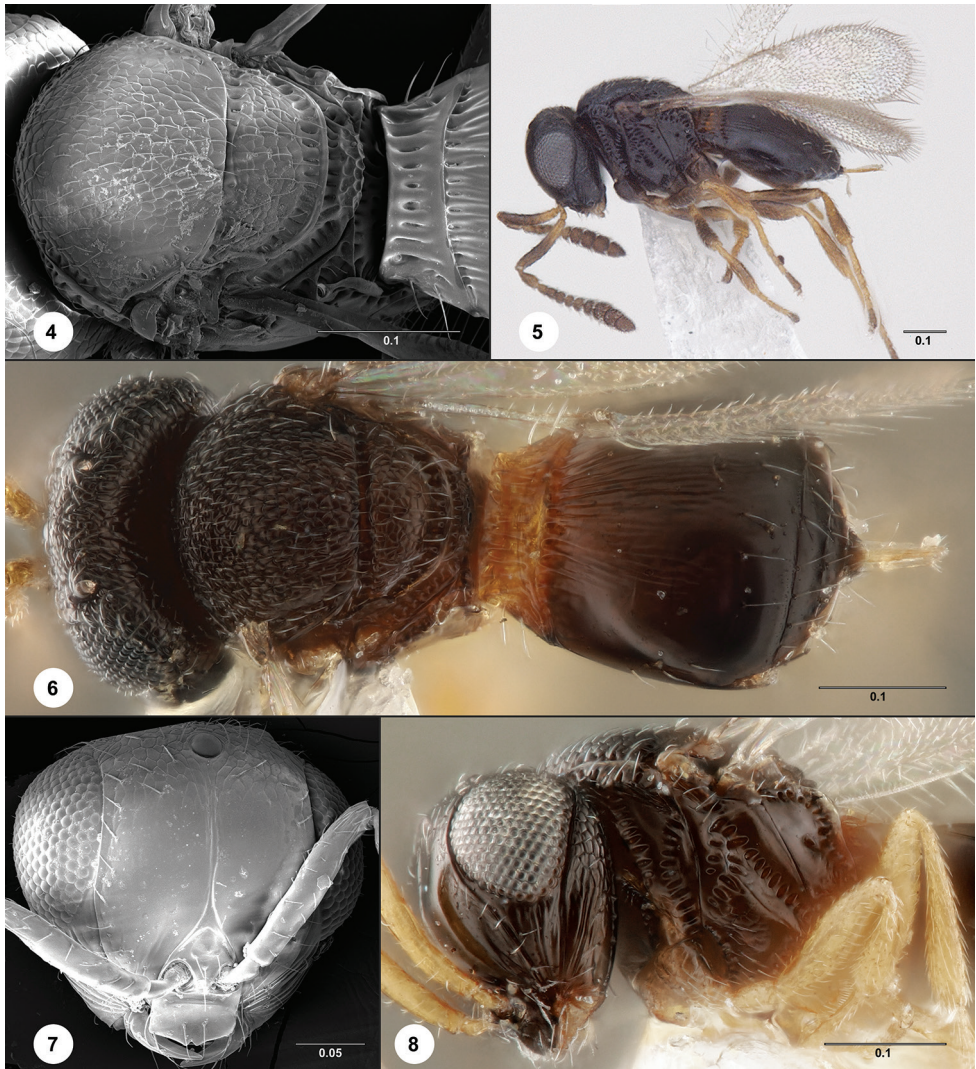
Head. Frons mostly smooth with coriaceous sculpture dorsally; central keel attenuated dorsally, not bifurcating around median ocellus; submedian carina absent; orbital carina present; a single row of equidistant setae present along orbital carina; gena dorsally coriaceous, as on vertex, but smooth toward mandibular articulation; occipital carina incomplete medially; crenulae arising from occipital carina short; labrum pentagonal, slightly more than 2× wider than long, apex bidentate medially; antennal clava 4-merous; claval formula A11–A8: 1-2-2-1; A5 in males with tyloid.

Mesosoma. Notauli absent to weakly present posteriorly; mesoscutum with coriaceous sculpture; parapsidal lines present; mesoscutal humeral sulcus and mesoscutal suprahumeral sulcus indicated by cells; transscutellar articulation narrowed medially, wider and crenulate laterally; foveae of posterior mesoscutellar sulcus of uniform size; mesoscutellum abutting mesoscutum medially; disc of mesoscutellum semicircular, with coriaceous sculpture; setal bases on mesoscutellum simple, not pustulate; metascutellum rugulose; mesopleural carina absent; intercoxal space narrow, not completely occluded by postacetabular and mesopleural epicoxal sulci; acetabular field small, finely setose, and coriaceous; episternal fovea present; femoral depression weakly indicated; prespecular sulcus present; metapleural triangle present; metapleural carina present; paracoxal sulcus absent; posterodorsal metapleural sulcus present.

Metasoma. T1 longitudinally costate, with two lateral setae; T2 striate, striae absent in lateral and posterior portions of tergite.

Male. Similar to female, except antennae filiform and metasoma with 8 external tergites and 7 external sternites.

Diagnosis. *Paratelenomus anu* does not fully follow either lead of the first couplet in the key to species of *Paratelenomus* by Johnson (1996) because the notauli are weakly present at the posterior margin of the metasoma (best seen in anterodorsal view) and may appear absent. Otherwise, *P. anu* matches the second lead based on the medially narrowed transscutal articulation and the presence of just two lateral setae on T1. By following the second lead of the couplet one would arrive at *P. saccharalis*, which is morphologically very similar to *P. anu*. They can be separated by the notaulus, which is well developed in *P. saccharalis* and extends for more than half the length of the mesoscutum; the central keel,



Figures 4–8. *Paratelenomus anu* **4** female (FSCA 00090272) mesosoma, dorsal view **5** holotype female (ZSI/WGRS/I.R-INV.5069) lateral habitus **6** female paratype (CNC494970), head, mesosoma, metasoma, dorsal view **7** female paratype (FSCA 00090272), head, anterior view **8** female paratype (CNC494969), head and mesosoma, lateral view. Scale bars: in millimeters.

which does not bifurcate around the median ocellus in *P. anu*; and the interorbital space, which in *P. anu* is 1.25× eye height and in *P. saccharalis* is slightly less than eye height.

Etymology. The species is named ‘anu’ because of its small size. (In Sanskrit ‘anu’ is the equivalent for the smallest unit of matter). The name is treated as a noun in apposition.

Material examined. Holotype, female: **INDIA:** Kerala St., Malapparamba, near Providence College, 9.VI.2015, J. Sachin, ZSI/WGRS/I.R-INV.5069 (deposited in ZSIK). Paratypes: **INDIA:** 17 females, 2 males, CNC494969–494970 (CNCI); 21987/H3–21999/H3 (ZSIC); ZSI/WGRS/I.R-INV.5070–5073 (ZSIK).

Comments. A central keel that dorsally bifurcates around the medial ocellus was listed by Johnson (1996) as a generic character for *Paratelenomus* and was used to distinguish it from *Psix* Kozlov & Lê. In *P. anu*, the central keel dorsally attenuates and does not bifurcate around the median ocellus and thus this character does not unambiguously separate *Psix* from *Paratelenomus*, although it remains useful for identifying other species of *Paratelenomus*. The other characters presented by Johnson (1996) remain valid for *Paratelenomus* and it is based on these that we are confident in the generic placement of *P. anu*: head and mesosoma without rugose-reticulate sculpture; mandibles narrow, sicklelike, unidentate and broadly overlapping; paracoxal and meta-pleural sulci absent.

Sequence analysis. The CO1 sequence of *Paratelenomus anu* (KT896660.1) was analyzed using the online BLAST tool of NCBI for comparison with other sequences in the GenBank database. We found *P. anu* showed 85% sequence identity with *P. saccharalis* (KC778442.1) with 520/628 identities, and 7 gaps that accounted for about 1% of the total alignment length. This degree of sequence divergence is congruent with treatment of *P. saccharalis* and *P. anu* as separate species.

Parasitism. The host eggs collected from all locations contained both parasitized and unparasitized eggs. In the laboratory, *M. cribraria* nymphs emerged from almost all unparasitized eggs within five days of collection, while the parasitoids emerged within 11–13 days. Male wasps were usually the first to emerge and remained on the egg mass for emergence of the females, with which they immediately mated for 12–15 sec. Following copulation, males continued waiting for the emergence of additional females. Among all the egg batches collected, the maximum number of males that emerged from an egg mass was four. Each egg mass had an average of 22.97 ± 6.41 eggs. The percent emergence of male and female parasitoids was 10.3 % and 63.2 % whereas the remainder (26.4%) were nymphs. This female-biased sex ratio enhances the potential of this parasitoid to be developed as a biocontrol agent against *M. cribraria* (Ode and Hardy 2008) (Table 2). It was also observed in the laboratory that, immediately after mating, the parasitoid females mounted the dorsal abdomen of *M. cribraria* in the vicinity and remained phoretic.

Parasitoid efficiency. The parasitism rate was $73.7 \pm 7.3\%$ for field-collected egg masses and $75.9 \pm 3.5\%$ for egg masses reared in the laboratory. Among the parasitized egg masses, nymph emergence was 10.39% for field-collected eggs and 7.58% in the laboratory (Table 2).

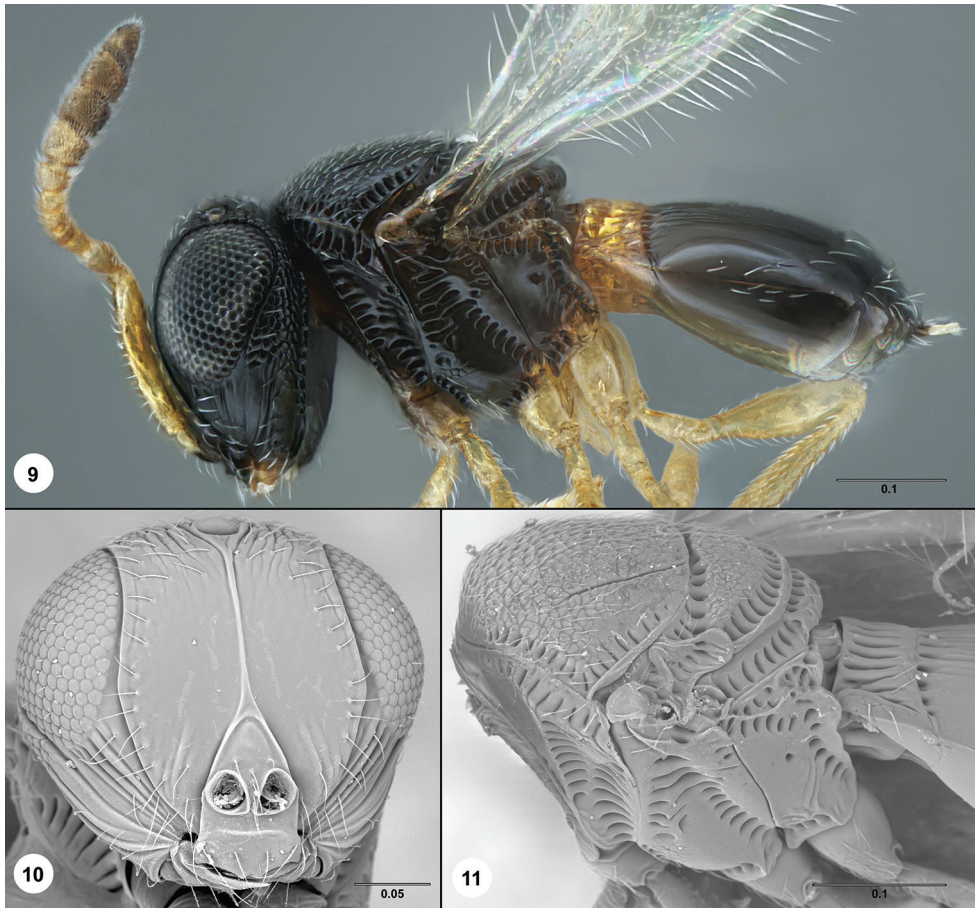
Table 2. Comparison of emergence rates of *Megacocta cribraria* nymphs and adults of *Paratelenomus anu* from laboratory-reared and field-collected egg masses. Percentages in parentheses are based on total number of eggs.

Locations	# of egg masses	total # of eggs	total # of nymphs emerged	total # of <i>P. anu</i> emerged	total # of male egg parasitoids emerged	total # of female egg parasitoids emerged	total # of unhatched eggs
Laboratory	31	686	52 (7.58%)	521 (75.95%)	67 (9.77%)	454 (66.18%)	165 (24.05%)
Field	64	1473	153 (10.39%)	1086 (73.73%)	150 (10.18%)	936 (63.54%)	387 (26.27%)

New Synonymies***Paratelenomus saccharalis* (Dodd)**http://bioguid.osu.edu/xbiod_concepts/3343

Figures 9–16

Telenomus saccharalis Dodd, 1914: 293 (original description).*Aphanurus Graeffei* Kieffer, 1917: 343 (original description); Johnson 1996 : 282 (junior synonym of *Telenomus saccharalis* Dodd); Johnson 1996 : 282 (junior synonym of *Paratelenomus saccharalis* (Dodd)).*Liophanurus saccharalis* (Dodd): Kieffer 1926 : 64, 71 (description, generic transfer, keyed).*Microphanurus graeffei* (Kieffer): Kieffer 1926 : 91, 100 (description, generic transfer, keyed).*Asolcus minor* Watanabe, 1954: 20, 21 (original description. Keyed); Johnson 1996 : 282 (junior synonym of *Telenomus saccharalis* Dodd); Johnson 1996 : 282 (junior synonym of *Paratelenomus saccharalis* (Dodd)).*Aporophlebus graeffei* (Kieffer): Kozlov 1970 : 216 (description, generic transfer); Kononova 1973 : 439 (description, keyed); Kozlov and Lê 1976: 348 (keyed); Mineo 1979 : 234 (description).*Archiphanurus graeffei* (Kieffer): Szabó 1975 : 269 (description, generic transfer, neotype designation); Kozlov 1978 : 646 (description); Kozlov and Kononova 1983: 136 (description); Kononova 1995 : 98 (keyed); Kononova 1995 : 98 (keyed).*Archiphanurus obtusus* Lê, 1982: 145 (original description); Lê 1997 : 24 (keyed); Lê 2000 : 249, 252 (description, keyed, type information).*Archiphanurus minor* (Watanabe): Bin and Colazza 1988: 33 (generic transfer); Yamagishi 1990 : 193 (systematic position, type information).*Paratelenomus saccharalis* (Dodd): Johnson 1988 : 231 (type information, generic transfer); Johnson 1992 : 564 (cataloged, type information); Johnson 1996 : 278, 282 (description, synonymy, keyed); Johnson 1996 : 278, 282 (description, synonymy, keyed); Rajmohana and Narendran 2007: 2523 (keyed); Saminet al. 2012: 19 (new distribution record for Iran); Rajmohana K. & Peter 2013 : 22 (description); Talamas et al. 2015: 52 (keyed).*Aporophlebus minor* (Watanabe): Ryu and Hirashima 1989: 50 (description).*Paratelenomus graeffei* (Kieffer): Johnson 1992 : 563 (cataloged, type information).*Paratelenomus minor* (Watanabe): Johnson 1992 : 564 (cataloged, type information).*Paratelenomus obtusus* (Lê) syn. nov.: Johnson 1992 : 564 (cataloged, type information).**Material examined.** Holotype, female, *Archiphanurus obtusus*: **VIETNAM**: Hanoi Prov., Hanoi, 29.V.1979, IEBR 0050 (deposited in IEBR).**Comments.** Our synonymy of *Paratelenomus obtusus* (Lê) is based on photographs of the holotype specimens provided by Talamas and Pham (2017) (Figs 12–16). This specimen matches the concept of *P. saccharalis* in the description and identification key of Johnson (1996) and likely was not considered by Lê in his later treatments of *Archiphanurus* Szabó (= *Paratelenomus*) (Lê 1997, 2000).



Figures 9–11. *Paratelenomus saccharalis* **9** female (USNMENT01109029), head, mesosoma, metasoma, lateral view **10** female (USNMENT00896364), head, anterior view **11** female (USNMENT00896364), mesosoma, dorsolateral view. Scale bars: in millimeters.

Paratelenomus tetartus (Crawford)

http://bioguid.osu.edu/xbiod_concepts/3345

Figures 17–27

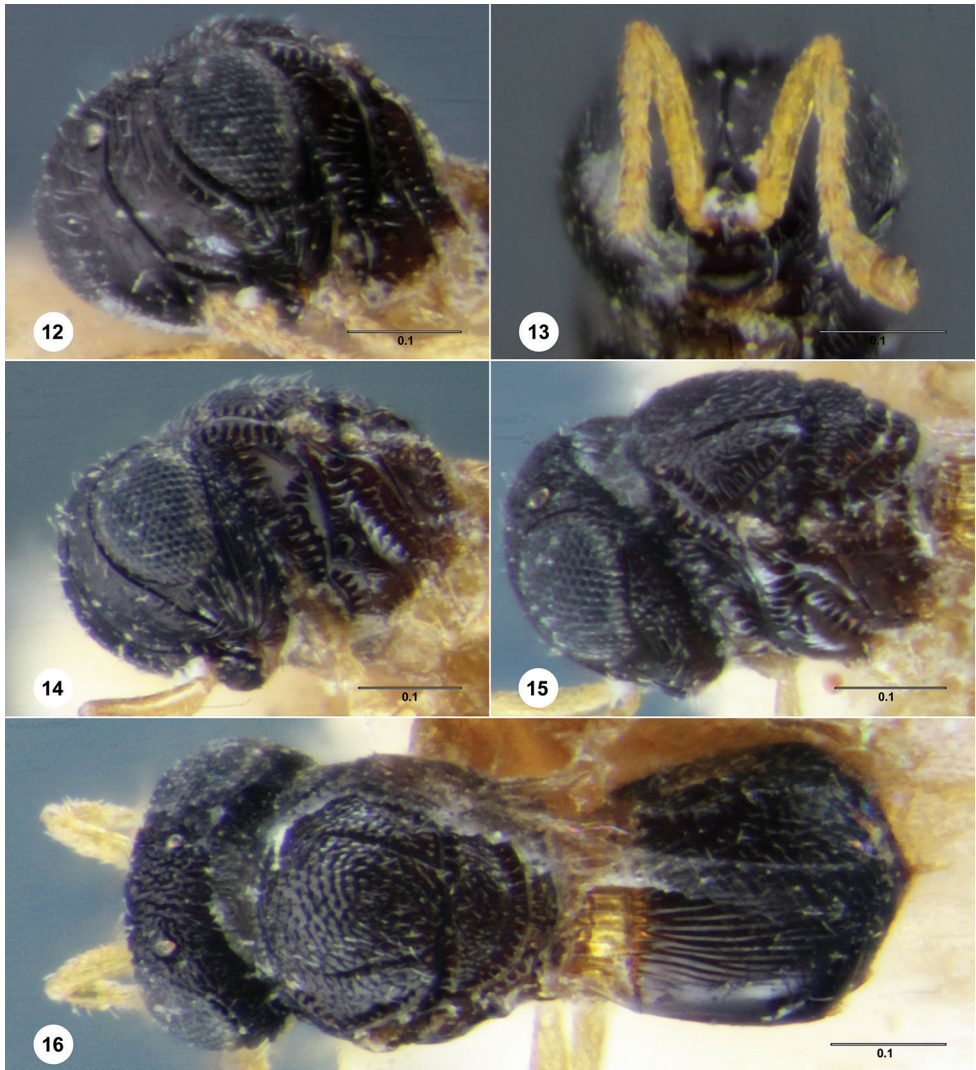
Dissolcus tetartus Crawford, 1911: 270 (original description); Kieffer 1926 : 124, 125 (description, keyed); Wall 1931 : 381 (repetition of Crawford (1911), variation).

Trissolcus tetartus (Crawford): Masner and Muesebeck 1968: 73 (type information).

Archiphanurus tetartus (Crawford): Johnson 1981 : 73 (generic transfer).

Paratelenomus tetartus (Crawford): Johnson 1992 : 564 (cataloged, type information); Johnson 1996 : 277, 286 (description, keyed); Johnson 1996 : 277, 286 (description, keyed).

Archiphanurus longus Kozlov & Lê syn. nov.: Lê 1997 : 24, 27 (original description, keyed); Lê 2000 : 251 (description, type information).



Figures 12–16. *Paratelenomus obtusus*, holotype female (IEBR 0050) **12** head and mesosoma, anterolateral view **13** head, anteroventral view **14** head and mesosoma, lateral view **15** head and mesosoma, dorsolateral view **16** head, mesosoma, metasoma, dorsal view. Scale bars: in millimeters.

Archiphanurus longgus Kozlov & Lê: Lê 2000 : 249 (keyed, misspelling).

Paratelenomus mangrovus Rajmohana & Narendran syn. nov., 2007: 2522, 2523 (original description, keyed).

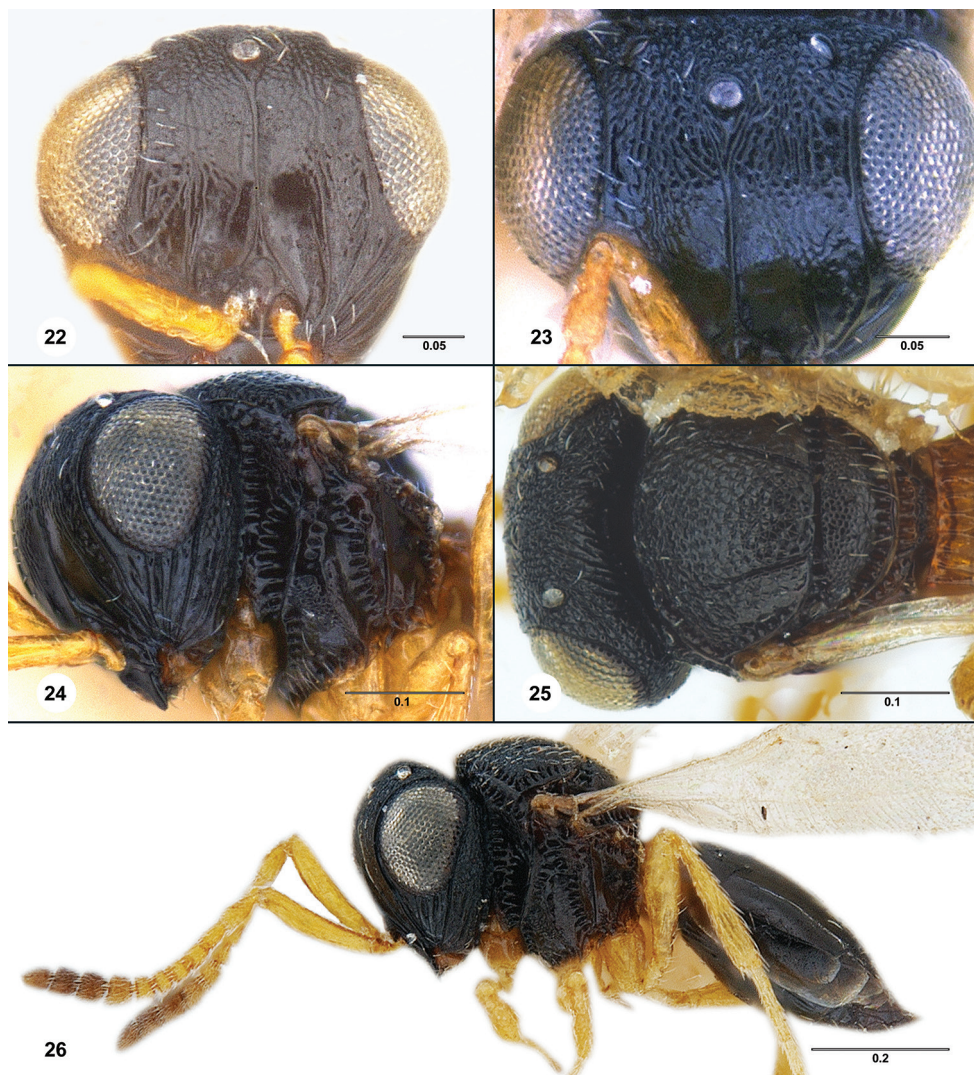
Material examined. Holotype, female, *Dissolcus tetartus*: **INDONESIA**: Sumatera Utara Prov., Sumatra Isl., Deli Land, Medan, no date, reared from egg, L. P. de Bussy, USNM-00989067 (deposited in USNM). Holotype, female, *Paratelenomus mangrovus*: **INDIA**: Kerala St., Kozhikode, Cheruvannur, 28.XI.2005, K. Rajmohana, ZSI/I/Hy/



Figures 17–21. *Paratelenomus tetartus* **17** female holotype of *P. tetartus* (USNMENT00989067), anterolateral view **18** female holotype of *P. longus* (IEBR 0049), head, anterolateral view **19** female holotype of *P. longus* (IEBR 0049) head and mesosoma, lateral view **20** female holotype of *P. longus* (IEBR 0049), head and mesosoma, dorsolateral view **21** female holotype of *P. longus* (IEBR 0049), head, mesosoma, metasoma, dorsal view. Scale bars: in millimeters.

Sc.-1 (ZSI/WGRS/I.R-INV.1934) (deposited in ZSIC). Holotype, female, *Archiphanurus longus*: **VIETNAM**: Son La Prov., Sông Mã (Shongma), 12.V.1986, A. Sharkov, IEBR 0049 (deposited in IEBR). Other material: (1 female) **MALAYSIA**: OSUC 398251.

Comments. The synonymy of *Paratelenomus longus* (Kozlov & Lê) is based on photographs of the holotype specimen provided by Talamas and Pham (2017) (Figs 18–



Figures 22–26. *Paratelenomus mangrovus*, female holotype (CUID) **22** head, anterior view **23** head, anterodorsal view **24** head and mesosoma, anterolateral view **25** head, mesosoma, T1, dorsal view **26** head, mesosoma, metasoma, lateral view. Scale bars in millimeters.

21) and images of the holotype of *P. tetartus* provided by Talamas et al. (2017) (Fig. 17). The mesopleuron on the holotype of *P. longus* is obscured by its foreleg and by glue (Fig. 19), making it impossible to confidently assess the characters of couplet 3 in the identification key of Johnson (1996). However, we can exclude the species that follow the first lead of the couplet because this specimen has microsculpture throughout the mesoscutum and mesoscutellum, well-developed submedian carinae on the frons, and T1 is xanthic and distinctly contrasting in color with the following metasomal segments. This combination of characters is not found in *P. angor* Johnson (Figs 28, 29),



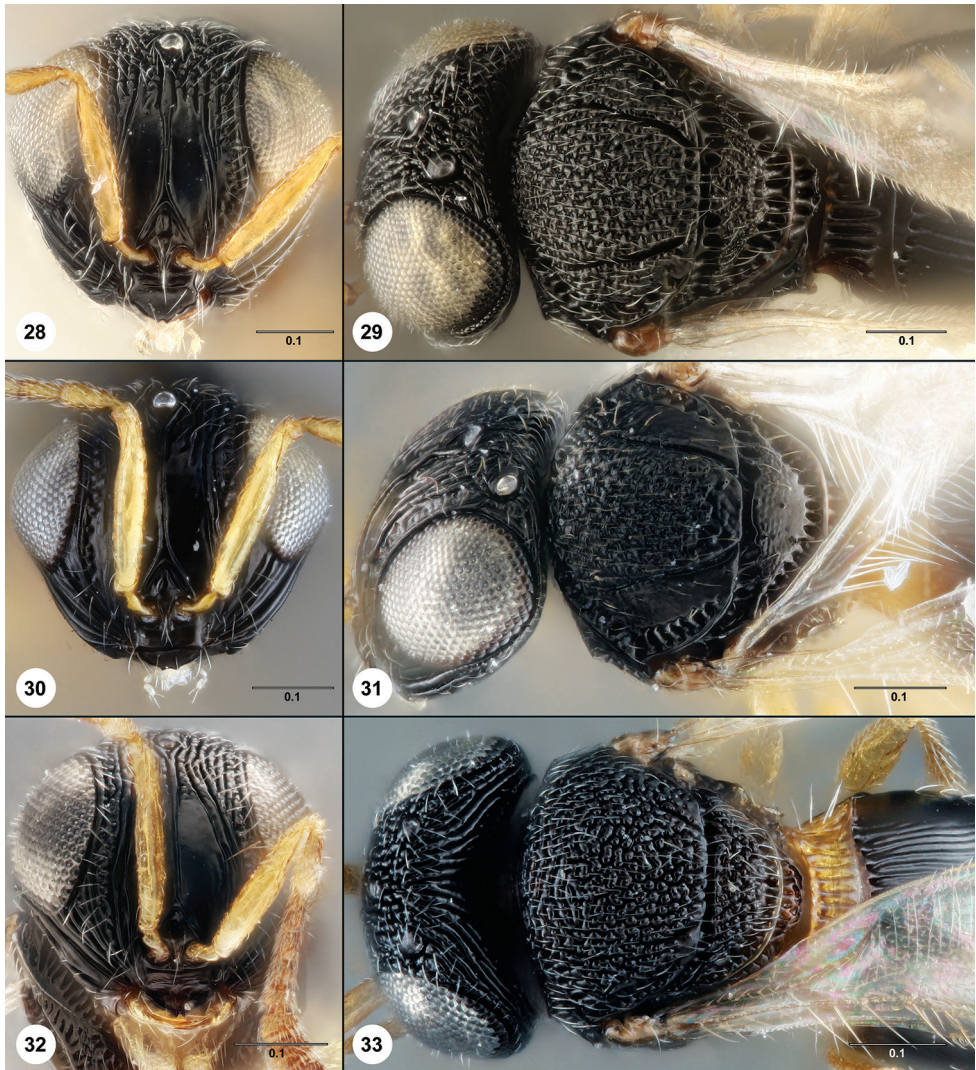
Figure 27. *Paratelenomus tetartus*, female (OSUC 398251), head, mesosoma, metasoma, lateral view. Scale bar: in millimeters.

P. matinalis Johnson (Figs 30, 31), or *P. striativentris* (Risbec) (Figs 32, 33). Following the second lead of the couplet results in an identification of *P. tetartus*, which matches the visible morphology and collection locality of *P. longus*.

Treatment of *P. mangrovus* as a junior synonym follows reexamination of the holotype of this species and reevaluation of the characters used by Rajmohana & Narendran (2007) to separate it from *P. tetartus*. Specifically, the length of the orbital carina and the proximity of the cells of the postacetabular and mesopleural epicoxal sulci are variable. The lateral habitus image of the holotype of *P. mangrovus* (Fig. 26) does not illustrate the presence of 4–5 episternal foveae, but instead illustrates the presence of 4–5 foveae immediately dorsal to the mesopleural carina, which is known to exist in *P. tetartus* (Fig. 27).

Comments on taxonomy of *Paratelenomus*

There remain two species of *Paratelenomus*, *P. aculus* (Lê) and *P. irritus* (Lê), for which the species concepts are unclear. Lê (1980) stated that *P. irritus* (= *Archiphanurus irritus*) had “notauli absent” yet illustrated this species with short notauli. Lê (1980) also stated “notauli usually short” for *P. aculus* (= *Archiphanurus aculus*), and the notauli for this species are illustrated in Lê (2000) as extending for half the length of the mesoscutum. Based on this evidence, we conclude that both species have notauli, which exclude these names as possibilities for the species we here describe as new. Treatment of *P. irritus* and *P. aculus* will require examination of additional type material, and we note that the holotype specimens of these species were not present in the Institute for Ecology and Biological Resources, Hanoi, Vietnam, during EJT’s visit to this collection in 2016.



Figures 28–33. **28** *Paratelenomus angor*, paratype female (OSUC 398127), head, anterior view **29** *Paratelenomus angor*, paratype female (OSUC 398127), head, mesosoma, T1–T2, dorsal view **30** *Paratelenomus matinalis*, paratype female (OSUC 398195), head, anterior view **31** *Paratelenomus matinalis* paratype female (OSUC 398195), head, mesosoma, T1–T2, dorsal view **32** *Paratelenomus striativentris* female (OSUC 398273), head, anterior view **33** *Paratelenomus striativentris* female (OSUC 398273), head, mesosoma, T1–T2, anterior view. Scale bars: in millimeters.

Discussion

Phoresy is common in the arthropod world (Ferrière 1926, Clausen 1976) but among insect parasitoids, it is mostly restricted to those that parasitize eggs (Clausen 1976). Females of about 35 egg parasitoid species are known to hitchhike on the adult hosts

to reach their egg-laying sites (Huigens and Fatouros 2013). Phoresy is a highly specialized strategy exploited by egg parasitoids to reduce the spatial and temporal discontinuity between where hosts mate and where host females oviposit (Clausen 1976, Vinson 1998, Fatouros and Huigens 2012) and facilitates dispersal of the parasitoids with their hosts. In phoretic species, the age and quality of the host eggs can be crucial for the success of parasitism.

Phoresy has now been documented in several scelionid genera: *Synoditella* Muesebeck, *Sceliocerdo* Muesebeck, and *Scelio* Latreille on grasshoppers (Acrididae) (Lanhams and Evans 1958, Brues 1917, Veenakumari et al. 2012, Noble 1935), *Thoronella* Masner on an aeshnid dragonfly, *Epiaeschna heros* (Fabr.) (Carlow 1992), *Mantibararia* Kirby on Mantodea (Kirby 1900), and *Protelenomus* on coreid bugs (Kohno 2002). This is the first report of phoretic behavior in *Paratelenomus*, which may be present in species other than *P. annu*. Both in captivity and in the field, females of *P. annu* were found to be phoretic on their bug hosts, with up to five wasps on a single host bug. Thus, the absence of reported phoresy in *P. saccharalis*, combined with the amount of attention it has received as a biological control agent, provides reasonable evidence that *P. saccharalis* is not phoretic. Biological data and a species-level phylogeny are needed to determine if phoresy in *P. annu* is an independent derivation or if it is phenomenon that arose earlier in the evolution of *Paratelenomus*. We surmise that the phoretic behavior of *P. annu* gives it a competitive advantage by enabling it to parasitize the eggs at the earliest possible moment. However, a cost to phoresy may exist because females of *P. annu* spend time attached to adult bugs instead of searching for egg masses, thus limiting their dispersal ability. In a comparison of *P. saccharalis* and *P. annu*, this idea is supported by the distributional data of the species: *P. saccharalis* is extremely widespread (Europe, Africa, tropical Asia, northern Australia (Johnson 1996)) while *P. annu* is known only from India. However, it must also be considered that the absence of *P. annu* from collections may be an artifact of collecting methods that are biased toward free-living, non-phoretic insects, such as Malaise and yellow pan traps.

Acknowledgments

The first author is thankful to Dr. Kailash Chandra, director of the Zoological Survey of India for all support extended. The second author is thankful to the Department of Science and Technology- Fund for Improvement of Science and Technology Infrastructure (2014) for providing financial support to adequately equip the laboratory. We are grateful to the principal of Malabar Christian College, Calicut, for providing infrastructure and encouragement; to Dr. Lubomír Masner (CNCI) who provided representatives of all *Paratelenomus* species treated by Johnson (1996); to Dr. H. M. Yeshwanth (University of Agricultural Sciences, Bangalore) for confirming the identity of the host bug; and to Smithsonian interns Anthony Cuminale and Ky Wildermuth, who contributed scanning electron micrographs. This work was supported in part by the Florida Department of Agriculture and Consumer Services- Division of Plant Industry.

References

- Bin F, Colazza S (1988) Egg parasitoids, Hym. Scelionidae and Encyrtidae, associated with Hemiptera Plataspidae. *Colloques de l'INRA* 43: 33–34.
- Brues T (1917) Adult hymenopterous parasites attached to the body of their host. *Proceedings of the National Academy of Sciences* 3: 136–140. <https://doi.org/10.1073/pnas.3.2.136>
- Carlow T (1992) *Thoronella* sp. (Hymenoptera: Scelionidae) discovered on the thorax of an Aeshnidae (Anisoptera). *Notulae Odonatologicae* 3: 149–150.
- Clausen CP (1976) Phoresy among entomophagous insects. *Annual review of Entomology* 21: 343–368. <https://doi.org/10.1146/annurev.en.21.010176.002015>
- Crawford JC (1911) Descriptions of new Hymenoptera. No. 3. *Proceedings of the United States National Museum* 41: 267–282. <https://doi.org/10.5479/si.00963801.41-1855.267>
- Dodd A, Nelson NQ (1914) Some proctotrypoid egg-parasites of sugar cane insects in Java. *The Canadian Entomologist* 46: 293–294. <https://doi.org/10.4039/Ent46293-8>
- Easton ER, Pun W-W (1997) Observations on some Hemiptera/Heteroptera of Macau, South-east Asia. *Proceedings of the Entomological Society of Washington* 99: 574–582.
- Eger Jr JE, Ames LM, Suiter DR, Jenkins TM, Rider DA, Halbert SE (2010) Occurrence of the Old World bug *Megacopta cribraria* (Fabricius) (Heteroptera: Plataspidae) in Georgia: a serious home invader and potential legume pest. *Insecta Mundi* 121: 1–11.
- Fatouros NE, Huigens ME (2012) Phoresy in the field: natural occurrence of *Trichogramma* egg parasitoids on butterflies and moths. *BioControl* 57: 493–502. <https://doi.org/10.1007/s10526-011-9427-x>
- Ferrière C (1926) L a phorésie chez les insectes. *Mitteilungen der Schweizerischen Entomologischen Gesellschaft* 13: 489–496.
- Gardner WA, Blount JL, Golec JR, Jones WA, Hu XP, Talamas EJ, Evans RM, Dong X, Ray C H Jr, Buntin GD (2013a) Discovery of *Paratelenomus saccharalis* (Dodd) (Hymenoptera: Platygasteridae), an egg parasitoid of *Megacopta cribraria* F. (Hemiptera: Plataspidae) in its expanded North American range. *Journal of Entomological Science* 48: 355–360. <https://doi.org/10.18474/0749-8004-48.4.355>
- Gardner WA, Peeler HB, LaForest J, Roberts PM, Sparks AN, Greene Jr JK, Reising DD, Suiter DR, Bachelier JS, Kidd K, Ray CH, Hu RC, Kemerait RC, Scocco EA, Eger JE, Ruberson JR, Sikora EJ, Herbert DA, Campana C, Halbert SE, Stewart SD, Buntin GB, Toews MD, Barger CT (2013b) Confirmed distribution and occurrence of *Megacopta cribraria* (F.) (Hemiptera: Heteroptera: Plataspidae) in the southeastern United States. *Journal of Entomological Science* 48: 118–127. <https://doi.org/10.18474/0749-8004-48.2.118>
- Hebert PDN, Penton EH, Burns JM, Janzen DH, Hallwachs W (2004) Ten species in one: DNA barcoding reveals cryptic species in the neotropical skipper butterfly *Astraptes fulgerator*. *Proceedings of the National Academy of Sciences of the United States of America* 101: 14812–14817. <https://doi.org/10.1073/pnas.0406166101>
- Hoffmann WE (1931) Notes on Hemiptera and Homoptera at Canton, Kwangtung province, Southern China 1924–1929. *USDA Insect Pest Survey Bulletin* 11: 131–151.
- Hoffmann WE (1932) Notes on the bionomics of some Oriental Pentatomidae (Hemiptera). *Archivio Zoologico Italiano (Torino)* 16: 1010–1027.

- Hua LZ (2000) List of Chinese insects. Volume I. Zhongshan (Sun Yat-sen) University Press, Guangzhou, P.R. China, 448 pp.
- Huigens ME, Fatouros NE (2013) A hitchhiker's guide to parasitism: Chemical ecology of phoretic insect parasitoids. In: Wajnberg E, Colazza S (Eds) Chemical Ecology of Insect Parasitoids. Wiley-Blackwell, Oxford, 328 pp. <https://doi.org/10.1002/9781118409589.ch5>
- Ishihara T (1950) The developmental stages of some bugs injurious to the kidney bean (Hemiptera). Transactions of the Shikoku Entomological Society 1: 17–31.
- Johnson NF (1981) New World species of the *Telenomus nigricornis* group (Hymenoptera: Scelionidae). Annals of the Entomological Society of America 74: 73–78. <https://doi.org/10.1093/aesa/74.1.73>
- Johnson NF (1988) Species of Australian Telenominae (Hymenoptera: Scelionidae) of A. P. Dodd and A. A. Girault. Proceedings of the Entomological Society of Washington 90: 229–243. <https://doi.org/10.5281/zenodo.23817>
- Johnson NF (1992) Catalog of world Proctotrupeoidea excluding Platygasteridae. Memoirs of the American Entomological Institute 51: 1–825. <https://doi.org/10.5281/zenodo.23657>
- Johnson NF (1996) Revision of world species of *Paratelenomus* (Hymenoptera: Scelionidae). The Canadian Entomologist 128: 273–291. <https://doi.org/10.4039/Ent128273-2>
- Kieffer JJ (1917) Über neue und bekannte Microhymenopteren. Entomologische Mitteilungen 11: 341–355. <https://doi.org/10.5281/zenodo.23832>
- Kieffer JJ (1926) Scelionidae. Das Tierreich. Vol. 48. Walter de Gruyter & Co., Berlin, 885 pp.
- Kirby WF (1900) Order 2. – Hymenoptera. In: Andrews (Ed.) A monograph of Christmas Island (Indian Ocean): physical features and geology; with descriptions of the fauna and flora by numerous contributors. British Museum (Natural History), London, 337 pp.
- Kohno K (2002) Phoresy by an egg parasitoid, *Protelenomus* sp. (Hymenoptera: Scelionidae), on the coreid bug *Anoplocnemis phasiana* (Heteroptera: Coreidae). Entomological Science 5: 281–285.
- Kononova SV (1973) Egg parasites of the genera *Aporophlebus* Kozlov, 1970 and *Platytelenomus* Dodd, 1914 (Hymenoptera, Scelionidae) in the fauna of the Ukraine. Entomologicheskoye Obozreniye 52: 658–664. <https://doi.org/10.5281/zenodo.23944>
- Kononova SV (1995) 25. Fam. Scelionidae. In: Lehr (Ed.) Key to insects of Russian Far East in six volume. vol. 4. Neuropteroidea, Mecoptera, Hymenoptera. Part 2. Hymenoptera. Dal'nauka, Vladivostok. 600 pp.
- Kozlov MA, Kononova SV (1983) Telenominae of the fauna of the USSR. Nauka, Leningrad, 336 pp.
- Kozlov MA (1970) Supergeneric groupings of Proctotrupeoidea (Hymenoptera). Entomologicheskoye Obozreniye 49: 203–226. <https://doi.org/10.5281/zenodo.23681>
- Kozlov MA (1978) Superfamily Proctotrupeoidea. In: Medvedev (Ed.) Determination of insects of the European portion of the USSR. Vol. 3, part 2. Nauka, Leningrad, 758 pp.
- Kozlov MA, Lê X-H (1976) Palearctic species of egg parasites of the genus *Aporophlebus* Kozlov (Hymenoptera, Scelionidae). Insects of Mongolia 4: 348–369. <https://doi.org/10.5281/zenodo.23934>
- Lanham UN, Evans FC (1958) Phoretic scelionids on grasshoppers of the genus *Melanoplus* (Hymenoptera: Scelionidae). Pan-Pacific Entomology 34: 213–214.

- Lê X-H (1980) Ba loại ong ki sinh moi thuoc cac giong *Archiphanurus* Szabo va *Platytenomus* Dodd (Hymenoptera, Scelionidae, Telenominae) o Viet Nam. Tap Chi Sinh Vat Hoc 2: 17–19.
- Lê X-H (1982) Two new species of the subfamily Telenominae (Hymenoptera, Scelionidae) from Viet Nam. [Pages 144–146] In: Medvedev (Ed.) *Zhivotnyi Mir Vietnam* [The animal world of Vietnam] Nauka, Moscow, 168 pp.
- Lê X-H (1997) Ong ky sinh ho Scelionidae (Hymenoptera) ky sinh trong trung bo xit (Heteroptera) o Viet Name. Tap Chi Sinh Hoc 19: 23–28.
- Lê X-H (2000) Egg-parasites of family Scelionidae (Hymenoptera). *Fauna of Vietnam*, vol. 3. Science and Technics Publishing House, Hanoi. 386 pp.
- Li YH, Pan ZS, Zhang JP, Li WS (2001) Observation of biology behavior of *Megacopta cribraria* (Fabricius). *Plant Protection Technology and Extension* 21: 11–12.
- Masner L, Muesebeck CFW (1968) The types of Proctotrupeoidea (Hymenoptera) in the United States National Museum. *Bulletin of the United States National Museum* 270: 1–143. <https://doi.org/10.5479/si.03629236.270>
- Medal J, Halbert S, Smith T, Santa Cruz A (2013) Suitability of selected plants to the bean plataspid, *Megacopta cribraria* (Hemiptera: Plataspidae) in no-choice tests. *Florida Entomologist* 96: 631–633. <https://doi.org/10.1653/024.096.0232>
- Mineo G (1979) Studies of the Scelionidae (Hym. Proctotrupeoidea). IX. Material for a revision of the genus *Gryon* Hal., with description of 4 new species (*G. austrfricanum*, *G. eremiogryon*, *G. laraichii*, *G. nicolai*) and notes on other scelionids. *Bollettino del Laboratorio di Entomologia Agraria “Filippo Silvestri” Portici* 36: 234–265. <https://doi.org/10.5281/zenodo.23812>
- Noble NS (1935) An egg parasite of the plague grasshopper. *Agricultural Gazette of New South Wales* 46: 513–518.
- Ode PJ, Hardy IC (2008) Parasitoid Sex Ratios and Biological Control. In: Wajnberg, Bernstein, van Alphen (Eds) *Behavioral Ecology of Insect Parasitoids*. Wiley-Blackwell, Malden, 464 pp.
- Rajmohana K, Narendran TC (2007) A new species of *Paratelenomus* (Hymenoptera: Scelionidae) from India. *Zoos’ Print Journal* 22: 2522–2523. <https://doi.org/10.11609/JoTT.ZPJ.1631.2522-3>
- Rajmohana K, Peter A (2013) Fauna of Bhadra Wildlife Sanctuary & Tiger Reserve. *Insecta: Platygastridae (Hymenoptera: Platygastroidea)*. Conservation Area Series 46: 11–23.
- Ryu J, Hirashima Y (1989) Taxonomic studies on the genera *Aporophlebus*, *Eumicrosoma*, and *Platytenomus* of Japan and Korea (Hymenoptera, Scelionidae, Telenominae). *Esakia* 28: 49–62.
- Sambrook JF, Russell DW (2001) *Molecular cloning: A laboratory manual*. 3rd edition (Cold Spring Harbor Laboratory Press, Cold Spring Harbor, New York, 2100 pp.
- Samin N, Radjabi GR, Asgari S (2012) A contribution to the knowledge of Scelionidae (Hymenoptera: Platygastridae) from Khuzestan Province, southwestern Iran. *Entomofauna Zeitschrift für Entomologie* 33: 17–24.
- Schaeffer CW, Panizzi AR (2000) *Heteroptera of economic importance*. Boca Raton, FL: CRC Press, 828 pp. <https://doi.org/10.1201/9781420041859>

- Srinivasaperumal S, Samuthiravelu P, Muthukrishnan J (1992) Host plant preference and life table of *Megacocta cribraria* (Fab.) (Hemiptera: Plataspidae). Proceedings of the National Academy of Sciences, India Section B: Biological Sciences 58: 333–340.
- Suiter DR, Eger Jr JE, Gardner WA, Kemerait RC, All JN, Roberts PM, Greene JK, Ames LM, Buntin GD, Jenkins TM, Dounce GK (2010) Discovery and distribution of *Megacocta cribraria* (Hemiptera: Heteroptera: Plataspidae) in northeast Georgia. Journal of Integrated Pest Management 1: 1–4. <https://doi.org/10.1603/IPM10009>
- Szabó JS (1975) Neue Gattungen und Arten der palaearktischen Telenominae (Hymenoptera, Scelionidae). Annales Historico-Naturales Musei Nationalis Hungarici 67: 265–278. <https://doi.org/10.5281/zenodo.23885>
- Talamas EJ, Buffington ML, Johnson NF (2015) Key to Nearctic species of *Trissolcus* Ashmead (Hymenoptera, Scelionidae), natural enemies of native and invasive stink bugs (Hemiptera, Pentatomidae). Journal of Hymenoptera Research 43: 45–110. <https://doi.org/10.3897/JHR.43.8560>
- Talamas EJ, Thompson J, Cutler A, Fitzsimmons Schoenberger S, Cuminale A, Jung T, Johnson NF, Valerio AA, Smith AB, Haltermann V, Alvarez E, Schwantes C, Blewer C, Bodenreider C, Salzberg A, Luo P, Meislin D, Buffington ML (2017) An online photographic catalog of primary types of Platygastridae (Hymenoptera) in the National Museum of Natural History, Smithsonian Institution. In: Talamas EJ, Buffington ML (Eds) Advances in the Systematics of Platygastridae. Journal of Hymenoptera Research 56: 187–224. <https://doi.org/10.3897/jhr.56.10774>
- Talamas EJ, Pham H-T (2017) An online photographic catalog of Platygastridae (Hymenoptera) in the Institute of Ecology and Biological Resources (Hanoi, Vietnam), with some taxonomic notes. In: Talamas EJ, Buffington ML (Eds) Advances in the Systematics of Platygastridae. Journal of Hymenoptera Research 56: 225–239. <https://doi.org/10.3897/jhr.56.10214>
- Veenakumari K, Rajmohana K, Prashanth M (2012) Studies on Phoretic Scelioninae (Hymenoptera: Platygastridae) from India along with description of a new species of *Mantibaria* Kirby. Linzer biologische Beiträge 44: 1715–1725.
- Vinson SB (1998) The general host selection behavior of parasitoid Hymenoptera and a comparison of initial strategies utilized by larvaphagous and oophagous species. Biological Control 11: 79–96. <https://doi.org/10.1006/bcon.1997.0601>
- Wall RE (1931) *Dissolcus tetartus* Crawford, a scelionid egg parasite of Plataspidinae in China. Lingnan Science Journal 9: 381–382.
- Wang ZX, Chen GH, Zi ZG, Tong CW (1996) Occurrence and control of *Megacocta cribraria* (Fabricius) on soybean (English abstract). Plant Protection 22: 7–9.
- Wang HS, Zhang CS, Yu DP (2004) Preliminary studies on occurrence and control technology of *Megacocta cribraria* (Fabricius). China Plant Protection 24: 45.
- Watanabe C (1954) Discovery of four new species of Telenominae, egg parasites of pentatomid and plataspid bugs, in Shikoku, Japan. Transactions of the Shikoku Entomological Society 4: 17–22. <https://doi.org/10.5281/zenodo.23942>
- Yamagishi K (1990) Notes on *Archiphanurus minor* (Watanabe) (Hymenoptera, Scelionidae). Esakia, Special Issue 1: 193–196. <https://doi.org/10.5281/zenodo.23936>

Zhang SM (1985) Economic insect fauna of China. Heteroptera Plataspidae. Science Press, Beijing. 31: 34–35.

Zhang Y, Hanula JL, Horn S (2012) The biology and preliminary host range of *Megacopta cribraria* (Heteroptera: Plataspidae) and its impact on kudzu growth. Environmental Entomology 41: 40–50. <https://doi.org/10.1603/EN11231>

Supplementary material 1

URI table of HAO morphological terms

Authors: Keloth Rajmohana, James P. Sachin, Elijah J. Talamas, Mukundan S. Shamyasree, S. K. Jalali, Ojha Rakshit

Data type: Microsoft Excel Spreadsheet (.xlsx)

Explanation note: This table lists the morphological terms used in this publication and their associated concepts in the Hymenoptera Anatomy Ontology

Copyright notice: This dataset is made available under the Open Database License (<http://opendatacommons.org/licenses/odbl/1.0/>). The Open Database License (ODbL) is a license agreement intended to allow users to freely share, modify, and use this Dataset while maintaining this same freedom for others, provided that the original source and author(s) are credited.

Link: <https://doi.org/10.3897/jhr.73.34262.suppl1>

Supplementary material 2

Barcode sequence of CO1 for *Paratelenomus anu*

Authors: Keloth Rajmohana, James P. Sachin, Elijah J. Talamas, Mukundan S. Shamyasree, S. K. Jalali, Ojha Rakshit

Data type: Microsoft Word Document (.docx)

Copyright notice: This dataset is made available under the Open Database License (<http://opendatacommons.org/licenses/odbl/1.0/>). The Open Database License (ODbL) is a license agreement intended to allow users to freely share, modify, and use this Dataset while maintaining this same freedom for others, provided that the original source and author(s) are credited.

Link: <https://doi.org/10.3897/jhr.73.34262.suppl2>

Field studies and molecular forensics identify a new association: *Idris elba* Talamas, sp. nov. parasitizes the eggs of *Bagrada hilaris* (Burmeister)

J. Refugio Lomeli-Flores¹, Susana Eva Rodríguez-Rodríguez¹,
Esteban Rodríguez-Levy¹, Héctor González-Hernández¹,
Tara D. Garipey², Elijah J. Talamas³

1 Colegio de Postgraduados, Posgrado en Fitosanidad, Programa de Entomología y Acarología, Montecillo, CP 56230. Texcoco, Estado de México, México **2** Agriculture and Agri-Food Canada, 1391 Sandford Street London, Ontario N5V 4T3, Canada **3** Florida State Collection of Arthropods, Division of Plant Industry, Florida Department of Agriculture and Consumer Services, Gainesville, FL 32608, USA

Corresponding author: *Elijah J. Talamas* (talamas.1@osu.edu)

Academic editor: *J. Fernandez-Triana* | Received 5 July 2019 | Accepted 26 August 2019 | Published 18 November 2019

<http://zoobank.org/31D390C3-85D1-4E44-BD8F-CA73D7B2DF7C>

Citation: Lomeli-Flores JR, Rodríguez-Rodríguez SE, Rodríguez-Levy E, González-Hernández H, Garipey TD, Talamas EJ (2019) Field studies and molecular forensics identify a new association: *Idris elba* Talamas, sp. nov. parasitizes the eggs of *Bagrada hilaris* (Burmeister). In: Talamas E (Eds) Advances in the Systematics of Platygastridae II. Journal of Hymenoptera Research 73: 125–141. <https://doi.org/10.3897/jhr.73.38025>

Abstract

A species of *Idris* Förster (Hymenoptera: Scelionidae) is found to parasitize the eggs of *Bagrada hilaris* (Hemiptera: Pentatomidae) and is described as new: *Idris elba* Talamas, **sp. nov.** This is the first association of an *Idris* species with a non-spider host, and the association is confirmed with molecular diagnostic tools that enable identification of parasitoid and host from the remains of parasitized eggs.

Keywords

Bagrada bug, natural enemies, egg parasitoid, diagnostics

Introduction

The bagrada bug, *Bagrada hilaris* (Burmeister) (Hemiptera: Pentatomidae), is an invasive alien species that has recently established in North America (Palumbo et al. 2016) and is one of the most important pests of Brassicaceae worldwide because of the eco-

conomic damage it causes in many crops. This pest has 74 host species in 23 botanical families, but it prefers crops of the Brassicaceae family (Obopile et al. 2008, Palumbo 2016, Palumbo et al. 2016). The main damage to the plants is caused by direct feeding: the suction of sap causes a decrease in vigor and photosynthetic area. *Bagrada hilaris* is native to West Africa or Southeast Asia (Howard 1906, Perring et al. 2013, Palumbo et al. 2016) and is currently an important pest in India, Africa, southern Europe, southern Asia and the Middle East (Palumbo et al. 2016). In North America, it was first detected in Los Angeles, California, USA, in 2008, and by 2014 it had already spread to brassica crops in other locations in California and Arizona (Garrison 2009, Arakelian 2010, Palumbo et al. 2016). In Mexico it was first detected in 2014, in Saltillo, Coahuila (Sánchez-Peña 2014), and in 2017 reached the state of Guanajuato (Hernández-Chávez et al. 2018). Over 70% of Mexico's production of broccoli is in Guanajuato and it is the leading region for exports of broccoli and cauliflower to the USA and Canada, either as frozen or fresh products (SIAP 2018). More recently, this species was found in Santiago, Chile, in 2016 (Faúndez et al. 2016). The losses in California during 2013 were estimated at \$679 million USD (Palumbo 2016). Even though quarantine measures have been taken for this pest, its distribution appears to have reached important commercial crop regions in the Americas and it threatens to spread to more ecosystems with potential economic impact in cruciferous and other crops (Carvajal et al. 2018). To date, control measures for *B. hilaris* rely primarily on the use of pyrethroid, carbamate, and neonicotinoid insecticides (Sachan and Purwar 2007, Obopile et al. 2008, Joseph et al. 2016). However, biological control using native or exotic natural enemies might offer an alternative to maintain pest populations below the economic threshold.

Invasive species have the potential to serve as an abundant host resource for native natural enemies if they can recognize and exploit this new resource (Cornell and Hawkins 1993). However, new host-parasitoid associations can be difficult to conclusively identify at the species level using traditional rearing approaches and misidentifications or contaminated rearing can result in questionable linkages (Shaw 1994, Quicke 1997). When reliable reference sequences (e.g., DNA barcodes) are available, the incorporation of molecular forensic approaches that detect and identify trace amounts of host and parasitoid DNA can be used to validate host-parasitoid associations obtained using traditional approaches (Rougerie et al. 2010, Hrcek et al. 2011; Garipey et al. 2019). Several species of parasitoid wasp (primarily in the family Scelionidae) are known to attack *B. hilaris* eggs in India and Pakistan (Palumbo et al. 2016, Mahmood et al. 2015, Martel et al. 2019). To date, no native parasitoids have been reported to attack *B. hilaris* in the field in the USA, although the adventive *Trissolcus hyalinipennis* Rajmohana & Narendran and the intentionally introduced *Trissolcus basalis* (Wollaston) have been detected from sentinel egg masses of *B. hilaris* in California (Ganjisaffar et al. 2018). In Mexico, studies to define the natural enemy community that exploit this newly established pest have identified two native scelionid species parasitizing *B. hilaris* eggs: *Telenomus podisi* Ashmead and *Gryon myrmecophilum* (Ashmead) (Felipe-Victoriano et al. 2019). Unlike most stink bugs, which lay their eggs in large contiguous masses directly on a plant, *B. hilaris* mostly oviposits singly or in small groups of eggs (~10 eggs) in the soil, which may decrease the likelihood of ex-

ploitation by native, generalist stink bug egg parasitoids that typically forage for hosts on foliage (Reed et al. 2013). Prior to the consideration of exotic natural enemies for a classical biological control program for the bagrada bug, the native natural enemy community associated with this pest in the field must be investigated to determine if the native fauna can contribute toward a biological control solution. During the 2018 field season, a natural enemy survey was conducted in Guanajuato, México, to detect and identify native parasitoid species that can exploit this new host resource.

Scelionid egg parasitoids of *B. hilaris* have been reported in natural field conditions from the native range of this species: *Gryon karnalensis* (Chacko and Katiyar 1961), *Telenomus samueli* (Mani and Sharma 1982), and *Psix* sp. (near *striaticeps*) (Cheema et al. 1973). In this study, traditional rearing and taxonomic treatment of emerged parasitoid adults were employed in conjunction with molecular forensics to definitively link the trophic association between host species and parasitoid species based on trace amounts of DNA in emerged eggs. With the combination of these methods we show that another scelionid, *Idris elba* sp. nov., can also successfully parasitize eggs of *B. hilaris* under natural field conditions.

Materials and methods

Field collections

Biweekly surveys were conducted between May and September 2018 in the municipalities of Abasolo and Juventino Rosas in Guanajuato, where large areas of broccoli, cauliflower and cabbage were planted. The sampling was conducted primarily in abandoned crops where insecticides were no longer used. In addition, crop edges where wild host plants (e.g., *B. campestris* L. and *B. nigra* (L.) W. D. J. Koch) of *B. hilaris* occur were inspected. When a population of *B. hilaris* was observed, the soil surrounding the plant was carefully inspected to collect the bug eggs. This material was separated from the substrate and placed in a Petri dish for transport to the laboratory.

Field-collected *B. hilaris* eggs were kept in Petri dishes with a broccoli leaf in the laboratory in a bioclimatic chamber (26 ± 1 °C, $75 \pm 5\%$ RH and 12:12 (L:D) photoperiod). The material was checked daily to observe evidence of parasitism. Emerged parasitoids were placed in 1.5mL Eppendorf tubes with ethyl alcohol (70%); subsequently, they were processed and mounted. Empty eggs from which either nymphs or parasitoids emerged were placed (dry) in separate 1.5mL Eppendorf tubes for subsequent molecular forensic analysis.

Taxonomy

The description of *I. elba* was generated by the online systematics and taxonomy tool, vSysLab (vsyslab.osu.edu). Specimen records of *I. elba* and other species used in the comparative analysis are deposited in the Hymenoptera Online Database (hol.osu.edu).

Morphological terms largely follow Mikó et al. (2007) and were matched to concepts in the Hymenoptera Anatomy Ontology using the text analyzer function and a table of these terms and URI links is provided in Suppl. material 1.

Photography

Images of bagrada bug eggs and the wings of *I. elba* were produced with a Zeiss Stereo Discovery.V20, and images were captured with AxioCam IC-ZEN 2 lite software. Photographs of the lectotype of *I. howardi* were made available by Talamas et al. (2017). All other images of *I. elba* and *Idris* species for comparative illustration were taken with a Macroscopic Solutions Macropod Micro Kit with optical slices rendered in Helicon Focus.

Collections

Specimens used in this study are deposited in the following collections:

- CEAM** Colegio de Postgraduados Insect Collection, Texcoco, Estado de México, México
CNCI Canadian National Collection of Insects, Ottawa, ON, Canada
FSCA Florida State Collection of Arthropods, Gainesville, FL, USA
USNM National Museum of Natural History, Smithsonian Institution, Washington, DC, USA

Abbreviations and characters annotated in the figures

- atc** acetabular carina (Figure 7)
eps episternal foveae (Figures 7, 10, 14)
lpa lateral propodeal area (Figures 16–19)
metd metasomal depression (Figures 16, 21)
mpit metapleural pit (Figure 6)
mpp mesopleural pit (Figure 7)
msct metascutellum (Figures 16–17)
nes netrion sulcus (Figures 8, 9, 13)
pcxs paracoxal sulcus (Figures 10, 11)
pdms posterodorsal metapleural sulcus (Figure 7)
prcs pronotal cervical sulcus (Figure 12)
pss pronotal suprahumeral sulcus (Figure 12)
sp2 anterior thoracic spiracle (Figure 13)
T1–T7 mediotergites 1–7 (Figures 20, 21)

Molecular analysis

Two parasitoid adult specimens that emerged from field-collected *B. hilaris* eggs were used as voucher material for DNA analysis to generate reference sequences. DNA from parasitoid adults was extracted non-destructively using a Chelex DNA extraction method (as described in Garipey et al. 2019) and amplified using universal COI barcode primers (LCO-1490 and HCO-2198; Folmer et al. 1994) following the protocol described by Hebert et al. (2003). In addition, DNA from emerged field-collected eggs was extracted and amplified following the protocol described by Garipey et al. (2019) for forensic analysis of empty stink bug eggs; eggs from which parasitoid adults (n=4) had emerged were processed using family-specific scelionid PCR primers (Scel-F1 and HCO-2198) (Garipey et al. 2019). Eggs from which stink bug nymphs had emerged (n=10) were processed with universal barcode primers (LCO-1490 and HCO-2198).

PCR products were visualized with a QIAxcel Advanced automated capillary electrophoresis system (Qiagen) using the DNA screening cartridge and method AL320. Results were scored with the Qiaxcel ScreenGel Software (version 1.2.0), and only samples of the expected fragment size with a signal strength exceeding 0.1 relative fluorescent units were scored as positive. Samples scored as positive were purified using ExoSAP-IT (Affymetrix, Santa Clara, California, USA) following the manufacturer's instructions. Purified PCR products were bidirectionally sequenced using the appropriate primers (SCEL-F1 and HCO-2198 for parasitized eggs or LCO-1490 and HCO-2198 for unparasitized eggs and parasitoid adults) on an ABI 3730 DNA Analyzer at the Robarts Research Institute (London Regional Genomics Centre, Ontario, Canada). Forward and reverse sequences were assembled and edited using CodonCode Aligner program, version 4.2.7 (CodonCode Corporation, Centerville Massachusetts, USA). Specimen data, assembled DNA sequences, and tracefiles for all samples that yielded sequences >400 bp were uploaded into BOLD under the project "Parasitoids of the genus *Idris* and their hosts" (IDRIS). DNA barcodes obtained from empty eggs were screened through the BOLD identification system to identify the host eggs based on publically-available DNA sequences in the identification engine. Parasitoid DNA obtained from the egg fragments was compared to the DNA barcode profiles generated from voucher *Idris* specimens for confirmation of species identity.

Results

A total of 88 *B. hilaris* eggs were collected across all sites surveyed in Guanajuato. Four parasitoids were recovered from 17 eggs collected May 31, 2018 (2 males, 2 females). These parasitoids emerged from eggs collected at the locality of Santa Cruz, municipality of Juventino Rosas, Guanajuato (20.622390N, 101.015655W). The parasitized eggs were collected in the soil near *Brassica nigra* plants, and the recovered species was

Table 1. Genbank Accession numbers for *Idris elba*.

Collecting Unit Identifier	Genbank Accession Number	Collection Locality
FSCA 00033237	MN135849	Santa Cruz, Guanajuato, Mexico
FSCA 00033238	MN135848	Santa Cruz, Guanajuato, Mexico
FSCA 00033127	MN135850	Sandoval County, New Mexico, USA

identified as a species in the genus *Idris* Förster (Hymenoptera: Scelionidae) based on the compact clava in females and other characters presented in Masner (1980).

DNA sequences were obtained for adult specimens and yielded a 649-bp COI fragment using the universal DNA barcode primers (LCO-1490, HCO-2198). Four out of 10 unparasitized stink bug eggs successfully amplified and sequenced using the universal COI barcode primers and were identified as *Bagrada hilaris* (100% identity) using the BOLD identification system (Genbank accession number MN135841–MN135844). The remaining unparasitized eggs yielded poor quality DNA sequences, likely due to insufficient or degraded DNA from unpreserved field-collected samples. Three out of the 4 parasitized eggs successfully amplified and sequenced using the scelionid PCR primers (Scel-F1, HCO-2198) (Genbank accession numbers MN135845–MN135847). The sequences were an exact match to the DNA barcode reference sequences obtained from the *I. elba* adults collected from the same site, thus corroborating the observational evidence that *I. elba* indeed emerged from field-collected *B. hilaris* eggs. COI sequences of these specimens and a specimen of *I. elba* from New Mexico have been uploaded to Genbank (Table 1).

Taxonomy

Idris elba Talamas, sp. nov.

<http://zoobank.org/26052F1D-C091-4398-9497-6689DC8AE0B7>

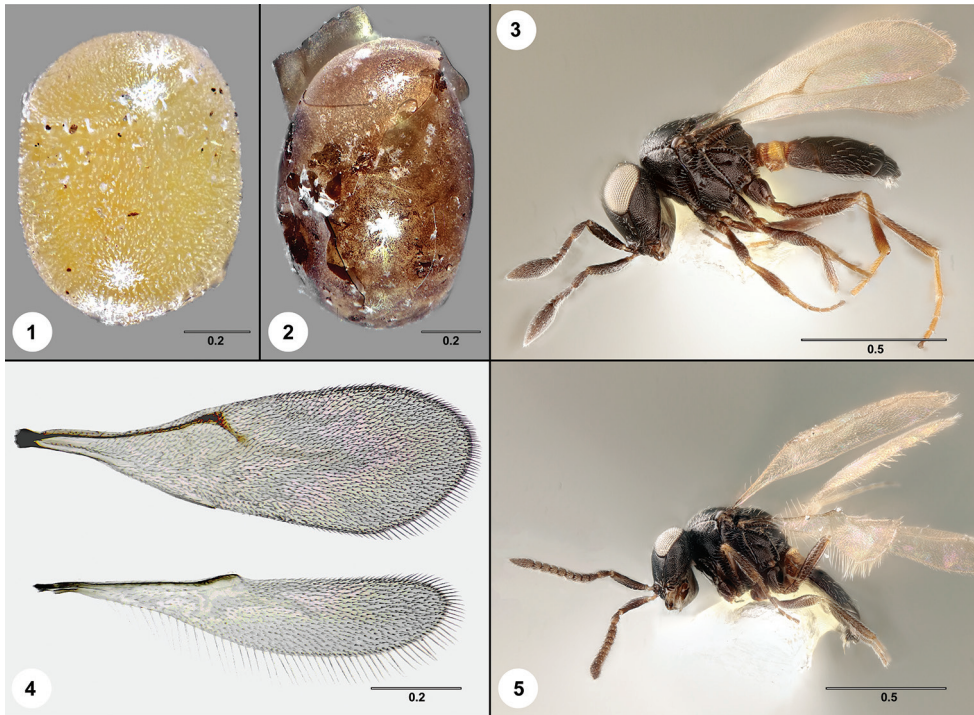
https://bioguid.osu.edu/xbiod_concepts/498223

Figures 3–5, 7, 9, 10, 16, 21

Description. Female body length: 0.85–1.16 mm (n=9). Male body length: 0.96–1.07 mm (n=2).

Head. Color of antenna: pale brown to black. Claval formula: 1-2-2-1. Mandible: tridentate, teeth of equal size. Number of clypeal setae: 6. Length of central keel: extending to midpoint of frons. Facial striae: short, not reaching ventral limit of compound eye. Malar striae: short and weakly indicated, not reaching ventral limit of compound eye. Hyperoccipital carina: present. Occipital carina: present ventrally, absent above midpoint of compound eye.

Mesosoma. Pronotal suprahumeral sulcus: absent. Epomial carina: absent. Pronotal cervical sulcus: absent. Dorsal terminus of netrion sulcus: ventral to anterior thoracic spiracle. Netrion sulcus: comprised of foveae, foveae elongate at midpoint of sulcus. Mesoscutal suprahumeral sulcus: foveate. Mesoscutal humeral sulcus: fove-



Figures 1–5. **1** unparasitized egg of *B. hilaris* **2** egg of *B. hilaris* from which *I. elba* emerged **3** *Idris elba*, holotype female (FSCA 00033238), lateral habitus **4** *Idris elba* paratype female (FSCA 00090587) fore and hind wings, dorsal view **5** *Idris elba*, paratype male (FSCA 00033237), lateral habitus. Scale bars: in millimeters.

ate. Scutoscutellar sulcus: smooth medially, foveate laterally in axillar area. Interior of axillar crescent: smooth. Posterior mesoscutellar sulcus: foveate, continuous around posterior and lateral margins of scutellar disc. Metanotal trough: foveate. Metascutellum: present as a smooth strip. Plical carina: absent. Lateral propodeal carinae: closely approximated medially. Perimeter of lateral propodeal area: foveate. Sculpture of lateral propodeal area: granulate; smooth. Sculpture of metasomal depression: radially striate; smooth. Propleural epicoxal sulcus: absent. Postacetabular sulcus: foveate. Mesopleural epicoxal sulcus: comprised of foveae. Intercostal space: narrow, cells of postacetabular and mesopleural epicoxal sulci confluent ventrally. Number of episternal foveae: 2. Prespecular sulcus: present, not extending to mesopleural pit. Paracoxal sulcus in ventral half of metapleuron: foveate. Metapleural epicoxal sulcus: comprised of elongate foveae anteriorly, absent posteriorly. Metapleural sulcus: extending anteriorly from metapleural pit as a smooth furrow. Posterodorsal metapleural sulcus: foveate, interrupted medially.

Metasoma. Color of metasoma: T1–S1, anterior T2–S2 yellow to pale brown, otherwise brown to black. Horn on T1 in females: absent; Sculpture of T1: longitudinally striate. Sculpture of T2: weakly striate posterior to transverse sulcus. Sculpture of T3–T6: uniform coriaceous microsculpture. T6–T7: located ventral to T4–T5, not visible

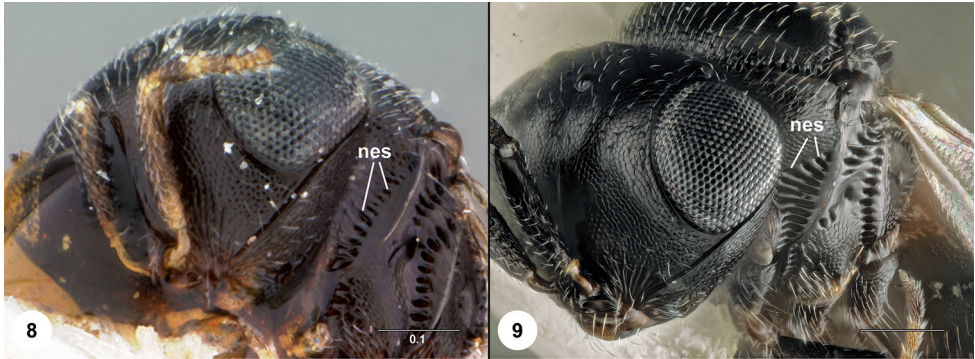


Figures 6, 7. *Idris howardi*, lectotype female (USNMMENT00989875), head, mesosoma, metasoma, lateral view **7** *Idris elba*, holotype female (FSCA 00033238), head, mesosoma, metasoma, lateral view. Scale bars: in millimeters.

in dorsal view. Sculpture of S1: longitudinally striate. Sculpture of S2: weakly striate posterior to transverse sulcus. Sculpture of S3–S6: uniform coriaceous microsculpture.

Variation. We observed notable variation in the degree of development of two characters. The microsculpture of the lateral propodeal area can be distinctly granulate (Figures 10, 21) or mostly smooth (Figure 16), and sculpture of the metasomal depression varies from radially striate (Figure 21) to mostly smooth (Figure 16)

Material examined. Holotype, female: **MEXICO**: 20.622390N, 101.015655W, Santa Cruz de Juventino Rosas, Guanajuato, 18.V.2018, reared from *Bagrada hilaris* egg, FSCA 00033238 (deposited in FSCA). Paratypes: (9 females, 3 males) **MEXICO**: 1 female, 2 males, FSCA 00090587–00090588 (CEAM); FSCA 00033237 (FSCA).

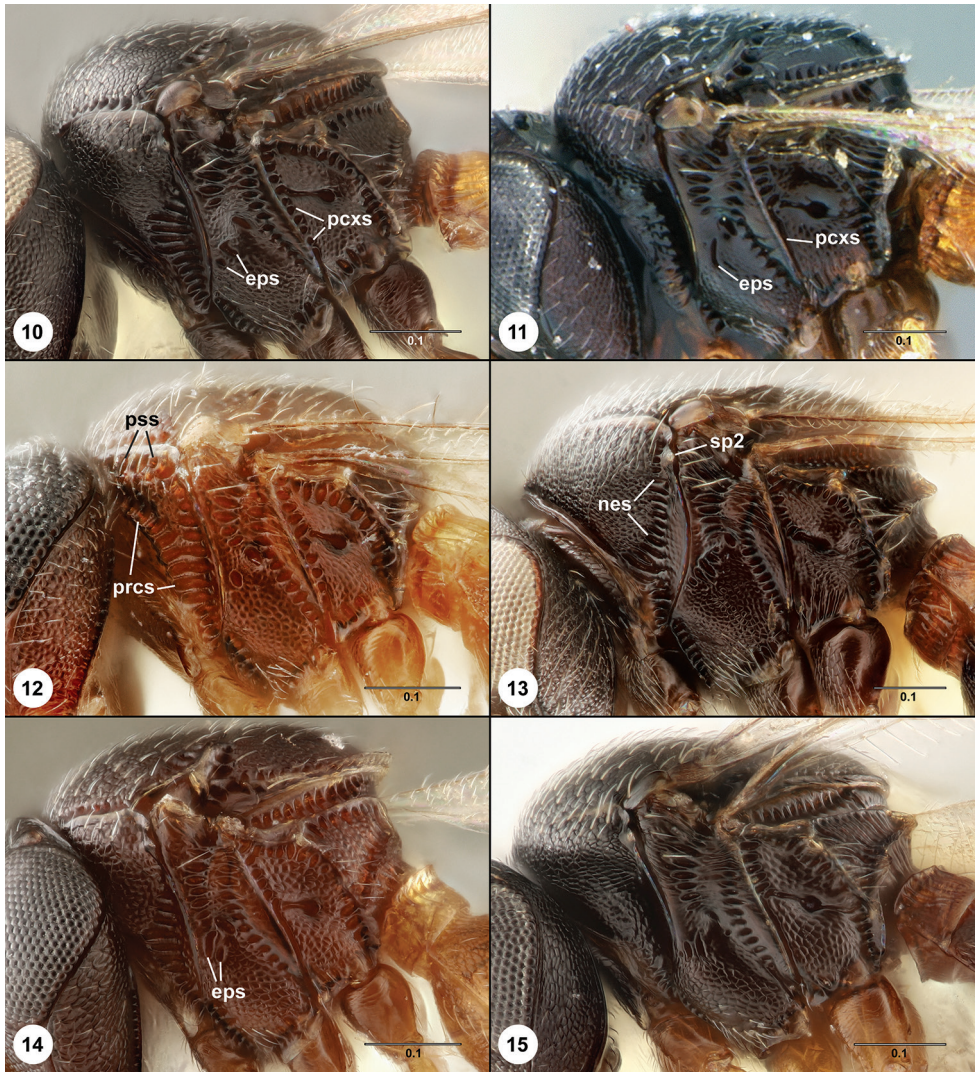


Figures 8, 9. **8** *Idris howardi*, lectotype female (USNMENT00989875), head and mesosoma, anterolateral view **9** *Idris elba*, holotype female (FSCA 00033238), head and mesosoma, anterolateral view. Scale bars: in millimeters.

UNITED STATES: 8 females, 1 male, FSCA 00090463 (CNCI); FSCA 00033127 (FSCA); USNMENT01335975–01335981 (USNM).

Diagnosis. It should be noted that our diagnosis is presented without full knowledge of the diversity of Nearctic *Idris* and additional comparison to the images, description, and sequence data here provided may be necessary to confirm the species identity. From the material that we have examined, *Idris elba* can be identified by the combination of the following characters: netrion sulcus complete and dorsally terminating ventral to the anterior thoracic spiracle; pronotal suprahumeral sulcus absent; pronotal cervical sulcus absent; episternal foveae arranged along a line between the mesopleural pit and the dorsal apex of the acetabular carina; paracoxal sulcus comprised mostly or entirely of foveae in the ventral half of the metapleuron; metapleural sulcus absent posterior to the metapleural pit; lateral propodeal area without rugae or longitudinal striation; T1 in females without horn; T6–T7 located ventral to T4–T5.

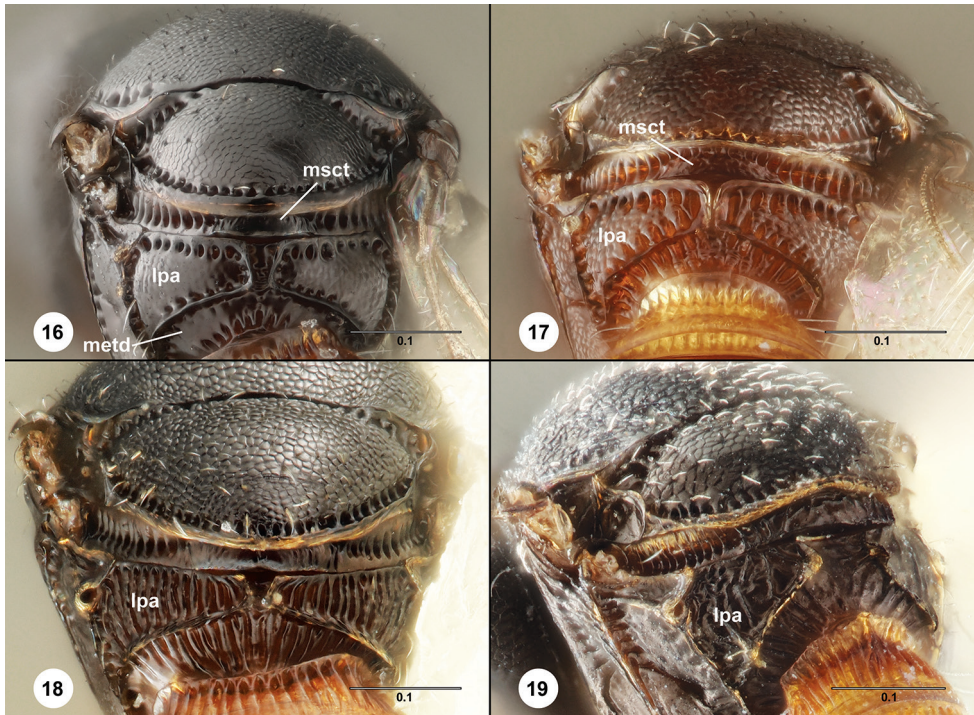
Two distinct characters are found in *I. elba* and numerous other species of Nearctic *Idris*, the color pattern of a dark body with a distinctly lighter T1/S1 and anterior T2/S2 (Figures 3, 5–7, 20, 21), and the form of the metasoma in which T6–T7 are oriented vertically and are largely obscured from dorsal view (Figures 20, 21). Among the described species of the Nearctic region, *I. howardi* is morphologically closest to *I. elba* and exhibits both traits. *Idris howardi* can be separated by the striate lateral propodeal area (Figure 20), the ventral portion of the paracoxal sulcus expressed as a simple furrow (Figure 11), and the small size of foveae of the netrion sulcus (compare Figures 8, 9). The absence of rugae or striae in the lateral propodeal area is very useful for diagnosing *I. elba* (compare Figures 10–19) but can be found in at least one other species from the region. This species can be separated by the paracoxal sulcus taking the form of a smooth furrow in the ventral half of the metapleuron, the episternal foveae arranged perpendicular to a line between the mesopleural pit and the dorsal apex of the acetabular sulcus (Figure 14) and the foveae of the metanotal trough forming a con-



Figures 10–15. **10** *Idris elba*, holotype female (FSCA 00033238), mesosoma, lateral view **11** *Idris howardi*, lectotype female (USNMENT00989875), mesosoma, lateral view **12** *Idris* sp., female (FSCA 00090464), mesosoma, lateral view **13** *Idris* sp., female (FSCA 00033145), mesosoma, lateral view **14** *Idris* sp., female (FSCA 00090465), mesosoma, lateral view **15** *Idris* sp., male (FSCA 00090467), mesosoma, lateral view. Scale bars: in millimeters.

tinuous line above the metascutellum (Figure 17). In female specimens of *I. elba*, the metascutellum interrupts the line of foveae across the metanotal trough (Figure 16).

We encountered one other species with the ventral portion of the paracoxal sulcus comprised of cells (Figure 12), and this species can easily be separated by the presence of distinct pronotal cervical and pronotal suprahumeral sulci on the lateral pronotum (Figure 12). We emphasize the utility of mesosomal sulci for future taxonomic studies, which exhibit an exceptional diversity of form in *Idris*. One remarkable species from

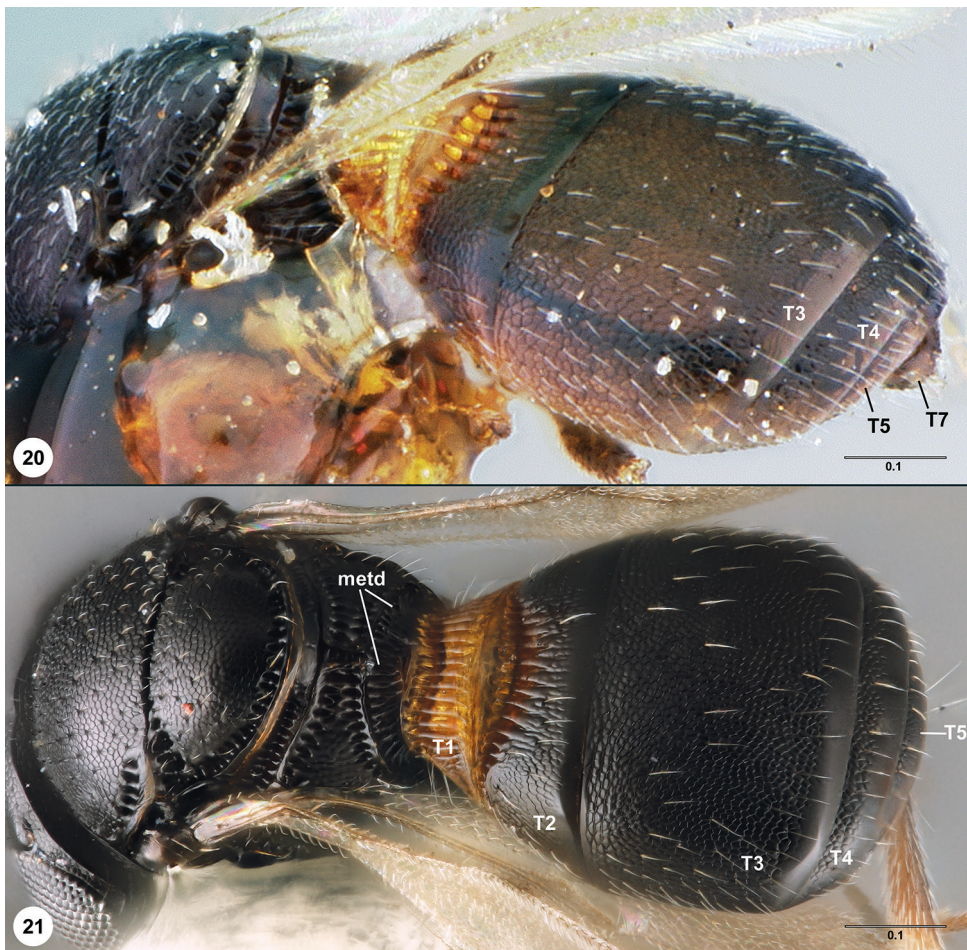


Figures 16–19. **16** *Idris elba*, paratype female (FSCA 00090463), mesosoma, posterolateral view **17** *Idris* sp., female (FSCA 00090465), mesosoma, posterolateral view **18** *Idris* sp., male (FSCA 00090467), mesosoma, posterolateral view **19** *Idris* sp., (FSCA 00090466), mesosoma, posterolateral view. Scale bars: in millimeters.

the mid-Atlantic USA features a netrion sulcus that terminates *anterior* to the anterior thoracic spiracle (Figure 13). Within Platygastroidea this unusual form is known to us only from *Nixonia* Masner (Nixoniidae) (Mikó et al. 2007).

Etymology. The epithet “elba” is an arbitrary combination of letters that is to be treated as a noun in apposition.

Comments. It is our opinion that the description of a new species from a genus as large and unexplored as *Idris* outside of the context of a thorough revision generally should be avoided. In the case of *Idris elba*, we justify our treatment based on the following: First, we are confident that *I. elba* has not been described previously from the Nearctic region. *Idris elba* clearly does not belong to the *I. melleus* species group treated by Masner and Denis (1996) based on the characters they presented, including “head moderately to remarkably large relative to the mesosoma and metasoma”, and “propodeum canaliculate (except in *I. pulvinus*)”. Images of all other species from the Nearctic are available via the online image database *Specimage* (specimage.osu.edu), provided by Norman Johnson (The Ohio State University) and Talamas et al. (2017). Based on these images, *Idris elba* can be separated from all described Nearctic species outside of the *melleus* group by the smooth lateral propodeal area, foveate mesoscutal humeral sulcus, and T6–T7 located ventral to T4–T5. Second, we considered the possibility



Figures 20, 21. **20** *Idris howardi*, lectotype female (USNMENT00989875), mesosoma and metasoma, dorsolateral view **21** *Idris elba*, holotype female (FSCA 00033238), mesosoma and metasoma, dorsal view. Scale bars: in millimeters.

that *I. elba* is an adventive species, given that the phenomenon of adventive populations of parasitoids following their invasive hosts is now well documented and has occurred with bagrada bug in North America (Ganjisaffar et al. 2018). We contend that this is highly unlikely because some specimens of *I. elba* were collected in New Mexico in 2008 (Sandoval Co.), two years prior to the first detection of *B. hilaris* in this state (Doña Ana Co.) (Bundy et al. 2012). Last, the host association of *Idris* with bagrada bug eggs is of agricultural consequence with implications for the ability of parasitoids to shift between phylogenetically distant hosts (Araneae and Hemiptera), and thus there is an immediate need to formally refer to this species. Revising the species of Nearctic *Idris* is a project requiring years of work and for which resources are not currently available. This situation exemplifies the need for a pre-existing taxonomic framework for parasitoid Hymenoptera, including taxa where the economic importance is not obvious. To that end, this publication may provide impetus for taxonomic revision of Nearctic *Idris*.

Discussion

Most hymenopteran parasitoids attack a narrow range of closely related host species, resulting from the coevolutionary arms race that restricts the ability of a parasitoid to develop in novel, phylogenetically distant host species (Godfray 1994, Rossinelli and Bacher 2014). However, there are some exceptions. For example, egg parasitoids belonging to the genus *Anastatus* Motschulsky (Hymenoptera: Eupelmidae) can often attack and develop in insects from different orders, and some can develop in eggs of pentatomids, mantids, and various Lepidoptera (Rao et al. 1971, Fritz et al. 1986, Jones 1988). The host range of a parasitoid is of considerable interest from ecological and evolutionary perspectives but is often difficult to interpret due to misidentifications of parasitoid and host species, contaminated rearing (Shaw 1994, Quicke 1997), and the logistical challenges of locating small, cryptically located hosts (eggs) in the environment. To overcome these difficulties, we used traditional rearing and a molecular forensic approach to detect and identify trace amounts of DNA to confirm the host-parasitoid associations in field-collected host eggs.

Members of the genus *Idris* are known to be solitary, primary parasitoids of spider eggs (Hickman 1967, Austin 1981, Masner and Denis 1996) and have not been reported previously from other arthropod hosts. *Idris* species are known from a variety of spider families and are thought to have a high degree of host group specificity (Iqbal and Austin 2000). However, there are no data available on the degree of host specificity within individual wasp species, and to date no egg parasitoids from the tribe Baeini (including *Idris*) have been reared from a host other than a spider (Johnson et al. 2018). The discovery of *I. elba* as a parasitoid of *B. hiliaris* is thus quite unexpected and suggests the potential for a much broader host range of *Idris* – one that includes both spider and insect hosts. The distinctive oviposition behavior of *B. hiliaris*, wherein eggs are laid in the soil (as opposed to on the plant like most pentatomids), suggests the possibility that the host selection and specificity of *Idris* may be based on habitat overlap between *B. hiliaris* eggs and spider eggs. As suggested by Strand and Obrycki (1996), shared ecology can be used to predict the host range of a natural enemy, where a parasitoid will attack a diversity of arthropods occurring in a defined habitat. This may be a case of accidental parasitism by *I. elba*, based on chance encounters with *B. hiliaris* eggs in the same habitat as its typical spider host. The physiological and developmental suitability of *B. hiliaris* eggs for *I. elba* is remarkable given the fact that the accidental host is not closely related to the hosts that are usually attacked by *Idris* species. Although largely speculative, it is possible that some of the strategies used to overcome host defenses are conserved within Scelionidae and confer some level of developmental success in a non-target host. To some extent this must be the case as numerous host shifts have occurred in the family (Austin et al. 2005). The degree of parasitism that *I. elba* can achieve on *B. hiliaris* is unknown, and further investigation on the frequency of occurrence, developmental success, and potential fitness consequences associated with development in *B. hiliaris* merits investigation, not only to determine its potential contribution to biological control strategies for this pest in Mexico, but also to provide improved understanding of this unlikely host-parasitoid association. The synergy of carefully executed field studies, traditional taxonomy and molecular forensics to identify the occurrence of *I. elba* in *B. hiliaris* shows the value of complementary methods in

the discovery of host-parasitoid associations and provides strong supporting evidence for associations that might otherwise be considered unlikely to occur in nature.

Acknowledgements

The authors are grateful to Oscar Hernández-Torres and Juan M. Vanegas-Rico for support and field work and to Matthew Buffington (USDA/SEL) for providing additional images of *Idris* holotypes. This project was sponsored by the Dirección General de Sanidad Vegetal of the Ministry of Agriculture (SENASICA-SADER), and the Colegio de Postgraduados. Support for EJT was provided by the Florida Department of Agriculture and Consumer Services-Division of Plant Industry, and the USDA/APHIS Farm Bill, Biological Control of Bagrada Bug.

References

- Arakelian G (2010) Bagrada Bug, *Bagrada hilaris*. Center for Invasive Species Research, University of California, Riverside. http://cistr.ucr.edu/bagrada_bug.html
- Austin AD (1981) The types of Australian species in the tribes Idrini, Baeni and Embidobiini (Hymenoptera: Scelionidae: Scelioninae). *General and Applied Entomology* 13: 81–92. <http://doi:10.5281/zenodo.23561>
- Austin AD, Johnson NF, Downton M (2005) Systematics, evolution, and biology of scelionid and platygastriid wasps. *Annual Review of Entomology* 50: 553–582. <https://doi.org/10.1146/annurev.ento.50.071803.130500>
- Bundy CS, Grasswitz TR, Sutherland C (2012) First report of the invasive stink bug *Bagrada hilaris* (Burmeister) (Heteroptera: Pentatomidae) from New Mexico, with notes on its biology. *Southwestern Entomologist* 37: 411–414. <https://doi.org/10.3958/059.037.0317>
- Carvajal MA, Alaniz AJ, Núñez-Hidalgo I, González-Céspedes C (2018) Spatial global assessment of the pest *Bagrada hilaris* (Burmeister) (Heteroptera: Pentatomidae): current and future scenarios. *Pest Management Science*. <https://doi.org/10.1002/ps.5183>
- Chacko MJ, Katiyar RN (1961) *Hadrophanurus karnalensis* sp. n. (Hymenoptera: Scelionidae), a parasite of *Bagrada cruciferarum* Kirkaldy (Hemiptera: Pentatomidae). *Proceedings of the Royal Entomological Society of London* 30: 161–163. <https://doi.org/10.1111/j.1365-3113.1961.tb00155.x>
- Cheema MA, Irshad M, Murtaza M, Ghani MA (1973) Pentatomids associated with Gramineae and their natural enemies in Pakistan. *Technical Bulletin of the Commonwealth Institute of Biological Control* 16: 47–67.
- Cornell HV, Hawkins BA (1993) Accumulation of Native Parasitoid Species on Introduced Herbivores A Comparison of Hosts as Natives and Hosts as Invaders. *American Naturalist* 141: 847–865. <https://doi.org/10.1086/285512>
- Faúndez EI, Lüer A, Cuevas ÁG, Rider DA, Valdebenito P (2016) First record of the painted bug *Bagrada hilaris* (Burmeister, 1835) (Heteroptera: Pentatomidae) in South America. *Arquivos Entomológicos* 16: 175–179.

- Felipe-Victoriano M, Talamas EJ, Sánchez-Peña SR (2019) Scelionidae (Hymenoptera) parasitizing eggs of *Bagrada hilaris* (Hemiptera: Pentatomidae) in Mexico. In: Talamas E (Eds) Advances in the Systematics of Platygastroidea II. Journal of Hymenoptera Research 73: 143–152. <https://doi.org/10.3897/jhr.73.36654>
- Folmer O, Black M, Hoeh W, Lutz R, Vrijenhoek R (1994) DNA primers for amplification of mitochondrial cytochrome c oxidase subunit I from diverse metazoan invertebrates. Molecular Marine Biology and Biotechnology 3: 294–299.
- Fritz GN, Frater AP, Owens JC, Huddleston EW, Richman DB (1986) Parasitoids and predators of *Hemileuca oliviae* (Lepidoptera: Saturniidae) in Chihuahua, Mexico. Annals of the Entomological Society of America 79:686–690. <https://doi.org/10.1093/aesa/79.4.686>
- Hrcek J, Miller SE, Quicke DL, Smith MA (2011), Molecular detection of trophic links in a complex insect host–parasitoid food web. Molecular Ecology Resources 11: 786–794. <https://doi.org/10.1111/j.1755-0998.2011.03016.x>
- Ganjisaffar F, Talamas EJ, Bon MC, Gonzalez L, Brown BV, Perring TM (2018) *Trissolcus hyalinipennis* Rajmohana & Narendran (Hymenoptera, Scelionidae), a parasitoid of *Bagrada hilaris* (Burmeister) (Hemiptera, Pentatomidae), emerges in North America. Journal of Hymenoptera Research 65: 111–130. <https://doi.org/10.3897/jhr.65.25620>
- Garipey TD, Bruin A, Konopka J, Scott-Dupree C, Fraser H, Bon M-C, Talamas EJ (2019) A modified DNA barcode approach to define trophic interactions between native and exotic pentatomids and their parasitoids. Molecular Ecology 28:456–470. <https://doi.org/10.1111/mec.14868>
- Garrison R (2009) Bagrada bug Pentatomidae: *Bagrada hilaris* (Burmeister). In: Gaimari S, O'Donnell M (Eds) California Plant Pest & Disease Report. California Department of Food & Agriculture, Plant Pest Diagnostics Branch, Sacramento, CA.
- Godfray HCJ (1994) Parasitoids: Behavioral and Evolutionary Ecology, Princeton University Press, Princeton, NJ, USA.
- Hebert PDN, Cywinska A, Ball SL, deWaard JR (2003) Biological identifications through DNA barcodes. Proceedings of the Royal Society of London B. 270: 313–321. <https://doi.org/10.1098/rspb.2002.2218>
- Hernández-Chávez L, Salas-Araiza MD, Martínez-Jaime OA, Flores Mejía S (2018) First report of *Bagrada hilaris* Burmeister, 1835 (Hemiptera: Pentatomidae) in the state of Guanajuato, Mexico. Entomological News 128: 72–74. <https://doi.org/10.3157/021.128.0110>
- Hickman VV (1967) New Scelionidae which lay their eggs in those of spider. Journal of the Entomological Society of Australia (N.S.W.) 4: 15–37.
- Howard CW (1906) The Bagrada bug (*Bagrada hilaris*). Transvaal Agriculture Journal 5: 168–173. https://hdl.handle.net/10520/AJA0000010_449
- Iqbal M, Austin AD (2000) Systematics of the wasp genus *Ceratobaeus* Ashmead (Hymenoptera: Scelionidae) from Australasia: parasitoids of spider eggs. Records of the South Australian Museum Monograph Series 6: 1–164.
- Johnson NF, Chen H, Huber BA (2018) New species of *Idris* Förster (Hymenoptera, Platygastroidea) from southeast Asia, parasitoids of the eggs of pholcid spiders (Araneae, Pholcidae). ZooKeys 811: 65–80. <https://doi.org/10.3897/zookeys.811.29725>

- Jones WA (1988) World Review of the Parasitoids of the Southern Green Stink Bug, *Nezara viridula* (L.) (Heteroptera: Pentatomidae). *Annals of the Entomological Society of America* 81: 262–273. <https://doi.org/10.1093/aesa/81.2.262>
- Joseph SV, Grettenberger I, Godfrey L (2016) Insecticides applied to soil of transplant plugs for *Bagrada hilaris* (Burmeister) (Hemiptera: Pentatomidae) management in broccoli. *Crop Protection* 87: 68–77. <https://doi.org/10.1016/j.cropro.2016.04.023>
- Mahmood R, Jones WA, Bajwa BE, Rashid K (2015) Egg parasitoids from Pakistan as possible classical biological control agents of the invasive pest *Bagrada hilaris* (Heteroptera: Pentatomidae). *Journal of Entomological Science* 50: 147–149. <https://doi.org/10.18474/JES14-28.1>
- Mani MS, Sharma SK (1982) Proctotrupeoidea (Hymenoptera) from India. *Oriental Insects* 16(2): 135–258. <https://doi.org/10.1080/00305316.1982.10434314>
- Martel G, Auge M, Talamas E, Roche M, Smith L, Sforza RFH (2019) First Laboratory evaluation of *Gryon gonikopalense* (Hymenoptera: Scelionidae), as potential biological control agent of *Bagrada hilaris* (Hemiptera: Pentatomidae). *Biological Control* 135: 48–56. <https://doi.org/10.1016/j.biocontrol.2019.04.014>
- Masner L (1980) Key to genera of Scelionidae of the Holarctic region, with descriptions of new genera and species (Hymenoptera: Proctotrupeoidea). *Memoirs of the Entomological Society of Canada* 113: 1–54. <https://doi.org/10.4039/entm112113fv>
- Masner L, Denis J (1996) The nearctic species of *Idris* Foerster. Part 1: the *Melleus*-group (Hymenoptera: Scelionidae). *The Canadian Entomologist* 128: 85–114. <https://doi.org/10.4039/Ent12885-1>
- Mikó I, Vilhelmsen L, Johnson NF, Masner L, Péntzes Z (2007) Skeletomusculature of Scelionidae (Hymenoptera: Platygastroidea): head and mesosoma. *Zootaxa* 1571: 1–78. <https://doi.org/10.11646/zootaxa.1571.1.1>
- Obopile M, Munthali DC, Matilo B (2008) Farmers' knowledge, perceptions and management of vegetable pests and diseases in Botswana. *Crop Protection* 27: 1220–1224. <https://doi.org/10.1016/j.cropro.2008.03.003>
- Palumbo JC (2016) Impact of bagrada bug on fall cole crops from 2010–2015. *Arizona Experiment Station. Veg IPM Update* 7: 1–6.
- Palumbo JC, Perring TM, Millar JG, Reed DA (2016) Biology, ecology, and management of an invasive stink bug, *Bagrada hilaris*, in North America. *Annual Review of Entomology* 61: 453–473. <https://doi.org/10.1146/annurev-ento-010715-023843>
- Perring TM, Reed DA, Palumbo JC, Grasswitz T, Bundy CS, Jones W, Papes M, Royer T (2013) National Pest Alert, Bagrada Bug *Bagrada hilaris* (Burmeister) Family Pentatomidae. Invasive and Exotic Pests, UC Statewide IPM Program (UC IPM). <https://www.ncipmc.org/action/alerts/bagradabug.pdf>
- Quicke D (1997) Parasitic wasps. Chapman and Hall, London, UK.
- Rao VP, Ghani MA, Sankaran T, Mathur KC (1971) A review of the biological control of insects and other pests in south-east Asia and the Pacific region. *Commonwealth Institute of Biological Control, Technical Communication* 6.
- Reed DA, Palumbo JC, Perring TM, May C (2013) *Bagrada hilaris* (Hemiptera: Pentatomidae), An Invasive Stink Bug Attacking Cole Crops in the Southwestern United States, *Journal of Integrated Pest Management* 4: C1–C7. <https://doi.org/10.1603/IPM13007>

- Rossinelli S, Bacher S (2014) Higher establishment success in specialized parasitoids: support for the existence of trade-offs in the evolution of specialization. *Function Ecology* 29: 277–284. <https://doi.org/10.1111/1365-2435.12323>
- Rougerie R, Smith MA, Fernandez-Triana J, Lopez-Vaamonde C, Ratnasingham S, Hebert PD (2011) Molecular analysis of parasitoid linkages (MAPL): gut contents of adult parasitoid wasps reveal larval host. *Molecular Ecology* 20: 179–186. <https://doi.org/10.1111/j.1365-294X.2010.04918.x>
- Sánchez-Peña SR (2014) First record in Mexico of the invasive stink bug *Bagrada hilaris*, on cultivated crucifers in Saltillo. *Southwestern Entomologist* 39(2): 375–377. <https://doi.org/10.3958/059.039.0219>
- Sachan GC, Purwar JP (2007) Integrated pest management in rapeseed and mustard. In: Jain PC, Bhargava MC (Eds) *Entomology, Novel Approaches*. New Delhi, New India Publishing, 413–416.
- Shaw MR (1994) Parasitoid host ranges. In: Hawkin BA, Sheehan W (Eds) *Parasitoid Community Ecology*. Oxford University Press, New York.
- SIAP (2018) Atlas Agroalimentario 2012–2018. Servicio de Información Agroalimentaria y Pesquera (SIAP): 1–222. https://nube.siap.gob.mx/gobmx_publicaciones_siap/pag/2018/Atlas-Agroalimentario-2018
- Strand MR, Obrycki JJ (1996) Host Specificity of Insect Parasitoids and Predators: Many factors influence the host ranges of insect natural enemies. *BioScience* 46: 422–429. <https://doi.org/10.2307/1312876>
- Talamas EJ, Thompson J, Cutler A, Fitzsimmons Schoenberger S, Cuminale A, Jung T, Johnson NF, Valerio AA, Smith AB, Haltermann V, Alvarez E, Schwantes C, Blewer C, Bodenreider C, Salzberg A, Luo P, Meislin D, Buffington ML (2017) An online photographic catalog of primary types of Platygastroidea (Hymenoptera) in the National Museum of Natural History, Smithsonian Institution. In: Talamas EJ, Buffington ML (Eds) *Advances in the Systematics of Platygastroidea*. *Journal of Hymenoptera Research* 56: 187–224. <https://doi.org/10.3897/jhr.56.10774>

Supplementary material I

URI table of HAO morphological terms

Authors: J. Refugio Lomeli-Flores, Susana Eva Rodríguez-Rodríguez, Esteban Rodríguez-Levy, Hector González-Hernández, Tara D. Garipey, Elijah J. Talamas

Data type: species data

Explanation note: This table lists the morphological terms used in this publication and their associated concepts in the Hymenoptera Anatomy Ontology.

Copyright notice: This dataset is made available under the Open Database License (<http://opendatacommons.org/licenses/odbl/1.0/>). The Open Database License (ODbL) is a license agreement intended to allow users to freely share, modify, and use this Dataset while maintaining this same freedom for others, provided that the original source and author(s) are credited.

Link: <https://doi.org/10.3897/jhr.73.38025.suppl1>

Scelionidae (Hymenoptera) parasitizing eggs of *Bagrada hilaris* (Hemiptera, Pentatomidae) in Mexico

Moisés Felipe-Victoriano¹, Elijah J. Talamas², Sergio R. Sánchez-Peña¹

1 Departamento de Parasitología Agrícola, Universidad Autónoma Agraria Antonio Narro (UAAAN), Saltillo, Coahuila 25315, México **2** Florida State Collection of Arthropods, Division of Plant Industry, Florida Department of Agriculture and Consumer Services, Gainesville, Florida, USA

Corresponding author: Sergio R. Sánchez-Peña (sanchezcheco@gmail.com)

Academic editor: J. Fernandez-Triana | Received 30 May 2019 | Accepted 30 July 2019 | Published 18 November 2019

<http://zoobank.org/590CC4D6-EFFC-4F99-8365-08676A181271>

Citation: Felipe-Victoriano M, Talamas EJ, Sánchez-Peña SR (2019) Scelionidae (Hymenoptera) parasitizing eggs of *Bagrada hilaris* (Hemiptera: Pentatomidae) in Mexico. In: Talamas E (Eds) Advances in the Systematics of Platygastroidea II. Journal of Hymenoptera Research 73: 143–152. <https://doi.org/10.3897/jhr.73.36654>

Abstract

The painted bug or bagrada bug, *Bagrada hilaris* (Burmeister) (Hemiptera: Pentatomidae), is a key pest of crops in the family Brassicaceae. In this work, three species of Scelionidae (Hymenoptera) are reported for the first time as parasitoids of painted bug eggs in Mexico, at Saltillo, state of Coahuila: *Gryon myrmecophilum* (Ashmead), *Telenomus podisi* Ashmead and *Trissolcus basalís* (Wollaston). This is also the first report of a species of the widespread genus *Telenomus* as an egg parasitoid of *B. hilaris*. Total percent parasitism, high resolution images, and CO1 sequences are provided for each species. In the future, research in Mexico should be carried out on parasitoid species presented in this work to determine their potential as biological control agents and the feasibility of augmentative, classical or inoculative biocontrol strategies for integrated pest management.

Keywords

Heteroptera, stink bug, biological control, parasitoid

Introduction

Bagrada hilaris (Burmeister) (Hemiptera: Pentatomidae), known in Mexico with the common names of bagrada bug or painted bug, is a key pest of cole crops (family Brassicaceae) originally distributed in Africa and Asia (Howard 1906; Ahuja et al. 2008; Kavita et al. 2014). This pest first invaded California, USA, in 2008 (Palumbo et al.

2016) and in 2014 was detected in Saltillo, southeastern Coahuila, Mexico, causing economic damage in broccoli (*Brassica oleracea* L. var. *italica*), cabbage (*B. oleracea* var. *capitata*), and cauliflower (*B. oleracea* var. *capitata*) (Sanchez-Peña 2014; Torres-Acosta and Sánchez-Peña 2016).

The family Scelionidae is a cosmopolitan group of parasitoids that attacks the eggs of a variety of arthropods, including Hemiptera. In the Old World, several authors have reported parasitoids of this family attacking painted bug eggs. In India, *Gryon karnalense* (Chacko and Katiyar) and *Telenomus samueli* Mani were reported from the eggs of *B. hilaris* (as *Bagrada cruciferarum* Kirkaldy) (Chacko and Katiyar 1961; Mani and Sharma 1982). In Pakistan, sentinel eggs of *B. hilaris* placed in the field for four days and subsequently incubated in the laboratory yielded three species of hymenopteran parasitoids: *Trissolcus hyalinipennis* Rajmohana & Narendran, *Gryon gonikopalense* Sharma and a species of *Ooencyrtus* Ashmead (Encyrtidae) (Mahmood et al. 2015; Sforza et al. 2019). In the USA, Ganjisaffar et al. (2018) reported *Trissolcus basalis* and *Tr. hyalinipennis* parasitizing painted bug eggs in California. The objective of this work is to determine the presence of parasitoids of painted bug through sentinel eggs in northwestern Mexico and facilitate future work in this line of research.

Materials and methods

Field site

The work was carried out in the experimental fields of the Universidad Autónoma Agraria Antonio Narro (UAAAN) in Saltillo, state of Coahuila, México (25°21'15.80"N, 101°2'17.98"W, 1746 meters above sea level. The specific irrigated field (0.07 hectares) was planted with an assortment of Brassicaceae cultivars in equal numbers of the following plants: Arugula (*Eruca vesicaria* L. ssp. *sativa*), broccoli, cabbage, cauliflower, kohlrabi (*Brassica napobrassica* Miller. 1768), mustard (*Sinapis alba* L. 1753), radish (*Raphanus sativus* L. 1753) and turnip (*Brassica rapa* L. 1753 subsp. *rapa*).

Detection of parasitoids of painted bug through sentinel eggs.

Eggs were obtained by rearing field-collected mating pairs of painted bugs in the laboratory. Eight mating pairs were placed in Petri dishes at a temperature of 26–28 °C with diffuse overhead daylight. After 12 hours in the laboratory, mating pairs in the Petri dishes produced an average of 270 eggs (range of 85–580). The mating pairs were removed and the eggs (on the same uncovered Petri dish bottom they were laid on) were placed on the soil surface at a distance of approximately 5 cm from a broccoli stem. If it was necessary to handle the eggs, a soft number 2 brush (Pinceles Rex, Mexico City) was used.

The sentinel egg tests were conducted monthly in the field from 25 November 2017 – 20 December 2018. The eggs were exposed 7–8 days in the field, and subsequently incubated at 24–28 °C and a relative humidity of 60% in the laboratory until

the emergence of parasitoids. The wasps that emerged were placed in 96% ethanol until their subsequent identification.

DNA analysis

Specimens were softened in 70% ethanol for two hours, then DNA was extracted using a DNeasy Blood and Tissue Kit (Qiagen). DNA extracts were quantified using a NanoDrop 2000 spectrophotometer (Thermo Scientific). At least 20 ng of genomic DNA was used per PCR. The 5'-CO1 barcode region was PCR-amplified using the primers LCO1490 and HCO2198 (Folmer et al. 1994). PCRs were performed at 25 µl volumes using HiFi HotStart DNA Polymerase (Kapa Biosystems). PCR thermo-cycle conditions were: 1) initial denaturing at 95 °C for 2:00 minutes followed by 32 cycles of steps 2–4, 2) 98 °C for 30 seconds, 3) 50 °C for 30 seconds, 4) 72 °C for 40 seconds, and 5) final extension at 72 °C for 7:00 minutes. PCR products were verified by gel electrophoresis and cleaned for sequencing with QIAquick Gel Extraction Kits (Qiagen). Purified PCR products were Sanger sequenced in both directions using Big-Dye Terminator v3.1 (Applied Biosystems) chemistry on a SeqStudio Genetic Analyzer (Applied Biosystems). Sequence reads were trimmed and sequence contigs were assembled in Sequencher 5.4.6 (Gene Codes Corporation). CO1 barcodes generated during this study were deposited in GenBank. Accession numbers for these sequences are presented in Table 1.

Morphological identification

Specimens of *G. myrmecophilum* and *Te. podisi* were identified to species using the keys of Masner (1980) and Johnson (1984), respectively. Specimens of *Tr. basalis* were identified using Talamas et al. (2015) and the description by Ganjisaffar et al. (2018) of morphological variation present in individuals that emerge from *B. hiliaris* eggs.

Stacks of photographs were taken with a Macropod imaging system and rendered using HeliconFocus. Specimen collection data and host associations are deposited in the Hymenoptera Online Database (<http://hol.osu.edu>). Voucher specimens for all scelionid species are deposited at the Florida State Collection of Arthropods (FSCA), Gainesville, Florida, and the Entomology collection, Universidad Autónoma Agraria Antonio Narro, Saltillo, Mexico.

Table 1. Accession numbers for specimens of Scelionidae used for DNA sequencing.

Species	Locality	Collection Unit Identifier	GenBank Accession Number
<i>Trissolcus basalis</i>	Saltillo, Mexico	FSCA 00090267	MK720829
<i>Telenomus podisi</i>	Saltillo, Mexico	FSCA 00090266	MK720830
<i>Gryon myrmecophilum</i>	Saltillo, Mexico	FSCA 00090442	MK720831
<i>Gryon myrmecophilum</i>	Saltillo, Mexico	FSCA 00090443	MK720832
<i>Gryon myrmecophilum</i>	Rutgers, NJ, USA	FSCA 00090445	MK937524

Results

Scelionid wasps were detected only in November 2017 and June, July and August 2018. In a subsequent paper we will discuss in detail the phenology of the parasitoid complex on painted bug eggs at this location in Mexico.

Trissolcus basalis (Wollaston)

Figs 1–3

As reported by Ganjisaffar et al. (2018), specimens of *Tr. basalis* that emerge from the eggs of *B. hiliaris* have reduced episternal foveae and fainter striation on T2 relative to specimens that emerge from larger stink bug eggs (Figs 2–3).

BLAST comparison of the CO1 sequence from specimen FSCA 00090267 resulted in a 100% identity to a *Tr. basalis* sequence in Genbank from the USA ([MK188338.1](#)), providing confirmation of the morphological identification.

On the collection date of 25 November 2017, a total of 29 *Tr. basalis* were collected (this date was the only time *Tr. basalis* emerged from sentinel eggs) and the percentage of parasitism was 12.4% (n= 234 eggs).

Telenomus podisi (Ashmead)

Figs 4–6

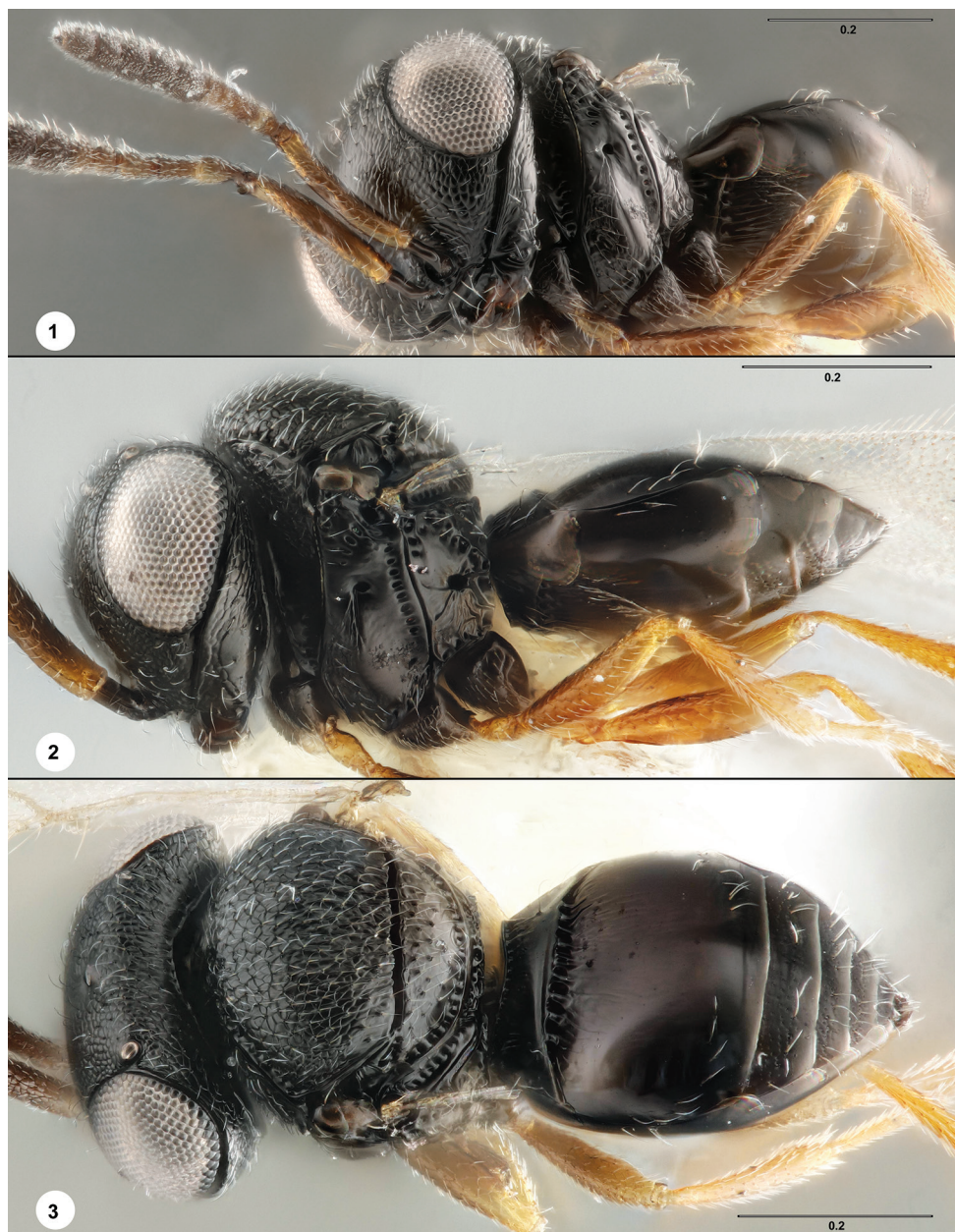
The small size of *B. hiliaris* eggs does not influence the diagnostic morphology of *Te. podisi* and no relevant differences were found between the specimens in this study and *Te. podisi* reared from other stink bug eggs. BLAST comparison of the CO1 sequence from specimen FSCA 00090266 resulted in 98.9% sequence identity with *Te. podisi* sequence [KR870961.1](#) from Genbank.

On the monthly collection dates between January–December 2018, a total of 51 *Te. podisi* was collected in the months of June and July, resulting in 9.2 and 9.9% of parasitism respectively (n= 532 eggs).

Gryon myrmecophilum (Ashmead)

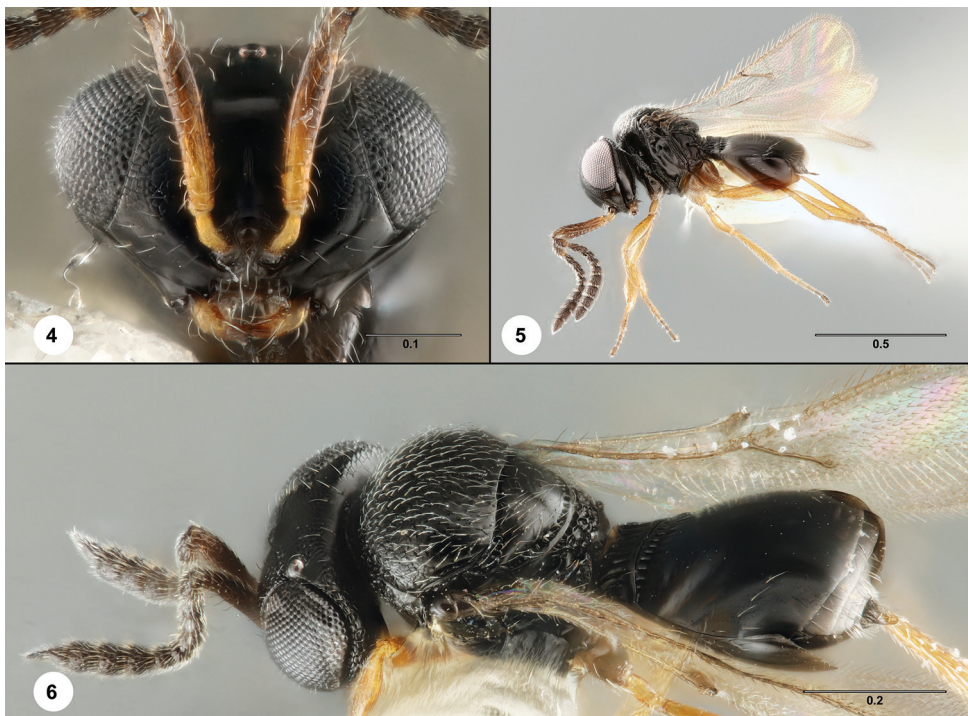
Figs 7–11

Our identification of this species is based on the revision of the genus by Masner (1980) and the specimens in this study were compared to photographs of the holotype specimen made available by Talamas et al. (2017). The systematics of *Gryon* is currently under revision by the second author. Preliminary analysis indicates that *G. myrmecophilum* belongs to a cosmopolitan cluster of similar species, some of which may have intercontinental distributions. A specimen of *G. myrmecophilum* from New



Figures 1–3. *Trissolcus basalis* female (FSCA 00090267) **1** head, mesosoma, metasoma, ventrolateral view **2** head, mesosoma, metasoma, lateral view **3** head, mesosoma, metasoma, dorsolateral view. Scale bars: in millimeters.

Jersey (FSCA 00090445) was sequenced to provide a comparison with a specimen closer to the type locality (Washington, DC). Comparison of the sequences from Mexico and New Jersey showed 88% sequence identity, indicating that *G. myrmecophilum*



Figures 4–6. *Telenomus podisi* **4** female (FSCA 00033549) head, anterior view **5** female (FSCA 00090266) habitus, lateral view **6** female (FSCA 00033275) head, mesosoma, metasoma, dorsolateral view. Scale bars: in millimeters.

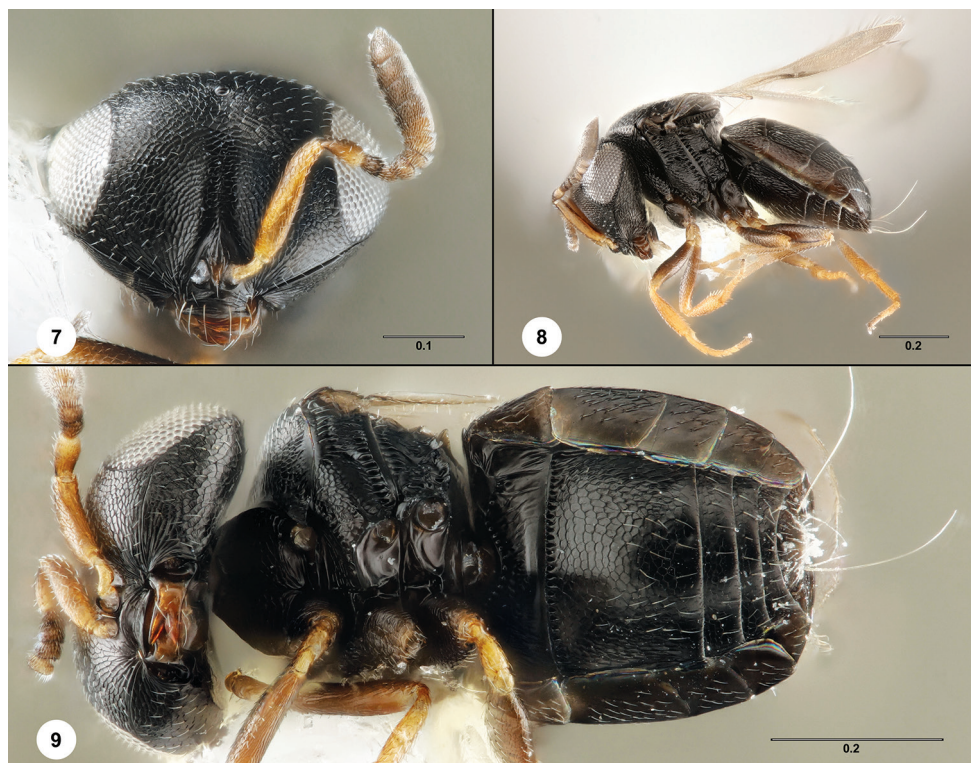
exhibits a high degree of variability in this gene region, or it is possibly a cryptic species complex.

On the monthly collection dates between January–December 2018, a total of 115 *G. myrmecophilum* were collected in the months of June, July and August, resulting in 3.0, 7.6 and 43.2% of parasitism respectively (n=786 eggs).

Discussion and conclusion

In 2017, only *Tr. basalis* emerged from eggs, in the month of November (29 specimens), for 12.4% of parasitism. This wasp is a near-cosmopolitan parasitoid of stink bug eggs for which one widespread host is the southern green stink bug, *Nezara viridula* (L.) (Powell and Shepard 1982).

During the 2018 monthly sampling dates, scelionid wasps were detected only in June–August. The percentages of egg parasitism by all Scelionidae in the months of June, July and August 2018 correspond to 12.2, 17.4 and 49.6% respectively (total of 166 wasp specimens). Out of the total monthly percent parasitism, *Gryon myrmecophilum* contributed with 24.2, 43.5 and 100% in June, July and August, respectively (115 specimens total); and *Tè. podisi* contributed with 75.8 and 56.5%, for the months

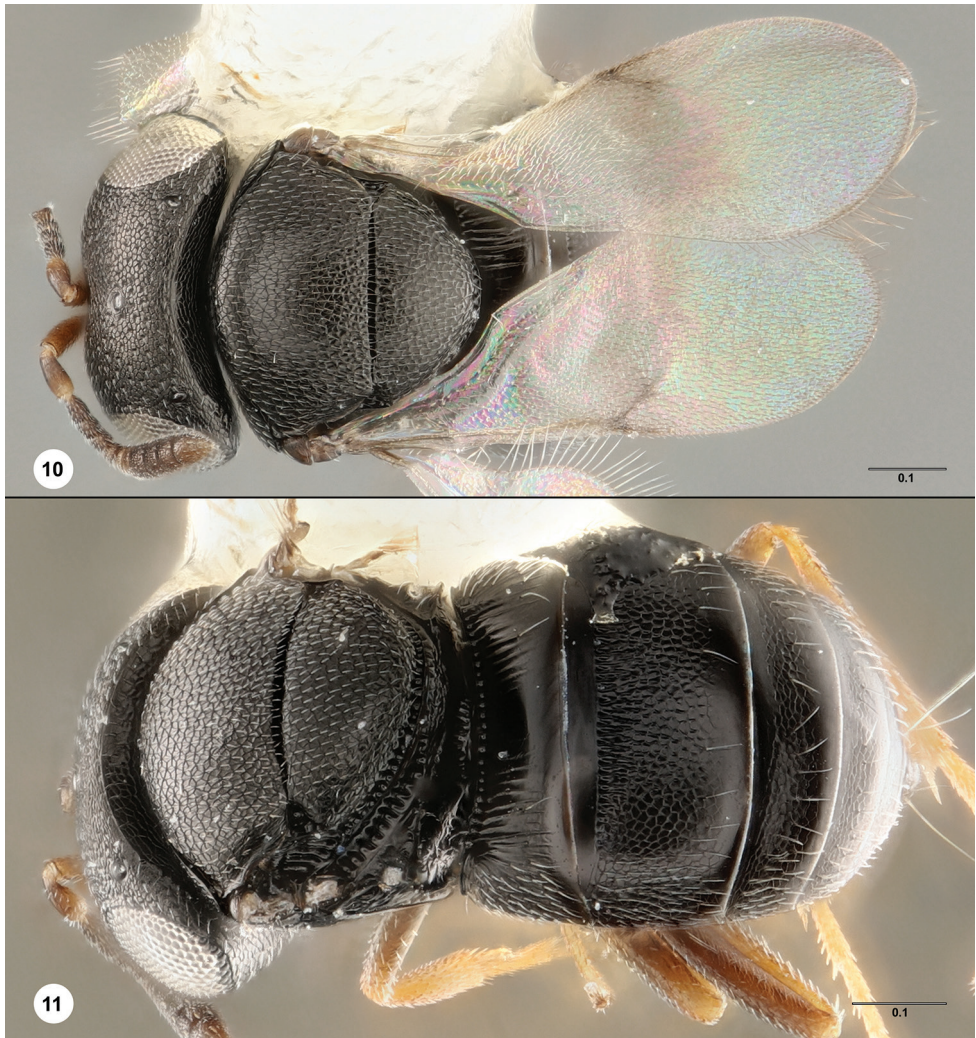


Figures 7–9. *Gryon myrmecophilum* **7** female (FSCA 00090446) head, anterior view **8** female (FSCA 00090447) habitus, lateral view **9** female (FSCA 00090446) head, mesosoma, metasoma, ventral view. Scale bars: in millimeters.

of June and July, respectively (51 specimens total). Species of *Telenomus* have been reported as parasitoids of other stink bugs, including *Euschistus heros* (F.), *Halyomorpha halys* (Stål), *Oebalus insularis* Stål, *Piezodorus guildinii* (Westwood) and *Tibraca limbativentris* (Stål).

In Pakistan, Mahmood et al. (2015) reported that *Tr. hyalinipennis* and *G. gonikopalense* had a combined parasitism rate of 32–38%. This level is similar to the parasitism level obtained in our work. In California, USA, Ganjisaffar et al. (2018) reported that *Tr. basalis* and *Tr. hyalinipennis* parasitized 4.0–20.0% of *B. hiliaris* sentinel eggs in January of 2018. We did not observe parasitism by scelionids in January, but it should be noted that our study includes only a small number of sampling dates. Additional sampling is required to describe the phenology of these wasps on *Bagrada* eggs.

To our knowledge, the present work reports the highest percentage of field parasitism of painted bug eggs in the USA and Mexico. It is also the first report of *Te. podisi* parasitizing painted bug eggs. We continue studying the identity, distribution and population fluctuation of beneficial wasps associated with painted bug eggs at selected localities in Mexico. Future research should be carried out on these species, and possibly others that have yet to be detected, to determine their potential



Figures 10–11. *Gryon myrmecophilum*, female (FSCA 00090447) **10** head and mesosoma, dorsal view **11** habitus, dorsal view. Scale bars: in millimeters.

as biological control agents. In particular, there is a need for critical comparative analysis of the different modalities of biological control (classical, augmentative or inoculative) that can utilize parasitic wasps in the integrated pest management of the painted bug in Mexico.

Acknowledgments

This work was supported by Consejo Nacional de Ciencia y Tecnología (CONACYT) scholarship 300868 to MFV; Dirección de Investigación, UAAAN, project

2109; USDA APHIS Farm Bill, Biological Control of Bagrada Bug, and the Florida Department of Agriculture and Consumer Services – Division of Plant Industry. We also thank Matthew Moore and Cheryl Roberts (FDACS/DPI) for performing the PCR and sequencing reactions, and to Paul Skelley, Zee Ahmed and Susan Halbert (FDACS/DPI) for reviewing earlier version of the manuscript.

References

- Ahuja B, Kalyan R, Ahuja U, Singh S, Sundria M, Dhandapani A (2008) Integrated management strategy for painted bug, *Bagrada hilaris* (Burm.) inflicting injury at seedling stage of mustard (*Brassica juncea*) in arid western Rajasthan. Pesticide Research Journal 20: 48–51.
- Chacko MJ, Katiyar RN (1961) *Hadrophanurus karnalensis* sp. n. (Hymenoptera: Scelionidae), a parasite of *Bagrada cruciferarum* Kirkaldy (Hemiptera: Pentatomidae). Systematic Entomology 30: 161–163. <https://doi.org/10.1111/j.1365-3113.1961.tb00155.x>
- Folmer O, Black M, Hoeh W, Lutz R, Vrijenhoek R (1994) DNA primers for amplification of mitochondrial cytochrome c oxidase subunit I from diverse metazoan invertebrates. Molecular Marine Biology and Biotechnology 3: 294–299.
- Ganjisaffar F, Talamas EJ, Bon MC, Gonzalez L, Brown BV, Perring TM (2018) *Trissolcus hyalinipennis* Rajmohana & Narendran (Hymenoptera, Scelionidae), a parasitoid of *Bagrada hilaris* (Burmeister) (Hemiptera, Pentatomidae), emerges in North America. Journal of Hymenoptera Research 65: 111–130. <https://doi.org/10.3897/jhr.65.25620>
- Howard CW (1906) The Bagrada bug (*Bagrada hilaris*). Transvaal Agriculture Journal 5: 168–173.
- Johnson NF (1984) Systematics of Nearctic *Telenomus*: classification and revisions of the *podisi* and *phymatae* species groups (Hymenoptera: Scelionidae). Bulletin of the Ohio Biological Survey 6: 1–112.
- Kavita D, Arvind K, Singh D, Yadav P (2014) Studies of the ecological parameter, site of oviposition, population dynamics and seasonal cycle of *Bagrada cruciferarum* on *Brassica campestris*. Journal of Experimental Zoology, India 17: 331–336.
- Mahmood R, Jones WA, Bajwa BE, Rashid K (2015) Egg parasitoids from Pakistan as possible classical biological control agents of the invasive pest *Bagrada hilaris* (Heteroptera: Pentatomidae). Journal of Entomological Science 50: 147–149. <https://doi.org/10.18474/JES14-28.1>
- Mani MS, Sharma SK (1982) Proctotrupeoidea (Hymenoptera) from India: a review. Oriental Insects 16: 135–258. <https://doi.org/10.1080/00305316.1982.10434314>
- Masner L (1980) Key to genera of Scelionidae of the Holarctic region, with descriptions of new genera and species (Hymenoptera: Proctotrupeoidea). The Memoirs of the Entomological Society of Canada 112: 1–54. <https://doi.org/10.4039/entm112113fv>
- Palumbo JC, Perring TM, Millar JG, Reed DA (2016) Biology, ecology, and management of an invasive stink bug, *Bagrada hilaris*, in North America. Annual Review of Entomology 61: 453–473. <https://doi.org/10.1146/annurev-ento-010715-023843>
- Powell JE, Shepard M (1982) Biology of Australian and United States strains of *Trissolcus basalis*, a parasitoid of the green vegetable bug, *Nezara viridula*. Australian Journal of Ecology 7: 181–186. <https://doi.org/10.1111/j.1442-9993.1982.tb01591.x>

- Sánchez-Peña SR (2014) First record in Mexico of the invasive stink bug *Bagrada hilaris*, on cultivated crucifers in Saltillo. *Southwestern Entomologist* 39: 375–377. <https://doi.org/10.3958/059.039.0219>
- Sforza RFH, Martel G, Roche M, Talamas E, Augé M, Smith L (2019) First Laboratory evaluation of *Gryon gonikopalense* (Hymenoptera: Scelionidae) as potential biological control agent of *Bagrada hilaris* (Hemiptera: Pentatomidae). *Biological Control* 135: 48–56. <https://doi.org/10.1016/j.biocontrol.2019.04.014>
- Talamas EJ, Johnson NF, Buffington M (2015) Key to Nearctic species of *Trissolcus* Ashmead (Hymenoptera, Scelionidae), natural enemies of native and invasive stink bugs (Hemiptera, Pentatomidae). *Journal of Hymenoptera Research* 43: 45–118. <https://doi.org/10.3897/JHR.43.8560>
- Talamas EJ, Thompson J, Cutler A, Fitzsimmons Schoenberger S, Cuminale A, Jung T, Johnson NF, Valerio AA, Smith AB, Haltermann V, Alvarez E, Schwantes C, Blewer C, Bodenreider C, Salzberg A, Luo P, Meislin D, Buffington ML (2017) An online photographic catalog of primary types of Platygastroidea (Hymenoptera) in the National Museum of Natural History, Smithsonian Institution. In: Talamas EJ, Buffington ML (Eds) *Advances in the Systematics of Platygastroidea*. *Journal of Hymenoptera Research* 56: 187–224. <https://doi.org/10.3897/jhr.56.10774>
- Torres-Acosta RI, Sánchez-Peña SR (2016) Geographical distribution of *Bagrada hilaris* (Hemiptera: Pentatomidae) in Mexico. *Journal of Entomological Science* 51: 165–167. <https://doi.org/10.18474/JES15-41.1>

A morphological, biological and molecular approach reveals four cryptic species of *Trissolcus* Ashmead (Hymenoptera, Scelionidae), egg parasitoids of Pentatomidae (Hemiptera)

Francesco Tortorici¹, Elijah J. Talamas², Silvia T. Moraglio¹, Marco G. Pansa¹, Maryam Asadi-Farfar³, Luciana Tavella¹, Virgilio Caleca⁴

1 Dipartimento di Scienze Agrarie, Forestali e Alimentari (DISAFA), Entomologia Generale e Applicata, University of Torino, Largo P. Braccini 2, 10095 Grugliasco (TO), Italy **2** Florida Department of Agriculture and Consumer Service, Division of Plant Industry, Gainesville, Florida, USA **3** Department of Plant Protection, Faculty of Agriculture, Urmia University, Urmia, Iran **4** Department of Agricultural, Food and Forest Sciences, University of Palermo, Edificio 5, Viale delle Scienze, 90128 Palermo, Italy

Corresponding author: *Elijah J. Talamas* (talamas.1@osu.edu)

Academic editor: *G. Broad* | Received 13 August 2019 | Accepted 1 November 2019 | Published 18 November 2019

<http://zoobank.org/>

Citation: Tortorici F, Talamas EJ, Moraglio ST, Pansa MG, Asadi-Farfar M, Tavella L, Caleca V (2019) A morphological, biological and molecular approach reveals four cryptic species of *Trissolcus* Ashmead (Hymenoptera, Scelionidae), egg parasitoids of Pentatomidae (Hemiptera). In: Talamas E (Eds) Advances in the Systematics of Platygastroidea II. Journal of Hymenoptera Research 73: 153–200. <https://doi.org/10.3897/jhr.73.39052>

Abstract

Accurate identification of parasitoids is crucial for biological control of the invasive brown marmorated stink bug, *Halyomorpha halys* (Stål). A recent work by Talamas et al. (2017) revised the Palearctic fauna of *Trissolcus* Ashmead, egg-parasitoids of stink bugs, and treated numerous species as junior synonyms of *T. semistriatus* (Nees von Esenbeck). In the present paper, we provide a detailed taxonomic history and treatment of *T. semistriatus* and the species treated as its synonyms by Talamas et al. (2017) based on examination of primary types, molecular analyses and mating experiments. *Trissolcus semistriatus*, *T. belemus* (Walker), *T. colemani* (Crawford), and *T. manteroi* (Kieffer) are here recognized as valid and a key to species is provided. The identification tools provided here will facilitate the use of *Trissolcus* wasps as biological control agents and as the subject of ecological studies.

Keywords

Biological control, taxonomy, brown marmorated stink bug

Table of contents

Abstract.....	1
Introduction.....	2
Taxonomic history of <i>T. semistriatus</i> and related species.....	3
Material and methods.....	7
Collections.....	7
Geographical distribution and host association.....	8
Cybertaxonomy.....	8
Photography.....	9
Morphology.....	9
Insect collecting and rearing.....	10
Molecular analyses.....	10
Mating tests and reproductive isolation between <i>T. belenus</i> and <i>T. semistriatus</i> ..	11
Results.....	12
Morphological analysis.....	12
Molecular analysis.....	13
Mating tests.....	13
Key to <i>Trissolcus</i> of the Palearctic region (females).....	15
<i>Trissolcus belenus</i> (Walker).....	16
<i>Trissolcus colemani</i> (Crawford).....	23
<i>Trissolcus manteroi</i> (Kieffer).....	29
<i>Trissolcus semistriatus</i> (Nees von Esenbeck).....	33
Discussion.....	39
Acknowledgements.....	40
References.....	41
Supplementary material 1.....	46
Supplementary material 2.....	47
Supplementary material 3.....	47
Supplementary material 4.....	48
Supplementary material 5.....	48
Supplementary material 6.....	49

Introduction

Taxonomy of the genus *Trissolcus* Ashmead has received renewed attention in recent years (Talamas et al. 2015, 2017), largely because accurate identification of these wasps is needed to use them as biological control agents against the invasive brown marmorated stink bug (*Halyomorpha halys* (Stål)) in Europe and North America. Morphological similarity, sharing of hosts by various species of *Trissolcus*, and the historical complications presented in Talamas et al. (2017) and Buffington et al. (2018) are some of the challenges faced by taxonomists working with this group.

The revision of Palearctic *Trissolcus* (Talamas et al. 2017) provided keys to species, complete redescriptions, illustrations, and the utilization of new morphological characters. Many new synonymies were presented, including *T. grandis* (Thomson), *T. artus* Kozlov & Lê, *T. colemani* (Crawford), *T. djadetsbko* (Rjachovskij), *T. manteroi* (Kieffer), *T. nigripedius* (Nakagawa), *T. pentatoma* (Rondani) and *T. pseudoturesis* (Rjachovskij) as junior synonyms of *T. semistriatus* (Nees von Esenbeck).

In support of studies on the egg-parasitoid complex of European Pentatomoidea, a survey of egg masses was conducted and previously collected specimens were also examined. Using the key to species provided by Talamas et al. (2017), *Trissolcus* specimens that emerged from *Aelia rostrata* Boheman, *Arma custos* (F.), *Carpocoris* spp., *Eurygaster maura* (L.), *Graphosoma lineatum* (L.), *Palomena prasina* (L.) collected between 1996 and 2017 in Piedmont (NW Italy) were identified as *T. semistriatus*. However, some consistent morphological differences were detected among the specimens, which instigated closer examination using multiple methods. The focus of this paper is the morphological and molecular analysis of species synonymized under *T. semistriatus* by Talamas et al. (2017), and the integration of mating tests, when possible, to confirm species delimitation.

Taxonomic history of *T. semistriatus* and related species

Species described by Walker

Telenomus belenus was described by Walker (1836), then transferred by Kieffer (1912) to *Aphanurus* Kieffer, then transferred to *Microphanurus* Kieffer (Kieffer 1926). Walker (1838) described *Telenomus arminon* but did not provide distinctive characters by which it could be identified or separated from *Telenomus belenus*. Kieffer (1912) transferred *Tē. arminon* to *Allophanurus* Kieffer and provided a redescription. Kieffer did not mention if his treatment was based on type material, and we consider it unlikely that it was. Lectotypes for *Tē. belenus* and *Tē. arminon* were designated by Fergusson (1984, 1983), respectively, from material housed in the National Museum of Ireland, Dublin. Despite their antiquity, and thus priority, these species received no further taxonomic treatment.

Trissolcus semistriatus vs. *T. grandis*

In taxonomic literature, the distinction between *T. semistriatus* and *T. grandis* has long been questioned. Mayr (1879) and Nixon (1939) ascertained *T. semistriatus* to be a highly variable species. Masner (1959) wrote “On base of the check of type of *Asolcus grandis* (Thomson), the latter species was synonymized with *semistriatus*”. However, the meaning of this sentence is unclear because we have not found in the literature previous synonymy of *T. grandis* under *T. semistriatus*, and it is not clear that Masner

sought to synonymize them for the first time. In this paper, Masner addressed characters considered to distinguish *T. grandis* and *T. semistriatus* (rugosity of the frons, leg color, longitudinal sculpture on the posterior mesoscutum, body length) based on the comparison of ~500 reared specimens and stated that these characters were variable within *T. semistriatus*. Viktorov (1967) considered *T. grandis* to be conspecific with *T. semistriatus*, but he did not formally treat it as a junior synonym. Subsequent authors considered *T. semistriatus* and *T. grandis* as different species, but without clearly defining the boundaries between them. Delucchi (1961) provided the first reliable character to distinguish *T. semistriatus* from *T. grandis*: the external surface of the hind femur is almost totally covered by setation in *T. grandis* (Figure 1), and he coupled this character with the color of the tibiae: reddish yellow in *T. semistriatus*, dark or black in *T. grandis*. Most authors continued to distinguish *T. semistriatus* and *T. grandis* by tibial color and ignored setation of the hind femora. This color-based distinction was employed in numerous previous and following papers (Delucchi 1961; Javahery 1968; Kozlov 1968, 1978; Safavi 1968; Voegelé 1969; Fabritius 1972; Kozlov and Lê 1977; Kozlov and Kononova 1983), and no substantial change was indicated in keys to species by Kononova (1995, 2014, 2015). Talamas et al. (2017) did not use tibial setation to differentiate between these species, but listed a new character, the form of the mesoscutal humeral sulcus, and mentioned setation of the first laterotergite, which was first presented as a character for species of *Trissolcus* by Johnson (1987). Although Talamas et al. (2017) treated these characters as variable within *T. semistriatus*, analysis of these characters in light of molecular and mating experiments has allowed us to use them for species delimitation.

In a study on larval stages, Voegelé (1964) provided information about pigmentation of the membrane secreted by the larvae of different *Trissolcus* species reared in eggs of *Eurygaster austriaca* (L.). He distinguished *T. semistriatus* from *T. grandis* by the width of the pigmented band close to the margin of host egg operculum (see fig. 4 in Voegelé, 1964). In his key to species, Safavi (1968) coupled color of the hind tibia (instead of mid tibia), and width of the pigmented band in larval membrane shown by Voegelé (1964), also adding different length ratios of the first two flagellomeres in males.

Trissolcus artus was distinguished by Kozlov and Kononova (1983) and Kononova (1995) from *T. grandis* (black tibiae) by its reddish-yellow tibiae, and from *T. semistriatus* by having a more elongate clava and infuscation in the fore wing. This last feature is used in the key by Kononova (2014, 2015) to distinguish *T. artus* from both *T. grandis* and *T. semistriatus*.

Trissolcus manteroi

Trissolcus manteroi was described by Kieffer (1909) as having the postmarginal vein (pm) slightly longer than the stigmal vein (st). In Kozlov and Kononova (1983), Koçak and Kilinçer (2003) and Kononova (2014, 2015), *T. manteroi* was distinguished by its postmarginal vein 1.3× as long as the stigmal vein, compared to 1.8× in *Trissolcus rufiventris* (Mayr), and 2× in *T. grandis* (= *T. belenus*) and *T. semistriatus*. Kononova

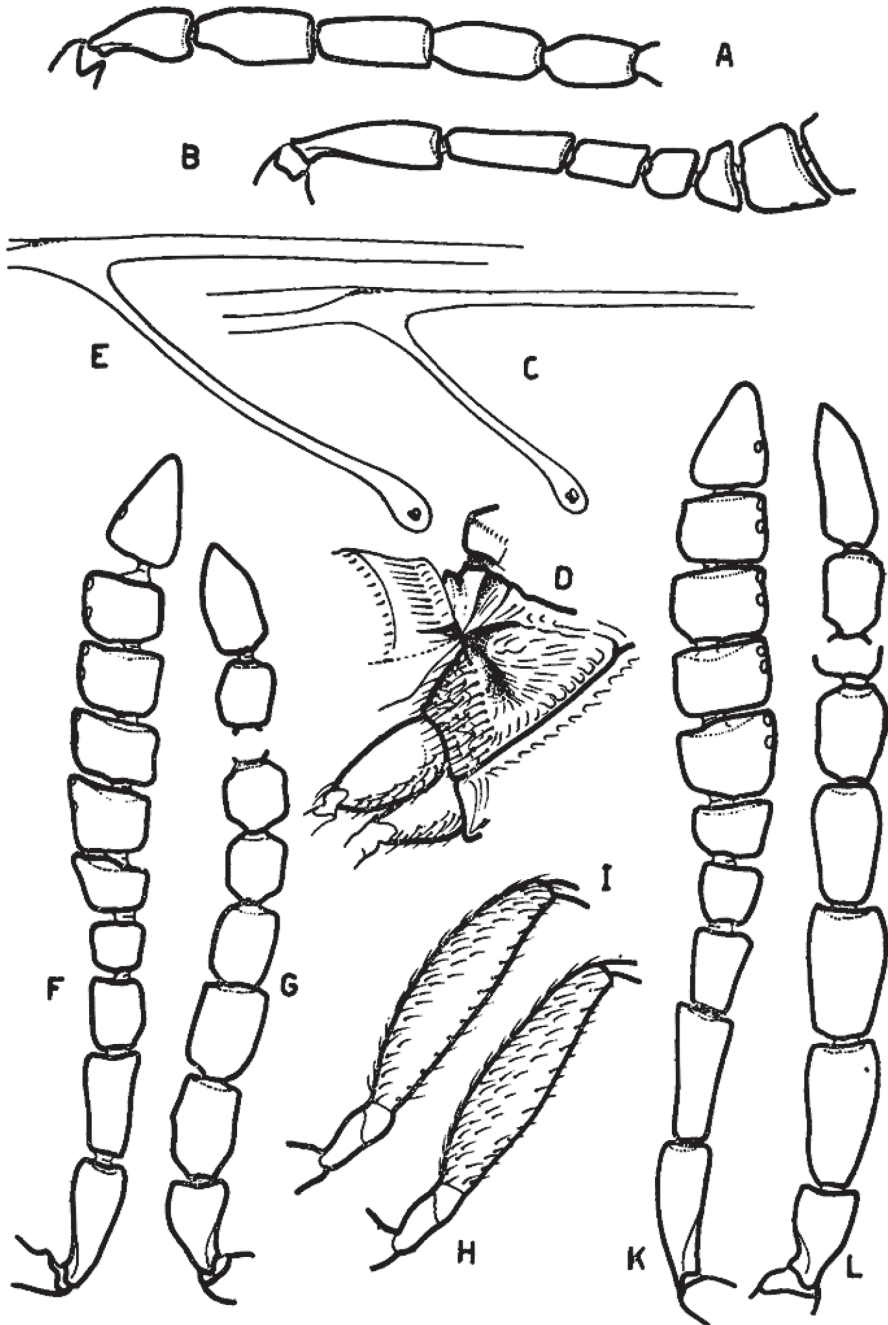


FIG. III — *A. ghorfii* DEL. et VÆG. (A - D), *A. vassilievi* MAYR (E), *A. grandis* THOMSON (F - H) et *A. semistriatus* NEES (I - L). Antennes de la femelle (B, F, K), antennes du mâle (A, G, L). Angle formé par les nervures postmarginale et stigmale de l'aile antérieure (E, C), pubescence de la metapleure (D) et des fémurs postérieurs (H, I).

Figure 1. Illustrations published by Delucchi (1961) where differences in the bare area of the external side of hind femora of *Asolcus semistriatus* (Fig III, I) and *A. grandis* (Fig. III, H) are shown.

(2014, 2015) also distinguished *T. manteroi* by the sculpture of T2, in which short longitudinal rugae are arranged medially and do not extend to the posterior half of the tergite, contrasting with longitudinal rugae throughout the anterior two thirds of T2 in *T. belenus* and *T. semistriatus*.

Trissolcus colemani

Crawford (1912) described *Telenomus colemani* from specimens that emerged from an egg mass of *Dolycoris indicus* Stål, collected in India. Masner and Muesebeck (1968) transferred this species into *Trissolcus* and no other information was recorded until its treatment as a junior synonym of *T. semistriatus* in Talamas et al. (2017).

Trissolcus pseudoturesis* and *T. djadetshko

The original description of *Microphanurus* (= *Trissolcus*) *pseudoturesis* Rjachovskij (Rjachovskij 1959) distinguished this species from *M. djadetshko* Rjachovskij and *M. semistriatus* by tibial color: completely yellow in *M. pseudoturesis*; reddish or yellow in *M. djadetshko*; almost black in *M. semistriatus*. Viktorov (1964) distinguished *Asolcus* (= *Trissolcus*) *djadetshko* and *A. rufiventris* by the lack of longitudinal striae on the posterior margin of the mesoscutum in contrast to their presence in *A. pseudoturesis* and *A. semistriatus*. Viktorov (1967) then modified his concept, considering the color of the hind tibia as a valid character to distinguish *T. djadetshko* from *T. semistriatus* and the color of femora to distinguish *T. djadetshko* from *T. pseudoturesis*. The keys to species by Kozlov (1968) and Fabritius (1972) distinguished *T. djadetshko* from *T. grandis*, *T. pseudoturesis* and *T. semistriatus* by the absence of longitudinal striation on the posterior mesoscutum and an absence of transverse striation on the frons, and *T. pseudoturesis* from *T. grandis* and *T. semistriatus* by color of the femora. Kozlov and Kononova (1983) separated *T. djadetshko* from both *T. grandis* and *T. semistriatus* by the absence of longitudinal striation on the posterior mesoscutum. Safavi (1968) and Voegelé (1969) separated *T. djadetshko* and *T. pseudoturesis* by their “ochraceous” femora from *T. semistriatus* and *T. grandis* (black femora), and separated *T. djadetshko* from *T. pseudoturesis* by longitudinal striae on the posterior margin of mesoscutum (vs. striate throughout) and the presence of parapsidal furrows. Koçak and Kiliñer (2003) distinguished *T. djadetshko* by its femora being reddish-yellow in contrast with dark brown or black femora in *T. semistriatus* and *T. grandis*, and separated *T. djadetshko* from *T. pseudoturesis* by sculpture on mesoscutum as in Voegelé (1969). Petrov (2013) again distinguished *T. djadetshko* on the basis of the mesoscutum without longitudinal wrinkles, contrasting with the clear longitudinal wrinkles of *T. grandis*, *T. pseudoturesis* and *T. semistriatus*, and he separated *T. pseudoturesis* from *T. grandis* and *T. semistriatus* by the color of femora. Kononova (2014, 2015) differentiated *T. djadetshko* by its yellow legs and mesoscutum without longitudinal rugae posteriorly from *T. semistriatus*

and *T. grandis* having all femora black and mesoscutum with longitudinal rugae posteriorly, and *T. pseudoturesis* from *T. grandis* and *T. semistriatus* as in Kozlov (1968). *Trissolcus djadetschko* and *T. pseudoturesis* were treated as junior synonyms of *T. semistriatus* in Talamas et al. (2017).

Trissolcus waloffae*, *T. nixomartini* and *T. silwoodensis

Javahery (1968) described and keyed *T. waloffae* (Javahery) using leg color (predominantly brownish to reddish-yellow) and weakly indicated parapsidal furrows to separate it from *T. grandis*, *T. semistriatus*, *T. nixomartini* and *T. silwoodensis*, which he considered to have black femora in both sexes and be without parapsidal furrows. Characters provided to distinguish each of the last four species from each other were black vs. brown front tibiae, presence of infuscation of wings, color of wing venation, ratio between first flagellar segment and pedicel of male, sculpture of the head, distance between lateral ocelli and compound eye, and 'weakly concave' vs. 'somewhat concave' head. *Trissolcus silwoodensis* and *T. nixomartini* were previously treated as synonyms of *T. grandis* by Kozlov and Lê (1977).

Trissolcus crypticus

During a program for classical biological control of *Nezara viridula* L. in Australia, several 'strains' of different geographical populations of *Trissolcus basalis* (Wollaston) were introduced, starting in the 1930s (Clarke 1990). Of the strains introduced in subsequent years to the interior of Australia, one population imported from Pakistan (1961) was not able to efficiently control *N. viridula* (Clarke 1990). Clarke (1993) demonstrated that this 'strain' was indeed a different species, which he described as *Trissolcus crypticus* Clarke. Comparing *T. crypticus* with *T. basalis*, he considered the complete nethion sulcus (figure 1 in Clarke 1993) as the main diagnostic character for *T. crypticus*. Clarke analyzed specimens of *Trissolcus rungsi* (Voegelé) labelled by Voegelé and deposited in NHMUK and concluded that they were not the same species as *T. crypticus*, but did not present characters to support his hypothesis (Clarke 1993).

Material and methods

Collections

Primary types

Due to the challenge of historic confusion regarding species close to *T. semistriatus*, we treat only species for which the primary types were directly examined, or the diagnostic characters are clearly visible in photographs.

Images of the primary types of *Telenomus colemani* Crawford, *Microphanurus djadetsbko* Rjachovskij, *Trissolcus grandis* Thomson, *Telenomus Manteroi* Kieffer, *Microphanurus pseudoturesis* Rjachovskij and *Teleas semistriatus* Nees von Esenbeck were made available via Specimage (specimage.osu.edu) by Talamas et al. (2017). Images of the lectotype of *Telenomus nigripes* Thomson, syntypes of *Telenomus ovulorum* Thomson, and additional images of the lectotype of *Telenomus grandis* were provided by Dr Hege Vårdal (Naturhistoriska Riksmuseet, Stockholm, Sweden).

Institutional acronyms

CNCI	Canadian National Collection of Insects – Ottawa, Canada;
DISAFA	Dipartimento di Scienze Agrarie, Forestali e Alimentari, University of Torino – Torino, Italy;
EIHU	Hokkaido University Museum, Entomology – Sapporo, Japan;
HMIM	Hayk Mirzayans Insect Museum, Plant Pests and Diseases Research Institute – Tehran, Iran;
NHMUK, BMNH	The Natural History Museum – London, United Kingdom;
NHMW	Naturhistorisches Museum Wien – Wien, Austria;
NMID	National Museum of Ireland – Dublin, Ireland;
MSNG, MCSN	Museo Civico di Storia Naturale “Giacomo Doria” – Genoa, Italy;
MZUF	Museo di Storia Naturale di Firenze, Sezione di Zoologia “La Specola”, Università degli Studi di Firenze – Florence, Italy;
NHRS	Naturhistoriska Riksmuseet, Entomology – Stockholm, Sweden;
UCRC	University of California, Riverside – CA, USA;
UNIPA	Dipartimento di Scienze Agrarie, Alimentari e Forestali, Università degli Studi di Palermo – Palermo, Italy;
USNM	National Museum of Natural History, Smithsonian Institution – Washington, DC, USA;
ZIN	Zoological Museum, Academy of Sciences – St. Petersburg, Russia.

Geographical distribution and host association

The identification tools of previous literature are not reliable for identifying the species that we treat here. Hence, the geographical distribution and host associations presented in Material Examined sections derive only from specimens examined as part of this study.

Cybertaxonomy

Specimens used in this study were assigned collecting unit identifiers (CUIDs) and their associated collection and host association data were deposited in Hymenoptera

Online (hol.osu.edu). In addition to the abbreviated Material examined sections, a DarwinCore archive is provided for each species (Suppl. material: S2–S5). These files contain the totality of specimens for which data is deposited in Hymenoptera Online, including specimens for which updated identification has not yet occurred, which can be assessed by the dates of determination. Taxonomic synopses, descriptions, and material examined sections were generated in the online, matrix-based program vSysLab (vsyslab.osu.edu) with a matrix based on that of Talamas et al. (2017).

Photography

A Leitz Großfeld-Stereomikroskop TS with magnification up to 160×, a Stereomicroscope Wild M3B with oculars 15×, and a spot light Leica CLS 150× were used for biometric diagnosis. A semi-transparent light shield was used to reduce glare and to diffuse the light. The lectotypes of *T. belemus* and *T. arminon* were photographed with a Macroscopic Solutions Macropod MicroKit with individual slices rendered in Helicon Focus 6. All other images were produced using a Leitz Dialux 20 EB compound microscope with a Leica DFC 290 Camera with LED spot light or dome light based on different points of view after techniques summarized in Buffington et al. (2005), Kerr et al. (2008) and Buffington and Gates (2008). LEICA APPLICATION SUITE V 3.7.0 software was used to manage image acquisition and ZERENE STACKER was used for merging of the image series into a single in-focus image.

Morphology

Terminology for surface sculpture follows the glossary by Harris (1979), Mikó et al. (2007), Yoder et al. (2010) and Talamas et al. (2017). Measurements of the head, mesosoma, metasoma, total body, and wing venation follow Masner (1980) and Tortorici et al. (2016). In the wing ratio expressed as st:pm:mg, the stigmal vein is treated as the benchmark unit (=1). Morphological terms largely follow Mikó et al. (2007) and were matched to concepts in the Hymenoptera Anatomy Ontology (Yoder et al. 2010) using the text analyzer function and a table of these terms and URI links is provided in Suppl. material: S1.

Additional abbreviations and terminology used in this paper: HL: head length; HW: head width; HH: head height, from vertex to distal end of clypeus; FCI: frontal cephalic index (HW/HH); LCI: lateral cephalic index (HH/HL); OOL:POL:LOL: ocular distance ratio, OOL as the benchmark unit (=1); IOS: interorbital space (Mikó et al. 2010); claval formula: the sequence of sensilla, from the apical antennomere (A11) to the last functional clavomere (Bin 1981), i.e. the last antennomere bearing one or two multiporous gustatory sensilla, as defined by Isidoro et al. (1996); compound eye height and width: measured when eye longitudinal axis is parallel to the focal plane.

Insect collecting and rearing

A host colony of *E. maura* used for rearing *Trissolcus* was established from adults collected on wheat in Piedmont (NW Italy) and maintained in cages under laboratory conditions (climatized chambers at 24 ± 1 °C, $65 \pm 5\%$ RH, L:D = 16:8). All eggs laid in the cages were collected and frozen at -20 °C. Because of the short egg-laying period of *E. maura*, freezing the eggs allowed the eggs to be used for a much longer time.

To obtain *Trissolcus* specimens, egg masses of *E. maura* and *P. prasina* were collected in the field in Piedmont (NW Italy) in the spring and summer of 2017. The field-collected egg masses were reared and checked daily. *Trissolcus* specimens that emerged from field-collected egg masses were allowed to mate. Some females were isolated in small plastic boxes ($64.5 \times 40.9 \times 16$ mm), fed with water and honey, and provided with *E. maura* frozen egg masses to produce progeny for use in subsequent tests.

For interbreeding experiments, specimens were isolated immediately following emergence to prevent mating, and females and males were maintained singly in plastic boxes as described above. When the parasitoids reach the early pupal stage inside the eggs, their red eyes are clearly visible through the transparent operculum of the host egg. Following observation of this feature (Figure 2), the eggs were checked at a frequency of 4–5 times per day to ensure that they were isolated prior to mating.

Some of the progeny from isolated, mated females were selected for preservation, identification and molecular analysis. The remaining progeny were used in breeding experiments.

Molecular analyses

Molecular analyses were performed to confirm morphological identification and characterize the species. Genomic DNA was extracted from the metasoma of specimens from rearing experiments and pinned collection specimens according to Kaartinen et al. (2010), but doubling the proteinase K dose (5 µl of 20 mg ml⁻¹ proteinase K). The barcode region of the cytochrome oxidase I (COI) gene was amplified using universal PCR primers for insects LCO1490 (5'-GGT CAA CAA ATC ATA AAG ATA TTG G-3') and HCO2198 (5'-TAA ACT TCA GGG TGA CCA AAA AAT CA-3') (Folmer et al. 1994). The PCR was performed in a 50 µl reaction volume: 2 µl of DNA, 37.9 µl molecular grade water, 5 µl 10× Qiagen PCR buffer, 3 µl dNTPs (25 mM each), 1.5 µl MgCl₂, 0.2 µl of each primer (0.3 µM each), 0.2 µl Taq DNA Polymerase (Qiagen, Hilden, Germany). Thermocycling conditions were optimized to shorten reaction times and included initial denaturation at 94 °C for 300 s, followed by 35 cycles of 94 °C for 30 s, annealing at 52 °C for 45 s and extension at 72 °C for 60 s; then further 600 s at 72 °C for final extension. PCR products were purified using a commercially available kit (QIAquick PCR Purification Kit, Qiagen GmbH, Hilden, Germany) following the manufacturer's instructions, and sequenced by a commercial service (Genechron S.r.l., Rome, Italy). The sequences were compared with the GenBank database and each other using the Basic Local Alignment Search Tool (<http://www.ncbi.nlm>



Figure 2. Pupal stage of *Trissolcus* sp. in *Halyomorpha halys* eggs, clearly indicated by the presence of eyes and ocelli, which are visible through the semi-transparent host egg.

[nih.gov/BLASTn](https://www.ncbi.nlm.nih.gov/BLASTn)). All sequences were aligned using ClustalW with default settings as implemented in Mega X. The pairwise nucleotide sequence distances among and within taxa were estimated using the Kimura 2-parameter model (K2P) of substitution (Kimura, 1980) using Mega X (Kumar et al. 2018). The sequences generated from this study are deposited in the GenBank database. All residual DNA is archived at DISAFA.

Mating tests and reproductive isolation between *T. belenus* and *T. semistriatus*

For mating experiments, 1–2-day old virgin females and males were used. Four combinations for mating tests were done: *T. semistriatus* (♀) × *T. belenus* (♂); *T. belenus* (♀) × *T. semistriatus* (♂); *T. semistriatus* (♀) × *T. semistriatus* (♂); *T. belenus* (♀) × *T. belenus* (♂). The total number of interbreeding tests was 24: four replicates for each intraspecific mating combination and eight replicates for each interspecific mating combination. Each pair of wasps was observed at the stereomicroscope until the end of copulation or for 10 minutes if copulation did not occur. The pair then remained together in isolation for 24 hours. After the mating test, an egg mass of *E. maura* was provided to each female wasp for 24 hours of exposure. The egg masses were then moved to other plastic boxes until offspring emergence. Each mating test was considered successful when emerged offspring included females, because in all known *Trissolcus* species, only mated females can produce female offspring. We compared the percentage of mating success among the four combinations and the significance of the results was assessed with a chi-square test.

Results

Morphological analysis

The easiest task regarded the distinction of *T. manteroi* from *T. semistriatus*, *T. belenus* and *T. colemani*. *Trissolcus manteroi* clearly has a shorter postmarginal vein, only slightly longer than the stigmal vein; A7 has only one papillary sensillum instead of two in the other three species; and *T. manteroi* has no episternal foveae. The holotype of *T. manteroi* is thus morphologically very close to *T. rufiventris*, from which it can be differentiated by the length of the postmarginal vein.

The distinction of *T. belenus* and *T. colemani* from *T. semistriatus* is more nuanced and required an integrative approach to determine which morphological characters were congruent with the biological and molecular data. The results of this in-depth analysis demonstrate that some of the characters that Talamas et al. (2017) treated as intraspecifically variable have diagnostic power.

The presence or absence of setation on the external face of the hind femur, described in the key and figure III (I) (H) in Delucchi (1961), is a reliable character to distinguish *T. grandis* from *T. semistriatus*. However, in the lectotype of *T. grandis* and neotype of *T. semistriatus* this character is opposite to what was stated by Delucchi (1961). Furthermore, the holotype of *T. colemani* has the external surface of hind femur setose, as in the lectotype of *T. grandis*. The association proposed in Delucchi (1961): ‘external face of hind femora uncovered by hair’ – ‘reddish yellow tibiae’ is the typical combination for *T. colemani*, while Delucchi (1961) proposed it for *T. semistriatus*, and ‘external face of hind femora covered by hair’ – ‘dark or black tibiae’ is the typical combination for *T. semistriatus*. We conclude that this interpretation is contrary to what is found in type material.

Synonymy in *T. belenus*

In the analysis of original descriptions and images of lectotype of *T. arminon* and *T. grandis*, no remarkable characters were recognized to distinguish them from *T. belenus*, which we therefore consider it to be their senior synonym. In the analysis of type material of *T. silwoodensis* and *T. nixomartini*, previously considered junior synonym of *T. grandis* (Kozlov & Lê, 1977), we confirmed the findings of previous authors, and thus treat these species as junior synonyms of *T. belenus*. Mayr (1879) considered *Telenomus ovulorum* Thomson to be a junior synonym of *Telenomus semistriatus* Nees von Esenbeck, but through analysis of the photographs of type material of *T. ovulorum* Thomson, we recognized the character states of *T. belenus*, and therefore treat *T. ovulorum* as a junior synonym of *T. belenus*.

Synonymy in *T. colemani*

One paratype of *T. djadetschko* and three syntypes of *T. pseudoturesis* were analyzed via photographs and compared with the original description and photographs of the holo-

type of *T. colemani*. The character states of the two first species matched perfectly with those of the latter, leading us to treat *T. colemani* as the senior synonym of *T. djadetschko* and *T. pseudoturesis*. We conclude that the characters of *T. crypticus* match those in the holotype of *T. colemani* based on examination of *T. crypticus* paratypes collected in Pakistan and its original description (see figs 1, 3, 5 in Clarke 1993). We thus treat *T. crypticus* as a junior synonym of *T. colemani*.

Clarke (1993) also reported that “Examination of material of *T. rungsi* labelled by Voegelé (deposited in NHMUK) shows that this species is not the same of *T. crypticus*” but he did not provide any distinguishing characters between the two species. Contrary to what was reported by Clarke (1993), in our analysis of the material deposited at NHMUK, 37 specimens labelled as “*Asolcus rungsi* Voegelé” were identified as *T. colemani* and four specimens labelled as “*rungs* 1965 Voegele” were identified as *T. basalis*, while other 25 with the same last cumulative label were identified as *T. colemani*. This confirms our interpretation of the description and analysis of figures regarding *A. rungsi* and demonstrates confusion of species in the Moroccan rearing efforts at École Nationale d’Agriculture in Meknès.

The original description of *Asolcus rungsi* mentioned the presence of short traces of notauli (fig. 1, c. in Voegelé 1965); these traces are visible in all specimens *T. colemani* (Figure 23). However, because the location of the holotype of *A. rungsi* is not known, we were unable to examine it and at this time do not treat this species name as a synonym. The morphological analyses of the holotype and paratypes of *T. waloffae* showed the conspecificity of this species with *T. colemani*.

Molecular analysis

Barcode sequences were obtained from 17 *Trissolcus* specimens (Table 1). The Blast search showed that the sequences of *T. semistriatus* from Italy and from Iran had a 98% sequence identity with the GenBank sequence from *Trissolcus nigripedius* (accession no. [AB971830](#)). The sequences from the two specimens of *T. colemani* showed a 98% identity with a GenBank sequence with a *Platygastridae* sp. (accession no. [KY839581](#)), while the sequences from the specimens of *T. manteroi*, *T. belenus* and *T. rufiventris* showed a lower similarity with GenBank sequences. The final alignment consisted of 548 characters. Pairwise distance values within and among analyzed species are shown in Table 2. The genetic distances between the specimens identified as of the same species (which averaged between 0.000 ± 0.000 and 0.005 ± 0.002), were much lower than the mean pairwise distances observed between the specimens identified as of different species (from 0.105 ± 0.001 to 0.149 ± 0.000).

Mating tests

Specimen pairs tested for intraspecific combination mated within ten minutes; pairs tested for interspecific combination did not mate within the 10-minute observation period.

Table 1. Specimen information and GenBank Accession Number for the sequences generated by this study.

Species	Sex	Country	Year of collection	GenBank accession number	Collecting unit identifier
<i>Trissolcus manteroi</i>	f	ITALY	2010	MK906047	DISAFA-draw1465-HYM-0424
	f	ITALY	2010	MN603796	DISAFA-draw1465-HYM-0425
<i>Trissolcus semistriatus</i>	f	ITALY	2017	MK906048	DISAFA-draw1465-HYM-0233
	f	IRAN	2015	MK906049	USNMENT01223088
	f	ITALY	2017	MN603799	DISAFA-draw1465-HYM-0238
	f	ITALY	2017	MN603800	DISAFA-draw1465-HYM-0240
	f	ITALY	2016	MN603798	DISAFA-draw1465-HYM-0242
	f	ITALY	2016	MN603797	DISAFA-draw1465-HYM-0283
<i>Trissolcus belenus</i>	f	ITALY	2017	MK906050	DISAFA-draw1465-HYM-0014
	f	ITALY	2017	MN603802	DISAFA-draw1465-HYM-0012
	f	ITALY	2017	MN603803	DISAFA-draw1465-HYM-0013
	f	ITALY	2017	MN603804	DISAFA-draw1465-HYM-0016
	f	ITALY	2017	MN603806	DISAFA-draw1465-HYM-0018
	f	ITALY	2017	MN603805	DISAFA-draw1465-HYM-0019
<i>Trissolcus colemani</i>	f	IRAN	2015	MK906051	USNMENT01223460
	f	IRAN	2015	MN603801	USNMENT01223455
<i>Trissolcus rufiventris</i>	f	IRAN	2015	MN603807	UNIPA-HYM-S01347

Table 2. Barcode mean pairwise genetic distances (\pm SE) between *T. manteroi*, *T. semistriatus*, *T. belenus*, *T. colemani* and *T. rufiventris* (under the diagonal), and within taxa (along the diagonal). n = number of sequences.

	<i>T. manteroi</i> (n = 2)	<i>T. semistriatus</i> (n = 6)	<i>T. belenus</i> (n = 6)	<i>T. colemani</i> (n = 2)
<i>T. manteroi</i> (n = 2)	0.000	–	–	–
<i>T. semistriatus</i> (n = 6)	0.139 \pm 0.000	0.005 \pm 0.002	–	–
<i>T. belenus</i> (n = 6)	0.139 \pm 0.000	0.109 \pm 0.000	0.000 \pm 0.000	–
<i>T. colemani</i> (n = 2)	0.138 \pm 0.000	0.105 \pm 0.001	0.107 \pm 0.000	0.000
<i>T. rufiventris</i> (n = 1)	0.144 \pm 0.000	0.141 \pm 0.001	0.149 \pm 0.000	0.133 \pm 0.00

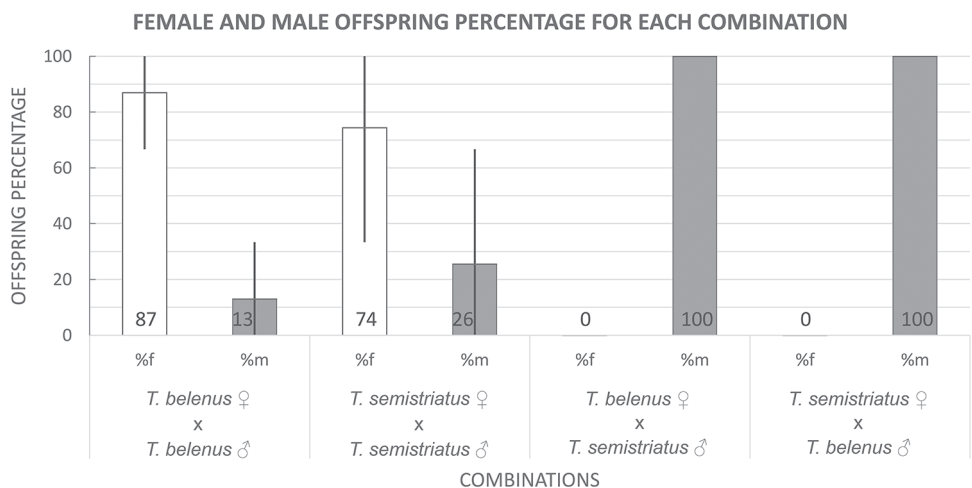


Figure 3. Sex ratio of emerged specimens. Combinations: *T. belenus* (♀ x ♂), n = 4; *T. semistriatus* (♀ x ♂), n = 4; *T. belenus* (♀) x *T. semistriatus* (♂), n = 8; *T. semistriatus* (♀) x *T. belenus* (♂), n = 8. Bars indicate standard deviation.

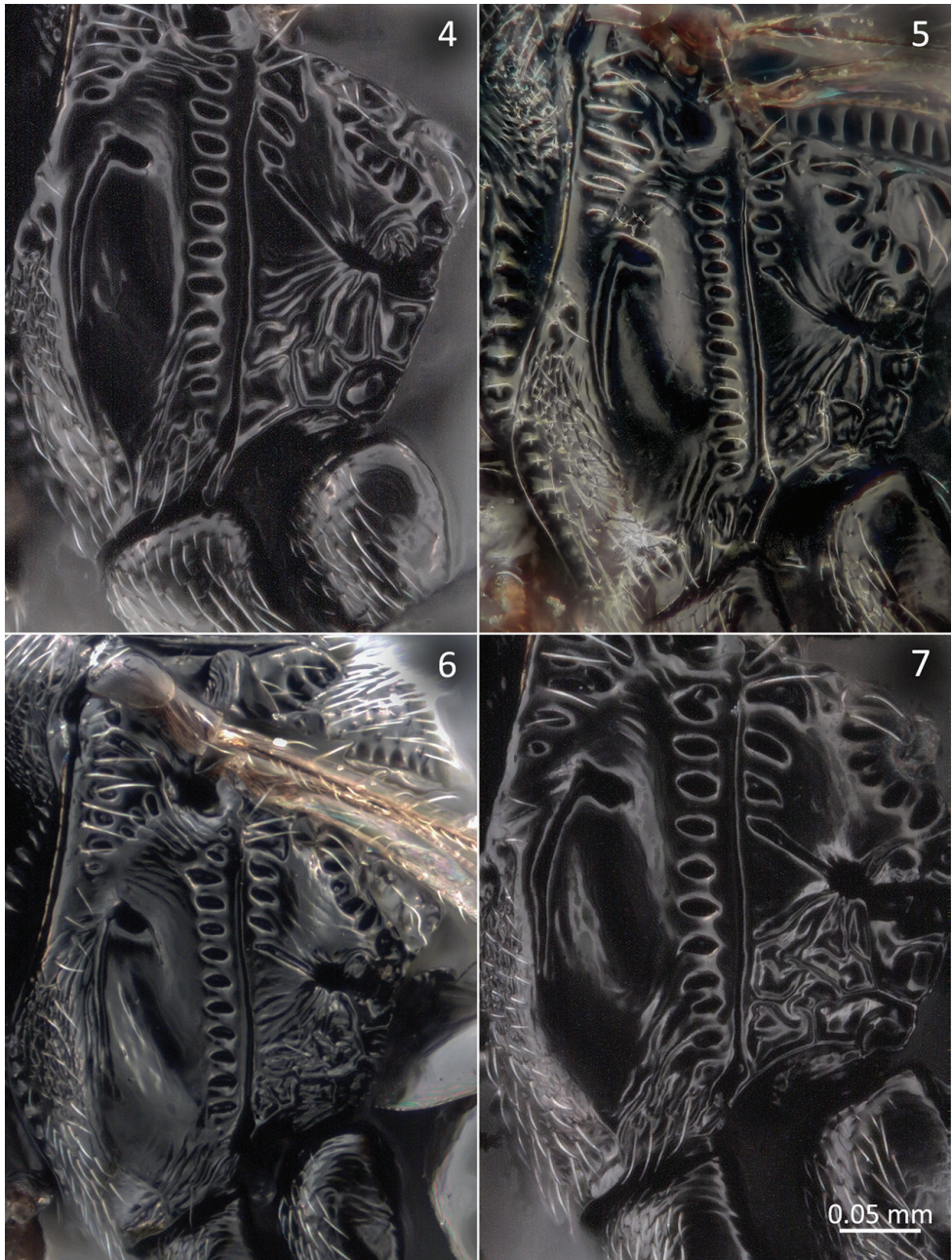
All females used for the two intraspecific combinations successfully produced female offspring (Figure 3); as expected the sex ratio was similar, in *T. belenus* (♀ × ♂) combination 31 females and 5 males emerged, and in *T. semistriatus* (♀ × ♂) 21 females and 4 males emerged. Females used for the two interspecific combinations produced only male offspring, 78 males in the *T. belenus* (♀) × *T. semistriatus* (♂) combination, and 65 males in the *T. semistriatus* (♀) × *T. belenus* (♂) combination. A total of 3 females failed to reproduce, producing no offspring in either the intraspecific or interspecific combinations.

Key to *Trissolcus* of the Palearctic region (females)

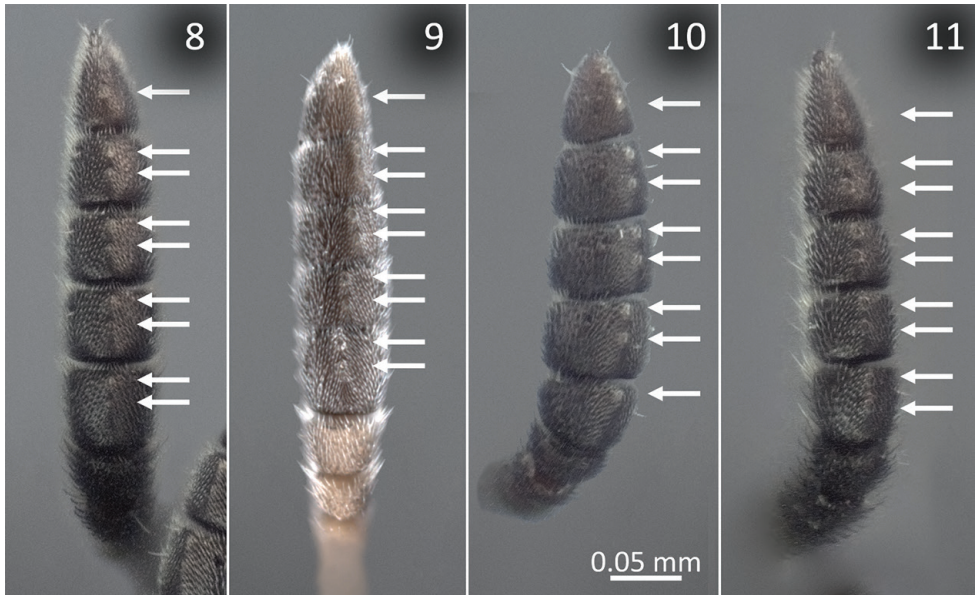
Modified couplets for the Key to *Trissolcus* of the Palearctic region (females) in Talamas et al. (2017)

- 29 Ventral mesopleuron distinctly bulging; mesocoxa oriented parallel to long axis of body; dorsal frons with sculpture effaced, sometimes entirely smooth and shining; A7 with two papillary (basiconic) sensilla (figures 128–132 in Talamas et al. 2017)..... ***Trissolcus perepelovi* (Kozlov)**
- Ventral mesopleuron not distinctly bulging; mesocoxa oriented at an angle of ~45° relative to long axis of body (Figure 6); dorsal frons evenly and densely covered in microsculpture; A7 with one papillary (basiconic) sensillum (Figure 10)..... **29A**
- 29A Postmarginal vein in fore wing about twice as long as stigmal vein (Figure 14); metasoma yellow to dark brown, typically reddish-brown..... ***Trissolcus rufiventris* (Mayr)**
- Postmarginal vein only slightly longer than stigmal vein (Figure 13); metasoma dark brown to black (Figure 18)..... ***Trissolcus manteroi* (Kieffer)**
- 32 Lateral mesoscutum with mesoscutal humeral sulcus present as a smooth furrow (Figure 25)..... **32A**
- Lateral mesoscutum with mesoscutal humeral sulcus comprised of distinct foveae (Figures 20–23)..... **32B**
- 32A Lateral pronotum with netrion sulcus incomplete dorsally, netrion often poorly defined; medial part of occipital carina rounded in dorsal view..... ***Trissolcus basalis* (Wollaston)**
- Lateral pronotum with netrion sulcus complete dorsally (Figures 5, 50, 53, 55, 60), netrion distinct; medial part of occipital carina angled (Figure 36), vertex of angle with short carina directed toward median ocellus..... ***Trissolcus semistriatus* (Nees von Esenbeck)**
- 32B Laterotergite 1 with line of 3 setae (Figures 30, 45)..... ***Trissolcus belenus* (Walker)**
- Laterotergite 1 without setae (Figure 32)..... ***Trissolcus colemani* (Crawford)**

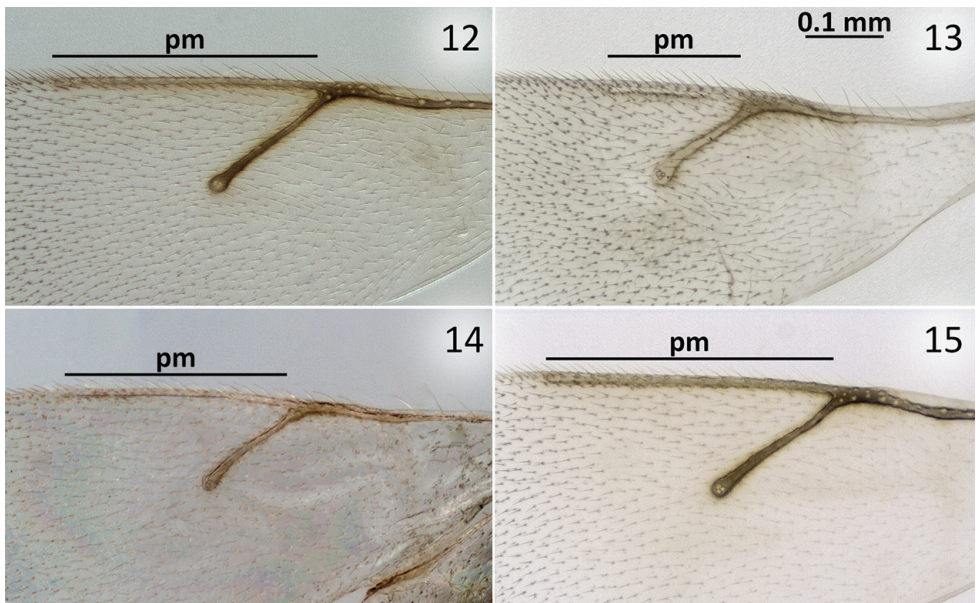
A matrix of the diagnostic characters used in this key is provided in Suppl. material: S6.



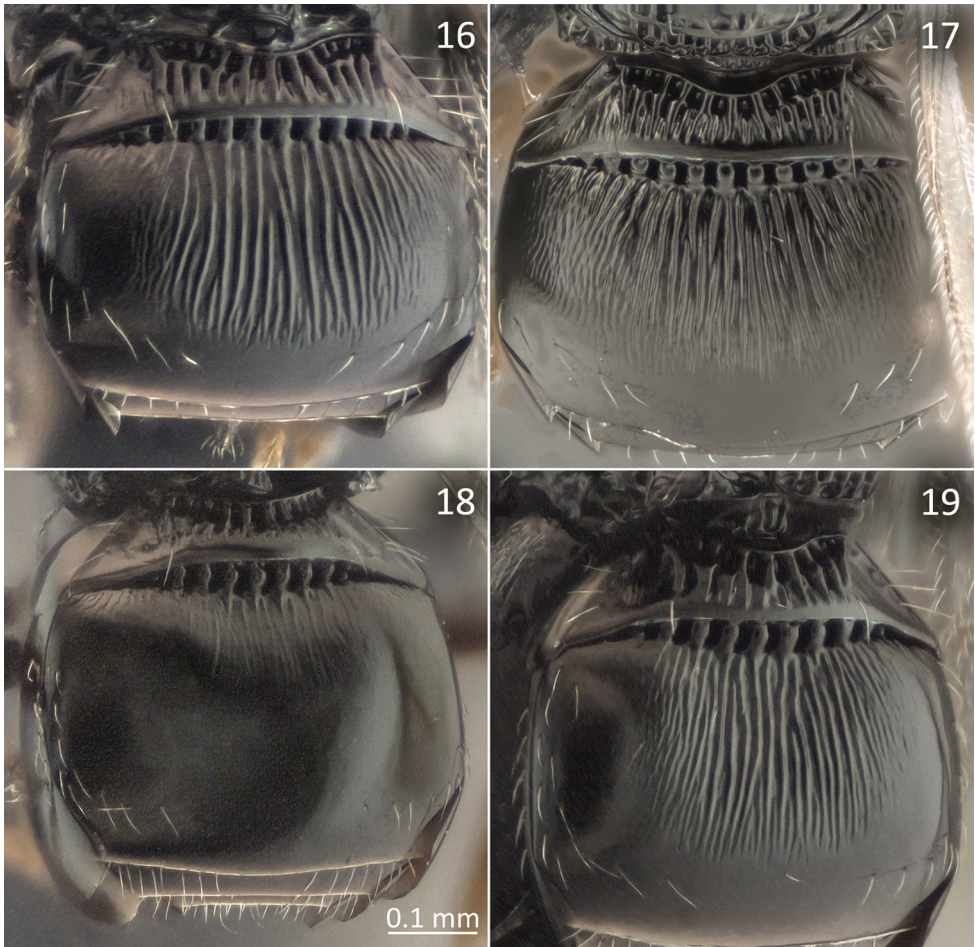
Figures 4–7. EPS, metapleural epicoxal sulcus, anterolateral extension of metapleuron: **4** *Trissolcus belenus* [DISAFA-draw1465-HYM-0009] **5** *T. colemani* [DISAFA-draw1466-HYM-0484] **6** *T. manteroi* [DISAFA-draw1465-HYM-0430] **7** *T. semistriatus* [DISAFA-draw1465-HYM-0227].



Figures 8–11. Basiconic sensilla, indicated by arrows, in the ventral surface of female antennal clava: **8** *Trissolcus belenus* [DISAFA-draw1465-HYM-0009] **9** *T. colemani* [DISAFA-draw1466-HYM-0484] **10** *T. manteroi* [DISAFA-draw1465-HYM-0430] **11** *T. semistriatus* [DISAFA-draw1465-HYM-0227].



Figures 12–15. Fore wing venations: **12** *Trissolcus belenus* [DISAFA-draw1465-0010] **13** *T. manteroi* [DISAFA-draw1465-0430] **14** *T. rufiventris* [USNMENT01223145] **15** *T. semistriatus* [DISAFA-draw1465-0229].



Figures 16–19. Metasomal tergites: **16** *Trissolcus belenus* [DISAFA-draw1465-HYM-0009] **17** *T. colemani* [DISAFA-draw1466-HYM-0484] **18** *T. manteroi* [DISAFA-draw1465-HYM-0430] **19** *T. semistriatus* [DISAFA-draw1465-HYM-0227].

***Trissolcus belenus* (Walker)**

https://bioguid.osu.edu/xbiod_concepts/3190

Figures 4, 8, 12, 16, 20, 21, 26, 30, 33, 37, 41, 45–51.

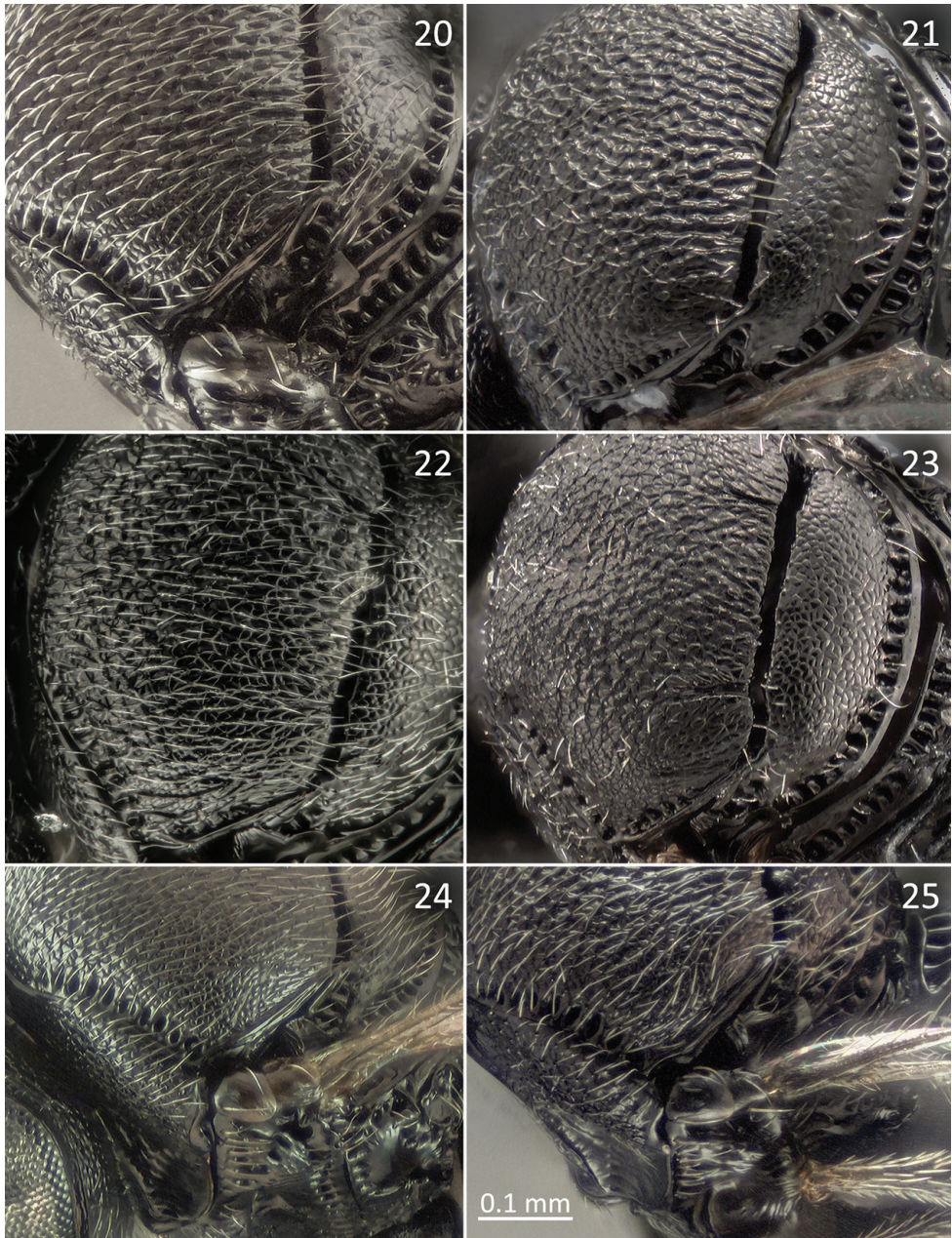
Telenomus Belenus Walker, 1836: 352 (original description).

Telenomus arminon Walker, 1838: 457 (original description).

Telenomus Nigrita Thomson, 1860: 172 (original description, synonymized by Kozlov (1968)); Kozlov, 1968: 214 (junior synonym of *Trissolcus grandis* (Thomson)).

Telenomus frontalis Thomson, 1860: 170 (original description, synonymized by Kozlov (1968)); Kozlov, 1968: 214 (junior synonym of *Trissolcus grandis* (Thomson)).

Telenomus grandis Thomson, 1860: 169 (original description).



Figures 20–25. Mesonotum; mshs and traces of notauli: **20** *Trissolcus belenus* [DISAFA-draw1465-HYM-0009] **21** *T. belenus* [DISAFA...] after treatment in potassa solution to remove setae **22** *T. colemani* [DISAFA-draw1466-HYM-0484] **23** *T. colemani* [DISAFA-draw1466-HYM-0483] after treatment in potassa solution to remove setae **24** *T. manteroi* [DISAFA-draw1465-HYM-0430] **25** *T. semistriatus* [DISAFA-draw1465-HYM-0227].



Figures 26–29. Hind femur: **26** *Trissolcus belenus* [DISAFA-draw1465-HYM-0009] **27** *T. colemani* [DISAFA-draw1466-HYM-0484] **28** *T. manteroi* [DISAFA-draw1465-HYM-0430] **29** *T. semistriatus* [DISAFA-draw1465-HYM-0227].

Telenomus nigripes Thomson, 1860: 170 (original description, synonymized by Kozlov (1968)); Kozlov, 1968: 214 (junior synonym of *Trissolcus grandis* (Thomson)); Fergusson, 1984: 230 (lectotype designation); Johnson, 1992: 629 (type information).

Telenomus ovulorum Thomson, 1860: 171 (original description, synonymized by Mayr (1879)); Mayr, 1879: 704 (junior synonym of *Telenomus semistriatus* (Nees von Esenbeck)).

Teleas (?) *Pentatomae* Rondani: Rondani, 1874: 135 (nomen nudum).

Teleas pentatomae Rondani, 1877: 199 (original description).

Telenomus ovulorum Thomson: Mayr 1879: 704. Junior synonym of *Telenomus semistriatus* (Nees von Esenbeck)

Telenomus nigritus Thomson: Dalla Torre 1898: 517 (emendation).

Telenomus pentatomae (Rondani): Dalla Torre, 1898: 518 (generic transfer).

Allophanurus Arminon (Walker): Kieffer, 1912: 12 (description, generic transfer).

Aphanurus Belenus (Walker): Kieffer, 1912: 83 (description, generic transfer).

Aphanurus Frontalis (Thomson): Kieffer, 1912: 81 (description, generic transfer).

Aphanurus Grandis (Thomson): Kieffer, 1912: 76 (description, generic transfer).

Aphanurus Nigrita (Thomson): Kieffer, 1912: 79 (description, generic transfer).

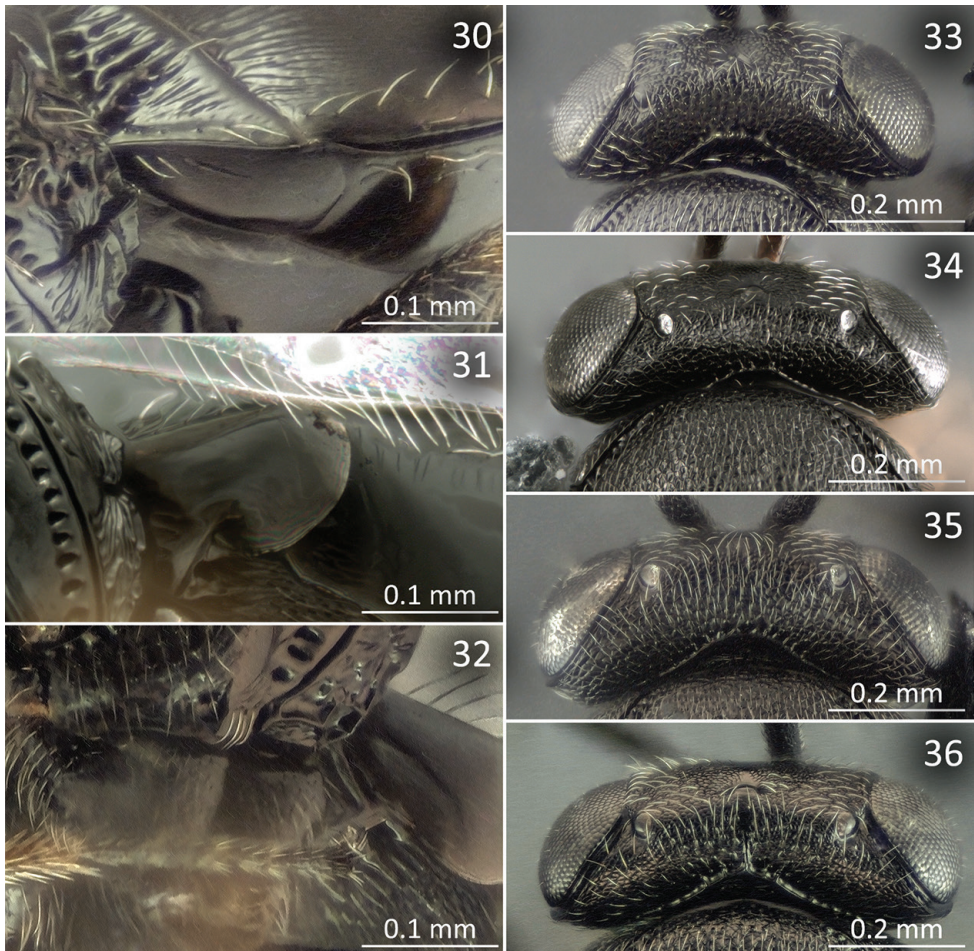
Aphanurus nigripes (Thomson): Kieffer, 1912: 75 (description, generic transfer).

Liophanurus Pentatomae (Rondani): Kieffer, 1912: 69 (description, generic transfer).

Allophanurus arminon (Walker): Kieffer, 1926: 23 (description, keyed).

Liophanurus pentatomae (Rondani): Kieffer, 1926: 71 (description).

Microphanurus belenus (Walker): Kieffer, 1926: 91, 102 (description, generic transfer, keyed).



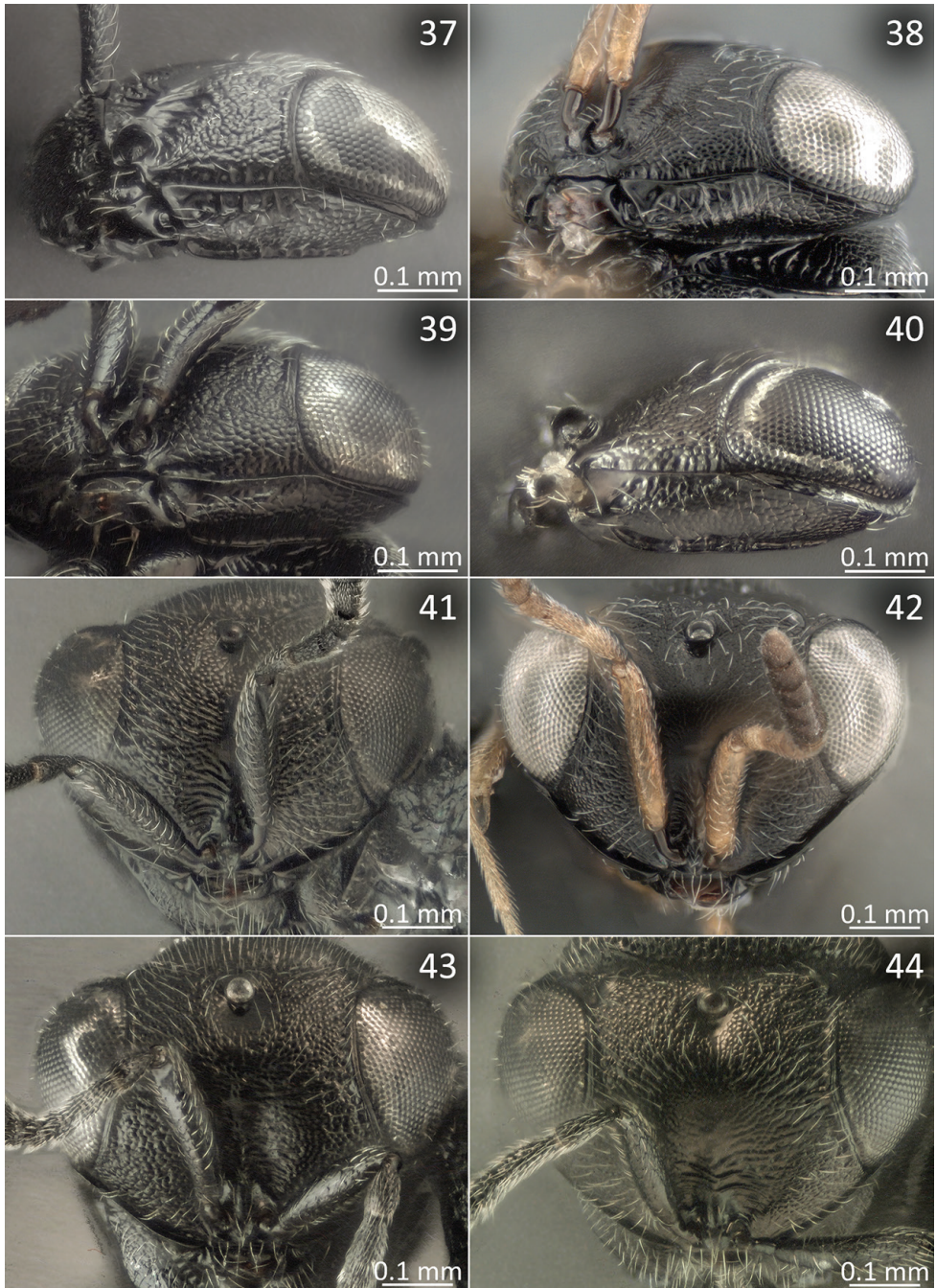
Figures 30–36. 30–32 Laterotergite 1 30 *Trissolcus belenus* [DISAFA-draw1465-HYM-0009] 31 *T. colemani* [DISAFA-draw1466-HYM-0484] 32 *T. semistriatus* [DISAFA-draw1465-HYM-0227] 33–36 Occipital carina 33 *Trissolcus belenus* [DISAFA-draw1465-HYM-0009] 34 *T. colemani* [DISAFA-draw1466-HYM-0484] 35 *T. manteroi* [DISAFA-draw1465-HYM-0430] 36 *T. semistriatus* [DISAFA-draw1465-HYM-0227].

Microphanurus frontalis (Thomson): Kieffer, 1926: 91, 103 (description, generic transfer, keyed).

Microphanurus grandis (Thomson): Kieffer, 1926: 91, 99 (description, generic transfer, keyed); Debauche, 1947: 256 (description).

Microphanurus nigripes (Thomson): Kieffer, 1926: 91, 98 (description, generic transfer, keyed).

Microphanurus nigritus (Thomson): Kieffer, 1926: 91, 100 (description, generic transfer, keyed).



Figures 37–44. 37–40 Head; malar area and gena **37** *Trissolcus belenus* [DISAFA-draw1465-HYM-0009] **38** *T. colemani* [DISAFA-draw1466-HYM-0484] **39** *T. manteroi* [DISAFA-draw1465-HYM-0430] **40** *T. semistriatus* [DISAFA-draw1465-HYM-0227] **41–44** Head in frontal view **41** *Trissolcus belenus* [DISAFA-draw1465-HYM-0009] **42** *T. colemani* [DISAFA-draw1466-HYM-0484] **43** *T. manteroi* [DISAFA-draw1465-HYM-0430] **44** *T. semistriatus* [DISAFA-draw1465-HYM-0227].

- Asolcus grandis* (Thomson): Masner, 1959: 376. (diagnosis, variation); Delucchi, 1961: 44, 60 (description, keyed); Voegelé, 1964: 28 (keyed); Javahery, 1968: 419 (keyed); Voegelé, 1969: 150 (keyed).
- Trissolcus grandis* (Thomson) syn. nov.: Viktorov, 1967: 91 (generic transfer, keyed); Safavi, 1968: 416 (keyed); Kozlov, 1968: 200, 214 (description, lectotype designation, synonymy, keyed); Fabritius, 1972: 32, 35. (keyed; host catalogue; distribution); Viggiani & Mineo, 1974: 156, 160, 161 (description, keyed); Kozlov & Lê, 1977: 512 (synonymy, keyed); Kozlov, 1978: 636 (description); Kozlov, 1981: 187 (keyed); Kozlov & Kononova, 1983: 110 (description); Johnson, 1992: 629 (cataloged, type information); Kononova, 1995: 96 (keyed); Doganlar, 2001: 112 (description); Koçak & Kilinçer, 2003: 302, 307 (keyed, description); Fabritius & Popovici, 2007: 158 (host informations, distribution); Buhl & O'Connor, 2010: 154 (distribution); Ali, 2011: 10 (keyed); Ghahari, Buhl & Kocak, 2011: 596 (host association, listed); Guz, Kocak & Kilincer, 2013: 87 (description, phylogenetic relationships); Petrov, 2013: 326 (keyed); Kononova, 2014: 1424 (keyed); Kononova, 2015: 262 (keyed); Talamas, Buffington & Hoelmer, 2017: 129, 135 (junior synonym of *Trissolcus semistriatus* (Nees von Esenbeck), type information).
- Asolcus nixomartini* Javahery, 1968: 419, 429 (original description, keyed, synonymized by Kozlov and Lê (1977)); Kozlov, and Lê 1977: 512 (junior synonym of *Trissolcus grandis* (Thomson)); Johnson, 1992: 629 (type information).
- Asolcus silwoodensis* Javahery, 1968: 419, 425 (original description, keyed, synonymized by Kozlov and Lê (1977)); Kozlov, and Lê 1977: 512 (junior synonym of *Trissolcus grandis* (Thomson)); Johnson, 1992: 629 (type information).
- Trissolcus pentatoma* (Rondani) syn. nov.: Bin, 1974: 463 (generic transfer, lectotype designation); Johnson, 1992: 634 (cataloged, type information); Talamas, Buffington & Hoelmer, 2017: 130, 135 (junior synonym of *Trissolcus semistriatus* (Nees von Esenbeck), type information).
- Trissolcus belemus* (Walker): Fergusson, 1978: 120 (generic transfer); Fergusson, 1984: 230 (lectotype designation); Johnson, 1992: 623 (cataloged, type information); Kononova, 2014: 1426 (possibly in *Telenomus*); Kononova, 2015: 264 (possibly in *Telenomus*).
- Trissolcus nigripes* (Thomson) syn. nov.: Fergusson, 1978: 120 (generic transfer).
- Trissolcus nixomartini* (Javahery) syn. nov.: Fergusson, 1978: 120 (generic transfer); Fergusson, 1984: 230 (type information).
- Trissolcus silwoodensis* (Javahery) syn. nov.: Fergusson, 1978: 120 (generic transfer); Fergusson, 1984: 230 (type information).
- Trissolcus arminon* (Walker) syn. nov.: Fergusson 1983: 208 (generic transfer, description, lectotype designation); Fergusson, 1984: 230 (type information); Johnson, 1992: 622 (cataloged, type information).
- Trissolcus ovulorum* (Thomson) comb. nov., syn. nov.

Diagnosis. The presence of setae on the first laterotergite (Figures 30, 45) allows *T. belemus* to be easily diagnosed, as only two other Palearctic species share this character: *T. saakowi* and *T. mitsukurii* (Ashmead). Both of these species have distinct notauli,

which are absent in *T. belenus* (Figures 20, 22). Additionally, the hyperoccipital carina is entirely absent in *T. belenus* (Figures 33, 47, 49), whereas it is complete in *T. saakowi* and present posterior to the lateral ocellus in *T. mitsukurii*.

Description. Body length: 1.03–1.1 mm, median = 1.06 mm, SD = 0.02, n = 20. Body color: head, mesosoma, and metasoma black.

Head. FCI = 1.4; LCI = 1.9; IOS = 0.3 mm; OOL:POL:LOL = 1:12:5.8. Color of radicle: dark brown. Length of radicle: about equal to width of clypeus. Color of A1–A6 in female: distal A2 yellow to light brown, otherwise black. Color of A7–A11 in female: black. Number of papillary sensilla on A6: 0. Number of papillary sensilla on A7: 2. Facial striae: absent. Number of clypeal setae: 6. Shape of gena in lateral view: narrow. Genal carina: present only at base of mandible. Malar striae: absent. Sculpture of malar sulcus: distinctly and sparsely striate. Orbital furrow: uniform in width between midpoint of eye and malar sulcus. Macrosculpture of frons directly dorsal to the antennal scrobe: coarsely rugose. Preocellar pit: present. Setation of lateral frons: sparse; moderately dense. Punctuation of lateral frons: sparse. Sculpture directly ventral to preocellar pit: dorsoventrally fluted. Rugae on lateral frons: weakly developed to absent. OOL: less than one ocellar diameter. Hyperoccipital carina: absent. Macrosculpture of posterior vertex: absent. Microsculpture on posterior vertex along occipital carina: granulate. Anterior margin of occipital carina: crenulate. Medial part of occipital carina in dorsal view: rounded.

Mesosoma. Epomial carina: present. Macrosculpture of lateral pronotum directly anterior to netrion: finely rugulose. Netrion sulcus: complete. Pronotal suprahumeral sulcus in posterior half of pronotum: undifferentiated from sculpture of dorsal pronotum. Number of episternal foveae: 2. Course of episternal foveae ventrally: distinctly separate from postacetabular sulcus. Course of episternal foveae dorsally: distinctly separate from mesopleural pit. Subacroleural sulcus: present. Speculum: transversely strigose. Mesopleural pit: extending ventrally into dorsoventral furrow parallel to mesopleural carina. Mesopleural carina: well defined anteriorly, poorly defined to absent posteriorly. Sculpture of femoral depression: smooth. Patch of striae at posteroventral end of femoral depression: present, striae oblique to long axis of femoral depression. Setal patch at posteroventral end of femoral depression: present as a line of setae. Microsculpture of anteroventral mesopleuron: present throughout. Macrosculpture of anteroventral mesopleuron: absent. Postacetabular sulcus: comprised of large cells. Mesopleural epicoxal sulcus: comprised of cells. Setation of posteroventral metapleuron: absent. Sculpture of dorsal metapleural area: absent. Posterodorsal metapleural sulcus: present as a line of foveae. Paracoxal sulcus in ventral half of metapleuron: indistinguishable from sculpture. Length of anteroventral extension of metapleuron: elongate, extending to base of mesocoxa. Apex of anteroventral extension of metapleuron: rounded. Metapleural epicoxal sulcus: present as coarse rugae. Mesoscutal humeral sulcus: comprised of cells. Median mesoscutal carina: absent. Microsculpture of mesoscutum: imbricate-punctate anteriorly, becoming longitudinally imbricate-strigate posteriorly. Mesoscutal suprahumeral sulcus: comprised of cells. Length of mesoscutal suprahumeral sulcus: two-thirds the length of anterolateral edge of mesoscutum. Parapsidal line: absent. Notaulus: absent. Median protuberance on anterior

margin of mesoscutellum: absent. Shape of dorsal margin of anterior lobe of axillar crescent: acute. Sculpture of anterior lobe of axillar crescent: dorsoventrally strigose. Area bound by axillar crescent: smooth. Macrosculpture of mesoscutellum: absent. Microsculpture on mesoscutellum: imbricate-punctate laterally to granulate medially. Median mesoscutellar carina: absent. Setation of posterior scutellar sulcus: present. Form of metascutellum: single row of cells. Metanotal trough: foveate, foveae occupying more than half of metanotal height. Metapostnotum: invaginated near lateral edge of metascutellum. Length of postmarginal vein: about twice as long as stigmal vein. Color of legs: coxae dark brown to black, femora and tibia dark brown with yellowish tips, trochanters and tarsi yellow to pale brown. Anteroventral area of hind femora: not covered by setae. Anteromedial portion of metasomal depression: smooth.

Metasoma. Width of metasoma: about equal to width of mesosoma. Longitudinal striae on T1 posterior to basal costae: pair of longitudinal submedial carinae separate a lateral smooth area from an internal area where striate sculpture starts with basal grooves. Number of sublateral setae (on one side): 1. Setation of laterotergite 1: present. Length of striation on T2: extending two-thirds the length of the tergite. Setation of T2: present in a transverse line and along lateral margin. Setation of laterotergite 2: present.

Host associations. Pentatomidae: *Aelia rostrata*; *Arma custos*; *Carpocoris* sp.; *Dolycoris* sp.; *Graphosoma italicum* Müller; *Palomena prasina*; *Picromerus bidens* (L.); *Piezodorus* sp.; sentinel frozen eggs of *Halyomorpha halys*. Scutelleridae: *Eurygaster integriceps* Puton; *Eurygaster maura*.

Link to distribution map. [<https://hol.osu.edu/map-large.html?id=3190>]

Material examined. Lectotype, male *Telenomus Belenus*: ENGLAND and WESTERN EUROPE: no date, NMINH_2018_11_49 (deposited in NMID); Lectotype, female, *Telenomus arminon*: UNITED KINGDOM: England, Dorset County, Lyme Regis, no date, NMINH_2018_11_46 (deposited in NMID); Holotype, female, *Asolcus nixomartini*: UNITED KINGDOM: England, Windsor and Maidenhead Unit. Auth., Silwood Park, 1966, reared from egg, M. Javahery, B.M. TYPE HYM. 9.798 (deposited in BMNH); Paratypes of *Asolcus nixomartini*: UNITED KINGDOM: 1 female, 2 males, UNIPA-HYM-S01317–S01318 (BMNH); OSUC 17734 (BMNH); Holotype, female, *Asolcus silwoodensis*: UNITED KINGDOM: England, Windsor and Maidenhead Unit. Auth., Silwood Park, 1966, reared from egg, M. Javahery, B.M. TYPE HYM. 9.797 (deposited in BMNH); Paratypes of *Asolcus silwoodensis*: UNITED KINGDOM: 4 females, 4 males, UNIPA-HYM-S01309–S01316 (BMNH). Syntype males, *Telenomus ovulorum* Thomson: SWEDEN: no date, Boheman, NHRS-HEVA 000006872 (deposited in NHRS). Lectotype, female, *Telenomus nigripes*: SWEDEN: Västra Götaland, no date, Boheman, NHRS-HEVA 000006873 (deposited in NHRS). Paratype of *T. nixomartini*: UNITED KINGDOM: 1 male, OSUC 17734 (BMNH). *Other material*: (437 females, 67 males, 21 pins with multiple specimens). CHINA: 1 female, OSUC 571231 (OSUC). IRAN: 16 females, HMIM-HYM-05–06, 08–09, 011–012, 014, 027, 039 (HMIM); USNMENT01223080–01223082, 01223425, 01223430, 01223435, 01223440 (UNIPA). ITALY: 366 females, 63 males, 17 pins with multiple specimens, DISAFA-draw1465-HYM-0006–0219 (DISAFA); MSNG -HYM-0001–0004, USNMENT01223249–01223258 (MCSN); USNMENT01223090–01223130, 01223132–01223139, 01223230–01223246 (UNIPA).

MOROCCO: 24 female, 1 pin with multiple specimens, OSUC 17729 (BMNH); USNMENT01223131 (UNIPA). PORTUGAL: 6 females, 1 male, 1 pin with multiple specimens, USNMENT00916191, 00916210–00916213, 00916217 (BMNH). RUSSIA: 4 females, 2 males, 2 pins with multiple specimens, OSUC 17796–17797 (BMNH). SWEDEN: 12 females, 2 males, UNIPA-HYM-S01306–S01307, USNMENT00916047, USNMENT00916051, USNMENT00916052, USNMENT00916070, USNMENT00916302–00916309 (BMNH). SWITZERLAND: 6 females, DISAFA-draw1465-HYM-0001–0005 (DISAFA); USNMENT01109059 (USNM). TANZANIA: 1 female, USNMENT01223480 (MZUF). UNITED KINGDOM: 1 female, 1 male, UNIPA-HYM-S01308 (BMNH); USNMENT00896318 (CNCI).

Trissolcus colemani (Crawford)

https://bioguid.osu.edu/xbiod_concepts/3203

Figures 5, 9, 17, 22, 23, 27, 31, 34, 38, 42, 52–55

Telenomus colemani Crawford, 1912: 2 (original description).

Microphanurus djadetshko Ryakhovskii, 1959: 84, 87 (original description, keyed).

Microphanurus pseudoturesis Ryakhovskii, 1959: 83, 85 (original description, keyed).

Microphanurus rossicus Ryakhovskii, 1959: 83, 86 (original description, keyed, synonymized by Viktorov (1964)); Viktorov, 1964: 1021 (junior synonym of *Trissolcus pseudoturesis* (Ryakhovskii)); Johnson, 1992: 635 (type information).

Asolcus nigribasalis Voegelé, 1962: 155 (original description); Voegelé, 1964: 28 (keyed); Voegelé, 1965: 96, 108 (variation, diagnosis, keyed); Voegelé, 1969: 151 (junior synonym of *Asolcus djadetshko* (Ryakhovskii)).

Asolcus djadetshko (Ryakhovskii): Viktorov, 1964: 1015, 1021 (description, generic transfer, removed from synonymy with *Telenomus scutellaris* Thomson, keyed); Voegelé, 1969: 151 (synonymy, keyed, spelling error).

Asolcus pseudoturesis (Ryakhovskii): Viktorov, 1964: 1013, 1021 (description, generic transfer, synonymy, keyed); Voegelé, 1969: 151 (synonymy, keyed).

Asolcus bennisi Voegelé, 1964: 119 (original description); Voegelé, 1965: 96, 108 (variation, diagnosis, keyed); Voegelé, 1969: 151 (junior synonym of *Asolcus pseudoturesis* (Ryakhovskii)).

Trissolcus djadetshko (Ryakhovskii) syn. nov.: Viktorov, 1967: 91 (generic transfer, keyed); Safavi, 1968: 415 (keyed); Kozlov, 1968: 200 (keyed); Fabritius, 1972: 31 (keyed); Kozlov & Lê, 1977: 512 (keyed); Kozlov, 1978: 636 (description); Kozlov, 1981: 187 (keyed); Kozlov & Kononova, 1983: 115 (description); Johnson, 1992: 626 (cataloged, type information); Kononova, 1995: 96 (keyed); Koçak & Kilinçer, 2000: 171 (description, diagnosis, new distribution record for Turkey); Koçak & Kilinçer, 2003: 303, 313 (keyed, description); Fabritius & Popovici, 2007: 159 (checklist, host information, distribution); Ghahari, Buhl & Kocak, 2011: 595 (listed); Petrov, 2013: 326 (keyed); Kononova, 2014: 1425 (keyed); Kononova, 2015: 263 (keyed); Talamas, Buffington & Hoelmer, 2017: 129 (junior synonym of *Trissolcus semistriatus* (Nees von Esenbeck)).

- Trissolcus pseudoturesis* (Ryakhovskii) syn. nov.: Viktorov, 1967: 91 (generic transfer, keyed); Safavi, 1968: 415 (keyed); Kozlov, 1968: 200 (keyed); Fabritius, 1972: 31 (keyed); Kozlov & Lê, 1977: 512 (keyed); Kozlov, 1978: 636 (description); Kozlov & Kononova, 1983: 114 (description); Johnson, 1992: 635 (cataloged, type information); Kononova, 1995: 96 (keyed); Koçak & Kiliçer, 2003: 302, 310 (keyed, description); Ghahari, Buhl & Kocak, 2011: 596 (listed); Petrov, 2013: 326 (keyed); Kononova, 2014: 1425 (keyed); Kononova, 2015: 263 (keyed).
- Trissolcus colemani* (Crawford): Masner & Muesebeck, 1968: 72 (type information, generic transfer); Johnson, 1992: 625 (cataloged, type information).
- Asolcus waloffae* Javahery, 1968: 419 (original description, keyed).
- Asolcus djadestshko* (Ryakhovskii): Voegelé, 1969: 151 (synonymy, keyed, spelling error).
- Trissolcus bennisi* (Voegelé): Kozlov & Lê, 1977: 516 (generic transfer, keyed); Kozlov, 1978: 637 (description); Kozlov & Kononova, 1983: 122 (description); Johnson, 1992: 623 (cataloged, type information); Kononova, 2014: 1425 (keyed); Kononova, 2015: 263 (keyed).
- Trissolcus nigribasalis* (Voegelé): Kozlov & Lê, 1977: 518 (keyed); Kozlov, 1978: 637 (description); Kozlov & Kononova, 1983: 124 (description); Johnson, 1992: 633 (cataloged, type information); Kononova, 2014: 1425 (keyed); Kononova, 2015: 263 (keyed).
- Trissolcus waloffae* (Javahery) syn. nov.: Kozlov & Lê, 1977: 516 (keyed, generic transfer); Kozlov, 1978: 637 (description); Kozlov & Kononova, 1983: 123 (description); Fergusson, 1984: 231 (type information); Johnson, 1992: 640 (cataloged, type information); Kononova, 2014: 1425 (keyed); Kononova, 2015: 263 (keyed).
- Trissolcus crypticus* Clarke syn. nov., 1993: 524 (original description); Ghahari, Buhl & Kocak, 2011: 595 (new distribution record for Iran, host association, listed); Kononova, 2014: 1426 (status unknown (not examined)); Kononova, 2015: 264 (status unknown (not examined)).

Diagnosis. *Trissolcus colemani* is identified by a combination of characters more than by the presence of a distinct feature. The foveate mesoscutal humeral sulcus (Figures 21, 23) separates it from all the species treated here with the exception of *T. belemus* (Figures 20, 22). *Trissolcus colemani* and *T. belemus* are very similar in general appearance and these two species can be separated most reliably by setation of laterotergite 1: present in *T. belemus* (Figures 30, 45) and absent in *T. colemani* (Figure 31, 53). The anteroventral extension of the metapleuron reaches the mesocoxa in lateral view in both *T. belemus* and *T. colemani* and exhibits difference in the shape of its apex between these species. In *T. colemani*, the anteroventral extension of the metapleuron is very slender (Figure 5) compared to *T. belemus*, in which it is thicker, and the apex is rounded (Figure 4).

Description. Body length: 0.96–1.10 mm, $m = 1.01$ mm, $SD = 0.03$, $n = 22$. Body color: head, mesosoma, and metasoma black.

Head. FCI = 1.5; LCI = 1.7; IOS = 0.31 mm; OOL:POL:LOL = 1:13:5.9. Color of radicle: brown. Length of radicle: about equal to width of clypeus. Color of A1–A6 in female: variably yellow to brown. Color of A7–A11 in female: brown to black. Number of papillary sensilla on A6: 0. Number of papillary sensilla on A7: 2. Facial

striae: absent. Number of clypeal setae: 6. Shape of gena in lateral view: narrow. Genal carina: present only at base of mandible. Malar striae: absent. Sculpture of malar sulcus: distinctly and sparsely striate. Orbital furrow: uniform in width between midpoint of eye and malar sulcus. Macrosculpture of frons directly dorsal to the antennal scrobe: weakly rugose. Preocellar pit: present. Setation of lateral frons: sparse; moderately dense. Punctuation of lateral frons: sparse. Sculpture directly ventral to preocellar pit: dorsoventrally fluted. Rugae on lateral frons: coarse. OOL: less than one ocellar diameter. Hyperoccipital carina: absent. Macrosculpture of posterior vertex: absent. Microsculpture on posterior vertex along occipital carina: granulate. Anterior margin of occipital carina: crenulate. Medial part of occipital carina in dorsal view: rounded.

Mesosoma. Epomial carina: present. Macrosculpture of lateral pronotum directly anterior to netrion: finely rugulose. Netrion sulcus: complete. Pronotal suprahumeral sulcus in posterior half of pronotum: undifferentiated from sculpture of dorsal pronotum. Number of episternal foveae: 2; 3. Course of episternal foveae ventrally: distinctly separate from postacetabular sulcus. Course of episternal foveae dorsally: distinctly separate from mesopleural pit. Subacroleural sulcus: present. Speculum: transversely strigose. Mesopleural pit: extending ventrally into dorsoventral furrow parallel to mesopleural carina. Mesopleural carina: well defined anteriorly, poorly defined to absent posteriorly. Sculpture of femoral depression: smooth. Patch of striae at posteroventral end of femoral depression: present, striae oblique to long axis of femoral depression. Setal patch at posteroventral end of femoral depression: present. Microsculpture of anteroventral mesopleuron: present throughout. Macrosculpture of anteroventral mesopleuron: absent. Postacetabular sulcus: comprised of large cells. Mesopleural epicoxal sulcus: comprised of cells. Setation of posteroventral metapleuron: absent. Sculpture of dorsal metapleural area: absent. Posterodorsal metapleural sulcus: present as a line of foveae. Paracoxal sulcus in ventral half of metapleuron: indistinguishable from sculpture. Length of anteroventral extension of metapleuron: elongate, extending to base of mesocoxa. Apex of anteroventral extension of metapleuron: acute. Metapleural epicoxal sulcus: present as coarse rugae. Mesoscutal humeral sulcus: comprised of cells. Median mesoscutal carina: absent. Microsculpture of mesoscutum: imbricate-punctate anteriorly, becoming longitudinally imbricate-strigate posteriorly. Mesoscutal suprahumeral sulcus: comprised of cells. Length of mesoscutal suprahumeral sulcus: two-thirds the length of anterolateral edge of mesoscutum. Parapsidal line: absent. Notaulus: presence of short traces. Median protuberance on anterior margin of mesoscutellum: absent. Shape of dorsal margin of anterior lobe of axillar crescent: acute. Sculpture of anterior lobe of axillar crescent: dorsoventrally strigose. Area bound by axillar crescent: smooth. Macrosculpture of mesoscutellum: absent. Microsculpture on mesoscutellum: imbricate-punctate. Median mesoscutellar carina: absent. Setation of posterior scutellar sulcus: present. Form of metascutellum: single row of cells. Metanotal trough: foveate, foveae occupying more than half of metanotal height. Metapostnotum: invaginated near lateral edge of metascutellum. Length of postmarginal vein: about twice as long as stigmal vein. Color of legs: coxae dark brown to black, femora yellow to light brown with yellowish tips, tibia trochanters and tarsi yellow to pale brown. Anteroventral area of hind femora: not covered by setae. Anteromedial portion of metasomal depression: smooth.

Metasoma. Width of metasoma: about equal to width of mesosoma. Longitudinal striae on T1 posterior to basal costae: pair of longitudinal submedial carinae separate a lateral smooth area from an internal area where striate sculpture starts with basal grooves. Number of sublateral setae (on one side): 1. Setation of laterotergite 1: absent. Length of striation on T2: extending two-thirds the length of the tergite. Setation of T2: present in a transverse line and along lateral margin. Setation of laterotergite 2: present.

Host associations. Pentatomidae: *Dolycoris indicus* (Type host); *Aelia acuminata* L.; *Aelia* sp.; *Brachynema germarii* (Kolenati); *Dolycoris* sp.; *Graphosoma semipunctatum* (F.); *Graphosoma* sp. Scutelleridae: *Eurygaster integriceps*; *Eurygaster maura*.

Link to distribution map. [<https://hol.osu.edu/map-large.html?id=3203>]

Material examined. Holotype, female, *Telenomus colemani*: INDIA: Karnataka St., Hongashenhalli (Hunsmannalli), 6.II.1909, L. C. Coleman, USNMMENT00989063 (deposited in USNM). Syntype, female, *Microphanurus pseudoturesis*: UKRAINE: Donetsk (Stalinskaya) Reg., V-1952/1953–VII-1952/1953, V. Rjachovsky, USNMMENT00954008 (deposited in ZIN). Syntype, female, *Microphanurus pseudoturesis*: UKRAINE: Donetsk (Stalinskaya) Reg., V-1952/1953–VII-1952/1953, V. Rjachovsky, USNMMENT00954010. Holotype, female, *A. waloffae*: UNITED KINGDOM: England, Windsor and Maidenhead Unit. Auth., Silwood Park, VI-1965, reared, B.M. TYPE HYM. 9.795 (deposited in BMNH). Paratypes of *Trissolcus crypticus*: PAKISTAN: 3 females, 3 males, OSUC 17744, UNIPA-HYM-S01319–S01323 (BMNH). Paratype of *Microphanurus djadetschko*: UKRAINE: 1 female, USNMMENT00954012 (ZIN). Paratypes of *Asolcus waloffae*: UNITED KINGDOM: 11 females, 11 males, 1 pin with multiple specimens, OSUC 17731, UNIPA-HYM-S01324, USNMMENT0119671–0119674 (BMNH).

Other material: (144 females, 52 males, 6 pins with multiple specimens) CHINA: 1 female, UCRC ENT 142649 (UCRC). FRANCE: 1 female, USNMMENT00896254 (CNCI). GREECE: 1 female, USNMMENT00896062 (CNCI). IRAN: 17 females, HMIM-HYM-015, 017–018, 020–021, 025, 028, 031, 036, 042 (HMIM); USNMMENT01223445, 01223450, 01223455, 01223460, 01223465, 01223470, 01223475 (UNIPA). ITALY: 82 females, 19 males, 2 pins with multiple specimens, DISAFA-draw1466-HYM-0483–0488 (DISAFA); USNMMENT01223144, 01223146–01223221, 01223481 (UNIPA). MOROCCO: 39 females, 31 males, 3 pins with multiple specimens, OSUC 17728, 17743 (BMNH); UNIPA-HYM-S01325 (BMNH). RUSSIA: 3 females, 1 pin with multiple specimens, USNMMENT01223222–01223223 (MCSN). SWEDEN: 2 males, USNMMENT00916067–00916068 (BMNH).

Trissolcus manteroi (Kieffer)

https://bioguid.osu.edu/xbiod_concepts/3260

Figures 6, 10, 13, 18, 24, 28, 35, 39, 43, 56–58

Telenomus Manteroi Kieffer, 1909: 268 (original description).

Aphanurus Manteroi (Kieffer): Kieffer 1912: 84 (description, generic transfer).

Microphanurus manteroi (Kieffer): Kieffer 1926: 91, 102. (description, generic transfer, keyed); Boldaruyev 1969: 163, 170 (description, keyed)

Trissolcus manteroi (Kieffer): Kozlov 1968: 199 (keyed); Fabritius 1972: 31 (keyed); Bin 1974: 462 (type information); Kozlov and Lê 1977: 514 (keyed); Kozlov 1978: 636 (description); Kozlov and Kononova 1983: 117 (description); Johnson 1992: 631 (cataloged, type information); Koçak and Kiliñer 2000: 174 (description, diagnosis, new distribution record for Turkey); Koçak and Kiliñer 2003: 302, 310 (keyed, description of female); Koçak and Kodan 2006: 41 (description of male); Fabritius and Popovici 2007: 159. (host information, distribution); Ghahari et al. 2011: 596 (listed); Kononova 2014: 1424 (keyed); Kononova 2015: 262 (keyed); Talamas et al. 2017: 129, 135 (junior synonym of *Trissolcus semistriatus* (Nees von Esenbeck), type information).

Diagnosis. *Trissolcus manteroi* and *T. rufiventris* are the only two species of Palearctic *Trissolcus* in which females exhibit a 1-2-2-2-1 claval formula (Figure 10). These two can be separated from each other by the length of the postmarginal vein in the fore wing: slightly longer than the stigmal vein in *T. manteroi* (Figure 13) and about twice as long as the stigmal vein in *T. rufiventris* (Figure 14). These two species can also be separated from each other by the form of the mesopleural epicoxal sulcus, which is comprised of cells in *T. manteroi* and is a smooth furrow in *T. rufiventris*.

Description. Female body length: 0.99–1.09 mm, m = 1.04 mm, SD = 0.02, n = 16. Body color: head, mesosoma, and metasoma black.

Head. FCI = 1.4; LCI = 1.8; IOS = 0.3 mm; OOL:POL:LOL = 1:12:5.3. Color of radicle: dark brown. Length of radicle: less than width of clypeus. Color of A1–A6 in female: distal A2 yellow to light brown, otherwise black. Color of A7–A11 in female: black. Number of papillary sensilla on A6: 0. Number of papillary sensilla on A7: 1. Facial striae: absent. Number of clypeal setae: 6. Shape of gena in lateral view: narrow. Genal carina: present only at base of mandible. Malar striae: absent. Sculpture of malar sulcus: weakly and densely striate. Orbital furrow: uniform in width between midpoint of eye and malar sulcus. Macrosculpture of frons directly dorsal to the anterior ocellus: weakly rugose. Preocellar pit: present. Setation of lateral frons: sparse; moderately dense. Punctuation of lateral frons: sparse. Sculpture directly ventral to preocellar pit: dorsoventrally fluted. Rugae on lateral frons: weakly developed to absent. OOL: less than one ocellar diameter. Hyperoccipital carina: absent. Macrosculpture of posterior vertex: absent. Microsculpture on posterior vertex along occipital carina: granulate. Anterior margin of occipital carina: crenulate. Medial part of occipital carina in dorsal view: rounded.

Mesosoma. Epomial carina: present. Macrosculpture of lateral pronotum directly anterior to netrion: finely rugulose. Netrion sulcus: complete. Pronotal suprahumeral sulcus in posterior half of pronotum: undifferentiated from sculpture of dorsal pronotum. Number of episternal foveae: 0. Subacropleurale sulcus: present. Speculum: transversely strigose. Mesopleural pit: extending ventrally into dorsoventral furrow parallel to mesopleural carina. Mesopleural carina: well defined anteriorly, poorly defined to absent posteriorly. Sculpture of femoral depression: smooth. Patch of striae at posteroventral end of femoral depression: present, striae oblique to long axis of femoral depression. Setal patch at posteroventral end of femoral depression: absent.



Figures 45–48. Holotype of *Trissolcus belemus* [NMINH_2018_11_49]: **45** mesoscutal humeral sulcus and laterotergite 1 in lateral view **46** body in lateral view **47** body in antero-lateral view **48** body in dorsal view.



Figures 49–51. Holotype of *Trissolcus arminon* [NMINH_2018_11_46]: **49** body in dorsal view **50** head and mesosoma in antero-lateral view **51** body in postero-lateral view.

Microsculpture of anteroventral mesopleuron: present throughout. Macrosculpture of anteroventral mesopleuron: absent. Postacetabular sulcus: comprised of large cells. Mesopleural epicoxal sulcus: comprised of cells. Setation of posteroventral metapleuron: absent. Sculpture of dorsal metapleural area: absent. Posterodorsal metapleural

sulcus: present as a line of foveae. Paracoxal sulcus in ventral half of metapleuron: indistinguishable from sculpture. Length of anteroventral extension of metapleuron: short, not extending to base of mesocoxa. Metapleural epicoxal sulcus: present as coarse rugae. Mesoscutal humeral sulcus: present as a simple furrow. Median mesoscutal carina: absent. Microsculpture of mesoscutum: imbricate-punctate anteriorly, becoming longitudinally imbricate-strigate posteriorly. Mesoscutal suprahumeral sulcus: comprised of cells. Length of mesoscutal suprahumeral sulcus: two-thirds the length of anterolateral edge of mesoscutum. Parapsidal line: absent. Notaulus: absent. Median protuberance on anterior margin of mesoscutellum: absent. Shape of dorsal margin of anterior lobe of axillar crescent: acute. Sculpture of anterior lobe of axillar crescent: dorsoventrally strigose. Area bound by axillar crescent: smooth. Macrosculpture of mesoscutellum: absent. Microsculpture on mesoscutellum: imbricate-punctate laterally to granulate medially. Median mesoscutellar carina: absent. Setation of posterior scutellar sulcus: present. Form of metascutellum: single row of cells. Metanotal trough: foveate, foveae occupying more than half of metanotal height. Metapostnotum: invaginated near lateral edge of metascutellum. Length of postmarginal vein: 1.1–1.2 times as long as stigmal vein. Color of legs: coxae dark brown to black, femora and tibia dark brown with yellowish tips, trochanters and tarsi yellow to pale brown. Anteroventral area of hind femora: not covered by setae. Anteromedial portion of metasomal depression: smooth.

Metasoma. Width of metasoma: about equal to width of mesosoma. Longitudinal striae on T1 posterior to basal costae: pair of longitudinal submedial carinae separate a lateral smooth area from an internal area where striate sculpture starts with basal grooves. Number of sublateral setae (on one side): 1. Setation of laterotergite 1: absent. Length of striation on T2: extending one-third the length of the tergite. Setation of T2: present in a transverse line and along lateral margin. Setation of laterotergite 2: present.

Host associations. Pentatomidae: *Carpocoris* sp. (Type host); *Aelia rostrata* Boheman; *Dolycoris* sp.

Link to distribution map. [<https://hol.osu.edu/map-large.html?id=13225>]

Material examined. Holotype, female, *T. Manteroi*: ITALY: Liguria, Genoa, 9.VIII.1997, G. Mantero, MCSN 0013 (deposited in MCSN). *Paratypes*: ITALY: 5 females, 1 male, 1 pin with multiple specimens, UNIPA-HYM-S01327, S01328 (MCSN). *Other material*: (20 females, 2 males, 1 pin with multiple specimens) ARMENIA: 3 females, 1 pin with multiple specimens, USNMENT00979995, 00979997 (ZIN). IRAN: 4 females, USNMENT01223224–01223227 (MCSN). ITALY: 13 females, 2 males, DISAFA-draw1465-HYM-0424–0438 (DISAFA).

***Trissolcus semistriatus* (Nees von Esenbeck)**

https://bioguid.osu.edu/xbiod_concepts/3305

Figures 7, 11, 15, 19, 25, 29, 32, 36, 40, 44, 59, 60.

Teles semistriatus Nees von Esenbeck, 1834: 290 (original description); Ratzeburg, 1852: 182 (description); Johnson, 1992: 519 (cataloged).

- Telenomus semistriatus* (Nees von Esenbeck): Thomson, 1860: 171 (description, generic transfer); Mayr, 1879: 699, 701, 704 (description, synonymy, keyed).
- Asolcus nigripedius* Nakagawa, 1900: 17 (original description); Watanabe, 1951: 21, 25 (description, type information, keyed); Watanabe, 1954: 22 (keyed).
- Aphanurus Semistriatus* (Nees von Esenbeck): Kieffer, 1912: 74 (description, generic transfer).
- Microphanurus semistriatus* (Nees von Esenbeck): Kieffer, 1926: 91, 97 (description, generic transfer, keyed); Nixon, 1939: 131, 134 (description, keyed); Meier, 1940: 80 (description, keyed); Ryakhovskii, 1959: 84 (keyed).
- Microphanurus alexeevi* Meier, 1949: 114 (original description, not seen: reference from Kozlov (1963), synonymized with *Asolcus semistriatus* (Nees von Esenbeck) by Kozlov (1963)); Ryakhovskii, 1959: 83 (keyed); Kozlov, 1963: 295 (junior synonym of *Asolcus semistriatus* (Nees von Esenbeck)).
- Microphanurus schtepetelnikovae* Meier, 1949: 114 (original description, not seen: reference from Kozlov (1963), synonymized with *Asolcus semistriatus* (Nees von Esenbeck) by Kozlov (1963)); Kozlov, 1963: 295 (junior synonym of *Asolcus semistriatus* (Nees von Esenbeck)).
- Asolcus semistriatus* (Nees von Esenbeck): Masner 1959: 376 (diagnosis, variation); Delucchi, 1961: 44, 59 (diagnosis, taxonomic status, keyed); Kozlov, 1963: 295 (synonymy); Viktorov, 1964: 1013, 1020 (variation, keyed); Kochetova, 1966: 558 (description of immature stages); Javahery, 1968: 419 (keyed); Voegelé, 1969: 150 (keyed); Szabó, 1976: 176, 178 (description, neotype designation, keyed).
- Microphanurus stschepletinikovae* Meier: Ryakhovskii, 1959: 83 (keyed, spelling error).
- Trissolcus nigripedius* (Nakagawa): Masner, 1964: 146 (generic transfer); Ryu & Hirasima, 1984: 37, 56 (description, keyed); Johnson, 1992: 633 (cataloged); He, Chen, Fan, Li, Liu, Lou, Ma, Wang, Wu, Xu, Xu & Yao, 2004: 321 (description); Fabritius & Popovici, 2007: 157 (host informations, distribution); Kononova, 2014: 1424 (keyed); Kononova, 2015: 261 (keyed); Talamas, Buffington & Hoelmer, 2017: 130 (junior synonym of *Trissolcus semistriatus* (Nees von Esenbeck), neotype designation).
- Trissolcus semistriatus* (Nees von Esenbeck): Safavi, 1968: 416 (keyed); Kozlov, 1968: 200 (keyed); Fabritius, 1972: 32, 34 (keyed, host catalogue; distribution); Kozlov & Lê, 1977: 512 (keyed); Kozlov, 1978: 636 (description); Kozlov & Kononova, 1983: 113 (description); Graham, 1984: 92 (variation); Johnson, 1992: 636 (cataloged, type information); Kononova, 1995: 96 (keyed); Koçak & Kilinçer, 2003: 302, 305 (keyed, description); Ali, 2011: 10 (keyed); Ghahari, Buhl & Kocak, 2011: 597 (listed); Guz, Kocak & Kilincer, 2013: 87 (description, phylogenetic relationships); Petrov, 2013: 326 (keyed); Kononova, 2014: 1425 (keyed); Kononova, 2015: 262 (keyed); Talamas, Buffington & Hoelmer, 2017: 20, 25, 128 (description, keyed, synonymy, type information, distribution).
- Trissolcus artus* Kozlov & Lê, 1977: 512, 519 (original description, keyed); Kozlov, 1978: 636 (description); Kozlov & Kononova, 1983: 112 (description); Johnson, 1992: 622 (cataloged, type information); Kononova, 1995: 96 (keyed); Kononova, 2014: 1424 (keyed); Kononova, 2015: 262 (keyed); Talamas, Buffington & Hoe-

lmer, 2017: 128, 135 (junior synonym of *Trissolcus semistriatus* (Nees von Esenbeck), type information).

Diagnosis. *Trissolcus semistriatus* is most similar to *T. belenus* and *T. colemani*, with which it overlaps in distribution and host range. It can be separated from both by the mesoscutal humeral sulcus present as a smooth furrow (Figure 25) and the short anteroventral extension of the mesopleuron, which does not extend to the base mesocoxa (Figure 7). Additionally, the angular form of the occipital carina in dorsal view, with a short carina extending toward the median ocellus, is found only in this species (Figure 36). The anteroventral area of the hind femur that is covered by setae (Figure 29) is useful when separating *T. semistriatus* from *T. belenus* (Figure 26), *T. colemani* (Figure 27) and *T. manteroi* (Figure 28).

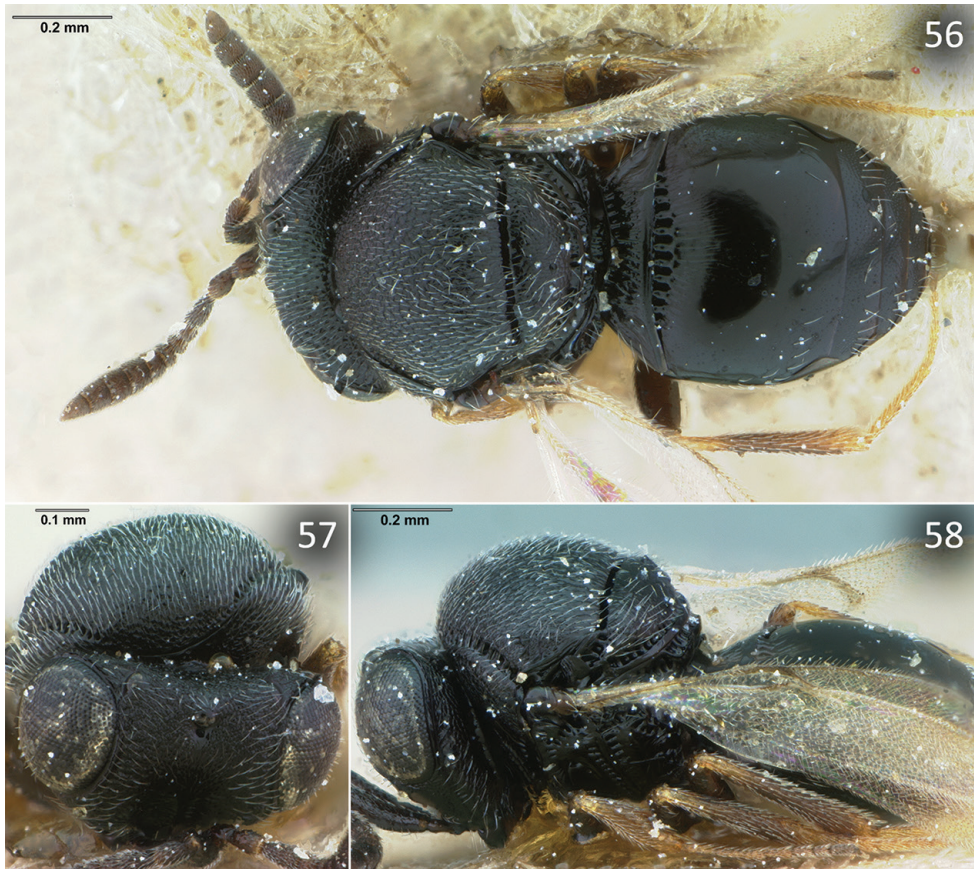
Description. Body length: 1.07–1.11 mm, median = 1.08 mm, SD = 0.01, n = 20. Body color: head, mesosoma, and metasoma black.

Head. FCI = 1.4; LCI = 1.9; IOS = 0.33 mm; OOL:POL:LOL = 1:12:5.4. Length of radicle: less than width of clypeus. Color of A1–A6 in female: distal A2 yellow to light brown, otherwise black. Color of A7–A11 in female: black. Number of papillary sensilla on A6: 0. Number of papillary sensilla on A7: 2. Facial striae: absent. Number of clypeal setae: 6. Shape of gena in lateral view: narrow. Genal carina: present only at base of mandible. Malar striae: absent. Sculpture of malar sulcus: weakly and densely striate. Orbital furrow: uniform in width between midpoint of eye and malar sulcus. Macrosculpture of frons directly dorsal to the antennal scrobe: coarsely rugose. Preocellar pit: present. Setation of lateral frons: sparse; moderately dense. Punctuation of lateral frons: sparse. Sculpture directly ventral to preocellar pit: dorsoventrally fluted. Rugae on lateral frons: weakly developed to absent. OOL: less than one ocellar diameter. Hyperoccipital carina: absent. Macrosculpture of posterior vertex: absent. Microsculpture on posterior vertex along occipital carina: granulate. Anterior margin of occipital carina: crenulate. Medial part of occipital carina in dorsal view: angled, vertex of angle with short carina directed toward median ocellus.

Mesosoma. Epomial carina: present. Macrosculpture of lateral pronotum directly anterior to netrion: finely rugulose. Netrion sulcus: complete. Pronotal suprahumeral sulcus in posterior half of pronotum: undifferentiated from sculpture of dorsal pronotum. Number of episternal foveae: 2. Course of episternal foveae ventrally: distinctly separate from postacetabular sulcus. Course of episternal foveae dorsally: distinctly separate from mesopleural pit. Subacroleural sulcus: present. Speculum: transversely strigose. Mesopleural pit: extending ventrally into dorsoventral furrow parallel to mesopleural carina. Mesopleural carina: well defined anteriorly, poorly defined to absent posteriorly. Sculpture of femoral depression: smooth. Patch of striae at posteroventral end of femoral depression: present, striae oblique to long axis of femoral depression. Setal patch at posteroventral end of femoral depression: absent. Microsculpture of anteroventral mesopleuron: present throughout. Macrosculpture of anteroventral mesopleuron: absent. Postacetabular sulcus: comprised of large cells. Mesopleural epicoxal sulcus: comprised of cells. Setation of posteroventral metapleuron: absent. Sculpture of dorsal metapleuron: absent. Posterodorsal metapleuron sulcus: present as a line of



Figures 52–55. Holotype of *Trissolcus colemani* [USNMENT00989063]: **52** body in dorsal view **53** body in lateral view **54** head in frontal view **55** head in ventral view and mesosoma in lateral view.



Figures 56–58. Holotype of *Trissolcus manteroi* [MCSN 0013]: **56** body in dorsal view **57** head in antero-lateral view **58** body in lateral view.

foveae. Paracoxal sulcus in ventral half of metapleuron: indistinguishable from sculpture. Length of anteroventral extension of metapleuron: short, not extending to base of mesocoxa. Metapleural epicoxal sulcus: present as coarse rugae. Mesoscutal humeral sulcus: present as a simple furrow. Median mesoscutal carina: absent. Microsculpture of mesoscutum: imbricate-punctate anteriorly, becoming longitudinally imbricate-strigate posteriorly. Mesoscutal suprahumeral sulcus: comprised of cells. Length of mesoscutal suprahumeral sulcus: two-thirds the length of anterolateral edge of mesoscutum. Parapsidal line: absent. Notaulus: absent. Median protuberance on anterior margin of mesoscutellum: absent. Shape of dorsal margin of anterior lobe of axillar crescent: acute. Sculpture of anterior lobe of axillar crescent: dorsoventrally strigose. Area bound by axillar crescent: smooth. Macrosculpture of mesoscutellum: absent. Microsculpture on mesoscutellum: imbricate-punctate laterally to smooth medially. Median mesoscutellar carina: absent. Setation of posterior scutellar sulcus: present. Form of metascutellum: single row of cells. Metanotal trough: foveate, foveae occupying more than half of metanotal height. Metapostnotum: invaginated near lateral edge of metascutellum.

Length of postmarginal vein: about twice as long as stigmal vein. Color of legs: coxae dark brown to black, femora and tibia dark brown with yellowish tips, trochanters and tarsi yellow to pale brown. Anteroventral area of hind femora: covered by setae. Anteromedial portion of metasomal depression: smooth.

Metasoma. Width of metasoma: about equal to width of mesosoma. Longitudinal striae on T1 posterior to basal costae: pair of longitudinal submedial carinae separate a lateral smooth area from an internal area where striate sculpture starts with basal grooves. Number of sublateral setae (on one side): 1. Setation of laterotergite 1: absent. Length of striation on T2: extending two-thirds the length of the tergite. Setation of T2: present in a transverse line and along lateral margin. Setation of laterotergite 2: present.

Host associations. Pentatomidae: *Aelia rostrata*; *Brachynema germarii* (Kolenati); *Carpocoris* sp.; *Dolycoris baccarum* (L.); *Graphosoma semipunctatum*; *Rhaphigaster* sp.; Scutelleridae: *Eurygaster maura*.

Link to distribution map. [<https://hol.osu.edu/map-large.html?id=3305>]

Material examined. Neotype, female, *Teleas semistriatus*: PALEARCTIC: no date, NHMW 0007A (deposited in NHMW). Paratype of *Trissolcus artus*: RUSSIA: 1 female, USNMENT00916276 (ZIN). *Neoparatype*: PALEARCTIC: 1 female, NHMW 0007B (NHMW).

Other material: (183 females, 50 males, 2 pins with multiple specimens) IRAN: 11 females, HMIM-HYM-022, 038 (HMIM); USNMENT01223083–01223089 (UNIPA); USNMENT01223228–01223229 (MCSN). ITALY: 189 females, 54 males, 2 pins with multiple specimen, DISAFA-draw1465-HYM-0226–0240, 0242–0423 (DISAFA); MSNG-HYM-0005–0013 (MCSN); UNIPA-HYM-S01329–01346, USNMENT01223140–01223142, 01223482 (UNIPA). JAPAN: 1 female, EIHU 0003 (EIHU). MOROCCO: 1 female, USNMENT01223143 (UNIPA). PORTUGAL: 3 females, USNMENT00916201–00916202, 00916236 (BMNH). SWEDEN: 1 female, UNIPA-HYM-S01326 (BMNH). SWITZERLAND: 1 female, DISAFA-draw1465-HYM-0241 (DISAFA).

Discussion

More than 180 years have passed between the original descriptions of *T. semistriatus* and *T. belenus* and the development of identification tools that can reliably distinguish them. This can be viewed as a glacial rate of progress, but also as an indication that modern methods can resolve long-standing taxonomic challenges. The taxonomy of *Trissolcus* illustrates that the examination of primary types and detailed comparison of specimens across a broad geographical range is necessary to advance the field, and that further refinement may be required even when these practices are implemented. Talamas et al. (2017) significantly advanced the taxonomy of Palearctic *Trissolcus* but additional analysis was needed to distill diagnostic characters from those that were treated as intraspecifically variable. Specifically, setation on the first laterotergite, the form of the mesoscutal humeral sulcus, and the length of the anteroventral extension of the metapleuron were treated as variable within *T. semistriatus*. Although the utility of these



Figures 59, 60. *Trissolcus semistriatus* [DISAFA-draw1465-HYM-0227]: **59** body in dorsal view **60** body in lateral view.

characters for separating *T. belemus* and *T. colemani* was not recognized, Talamas et al. (2017) did bring attention to them, as they had not yet been used in the taxonomy of Palearctic *Trissolcus*. Setation of the hind femora, not mentioned by Talamas et al. (2017), represents a case in which a diagnostic character was previously recognized, but

incorrectly associated with a taxon name (Delucchi 1961), and is now treated as useful for identifying *T. belenus*. *Trissolcus manteroi* is a different matter, in which reexamination of the type specimen was needed for its diagnostic characters (wing venation, claval formula, absence of episternal foveae) to be correctly characterized. These features place *T. manteroi* closer to *T. rufiventris* than to *T. semistriatus*, *T. belenus* or *T. colemani*.

The trail of photographic evidence provided by Talamas et al. (2017) enabled junior synonyms of *T. semistriatus* to be rapidly redistributed among *T. belenus* and *T. colemani* once the characters that delimit these species were identified, as well as the resurrection of *T. manteroi*. Given that producing a natural classification is an iterative process, explicit presentation of data that underlies taxonomic decisions accelerates further refinement. This is perhaps the only means by which the various quagmires of inadequate species descriptions in Platygastroidea can be transformed into a useful classification.

The need for reliable identification can be clearly seen in examples where quality taxonomy was absent. In the early part of the 20th century, *Trissolcus* specimens identified as *T. semistriatus* or *T. grandis* were reared and released in Russia and Iran as classical biological control agents against *Eurygaster* (Alexandrov 1947; Saakov 1903; Vaezi 1950; Vassiliev 1913; Zomorodi 1959). Some of these authors did not indicate how they identified the species, and in any case, the characters that reliably separate these species were not established. It is only by retroactively identifying voucher specimens, if they exist, that the results of these efforts can be interpreted in a meaningful way. The presence of *H. halys* in Europe has created a similar situation, with the same species involved in studies of its biological control. The refined species concepts presented here are thus of immediate relevance, given that *T. belenus* was recorded from frozen sentinel eggs of *H. halys* in Europe, and was previously identified as *T. semistriatus*.

Finally, it should be noted that independent testing of species concepts, ideally using multiple methods, is the best means by which they can be verified or improved. This study employed such an approach, using morphology, mating studies and molecular analysis to resolve four species from the concept of *T. semistriatus* provided in Talamas et al. (2017). In a manner conforming with this perspective, our results have been confirmed by a concomitant study by Talamas et al. (2019), in which a phylogeny of *Trissolcus* based on five molecular markers retrieved *T. belenus*, *T. colemani* and *T. semistriatus* as distinct entities.

Acknowledgements

We are grateful to: Dr. Hege Vårdal (NHRS) for photographing a number of Thomson types: *Telenomus frontalis*, *Telenomus nigripes*, *Telenomus nigrita*, *Telenomus ovulorum* and *Trissolcus grandis*; Dr. Matthew Buffington (USNM, USDA/SEL) for providing supplemental images of the holotype of *Telenomus colemani*; Valentina Guerini for transliteration from Cyrillic to Latin alphabet of labels; David Notton (BMNH), who hosted a visit of Virgilio Caleca; Dr. Paolo Visconti, who hosted a visit of Elijah Talamas to NMID which enabled the lectotypes of *T. belenus* and *T. arminon* to be studied and photographed and Dr. Norman Johnson (The Ohio State University), for maintaining Hymenoptera Online and vSysLab and assisting with data processing. Elijah Talamas

was supported in part by a cooperative agreement with Kim Hoelmer (USDA/BIIRU) and by the Florida Department of Agriculture and Consumer Services- Division of Plant Industry. This research was funded by Fondazione Cassa di Risparmio di Cuneo (project HALY-END) and Regione Piemonte (project BIOHALY).

References

- Alexandrov N (1947) *Eurygaster integriceps* Put. a Varamine et ses parasites. Entomologie et Phytopathologie Appliquees 5: 29–41.
- Ali WH (2011) The level of sunn pest oophagous parasitoids (Hymenoptera: Scelionidae) in infested wheat fields of northern governorate in Iraq with an identification key of *Trissolcus* species. Bulletin of the Iraq Natural History Museum 11: 7–15.
- Bin F (1974) The types of Scelionidae [Hymenoptera: Proctotrupoidea] in some Italian collections (Museums of Genoa and Florence, Institute of Portici). Entomophaga 19: 453–466. <https://doi.org/10.1007/BF02372781>
- Bin F (1981) Definition of female antennal clava based on its plate sensilla in Hymenoptera Scelionidae Telenominae. Redia 64: 245–261.
- Boldaruyev VO (1969) [Egg parasites of the subfamily Telenominae (Hymenoptera, Scelionidae), reared from the eggs of harmful insects.]. Trudy Buryatskogo Instituta Estestvennykh Nauk Buryatskii Filial Siirskogo Otdeleniya Akademii Nauk USSR 7: 156–171.
- Buffington ML, Burks RA, McNeil LA (2005) Advanced techniques for imaging parasitic Hymenoptera (Insecta). American Entomologist 51: 50–54. <https://doi.org/10.1093/ae/51.1.50>
- Buffington ML, Gates M (2008) Advanced Imaging Techniques II: Using a Compound Microscope for Photographing Point-Mount Specimens. American Entomologist 54: 222–224. <https://doi.org/10.1093/ae/54.4.222>
- Buffington ML, Talamas EJ, Hoelmer KA (2018) Team *Trissolcus*: Integrating Taxonomy and Biological Control to Combat the Brown Marmorated Stink Bug. American Entomologist 64: 224–232. <https://doi.org/10.1093/ae/tmy057>
- Buhl PN, O'Connor JP (2010) Five species of Ceraphronidae and Scelionidae (Hymenoptera) new to Ireland. Entomologists Monthly Magazine 146: 1–154.
- Clarke AR (1990) The Control of *Nezara viridula* L. with Introduced Egg Parasitoids in Australia. A Review of a “Landmark” Example of Classical Biological Control. Australian Journal of Agricultural Research 41: 1127–1146. <https://doi.org/10.1071/AR9901127>
- Clarke AR (1993) A new *Trissolcus* Ashmead species (Hymenoptera: Scelionidae) from Pakistan: Species description and its role as a biological control agent. Bulletin of Entomological Research 83: 523–527. <https://doi.org/10.1017/S0007485300039948>
- Crawford JC (1912) Descriptions of new Hymenoptera. No. 4. Proceedings of the United States National Museum 42: 1–10. <https://doi.org/10.5479/si.00963801.42-1880.1>
- Dalla Torre CG de (1898) Catalogus Hymenopterorum Hucusque Descriptorum Systematicus et Synonymicus (Vol. V). Chalcididae et Proctotrupidae. Sumptibus Guilelmi Engelmann, Lipsiae, 598 pp.
- Debauche (1947) Scelionidae de la faune belge (Hymenoptera Parasitica). Bulletin et Annales de la Société Entomologique de Belge 83: 255–285.

- Delucchi VL (1961) Le complexe des *Asolcus* Nakagawa (*Microphanurus* Kieffer) (Hymenoptera, Proctotrupeoidea) parasites oophages des punaises des cereales au Maroc et au Moyen-Orient. Cahiers de la Recherche Agronomique 14: 41–67.
- Doganlar M (2001) Egg parasitoids of *Rhaphigaster nebulosa* (Poda) (Hemiptera; Pentatomidae) with description of a new species of *Trissolcus* Ashmead (Hymenoptera: Scelionidae). Turkish Journal of Entomology 25: 109–114.
- Fabritius K (1972) Genul *Trissolcus* Ashmead 1893 (Hymenoptera, Scelionidae) în România și perspectivele utilizării acestui gen de entomofagi în combaterea biologică și integrată a ploșnițelor cerealelor. Lucrări Științifice – Zoologie, Constanța 1972: 27–42.
- Fabritius K, Popovici OA (2007) A Catalogue of Scelionidae from Romania (Hymenoptera, Platygastroidea). Entomologica Romanica 12: 133–161.
- Fergusson NDM (1978) Proctotrupeoidea and Ceraphonoidea. Pages 110–126 in Fitton, Graham, Boucek, Fergusson, Huddleston, Quinlan & Richards. 1978. A check list of British insects by George Sidney Kloet and the late Walter Douglas Hincks, second edition (completely revised). Pa. Handbooks for the Identification of British Insects 11: 1–159.
- Fergusson NDM (1983) The status of the genus *Allophanurus* Kieffer (Hymenoptera: Proctotrupeoidea, Scelionidae). Entomologist's Monthly Magazine 119: 207–209.
- Fergusson NDM (1984) The type-specimens and identity of the British species of *Trissolcus* Ashmead (Hym., Proctotrupeoidea, Scelionidae). Entomologist's Monthly Magazine 120: 229–232.
- Folmer O, Black M, Hoeh W, Lutz R, Vrijenhoek R (1994) DNA primers for amplification of mitochondrial cytochrome c oxidase subunit I from diverse metazoan invertebrates. Molecular Marine Biology and Biotechnology 3: 294–299.
- Ghahari H, Buhl PN, Koçak E (2011) Checklist of Iranian *Trissolcus* Ashmead (Hymenoptera: Platygastroidea: Scelionidae: Telenominae). International Journal of Environmental Studies 68: 593–601. <https://doi.org/10.1080/00207233.2011.617531>
- Graham MWR de V (1984) Madeira insects, mainly Hymenoptera Proctotrupeoidea, Ceraphonoidea, and Bethyloidea. Boletim do Museu Municipal do Funchal 36: 83–110.
- Guz N, Kocak E, Kilincer N (2013) Molecular phylogeny of *Trissolcus* species (Hymenoptera: Scelionidae). Biochemical Systematics and Ecology 48: 85–91. <https://doi.org/10.1016/j.bse.2012.12.010>
- Harris RA (1979) A Glossary of Surface Sculpturing. California Department of Food and Agriculture Division of Plant Industry Laboratory Services 28: 1–31.
- He J-H, Chen X-X, Fan J-J, Li Q, Liu C-M, Lou X-M, Ma Y, Wang S-F, Wu Y-R, Xu Z-H, Xu Z-F, Yao J (2004) [Hymenopteran Insect Fauna of Zhejiang.] Science Press, Beijing. 1373 pp.
- Isidoro N, Bin F, Colazza S, Vinson SD (1996) Morphology of antennal gustatory sensilla and glands in some parasitoids Hymenoptera with hypothesis on their role in sex and host recognition. Journal of Hymenoptera Research 5: 206–239.
- Javahery M (1968) The egg parasite complex of British Pentatomoidea (Hemiptera): taxonomy of Telenominae (Hymenoptera: Scelionidae). Transactions of the Royal Entomological Society of London 120: 417–436. <https://doi.org/10.1111/j.1365-2311.1968.tb00345.x>
- Johnson NF (1987) Systematics of New World *Trissolcus*, a genus of pentatomid egg-parasites (Hymenoptera: Scelionidae): Neotropical species of the *flavipes* group. Journal of Natural History 21: 285–304. <https://doi.org/10.1080/00222938700771021>

- Johnson NF (1992) Catalog of world Proctotrupeoidea excluding Platygasteridae. *Memoirs of the American Entomological Institute* 51: 1–825.
- Kaartinen R, Stone G, Hearn J, Lohse K, Roslin T (2010) Revealing secret liaisons: DNA barcoding changes our understanding of food webs. *Ecological Entomology* 35: 623–638. <https://doi.org/10.1111/j.1365-2311.2010.01224.x>
- Kerr PH, Fisher EM, Buffington ML (2008) Dome lighting for <https://doi.org/10.1093/ae/54.4.198> insect imaging under a microscope. *American Entomologist* 54: 198–200.
- Kieffer JJ (1909) Description de quelques nouveaux Scelionides d'Europe (Hym.). *Bulletin de la Société Entomologique de France* 15: 268–271. <https://doi.org/10.5962/bhl.part.13507>
- Kieffer JJ (1912) Proctotrypidae (3e partie). *Species des Hyménoptères d'Europe et d'Algérie*. 11: 1–160.
- Kieffer JJ (1926) Scelionidae. *Das Tierreich* (Vol. 48). Walter de Gruyter & Co., Berlin, 885 pp.
- Kimura M (1980) A simple method for estimating evolutionary rates of base substitutions through comparative studies of nucleotide sequences. *Journal of molecular evolution* 16(2): 111–120. <https://doi.org/10.1007/BF01731581>
- Koçak E, Kiliçer N (2000) Türkiye faydalı faunası için yeni kayıt *Trissolcus* (Hym.: Scelionidae) türleri. *Bitki Koruma Bülteni* 40: 169–177.
- Koçak E, Kiliçer N (2003) Taxonomic studies on *Trissolcus* sp. (Hymenoptera: Scelionidae), egg parasitoids of the sunn pest (Hemiptera: Scutelleridae: *Eurygaster* sp.), in Turkey. *Turkish Journal of Zoology* 27: 301–317.
- Koçak E, Kodan M (2006) *Trissolcus manteroi* (Kieffer, 1909) (Hymenoptera, Scelionidae): male nov. with new host from Turkey. *Journal of Pest Science* 79: 41–42. <https://doi.org/10.1007/s10340-005-0101-x>
- Kochetova NI (1966) [Development of *Asolcus semistriatus* Nees (Hymenoptera, Scelionidae) – egg parasite of the little tortoise bug and other Pentatomoidea (Hemiptera)]. *Zoologicheskii Zhurnal* 45: 558–567.
- Kononova SV (1995) [25. Fam. Scelionidae.]. In: Lehr PA (Ed.) *Key to Insects of Russian Far East in Six Volume* (Vol. 4). Neuropteroidea, Mecoptera, Hymenoptera. Part 2. Hymenoptera.]. *Dal'nauka, Vladivostok*, 57–121.
- Kononova SV (2014) Egg-parasitoids of the genus *Trissolcus* (Hymenoptera, Scelionidae, Telenominae) from the Palaearctic fauna (the *flavipes* morphological group). 1. New species of the genus *Trissolcus*. *Zoologicheskii Zhurnal* 93: 1420–1426. <https://doi.org/10.1134/S0013873814070112>
- Kononova SV (2015) Egg-parasitoids of the genus *Trissolcus* (Hymenoptera, Scelionidae, Telenominae) from the Palaearctic region. The *flavipes* morphological group: 2. A key to the species of the *flavipes* group. *Entomological Review* 95: 257–264. <https://doi.org/10.1134/S0013873815020086>
- Kozlov MA (1963) [New synonyms of species of the genus *Asolcus* Nak., *Gryon* Hal. and *Telenomus* Hal. (Hymenoptera, Scelionidae), egg parasites of *Eurygaster integriceps* Put.]. *Zoologicheskii Zhurnal* 63: 294–296.
- Kozlov MA (1968) Telenomines (Hymenoptera, Scelionidae, Telenominae) of the Caucasus – egg parasites of the sunn pest (*Eurygaster integriceps* Put.) and other grain bugs. *Trudy Vsesoyuznogo Entomologicheskogo Obshchestva* 52: 188–223.

- Kozlov MA (1978) [Superfamily Proctotrupeoidea]. In: Medvedev GS (Ed.) [Determination of Insects of the European Portion of the USSR.]. Nauka, Leningrad, 538–664.
- Kozlov MA (1981) The system and zoogeography of scelionids (Hymenoptera, Scelionidae). Entomologicheskoe Obozrenie 60: 174–182.
- Kozlov MA, Kononova SV (1983) [Telenominae of the Fauna of the USSR.]. Nauka, Leningrad.
- Kozlov MA, Lê XH (1977) Palearctic species of egg parasites of the genus *Trissolcus* Ashmead, 1893 (Hymenoptera, Scelionidae, Telenominae). Insects of Mongolia 5: 500–525.
- Kumar S, Stecher G, Li M, Knyaz C, Tamura K (2018) MEGA X: molecular evolutionary genetics analysis across computing platforms. Molecular biology and evolution 35(6): 1547–1549. <https://doi.org/10.1093/molbev/msy096>
- Masner L (1959) Some problems of the taxonomy of the subfamily Telenominae (Hym. Scelionidae). Transactions of the 1st International Conference on Insect Pathology and Biological Control, Prague 1958: 375–382.
- Masner L (1964) A comparison of some Nearctic and Palearctic genera of Proctotrupeoidea (Hymenoptera) with revisional notes. Casopis Československé Společnosti Entomologické 61: 123–155.
- Masner L (1980) Key to genera of Scelionidae of the Holarctic Region, with descriptions of new genera and species (Hymenoptera: Proctotrupeoidea). Memoirs of the Entomological Society of Canada 112: 1–54. <https://doi.org/10.4039/entm112113fv>
- Masner L, Muesebeck CFW (1968) The types of Proctotrupeoidea (Hymenoptera) in the United States National Museum. Bulletin of the United States National Museum 270: 1–143. <https://doi.org/10.5479/si.03629236.270>
- Mayr G (1879) Ueber die Schlupfwespengattung *Telenomus*. Verhandlungen der Zoologisch-Botanischen Gesellschaft in Wien 29: 697–714.
- Meier NF (1940) [Parasites reared in the USSR in 1938–1939 from eggs of the corn-bug (*Eurygaster integriceps* Osch.)]. Vestnik Zashchita Rastenii 3: 79–82.
- Meier NF (1949) [Toward knowledge of the species of egg-parasites of bugs found in recent years in the USSR.]. Trudy Vsesoyuznogo Instituta Zashchity Rastenii 2: 114–116.
- Mikó I, Masner L, Deans AR (2010) World revision of *Xenomerus* Walker (Hymenoptera: Platygastridae, Platygastridae). Zootaxa 2708: 1–73. <https://doi.org/10.11646/zootaxa.2708.1.1>
- Mikó I, Vilhelmsen L, Johnson NF, Masner L, Péntes Z (2007) Skeletomusculature of Scelionidae (Hymenoptera: Platygastridae): Head and mesosoma. Zootaxa 1571: 1–78. <https://doi.org/10.11646/zootaxa.1571.1.1>
- Nakagawa H (1900) [Illustrations of some Japanese Hymenoptera parasitic on insect eggs. I.]. Special Report of the Agricultural Experiment Station, Tokyo 6: 1–26.
- Nees von Esenbeck CG (1834) Hymenopterorum Ichneumonibus Affinium Monographiae, Genera Europaea et Species Illustrantes (Vol. 2). J. G. Cotta, Stuttgart, 448 pp. <https://doi.org/10.5962/bhl.title.26555>
- Nixon GEJ (1939) Parasites of hemipterous grain-pests in Europe (Hymenoptera: Proctotrupeoidea). Arbeiten über Morphologische und Taxonomische Entomologie aus Berlin-Dahlem 6: 129–136.

- Petrov S (2013) Three new species of *Trissolcus* Ashmead (Hymenoptera: Platygastridae: Scelionidae) from Bulgaria. *Biologia (Bratislava)* 68: 324–329. <https://doi.org/10.2478/s11756-013-0151-0>
- Ratzeburg JTC (1852) Die Ichneumoniden der Forstinsecten in Forstlicher und Entomologischer Beziehung (Vol. 3). Nicolaischen Buchhandlung, Berlin, 272 pp.
- Rjachovskij VV (1959) [Egg parasites of the sunn pest in the Ukrainian SSR.]. *Ukrainskii Nauchno-Issledovatel'skii Institut Zashchity Rastenii* 8: 76–88.
- Rondani C (1874) Nuove osservazioni sugli insetti fitofagi e sui loro parassiti. *Bullettino della Società Entomologica Italiana* 6: 130–136.
- Rondani C (1877) *Vesparia* parasita no vel minus cognita observata et descripta. *Bullettino della Società Entomologica Italiana* 9: 166–213.
- Ryu J, Hirashima Y (1984) Taxonomic studies on the genus *Trissolcus* Ashmead of Japan and Korea (Hymenoptera, Scelionidae). *Journal of the Faculty of Agriculture, Kyushu University* 29: 35–58.
- Saakov AI (1903) [The artificial breeding of egg parasites of the bread bug.]. *Trudy Byuro po Entomologii* 4: 1–12.
- Safavi M (1968) Etude biologique et ecologique des hymenopteres parasites des oeufs des punaises de cereales. *Entomophaga* 13: 381–495.
- Szabó JB (1976) Neue Daten zur Kenntnis der Gattung *Asolcus* Nakagawa, 1900 (Hymenoptera: Proctotrupoidea, Scelionidae). *Folia Entomologica Hungarica* 29: 175–191.
- Talamas EJ, Johnson NF, Buffington ML (2015) Key to Nearctic species of *Trissolcus* Ashmead (Hymenoptera, Scelionidae), natural enemies of native and invasive stink bugs (Hemiptera, Pentatomidae). *Journal of Hymenoptera Research* 43: 45–110. <https://doi.org/10.3897/JHR.43.8560>
- Talamas EJ, Buffington ML, Hoelmer K (2017) Revision of Palearctic *Trissolcus* Ashmead (Hymenoptera, Scelionidae). *Journal of Hymenoptera Research* 56: 3–185. <https://doi.org/10.3897/jhr.56.10158>
- Talamas EJ, Bon MC, Hoelmer KA, Buffington ML (2019) Molecular phylogeny of *Trissolcus* wasps (Hymenoptera: Scelionidae), natural enemies of stink bugs. In: Talamas E (Eds) *Advances in the Systematics of Platygastridae II*. *Journal of Hymenoptera Research* 73: 201–217. <https://doi.org/10.3897/jhr.73.39563>
- Thomson CG (1860) Sverges Proctotruper. Tribus IX. Telenomini. Tribus X. Dryinini. Öfversigt af Kongliga Vetenskaps-Akadamiens Förhandlingar 17: 169–181.
- Tortorici F, Caleca V, van Noort S, Masner L (2016) Revision of Afrotropical *Dyscritobaeus* Perkins, 1910 (Hymenoptera: Scelionidae). *Zootaxa* 4178: 1–59. <https://doi.org/10.11646/zootaxa.4178.1.1>
- Vaezi M (1950) Rapport du laboratoire d'élevage des parasites d'*Eurygaster integriceps* Put. *Entomologie et Phytopathologie Appliquées* 11: 27–41.
- Vassiliev JV (1913) [*Eurygaster integriceps* Put. and New Methods of Fighting it by the Aid of Parasites]. St. Petersburg, 81 pp.
- Viggiani G, Mineo G (1974) Identificazione dei parassitoidi del *Gonocerus acutepunctatus* (Goeze). *Bollettino dell'Istituto di Entomologia Agraria e dell'Osservatorio di Fitopatologia di Palermo* 8: 143–163.

- Viktorov GA (1964) [Food specialization of egg parasites of *Eurygaster integriceps* Put. and the role of this specialization for the diagnostics of species in the genus *Asolcus* Nakagawa (*Microphanurus* Kieffer) (Hymenoptera, Scelionidae).]. Zoologicheskii Zhurnal 43: 1011–1025.
- Viktorov GA (1967) [Problems in Insect Population Dynamics with Reference to the Sunn Pest.] Nauka, Moscow, 271 pp.
- Voegelé J (1962) Isolement d'une espece jumelle d'*Asolcus basalis* Wollaston (Hymenoptera, Proctotrupoidea). Al Awamia 4: 155–161.
- Voegelé J (1964) Contribution a la connaissance des stades larvaires des especes du genre *Asolcus* Nakagawa (*Microphanurus* Kieffer) (Hymenoptera, Proctotrupoidea). Al Awamia 10: 19–31.
- Voegelé J (1965) Nouvelle methode d'étude systematique des especes du genre *Asolcus*. Cas d'*Asolcus rungsi*. Al Awamia 14: 95–113.
- Voegelé J (1969) Les hymenopteres parasites oophages des *Aelia*. Al Awamia 31: 137–323.
- Walker F (1836) On the species of *Teleas*, &c. Entomological Magazine 3: 341–370.
- Walker F (1838) Descriptions of some Oxyuri. Entomological Magazine 5: 453–458.
- Watanabe C (1951) On five scelionid egg-parasites of some pentatomid and coreid bugs from Shikoku, Japan (Hymenoptera: Proctotrupoidea). Transactions of the Shikoku Entomological Society 2: 17–26.
- Watanabe C (1954) Discovery of four new species of Telenominae, egg parasites of pentatomid and plataspid bugs, in Shikoku, Japan. Transactions of the Shikoku Entomological Society 4: 17–22.
- Yoder MJ, Mikó I, Seltmann KC, Bertone MA, Deans AR (2010) A gross anatomy ontology for Hymenoptera. PLoS ONE 5(12). e15991. <https://doi.org/10.1371/journal.pone.0015991>
- Zomorodi A (1959) La lutte biologique contre la Punaise du blé *Eurygaster integriceps* Put. Part *Microphanurus semistriatus* Nees en Iran. Anzeiger Fur Schadlingskunde 3: 167–175.

Supplementary material I

URI table of HAO morphological terms

Authors: Francesco Tortorici, Elijah J. Talamas, Silvia T. Moraglio, Marco G. Pansa, Maryam Asadi-Farfar, Luciana Tavella, Virgilio Caleca

Data type: species data

Explanation note: This table lists the morphological terms used in this publication and their associated concepts in the Hymenoptera Anatomy Ontology.

Copyright notice: This dataset is made available under the Open Database License (<http://opendatacommons.org/licenses/odbl/1.0/>). The Open Database License (ODbL) is a license agreement intended to allow users to freely share, modify, and use this Dataset while maintaining this same freedom for others, provided that the original source and author(s) are credited.

Link: <https://doi.org/10.3897/jhr.73.39052.suppl1>

Supplementary material 2

Trissolcus belenus occurrence data

Authors: Francesco Tortorici, Elijah J. Talamas, Silvia T. Moraglio, Marco G. Pansa, Maryam Asadi-Farfar, Luciana Tavella, Virgilio Caleca

Data type: species data

Explanation note: This table provides a DarwinCore archive of occurrence records for *Trissolcus belenus*.

Copyright notice: This dataset is made available under the Open Database License (<http://opendatacommons.org/licenses/odbl/1.0/>). The Open Database License (ODbL) is a license agreement intended to allow users to freely share, modify, and use this Dataset while maintaining this same freedom for others, provided that the original source and author(s) are credited.

Link: <https://doi.org/10.3897/jhr.73.39052.suppl2>

Supplementary material 3

Trissolcus colemani occurrence data

Authors: Francesco Tortorici, Elijah J. Talamas, Silvia T. Moraglio, Marco G. Pansa, Maryam Asadi-Farfar, Luciana Tavella, Virgilio Caleca

Data type: species data

Explanation note: This table provides a DarwinCore archive of occurrence records for *Trissolcus colemani*.

Copyright notice: This dataset is made available under the Open Database License (<http://opendatacommons.org/licenses/odbl/1.0/>). The Open Database License (ODbL) is a license agreement intended to allow users to freely share, modify, and use this Dataset while maintaining this same freedom for others, provided that the original source and author(s) are credited.

Link: <https://doi.org/10.3897/jhr.73.39052.suppl3>

Supplementary material 4

Trissolcus manteroi occurrence data

Authors: Francesco Tortorici, Elijah J. Talamas, Silvia T. Moraglio, Marco G. Pansa, Maryam Asadi-Farfar, Luciana Tavella, Virgilio Caleca

Data type: species data

Explanation note: DarwinCore archive of occurrence records for *T. manteroi*.

Copyright notice: This dataset is made available under the Open Database License (<http://opendatacommons.org/licenses/odbl/1.0/>). The Open Database License (ODbL) is a license agreement intended to allow users to freely share, modify, and use this Dataset while maintaining this same freedom for others, provided that the original source and author(s) are credited.

Link: <https://doi.org/10.3897/jhr.73.39052.suppl4>

Supplementary material 5

Trissolcus semistriatus occurrence data

Authors: Francesco Tortorici, Elijah J. Talamas, Silvia T. Moraglio, Marco G. Pansa, Maryam Asadi-Farfar, Luciana Tavella, Virgilio Caleca

Data type: species data

Explanation note: DarwinCore archive of occurrence records for *Trissolcus semistriatus*.

Copyright notice: This dataset is made available under the Open Database License (<http://opendatacommons.org/licenses/odbl/1.0/>). The Open Database License (ODbL) is a license agreement intended to allow users to freely share, modify, and use this Dataset while maintaining this same freedom for others, provided that the original source and author(s) are credited.

Link: <https://doi.org/10.3897/jhr.73.39052.suppl5>

Supplementary material 6

Matrix of diagnostic characters

Authors: Francesco Tortorici, Elijah J. Talamas, Silvia T. Moraglio, Marco G. Pansa, Maryam Asadi-Farfar, Luciana Tavella, Virgilio Caleca

Data type: species data

Explanation note: This table provides a matrix of diagnostic characters to separate Palearctic species that are morphologically close to *Trissolcus semistriatus*.

Copyright notice: This dataset is made available under the Open Database License (<http://opendatacommons.org/licenses/odbl/1.0/>). The Open Database License (ODbL) is a license agreement intended to allow users to freely share, modify, and use this Dataset while maintaining this same freedom for others, provided that the original source and author(s) are credited.

Link: <https://doi.org/10.3897/jhr.73.39052.suppl6>

Molecular phylogeny of *Trissolcus* wasps (Hymenoptera, Scelionidae) associated with *Halyomorpha halys* (Hemiptera, Pentatomidae)

Elijah J. Talamas^{1,4}, Marie-Claude Bon², Kim A. Hoelmer³, Matthew L. Buffington⁴

1 Florida State Collection of Arthropods, Division of Plant Industry, Florida Department of Agriculture and Consumer Services, Gainesville, FL, USA **2** European Biological Control Laboratory, USDA/ARS, Montpellier, France **3** Beneficial Insects Introduction Research Unit, USDA/ARS, Newark, DE, USA **4** Systematic Entomology Laboratory, USDA/ARS c/o NMNH, Smithsonian Institution, Washington DC, USA

Corresponding author: *Elijah J. Talamas* (talamas.1@osu.edu)

Academic editor: *G. Broad* | Received 29 August 2019 | Accepted 1 November 2019 | Published 18 November 2019

<http://zoobank.org/>

Citation: Talamas EJ, Bon M-C, Hoelmer KA, Buffington ML (2019) Molecular phylogeny of *Trissolcus* wasps (Hymenoptera, Scelionidae) associated with *Halyomorpha halys* (Hemiptera, Pentatomidae). In: Talamas E (Eds) Advances in the Systematics of Platygastroidea II. Journal of Hymenoptera Research 73: 201–217. <https://doi.org/10.3897/jhr.73.39563>

Abstract

As the brown marmorated stink bug (*Halyomorpha halys*) has spread across the Northern Hemisphere, research on its egg parasitoids has increased accordingly. These studies have included species-level taxonomy, experimental assessments of host ranges in quarantine, and surveys to assess parasitism in the field. We here present a molecular phylogeny of *Trissolcus* that includes all species that have been reared from live *H. halys* eggs. Species-group concepts are discussed and revised in the light of the phylogenetic analyses. The analyses indicate that the ability to successfully parasitize *H. halys* eggs is not phylogenetically constrained, but the most effective parasitoids are all found in the *flavipes* species group.

Keywords

egg parasitoid, biological control, Pentatomoidea

Introduction

Research on the systematics of *Trissolcus* Ashmead (Hymenoptera: Scelionidae) has recently experienced a resurgence, driven primarily by the search for biological control agents of invasive pests. The first of these is the economically destructive brown marmorated stink bug (BMSB), *Halyomorpha halys* (Stål) (Heteroptera: Pentatomidae), a native of northeastern Asia that first appeared in the eastern USA in the 1990s (Leskey and Nielsen 2017). The invasion of the southeastern USA by another Asian species, the bean plataspid (or kudzu bug), *Megacopta cribraria* (F.) (Heteroptera: Plataspidae), a serious pest of soybeans, soon followed (Eger et al. 2010). In 2008, the bagrada bug, *Bagrada hilaris* (Burmeister) (Heteroptera: Pentatomidae), an Old-World pest of cruciferous crops, was discovered in the southwestern USA (Palumbo and Natwick 2010). The distribution of these pests has since expanded into Europe and South America (Faúndez et al. 2016, Faúndez and Rider 2017, Kriticos et al. 2017). In each newly invaded region, these bugs have encountered resident parasitoids to which they had not previously been exposed, including species of *Trissolcus*. A sound taxonomy has been critical to assess parasitism by parasitoids in the invaded range, identify the parasitoids that coevolved with these pentatomoids in their native range, and to accurately identify them when they appear adventively in new regions, often unexpectedly, which has happened with parasitoids of all three bugs (Gardner et al. 2013, Talamas et al. 2015b, Ganjisaffer et al. 2018).

This phylogenetic analysis follows a period of intensive taxonomic revision for *Trissolcus*. Talamas et al. (2015a), following the research by Johnson (1984a, 1985a–b), updated the identification tools for species of *Trissolcus* in the Nearctic region. Talamas et al. (2017) and Tortorici et al. (2019) clarified species limits across Europe, Asia, North Africa, and the Middle East. Host data has been reviewed, updated and significantly expanded, making management decisions regarding natural enemy recruitment and rearing more efficient and accurate, much of which is summarized by Buffington et al. (2018). Our effort to understand natural enemies of *H. halys* here analyzes the phylogenetic relationships among species of *Trissolcus* in the native and invaded ranges of *H. halys* to facilitate molecular diagnostics, redefine species groups, and assess the relationship between phylogenetic affinity and the ability of *Trissolcus* species to successfully parasitize *H. halys* eggs.

Phylogenetics and biological control

Classical biological control requires parasitoids to efficiently locate their hosts and exhibit a host range that is narrow enough to eliminate or reduce the chances of unwanted non-target effects. Phylogenies can reveal the mechanisms that contribute to these traits by determining if they are phylogenetically constrained or are highly variable within the genus. The primary candidate as a biological control agent for

H. halys is *Trissolcus japonicus* (Ashmead), a species for which adventive populations are now in USA, Canada, Switzerland, and Italy (Talamas et al. 2015a, Abram et al. 2019, Stahl et al. 2018, Sabbatini-Peverieri et al. 2018). However, it is not the only species of *Trissolcus* that can parasitize *H. halys*, and there are many species that attempt to parasitize of *H. halys* eggs with limited or no success. Our analysis examines how these traits of host acceptance and host competence are distributed within *Trissolcus*. Taxon sampling, while focused on species associated with *H. halys*, includes additional representatives for the *basalis*, *flavipes*, and *thyantae* species groups from the Holarctic. We consider this phylogeny to provide a backbone for future molecular studies on *Trissolcus* wasps that will undoubtedly occur as interest in the group continues to grow and specimens from a broader geographic sampling become available.

A history of phylogenetics in *Trissolcus*

The present study is not the first phylogenetic effort for *Trissolcus*. Johnson (1987) provided a phylogenetic hypothesis for *Trissolcus* species which was cladistic in its argumentation, but not computationally optimized (i.e. characters were optimized on a tree, but tree space was not searched). The result was a partially resolved phylogeny and only concerned Nearctic species. Later, Johnson (1991) improved the resolution of *Trissolcus* by employing a character matrix and analysis in PAUP. However, computer limitations prevented a complete data matrix, as a great deal of homoplasy occupied the tree memory storage of PAUP at that time. As a result, Johnson (1991) reduced the size of the matrix and relied on ground-plan coding for some taxa; the resulting data matrix recovered a single tree.

The first molecular sequence data for *Trissolcus* were provided by Murphy et al. (2007), who investigated higher level relationships in Platygastroidea using three gene fragments. The results of that study confirmed the placement of *Trissolcus* in Telenominae with very high bootstrap support. Guz et al. (2013) were the first to investigate the relationships within *Trissolcus* using molecular data. Here the focus was on *Trissolcus* species that were natural enemies of the sunn pest (*Eurygaster integriceps* Puton (Hemiptera: Scutelleridae) of wheat and barley. While the study has limited utility with respect to relationships within the genus, Guz et al. (2013) demonstrated the usefulness of the COI marker for species-level questions, and reported that due to insertions, ITS2 was difficult to align, and that 28S, 18S, and 5.8S were too conserved to be informative.

Taekul et al. (2014) included 12 species of *Trissolcus* in an analysis that redefined the limits of Telenominae. Their phylogeny was based on four molecular markers (18S, 28S, COI and Ef-1 α) and focused on shifts in host selection in Telenominae, *Gryon* Haliday, and the *Psix*-cluster of genera. Importantly, it demonstrated the utility of 18S and 28S sequence data for phylogenetic analysis of *Trissolcus* and its relatives.

Materials and methods

Taxonomy and specimen data

Species determinations were made with the identification tools provided in Talamas et al. (2015a), Talamas et al. (2017), and Tortorici et al. (2019). The data associated with these specimens, including host associations, are deposited in Hymenoptera Online (hol.osu.edu) and can be accessed via the Collectin Unit Identifiers listed in Suppl. material 1. Voucher specimens from this study are deposited in the National Museum of Natural History (Washington, DC) and the Florida State Collection of Arthropods (Gainesville, FL).

DNA extraction

Most specimens were collected alive and fixed in 95% or absolute ethanol and some were gleaned from material stored in ethanol in entomological collections. These specimens were used for nondestructive DNA extraction using the Qiagen DNeasy kit (Hilden, Germany) following the protocol published in Taekul et al. (2014), but with minor modifications specified in Sabbatini Peverieri et al. (2018). Individual specimens were bathed three times at room temperature in molecular grade water for five minutes prior to overnight incubation in lysis buffer at 55 °C. In step 7 of the Qiagen protocol, the elution buffer was warmed to 55 °C and allowed to rest on the membrane for 15 minutes before centrifugation. The collected flow-through was reloaded onto the spin column to increase the DNA yield. When we started this study, the nondestructive method was not employed, and therefore, some specimens were entirely ground using the Qiagen DNeasy kit (Hilden, Germany) following the manufacturer's recommendations. These specimens thus have no corresponding voucher specimen. A negative control (no insect tissue) was included in each extraction to detect potential contamination. The genomic DNA was stored at -24 °C for further use. All voucher specimens are deposited in the Florida State Collection of Arthropods (Gainesville, FL), and the National Insect Collection, National Museum of Natural History (Washington DC, USA).

Five molecular markers were sequenced. These included the mitochondrial 5' end of the cytochrome *c* oxidase subunit I gene (*COI*) also named the barcode region (~660bp), the nuclear ribosomal gene 18S rRNA (variable region V3-V5, ~780bp), the 28S rRNA (D2-D3 expansion regions, ~800bp), the internal transcribed spacer 2 (ITS2), (~550bp to 650bp), and the nuclear gene *Wingless* (exon, ~450bp). The choice of these markers was partly guided as a compromise between “top down” and “bottom up” approaches (Wiens et al. 2005). We apply the bottom up approach to resolve higher level relationships (the bottom of the tree) using relatively slowly evolving markers (18S rRNA, 28S rRNA, *Wingless*) and then apply the top down approach to resolve species level relationships (the top of the tree) using faster evolving markers (*COI*, ITS2). Primers and PCR conditions used in this study are described in Tables 1, 2, respectively. All PCRs were performed in a 30 µl total volume with 2 µl of DNA template, 0.2 mM of each dNTP, 0.3 µM

Table 1. List of primers used in this study.

Primer	Apis position	Sequence (5'-3')	Source
18SrRNA			
18S-H17F	430-449	AAATTACCCACTCCCGCA	Heraty et al. (2004)
18S-H35R	1251-1233	TGGTGAGGTTTCCCGTGT	
28S rRNA	–		
28S-D23F		GAGAGTTCAAGAGTACGTG	Park and O' Foighil (2000)
28S-Sb		TCGGAAGGAACCAGCTACTA	
Wg	–		Huayan 2018
ScWgIF-1		GTAAGTGTACGGGATGTC	
ScWgIR-1		TTGACTTCACAGCACCAGT	
ITS2	-		Germain et al. (2013)
Forward		TGTAAAACGACGGCCAGTTCGATGAAGAACGCAGCDAHTG	
5.8S_cbgp_F1_t1		TGTAAAACGACGGCCAGTTCGATGAAGAMCGCAGYTAAGT	
5.8S_cbgp_F2_t1		TGTAAAACGACGGCCAGTTCGATGAAAGACGCAGCAAAATG	
5.8S_cbgp_F3_t1			
Reverse		CAGGAAACAGCTATGACGATATGYTTAAATTCRSGGGT	
<i>COI</i>			
LCO1490	1810–1834	GGTCAACAAATCATAAAGATATTGG	Folmer et al. (1994)
HCO2198	2493–2518	TAAACTTCAGGGTGACCAAAAAATCA	Cruaud et al. (2010)
LCO1490puc	1810–1834	TTTCAACWAATCATAAAGATATTGG	
HCO2198puc	2493–2518	TAAACTTCWGGRTGWCCAAARAATCA	

Table 2. PCR conditions used in this study.

Primers (F)	Primers (R)	PCR conditions	No of cycles
18SH-17F	18SH-35R	94 °C/3 min; 94 °C/30s; 48 °C/45s; 72 °C/1 min	5
		94 °C/3 min; 94 °C/30s; 50 °C/45s; 72 °C/1 min; 72 °C/10 min	35
28S-D23F	28S-Sb	94 °C/3 min; 94 °C/30s; 55 °C/45s; 72 °C/1 min	5
		94 °C/3 min; 94 °C/30s; 57 °C/45s; 72 °C/1 min; 72 °C/10 min	35
ScWgIF-1	ScWgIR-1	94 °C/3 min; 94 °C/30s; 48 °C/45s; 72 °C/1 min	5
		94 °C/3 min; 94 °C/30s; 50 °C/45s; 72 °C/1 min; 72 °C/10 min	35
5.8S_cbgp_F1_t1	28S_cbgp_R1_t1	94 °C/3 min; 94 °C/30s; 45 °C/1 min; 72 °C/1 min 30 s	5
5.8S_cbgp_F2_t1		94 °C/3 min; 94 °C/30s; 55 °C/1min 30 s; 72 °C/1 min 30 s; 72 °C/10 min	35
5.8S_cbgp_F3_t1			
LCO1490	HCO2198	94 °C/3 min; 94 °C/30s; 48 °C/1 min; 72 °C/1 min	5
		94 °C/3 min; 94 °C/30s; 52 °C/1 min; 72 °C/1 min; 72 °C/10 min	35
LCO1490-puc	HCO2198-puc	94 °C/3 min; 94 °C/30s; 48 °C/1 min; 72 °C/1 min	5
		94 °C/3 min; 94 °C/30s; 52 °C/1 min; 72 °C/1 min; 72 °C/10 min	35

of each primer, 1× CoralLoad PCR Buffer (including 1.5mM of MgCl₂) and 1 Unit of *Taq* DNA Polymerase (Qiagen). PCR amplifications were run on a 9700 thermocycler (Applied Biosystem). The PCR products were purified and sequenced in both directions using the same sets of PCR primers, by Genoscreen, Lille, France, whereas others were cloned prior to sequencing (especially ITS2). Both strands for each overlapping fragment were assembled using the sequence editing software Bioedit, version 7 (Hall 1999). All sequences have been deposited in GenBank and accession numbers are provided in Suppl. material 1. All residual DNAs are archived (-24 °C) at the European Biological Control Laboratory (EBCL, USDA/ARS), Montpellier, France.

Sequence alignment

The protein coding genes *CO1* and *Wingless* were aligned using ClustalW with default gap opening, extension, and substitution costs as implemented in Mega 6 (Tamura et al. 2013). These sequences were checked for stop codons and frame shifts, and sequences were translated to amino acids using the invertebrate mitochondrial code and the standard code respectively as implemented in MEGA 6 (Tamura et al. 2013). Secondary structural alignments were implemented for ribosomal RNA sequences of 18S, 28S and ITS2. The ClustalW alignment conventions followed Kjer (1995) with slight modifications (Gillespie 2004). Ambiguous regions in ITS2 were excluded from the final analyses using GBlock as implemented in PhyML 3.0 (Guindon et al. 2010). The aligned, partitioned sequence data is provided in Suppl. material 2.

Phylogenetic reconstruction

Bayesian inference. The resulting concatenated matrix was exported from Mesquite for Mr. Bayes 3.2 applying the GTR+I+G rate matrix for each data partition (COI divided into three partitions, one for each position) and running 15 million generations with a burn-in of 25%; explanation and justification of these protocols are in Buffington et al. (2007).

Parsimony. The parsimony searches were conducted using PAUP* (Swofford 2002), employing an initial 10000 replicate searches of TBR under equal weights with branches of maximum length zero collapsed and steepest descent set to 'off'. For bootstrap analyses (Felsenstein 1985), a simple addition sequence was employed with *Telenomus* (*Te. californicus* complex sensu Johnson (1984b)) set as the reference taxon, followed by 1000 bootstrap replicates, with each employing 100 TBR swapping replications. As many equally parsimonious trees were found in the initial tree search, successive approximations (Farris 1969) were used to converge on a topology favored by the characters with the best tree score. A separate analysis was run in TNT (Goloboff et al. 2008) employing sectorial searches, parsimony ratchet, and tree fusing.

Maximum likelihood. These analyses were run using RAxML version 8.2.10. The model used was GTRGAMMA+I. Automatic bootstopping criterion was selected as the appropriate number of bootstraps; 300 replicates were run. Six partitions were identified using PartitionFinder 2. The proportion of gaps/undetermined sites in the alignment was 11.47%. All resulting trees were visualized in FigTree 1.3.1, and the out-group (*Telenomus*) was assigned; the final tree figure was generated using Adobe Illustrator. The commands used to perform each analysis are listed in Suppl. material 3.

Results

The topologies of the three phylogenetic analyses are largely congruent and the morphology-based delimitations of species were highly supported (>99 bootstrap support,

100% posterior probability), indicating that the molecular markers are well suited to resolve intraspecific relationships in *Trissolcus*. The topology of the strict consensus tree from TNT (not figured) was congruent with, and nearly identical to that in PAUP*: *T. saakowi*, *T. tumidus* and (*T. euschisti*+*T. edessae*) formed a polytomy and PAUP* retrieved *T. saakowi* and *T. tumidus* as sister species.

Species groups

flavipes group

The *flavipes* group sensu Talamas et al. (2017) was retrieved as a monophyletic clade in the parsimony analysis, but with *T. mitsukurii*, *T. latisulcus*, and *T. thyantae* included (Figure 3). The Bayesian and ML analyses both retrieved the *flavipes* group as two separate clades in a polytomy with the *basalis* group (Figs 1–2), with *T. mitsukurii* sister to a *flavipes* clade comprised of primarily Asian species. Talamas et al. (2017) treated *T. mitsukurii* and *T. latisulcus* as part of the *basalis* group based on the number of clypeal setae (6), absence of a hyperoccipital carina on the medial vertex, and glabrous metapleuron. However, each of the analyses indicate that *T. mitsukurii* is better accommodated in the *flavipes* group. A morphological character supports this new hypothesis: in *T. mitsukurii* the orbital furrow is expanded at its intersection with the malar sulcus, which is found only in the *flavipes* group, at least among the species in this phylogeny.

We thus retain much of the previous concept of the *flavipes* group, but the inclusion of *T. mitsukurii* means that the number of clypeal setae can be 2, 4, or 6. The number of clypeal setae remains a useful character because having 4 or fewer clypeal setae is limited to this group. We therefore redefine the *flavipes* group based on the following characters: clypeus with 2–6 clypeal setae; hyperoccipital carina usually complete, sometimes weakened or absent between lateral ocelli; orbital furrow often expanded at intersection with malar sulcus; metapleuron glabrous. This approach ignores the ambiguity of the polytomy in the Bayesian and ML analyses, and the presence of *T. latisulcus* and *T. thyantae* retrieved within the *flavipes* group by the parsimony analysis. Because the results do not fully agree, we prefer an approach that minimizes changes to the infrageneric organization until consensus and better supported resolution is achieved through increased sampling of species and molecular markers. To further examine the degree of homoplasy in morphological characters and their utility for delimiting species groups, we recommend that future efforts include species that do not fit into the current species groups (e.g. *T. atys* (Nixon), *T. tersus* Lê, *T. levicaudus* Talamas) and species from Asia and Africa that are morphologically similar to *T. mitsukurii*, of which there are many.

thyantae group

The *thyantae* group was represented by a single species, *T. thyantae*. The Bayesian and RaxML analyses retrieved it as the most basal lineage of *Trissolcus* (Figs 1–2), whereas

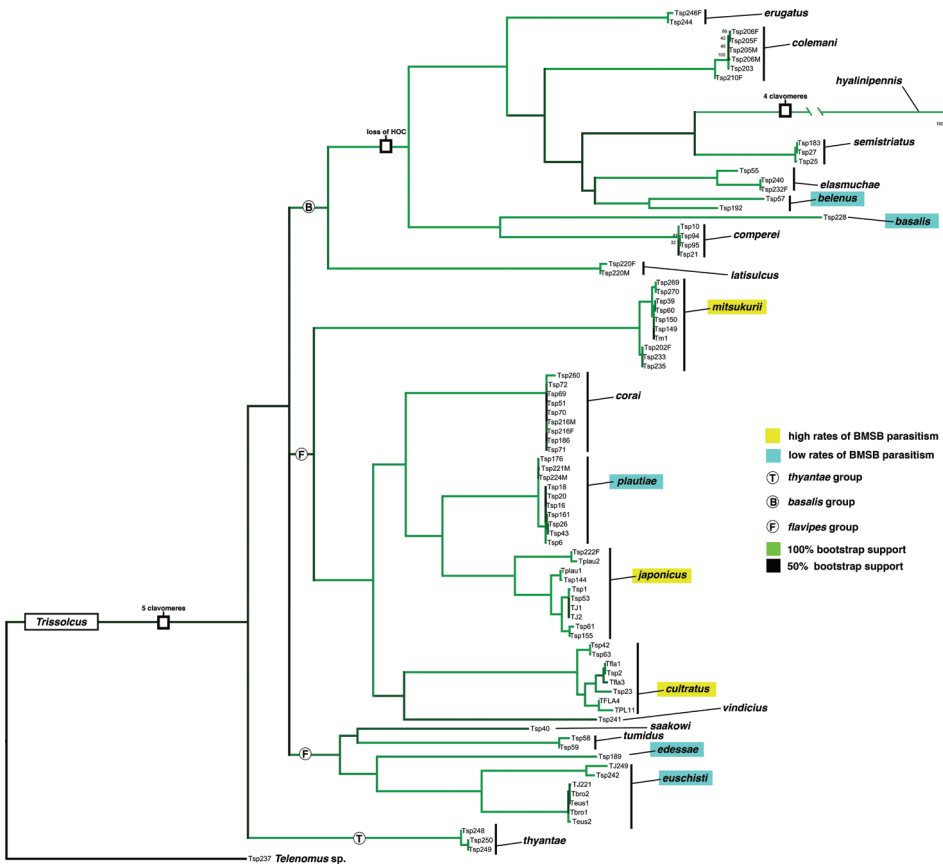


Figure 1. Phylogenetic tree, RaxML analysis.

the parsimony analysis placed it within the *flavipes* group as sister to *T. latusulcus* (Figure 3). However, *Trissolcus thyantae* and *T. latusulcus* are not morphologically similar to each other or to other species in the *flavipes* group. Increased taxon sampling is needed to address the ambiguity in the placement of the *thyantae* group and assess relationships between the morphologically similar species that constitute it.

basalis group

The *basalis* group remains largely unchanged regarding its constituent species and the characters that delimit it: clypeus with 6 or more setae; hyperoccipital carina absent between lateral ocelli; metapleuron glabrous; orbital furrow not expanded near intersection with malar sulcus. In both the Bayesian and RaxML analyses, *Trissolcus latusulcus* and *T. erugatus* were retrieved as a paraphyletic group sister to the other members of the *basalis* group (Figures 1–2). Excluding the aberrant placement of *T. latusulcus* in the parsimony analysis, the *basalis* group was consistently retrieved as monophyletic, but with varying topologies among its species.

The *T. semistriatus* complex

Numerous species were treated by Talamas et al. (2017) as junior synonyms of *T. semistriatus* (Nees von Esenbeck). Tortorici et al. (2019) reexamined characters previously treated as variable within *T. semistriatus* and further updated the classification of Palearctic *Trissolcus*, resurrecting *T. colemani* (Crawford) and *T. manteroi* (Kieffer) as valid species and establishing name usage for *T. belenus* (Walker). Although *T. belenus* was described in 1836, this species name was largely ignored in literature on Palearctic *Trissolcus* because it had not been reliably characterized. Tortorici et al. (2019) examined the lectotype of this species, established a means of separating it from other members of the *T. semistriatus* complex and provided records of it parasitizing *H. halys* eggs in Europe. Although our analysis did not include *T. manteroi*, it confirms the conclusion of Tortorici et al. (2019) that *T. belenus*, *T. colemani*, and *T. semistriatus* are distinct species.

Parasitism of *Halyomorpha halys*

The ability to develop in *H. halys* eggs is not constrained phylogenetically, but the species with high rates of successful parasitism are all found in the *flavipes* group (*T. mitsukurii* now included). The closest relative of *T. japonicus* in our analysis, *T. plautiae* (Watanabe), has been reared from *H. halys* eggs in Asia, but accounted for only 2% of parasitism in a study by Zhang et al. (2017). *Trissolcus cultratus* (Mayr) and *T. mitsukurii* have appreciable rates of parasitism on *H. halys* eggs (Zhang et al. 2017; Sabbatini-Peverieri et al. 2018), leading to host range testing for these species. *Trissolcus euschisti* (Ashmead) and *T. edessae* Fouts (*flavipes* group) have been reared from *H. halys* eggs in North America, but at very low rates if the eggs are viable, indicating that they recognize *H. halys* as a potential host but are largely unable to complete development (Abram et al. 2017). Outside of the *flavipes* group, *T. basalis* (Wollaston) and *T. solocis* Johnson (*basalis* group) have been reared from live, sentinel *H. halys* eggs (Balusu et al. 2019a, Balusu et al. 2019b), but these records are considered to be rare events.

A phenomenon that deserves future attention is the geographic division in the ability of *Trissolcus cultratus* to successfully develop in live *H. halys* eggs. Our analysis retrieved a European specimen of *T. cultratus* (TFLA4) nested well within a clade of Asian specimens, supporting the conclusion that this is a single widespread species. However, European populations of *T. cultratus* fully develop and emerge from *H. halys* eggs only if they were previously frozen or had defenses compromised by parasitism from another species (Haye et al. 2015, Konopka et al. 2016). Given the rate at which adventive populations of Asian parasitoids follow the movement of *H. halys*, it is likely that an Asian population of *T. cultratus* will eventually appear in Europe. If this occurs, identification of the exotic population will require molecular diagnostics because they

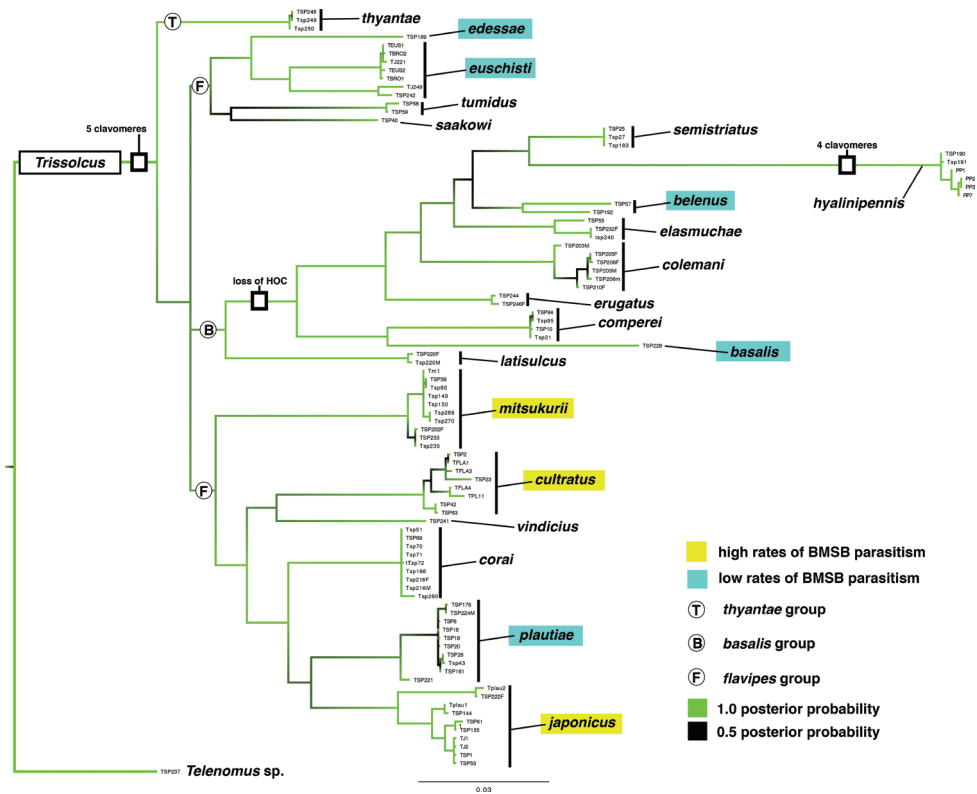


Figure 2. Phylogenetic tree, Bayesian analysis.

cannot be differentiated based on external morphology. In any biocontrol project such as this one, molecular characterizations of different populations should be done as soon as possible before population mixing has a chance to occur.

Molecular diagnostics

In recent years, DNA barcode sequences have increasingly been used to confirm morphology-based identification of *Trissolcus* species (Ganjisaffar et al. 2018, Balusu et al. 2019b, Talamas et al. 2015b, Abram et al. 2019, Stahl et al. 2018, Sabbatini Peverieri et al. 2018). In some cases, this is primarily a supplement to morphological diagnosis, and in others it is an invaluable means of confirmation. For example, in Ganjisaffar et al. (2018) the initial detection of *Trissolcus hyalinipennis* Rajmohana & Narendran in California was based on single male specimen that lacked some of the diagnostic female characters, and specimens of *Trissolcus basalis* had reduced morphology because of the diminutive size the bagrada bug eggs from which they emerged. For both species, the use of DNA barcoding provided an additional level of confidence in their identification. More recently, Garipey et al. (2018) published a method that enables identification of

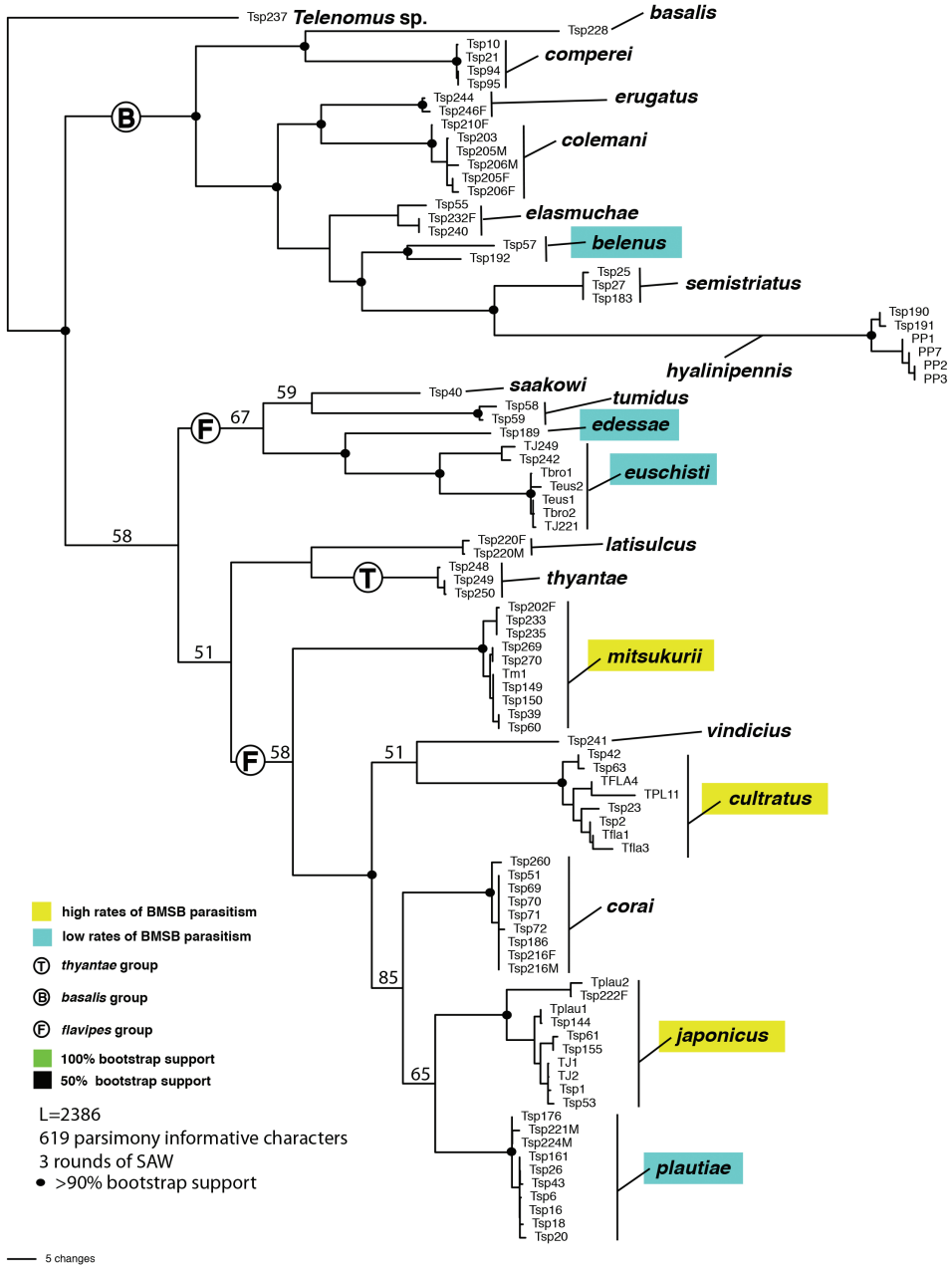


Figure 3. Phylogenetic tree, PAUP* analysis.

parasitoids via residual DNA in empty, parasitized eggs. This method has since been used to detect the first population of *Trissolcus japonicus* in eastern Canada (Garipey and Talamas 2019) and confirm that a species of *Idris* Förster (Scelionidae) parasitized bagrada

bug eggs, the first non-spider host for the genus (Lomeli-Flores et al. 2019). Each of these examples relied on a pre-existing library of CO1 sequences that were reliably matched to species names. In this study, we provide CO1 sequences for 20 species of *Trissolcus*. The names associated with these sequences are provided with the highest level of confidence possible, given that the specimens were identified in the context of the most recent and thorough taxonomic treatments and with direct comparison to primary types.

Acknowledgements

We are grateful to Fatiha Guermache (EBCL) for her valuable assistance during molecular work and to Zachary Lahey (The Ohio State University) for performing the Maximum Likelihood analysis on an analysis server. This project was funded in part by two USDA Farm Bills: Biological Control of Bagrada Bug and Monitoring, and Identification, monitoring, and redistribution of *Trissolcus japonicus* – Biological Control of Brown Marmorated Stink Bug (BMSB); a cooperative agreement between Kim Hoelmer (USDA/BIIRU) and Elijah Talamas (FDACS/DPI); and funding from USDA NIFA SCRI grants: 2011-51181-30937 and 2016-51181-25409. Elijah Talamas was supported by the Florida Department of Agriculture and Consumer Services-Division of Plant Industry. The USDA does not endorse any commercial product mentioned in this research. USDA is an equal opportunity provider and employer.

References

- Abram PK, Hoelmer KA, Acebes-Doria A, Andrews H, Beers EH, Bergh JC, Bessin R, Biddinger D, Botch P, Buffington ML, Cornelius ML, Costi E, Delfosse ES, Dieckhoff C, Dobson D, Donais D, Grieshop M, Hamilton G, Haye T, Hedstrom C, Herlihy MV, Hoddle MS, Hooks CRR, Jentsch P, Joshi NK, Kuhar TP, Lara J, Lee JC, Legrand A, Leskey TC, Lowenstein D, Maistrello L, Mathews CR, Milnes JM, Morrison III WR, Nielsen AN, Ogburn EC, Pickett CH, Poley K, Pote J, Radl J, Shrewsbury PM, Talamas EJ, Tavella L, Walgenbach JF, Waterworth R, Weber DC, Welty C, Wiman NG (2017) Indigenous arthropod natural enemies of the invasive brown marmorated stink bug in North America and Europe. *Journal of Pest Science* 90: 1009–1020. <https://doi.org/10.1007/s10340-017-0891-7>
- Abram PK, Talamas EJ, Acheampong S, Mason PG, Garipey TD (2019) First detection of the samurai wasp, *Trissolcus japonicus* (Ashmead) (Hymenoptera, Scelionidae), in Canada. *Journal of Hymenoptera Research* 68: 29–36. <https://doi.org/10.3897/jhr.68.32203>
- Balusu R, Cottrell T, Talamas E, Toews M, Blaauw B, Sial A, Buntin D, Vinson E, Fadamiro H, Tillman G (2019a) New record of *Trissolcus solocis* (Hymenoptera: Scelionidae) parasitising *Halyomorpha halys* (Hemiptera: Pentatomidae) in the United States of America. *Biodiversity Data Journal* 7: e30124. <https://doi.org/10.3897/BDJ.7.e30124>
- Balusu R, Talamas E, Cottrell T, Toews M, Blaauw B, Sial A, Buntin D, Fadamiro H, Tillman G (2019b) First record of *Trissolcus basalis* (Hymenoptera: Scelionidae) parasitizing *Halyo-*

- morpha halys* (Hemiptera: Pentatomidae) in the United States. Biodiversity Data Journal 7: 1–9. <https://doi.org/10.3897/BDJ.7.e39247>
- Buffington ML, Talamas EJ, Hoelmer KA (2018) Team *Trissolcus* : Integrating Taxonomy and Biological Control to Combat the Brown Marmorated Stink Bug. American Entomologist 64: 224–232. <https://doi.org/10.1093/ae/tmy057>
- Cruaud A, Jabbour-Zahab R, Genson G, Cruaud C, Couloux A, Kjellberg F, van Noort S, Rasplus JY (2009) Laying the foundations for a new classification of Agaonidae (Hymenoptera: Chalcidoidea), a multilocus phylogenetic approach. Cladistics 25: 1–29. <https://doi.org/10.1111/j.1096-0031.2009.00291.x>
- Eger Jr JE, Ames LM, Suiter DR, Jenkins TM, Rider DA, Halbert SE (2010) Occurrence of the Old World bug *Megacopta cribraria* (Fabricius) (Heteroptera: Plataspidae) in Georgia: A serious home invader and potential legume pest. Insecta Mundi 0121: 1–11.
- Faúndez EI, Lüer A, Cuevas AG, Rider DA, Valdebenito P (2016) First record of the painted bug *Bagrada hilaris* (Burmeister) (Heteroptera: Pentatomidae) in South America. Arquivos Entomológicos 16: 175–179.
- Faúndez EI, Rider DA (2017) The brown marmorated stink bug *Halyomorpha halys* (Stål 1885) (Heteroptera: Pentatomidae) in Chile. Arquivos Entomol 17: 305–330.
- Folmer O, Black M, Hoeh W, Lutz R, Vrijenhoek R (1994) DNA primers for amplification of mitochondrial cytochrome c oxidase subunit I from diverse metazoan invertebrates. Molecular Marine Biology and Biotechnology 3: 294–299.
- Ganjisaffar F, Talamas E, Bon M-C, Brown B, Gonzalez L, Perring T (2018) *Trissolcus hyalinipennis* Rajmohana & Narendran (Hymenoptera: Scelionidae), a parasitoid of *Bagrada hilaris* (Burmeister) (Hemiptera: Pentatomidae), emerges in North America. Journal of Hymenoptera Research 65: 111–130. <https://doi.org/10.3897/jhr.65.25620>
- Gardner WA, Blount JL, Golec JR, Jones WA, Hu XP, Talamas EJ, Evans RM, Dong X, Ray Jr CH, Buntin GD, Gerardo NM, Couret J (2013) Discovery of *Parateleonomus saccharalis* (Dodd) (Hymenoptera: Platygasteridae), an egg parasitoid of *Megacopta cribraria* F. (Hemiptera: Plataspidae) in its expanded North American range. Journal of Entomological Science 48: 355–359. <https://doi.org/10.18474/0749-8004-48.4.355>
- Garipey TD, Bruin A, Konopka J, Scott-Dupree C, Fraser H, Bon M-C, Talamas EJ (2019) A modified DNA barcode approach to define trophic interactions between native and exotic pentatomids and their parasitoids. Molecular Ecology 28: 456–470. <https://doi.org/10.1111/mec.14868>
- Garipey T, Talamas EJ (2019) Discovery of the samurai wasp, *Trissolcus japonicus*, in Ontario. The Canadian Entomologist 1–3. <https://doi.org/10.4039/tce.2019.58>
- Germain JF, Chatot C, Meusnier I, Artige E, Rasplus JY, Cruaud A (2013) Molecular identification of *Epitrix* potato flea beetles (Coleoptera: Chrysomelidae) in Europe and North America. Bulletin of Entomological Research 103: 354–362. <https://doi.org/10.1017/S000748531200079X>
- Gillespie JJ (2004) Characterizing regions of ambiguous alignment caused by the expansion and contraction of hairpin-stem loops in ribosomal RNA molecules. Molecular Phylogenetics and Evolution 33: 936–943. <https://doi.org/10.1016/j.ympev.2004.08.004>
- Goloboff PA, Farris JS, Nixon KC (2008) TNT, a free program for phylogenetic analysis. Cladistics 24: 774–783. <https://doi.org/10.1111/j.1096-0031.2008.00217.x>

- Guindon S, Dufayard JF, Lefort V, Anisimova M, Hordijk W, Gascuel O (2010) New Algorithms and Methods to Estimate Maximum-Likelihood Phylogenies: Assessing the Performance of PhyML 3.0. *Systematic Biology* 59: 307–321. <https://doi.org/10.1093/sysbio/syq010>
- Guz N, Kocak E, Kilincer N (2013) Molecular phylogeny of *Trissolcus* species (Hymenoptera: Scelionidae). *Biochemical Systematics and Ecology* 48: 85–91. <https://doi.org/10.1016/j.bse.2012.12.010>
- Hall TA (1999) BioEdit: A User-Friendly Biological Sequence Alignment Editor and Analysis Program for Windows 95/98/NT. *Nucleic Acids Symposium Series* 41: 95–98.
- Haye T, Fischer S, Zhang J, Garipey RD (2015a) Can native egg parasitoids adopt the invasive brown marmorated stink bug, *Halyomorpha halys* (Heteroptera: Pentatomidae), in Europe? *Journal of Pest Science* 88: 693–705. <https://doi.org/10.1007/s10340-015-0671-1>
- Heraty J, Hawks D, KostECKI JS, Carmichael A (2004) Phylogeny and behaviour of the Gollumiellinae, a new subfamily of the ant-parasitic Eucharitidae (Hymenoptera: Chalcidoidea). *Systematic Entomology* 29: 544–559. <https://doi.org/10.1111/j.0307-6970.2004.00267.x>
- Johnson NF (1984a) Revision of the Nearctic species of the *Trissolcus flavipes* group (Hymenoptera: Scelionidae). *Proceedings of the Entomological Society of Washington* 86: 797–807.
- Johnson NF (1984b) Systematics of Nearctic *Telenomus*: classification and revisions of the *podisi* and *phymatae* species groups (Hymenoptera: Scelionidae). *Bulletin of the Ohio Biological Survey* 6: 1–113.
- Johnson NF (1985a) Revision of the New World species of the *thyantae* group of *Trissolcus* (Hymenoptera: Scelionidae). *The Canadian Entomologist* 117: 107–112. <https://doi.org/10.4039/Ent117107-1>
- Johnson NF (1985b) Systematics of New World *Trissolcus* (Hymenoptera: Scelionidae): species related to *T. basalis*. *The Canadian Entomologist* 117: 431–445. <https://doi.org/10.4039/Ent117431-4>
- Johnson NF (1987) Systematics of New World *Trissolcus*, a genus of pentatomid egg-parasites (Hymenoptera: Scelionidae). *Journal of Natural History* 21: 285–304. <https://doi.org/10.1080/00222938700771021>
- Johnson NF (1991) Revision of Australasian *Trissolcus* species (Hymenoptera: Scelionidae). *Invertebrate Taxonomy* 5: 211–239. <https://doi.org/10.1071/IT9910211>
- Kjer KM (1995) Use of rRNA secondary structure in phylogenetic studies to identify homologous positions: an example of alignment and data presentation from the frogs. *Molecular Phylogenetics and Evolution* 4: 314–330.
- Konopka JK, Haye T, Garipey T, Mason P, Gillespie D, McNeil JN (2016) An exotic parasitoid provides an invasional lifeline for native parasitoids. *Ecology and Evolution* 2016 (7): 277–284. <https://doi.org/10.1002/ece3.2577>
- Kriticos DJ, Kean JM, Phillips CB, Senay SD, Acosta H, Haye T (2017) The potential global distribution of the brown marmorated stink bug, *Halyomorpha halys*, a critical threat to plant biosecurity. *Journal of Pest Science* 90: 1033–1043. <https://doi.org/10.1007/s10340-017-0869-5>
- Leskey T, Nielsen A (2017) Impact of the invasive brown marmorated stink bug in North America and Europe: history, biology, ecology and management. *Annual Review of Entomology* 63: 599–618. <https://doi.org/10.1146/annurev-ento-020117-043226>

- Lomeli-Flores JR, Rodríguez-Rodríguez SE, Rodríguez-Leyva E, González-Hernández H, Garipey TD, Talamas EJ (2019) Field studies and molecular forensics identify a new association: *Idris elba* Talamas, sp. nov. parasitizes the eggs of *Bagrada hilaris* (Burmeister). In: Talamas E (Eds) Advances in the Systematics of Platygastroidea II. Journal of Hymenoptera Research 73: 125–141. <https://doi.org/10.3897/jhr.73.38025>
- Murphy NP, Carey D, Castro LR, Dowton M, Austin AD (2007) Phylogeny of the platygastroid wasps (Hymenoptera) based on sequences from the 18S rRNA, 28S rRNA and cytochrome oxidase I genes: implications for the evolution of the ovipositor system and host relationships. Biological Journal of the Linnean Society 91: 653–669. <https://doi.org/10.1111/j.1095-8312.2007.00825.x>
- Palumbo JC, Natwick ET (2010) The bagrada bug (Hemiptera: Pentatomidae): A new invasive pest of cole crops in Arizona and California. Plant Health Progress. <https://doi.org/10.1094/PHP-2010-0621-01-BR>
- Park JK, Foighil DÓ (2000) Sphaeriid and corbiculid clams represent separate heterodont bivalve radiations into freshwater environments. Molecular Phylogenetics and Evolution 14: 75–88. <https://doi.org/10.1006/mpev.1999.0691>
- Sabbatini Peverieri G, Talamas E, Bon MC, Marianelli L, Bernardinelli I, Malossini G, Benvenuto L, Roversi PF, Hoelmer K (2018) Two Asian egg parasitoids of *Halyomorpha halys* (Stål) (Hemiptera, Pentatomidae) emerge in northern Italy: *Trissolcus mitsukurii* (Ashmead) and *Trissolcus japonicus* (Ashmead) (Hymenoptera, Scelionidae). Journal of Hymenoptera Research 67: 37–53. <https://doi.org/10.3897/jhr.67.30883>
- Stahl J, Tortorici F, Pontini M, Bon MC, Hoelmer K, Marazzi C, Tavella L, Haye T (2018) First discovery of adventive populations of *Trissolcus japonicus* (Ashmead) in Europe. Journal of Pest Science. <https://doi.org/10.1007/s10340-018-1061-2>
- Taekul C, Valerio AA, Austin AD, Klompen H, Johnson NF (2014) Molecular phylogeny of telenomine egg parasitoids (Hymenoptera: Platygastroidea s.l.: Telenominae): evolution of host shifts and implications for classification. Systematic Entomology 39: 24–35. <https://doi.org/10.1111/syen.12032>
- Talamas EJ, Johnson NF, Buffington M (2015a) Key to Nearctic species of *Trissolcus* Ashmead (Hymenoptera, Scelionidae), natural enemies of native and invasive stink bugs (Hemiptera, Pentatomidae). Journal of Hymenoptera Research 43: 45–110. <https://doi.org/10.3897/JHR.43.8560>
- Talamas EJ, Herlihy MV, Dieckhoff C, Hoelmer KA, Buffington ML, Bon M-C, Weber DC (2015b) *Trissolcus japonicus* (Ashmead) emerges in North America. Journal of Hymenoptera Research 43: 119–128. <https://doi.org/10.3897/JHR.43.4661>
- Talamas EJ, Buffington ML, Hoelmer K (2017) Revision of Palearctic *Trissolcus* Ashmead (Hymenoptera, Scelionidae). In: Talamas EJ, Buffington ML (Eds) Advances in the Systematics of Platygastroidea. Journal of Hymenoptera Research 56: 3–185. <https://doi.org/10.3897/jhr.56.10158>
- Tamura K, Stecher G, Peterson D, Filipiński A, Kumar S (2013) MEGA6: Molecular Evolutionary Genetics Analysis Version 6.0. Molecular Biology and Evolution 20: 2725–2729. <https://doi.org/10.1093/molbev/mst197>
- Tortorici F, Talamas EJ, Moraglio ST, Pansa MG, Asadi-Farfar M, Tavella L, Caleca V (2019) A morphological, biological and molecular approach reveals four cryptic species of

Trissolcus semistriatus (Nees von Esenbeck) (Hymenoptera Scelionidae) egg parasitoids of Pentatomidae (Heteroptera). Journal of Hymenoptera Research X: X–X.

Whiting MF, Carpenter JC, Wheeler QD, Wheeler WC (1997) The Strepsiptera problem: phylogeny of the holometabolous insect orders inferred from 18S and 28S ribosomal DNA sequences and morphology. Systematic Biology 46: 1–68. <https://doi.org/10.1093/sysbio/46.1.1>

Zhang J, Zhang F, Garipey T, Mason P, Gillespie D, Talamas E, Haye T (2017) Seasonal parasitism and host specificity of *Trissolcus japonicus* in northern China. Journal of Pest Science 90: 1127–1141. <https://doi.org/10.1007/s10340-017-0863-y>

Supplementary material 1

Specimen information table

Authors: Elijah J. Talamas, Marie-Claude Bon, Kim A. Hoelmer, Matthew Buffington

Data type: specimens data

Explanation note: This table provides a table of information associated with the specimens used in this study, including collecting unit identifier, isolate code, sampling locality, collector, and GenBank accession numbers.

Copyright notice: This dataset is made available under the Open Database License (<http://opendatacommons.org/licenses/odbl/1.0/>). The Open Database License (ODbL) is a license agreement intended to allow users to freely share, modify, and use this Dataset while maintaining this same freedom for others, provided that the original source and author(s) are credited.

Link: <https://doi.org/10.3897/jhr.73.39563.suppl1>

Supplementary material 2

Sequence alignment used for phylogenetic analysis

Authors: Marie-Claude Bon, Matthew Buffington

Data type: molecular data

Explanation note: This file contains a NEXUS file of the aligned sequence data used for phylogenetic analysis, partitioned by molecular marker.

Copyright notice: This dataset is made available under the Open Database License (<http://opendatacommons.org/licenses/odbl/1.0/>). The Open Database License (ODbL) is a license agreement intended to allow users to freely share, modify, and use this Dataset while maintaining this same freedom for others, provided that the original source and author(s) are credited.

Link: <https://doi.org/10.3897/jhr.73.39563.suppl2>

Supplementary material 3

Command lines for phylogenetic analyses

Authors: Matthew Buffington, Zachary Lahey

Data type: phylogenetic data

Explanation note: This file contains a list of the operations used to generate the phylogenetic trees in this study.

Copyright notice: This dataset is made available under the Open Database License (<http://opendatacommons.org/licenses/odbl/1.0/>). The Open Database License (ODbL) is a license agreement intended to allow users to freely share, modify, and use this Dataset while maintaining this same freedom for others, provided that the original source and author(s) are credited.

Link: <https://doi.org/10.3897/jhr.73.39563.suppl3>



■ *Advances in the Systematics of Platygastroidea II* builds on many of the subjects of the first issue, including the taxonomy of Cretaceous species, the evolution of ovipositor morphology, and systematics of parasitoids that attack the eggs of invasive pests. Classical taxonomy features prominently, including species-level revision of two extant genera, *Pulchrisolia* and *Aleyroctonus* (Sceliotrachelinae) and the extinct *Proterosceliopsis*, now raised to the rank of family. Revision of the latter is the largest to date for fossil platygastroids, reflecting the diversity of the Cretaceous fauna and the excellent preservation afforded by Burmese amber. In contrast with the the first issue, molecular data and field studies are featured in six of the nine article and support studies of species with potential as biological control agents. Here, molecular sequences form the basis for phylogenetic inference and forensic analysis of host associations, and provide independent support for morphological diagnoses. Field studies reveal new behaviors, novel host associations, and expanded geographical distributions.